Targeting of the PI3K/AKT/mTOR pathway in human prostate cancer

Dominika Ewelina Butler

PhD

University of York

Biology

September 2014

ABSTRACT

The tumour suppressor PTEN is frequently lost in advanced prostate cancer leading to over-activation of the PI3K/AKT/mTOR pathway. Therefore targeting of the PI3K signalling with pathway-specific inhibitors has been proposed as a therapeutic strategy.

Inhibition of AKT and mTOR kinases in prostate cancer cell lines showed a decrease in cell viability and reduction in phospho-biomarkers expression. Although apoptosis was not induced, a decrease in cell migration and G1 cell growth arrest were observed in LNCaP cells.

However, in primary prostate cultures activation of the Ras/MEK/ERK compensatory pathway was observed following treatment with AKTi. Moreover, cell viability was less affected than in cell lines and autophagy was induced following treatment with AKTi. Surprisingly, treatment with a combination of AKTi and MEK1/2 inhibitors (MEK1/2i and RO-512) did not reduce phosphorylation of ERK1/2 in primary prostate cultures, but irreversible growth arrest-senescence, was evident. Additionally, *ex vivo* treatment of a 'near-patient' prostate xenograft with a combination of AKTi and mTORi significantly reduced tumour frequency.

These results demonstrate that targeting the PI3K/AKT/mTOR pathway triggers activation of the Ras/MEK/ERK compensatory pathway and therefore blockade of one pathway is not sufficient to treat prostate cancer. This study also highlights the importance of using patient-derived tumour cells in preclinical assessment of new drugs rather than relying solely on cancer cell lines.

LIST OF CONTENTS

LIST OF TABLES

TABLES

LIST OF FIGURES

ACKNOWLEDGEMENTS

I would like to thank BBSRC and AstraZeneca for funding this project and my supervisors Norman Maitland and Barry Davies for giving me the opportunity to carry out this work.

I am especially grateful to Anne Collins for her guidance and advice throughout this project, for her support during my life-changing events and most importantly, for being my friend sharing dog-walking and science passion.

Special thanks to Michelle Scaife, Hannah Walker and Adam Hirst for being my 'support group', for the outbursts of laughter and the tears of joy. I will miss you dearly.

I would especially like to thank Fiona Frame for keeping me sane for the last few weeks of writing this thesis, and most importantly for being 'my person' when I needed the most encouragement and support.

Also, a special thanks to Paul Berry, Marie Labarthe-Last and Caty Hyde for their assistance in *in vivo* study.

A special thanks to everyone at the CRU, past and present, for making the laboratory such a friendly work environment.

I would also like to thank my husband Mark Butler who supported me during the years and never stopped believing in me.

I dedicate this work to my children, Brandon and Scarlett Butler, who came to this world during my PhD and made it the most incredible experience of my life.

AUTHOR'S DECLARATION

I declare that this thesis represents my own unaided work, except where acknowledged otherwise in the text, and has not been submitted previously in consideration for a degree at this, or at any other university.

Chapter 1

Introduction

1. INTRODUCTION

1.1. Human prostate gland anatomy

The prostate is a walnut-sized major secretory gland of the male reproductive system. It is located in front of the rectum and just below the bladder, where it wraps around the upper part of the urethra (Figure 1.1 A). The human prostate is a heterogeneous organ, which can be divided into four zones: peripheral zone (70% of prostate glandular tissue), central zone (25%), transition zone (5%) and anterior zone, which is composed of muscular and fibrous tissue, but lacks any glandular structures (Figure 1.1 B) (McNeal, 1981). The peripheral zone is the most common area in which prostate cancer arises. It accounts for up to 70% of all prostate cancers, compared to 20% arising in the transition zone and 10% in the central zone (McNeal, 1988).

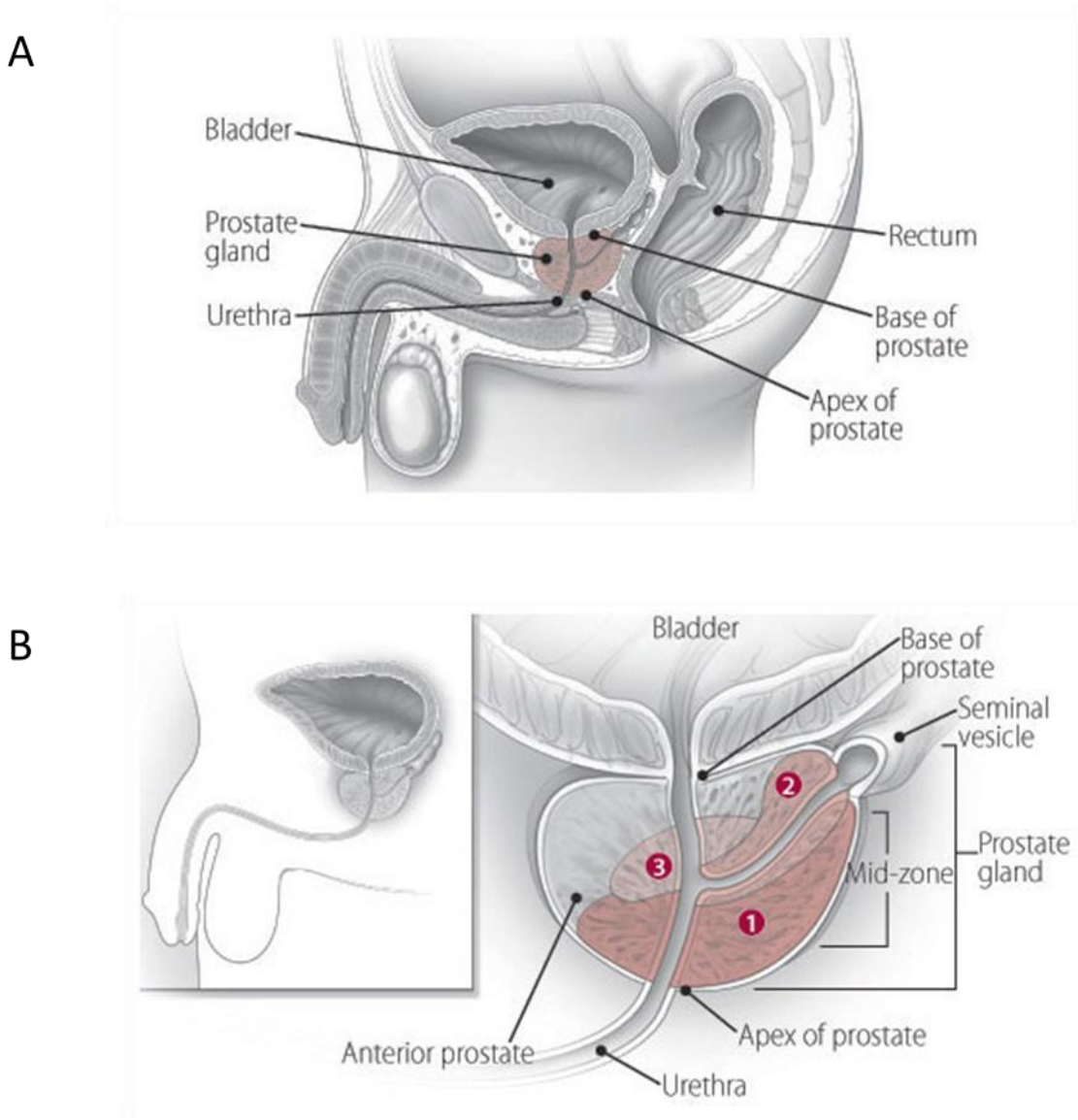

Figure 1.1. Schematic illustration of location and organisation of the human prostate gland. The human prostate is located at the base of the bladder, where it surrounds the urethra (A). It consists of peripheral zone – 1, central – 2 and transition zone – 3 (B). Image adapted from (Harvard Prostate Knowledge).

1.1.1. Cellular organisation of the prostate epithelium

The prostate epithelium consists of basal, secretory luminal and rare neuroendocrine cells. The luminal cells represent the major cell type in the prostate, they are terminally differentiated and secrete prostate-specific antigen (PSA) and prostatic acid phosphatase (PAP) into the glandular lumen (Figure 1.2 A). Luminal cells, unlike the basal cells, express high levels of androgen receptor (AR) and are dependent on androgens for their survival, whereas the basal cells are located at the basement membrane, express low levels of AR and do not have any secretory activity (Sar et al., 1990, Kyprianou and Isaacs, 1988, Lilja and Abrahamsson, 1988, Bonkhoff and Remberger, 1993). Basal cells can be further subdivided into distinct subpopulations: stem cells, transit-amplifying and committed basal cells on the basis of expression of cell surface markers, including $\alpha_2\beta_1$ integrins, CD44 and CD133 (Figure 1.2 B).

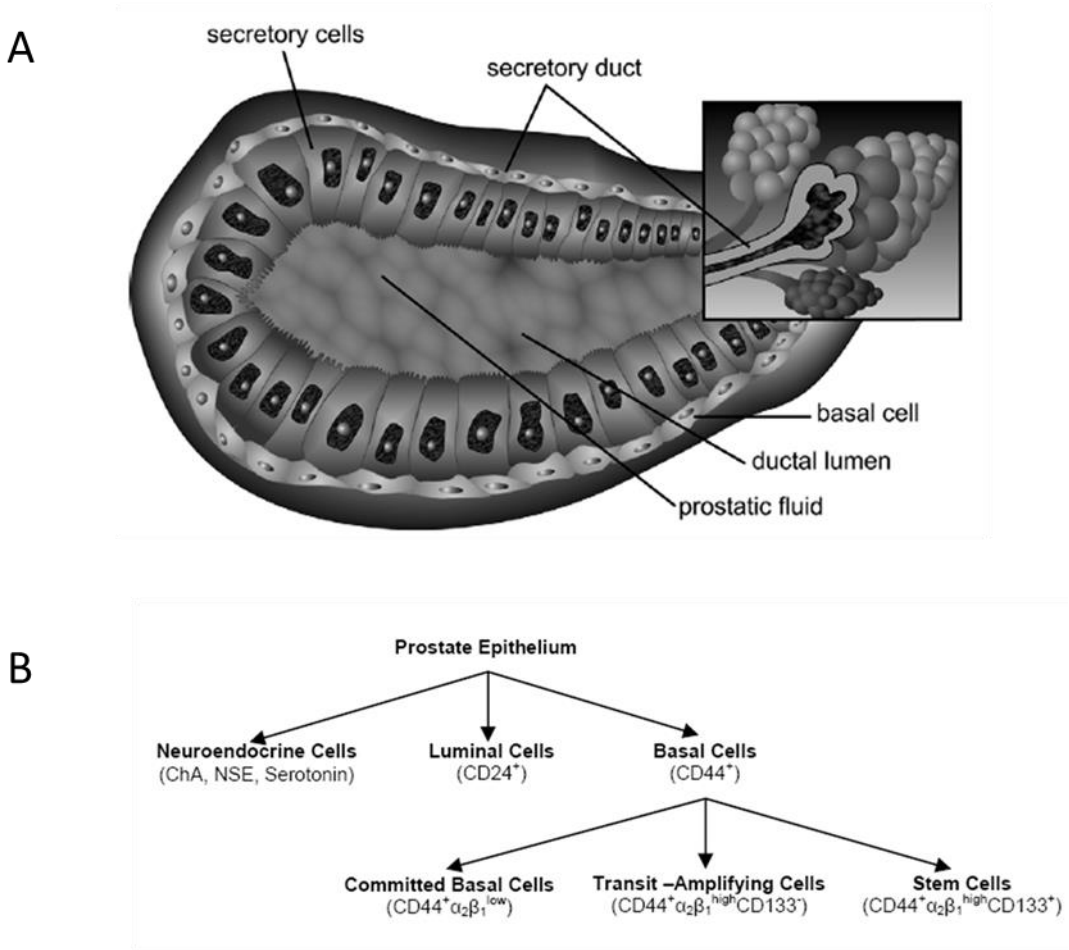

Figure 1.2. Anatomy and organisation of the human prostate gland.

Cross-section of the prostatic duct showing organisation of the epithelial cells (A) and schematic organisation of the prostate epithelium (B). Adapted from (Collins and Maitland, 2006).

Basal and luminal cells can be discriminated on the basis of their localisation, morphology and expression of specific cytokeratins (CK), such as cytokeratin 5 and 14 (expressed by basal cells) and cytokeratin 8 and 18 (expressed predominantly by luminal cells) (Sherwood et al., 1991).

Neuroendocrine cells are principally located within the basal compartment, they are terminally differentiated and androgen-independent (Bonkhoff et al., 1995). They are responsible for the production and secretion of neuroendocrine peptides, such as calcitonin, chromogranin and serotonin and therefore essential for homeostatic regulation of the secretory processes in the prostate gland (Abrahamsson, 1999).

The basal layer of cells strongly adheres to the basement membrane, which forms a structural barrier between the epithelial compartment and the stroma (Figure 1.3). The prostatic stromal cells secrete growth factors, including epidermal growth factor (EGF) and fibroblast growth factor (FGF), which are essential for epithelial cell maintenance and differentiation (Hall et al., 2002, Berry et al., 2008).

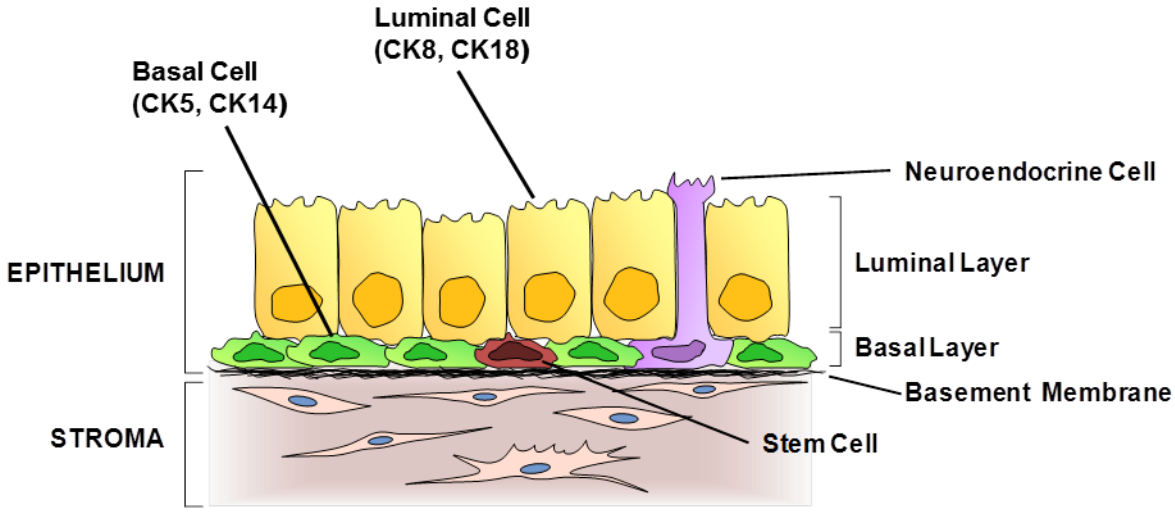

Figure 1.3. Schematic representation of the architecture of the human prostate epithelium.

Stem cells and neuroendocrine cells are located in the basal compartment of the prostate and together with luminal layer form the prostate epithelium. Stromal cells, including myofibroblasts, fibroblasts and smooth muscle cells, are separated from the epithelium by the basement membrane. Adapted from (Oldridge et al., 2012).

1.1.1.1. Prostate epithelial stem cells

Multipotent adult stem cells are an essential component of tissue homeostasis and their main functions include tissue regeneration following injury or replacement of terminally differentiated cells. Adult stem cells have limited differentiation potential depending on the specific lineages of the tissue in which they reside. However, these cells are able to self-renew and differentiate throughout the lifespan of an adult because of their unlimited growth and asymmetrical division capacity (Morrison and Kimble, 2006). The progeny of adult stem cells named transit amplifying (TA) cells, have limited proliferative capacity before they terminally differentiate (Figure 1.4) (Hall and Watt, 1989).

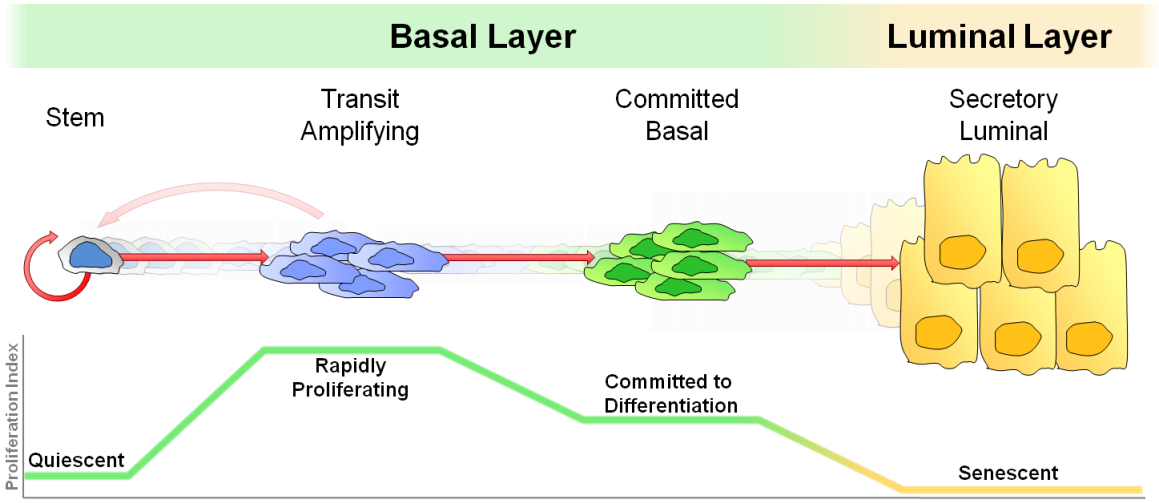

Figure 1.4. Hierarchical organisation of the human prostate epithelium.

Quiescent stem cells produce rapidly proliferating transit amplifying progeny, which then produce cells committed to differentiation. Committed basal cells differentiate further to secretory luminal cells, which are mainly senescent. Adapted from (Oldridge et al., 2012).

1.2. Diseases of the prostate

1.2.1. Prostatitis

Prostatitis is an inflammatory disorder of the prostate whose main symptom is difficulty or pain in passing urine. It is the most common disease of the prostate in men age 36 to 65 with an incidence rate of 2-10% (Krieger, 2004). There are many potential causes of the disease, such as acute and chronic bacterial infections, stress, physical injury or autoimmune reaction. Prostatitis can be successfully treated with antibiotics or anti-inflammatory drugs (Stevermer and Easley, 2000). Research evidence suggests that inflammation of the prostate is a significant factor for benign prostatic hyperplasia (BPH) initiation in older men (Kramer and Marberger, 2006, Kramer et al., 2007).

1.2.2. Benign prostatic hyperplasia (BPH)

BPH is a non-malignant, age-related disease, which originates in the transition zone of the prostate gland. Clinical symptoms are associated with an enlarged prostate and they include decrease in force and calibre of urinary stream and the sensation of incomplete bladder emptying (Figure 1.5) (Oesterling, 1991). Transurethral resection of the prostate (TURP) is often performed in order to alleviate symptoms (Schroder and Blom, 1989). Other treatment options for BPH include:

- Alpha blockers, for example tamsulosin and alfuzosin which relax the smooth muscle of the prostate and bladder improving urine flow (Urology Care Foundation, 2013, National Health Service UK, 2013);

- 5-alpha-reductase inhibitors such as finasteride and dutasteride which block the effects of hormone dihydrotestosterone (DHT) and reduce the enlarged prostate (Urology Care Foundation, 2013, National Health Service UK, 2013);

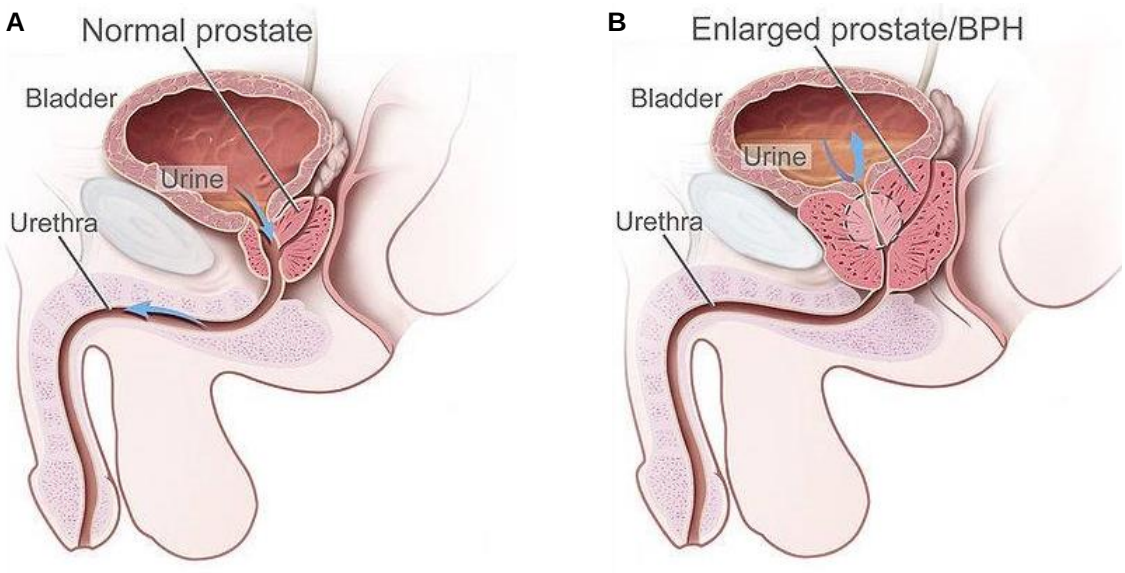

Figure 1.5. Schematic representation of the normal prostate and BPH.

The illustration shows a normal prostate and undisturbed flow of urine through the urethra (A) and an enlarged prostate, due to BPH, pressing on the bladder and urethra blocking the flow of urine (B). Adapted from (National Cancer Institute).

1.2.3. Prostatic intraepithelial neoplasia (PIN)

Prostatic intraepithelial neoplasia (PIN) represents a precancerous stage of the prostate. Two grades of PIN are recognized: low and high grade. In low grade PIN, the cells within ducts and acini are irregularly spaced, their nuclei are elongated and nucleoli are small, whereas in high grade PIN, the cells are crowded, their nuclei are enlarged and often multiple nucleoli are present (Bostwick et al., 2004). PIN is characterised by abnormal cellular proliferation which disturbs the bilayer of the prostatic epithelium, but the basement membrane remains intact. The most common location for PIN is the peripheral zone of the prostate, the area in which the majority (70%) of prostatic carcinomas occur. The frequency and severity of PIN in prostates with cancer is significantly increased when compared with prostates without cancer. High grade PIN is considered the ultimate pre-invasive stage of invasive carcinoma (Bostwick et al., 2004).

1.2.4. Prostate cancer

Prostate cancer is a slow-growing, heterogeneous disease; with the majority (>70%) of tumours originating in the peripheral zone, 15-20% in the central zone and the remaining 10-15% in the transitional zone. Prostate cancer progression has been shown to correlate with loss of tumour suppressor genes, such as phosphatase and tensin homolog deleted on chromosome ten (*PTEN)*, Retinoblastoma (*Rb)* and *p53* (Figure 1.6) (Shen and Abate-Shen, 2010, Abate-Shen and Shen, 2000).

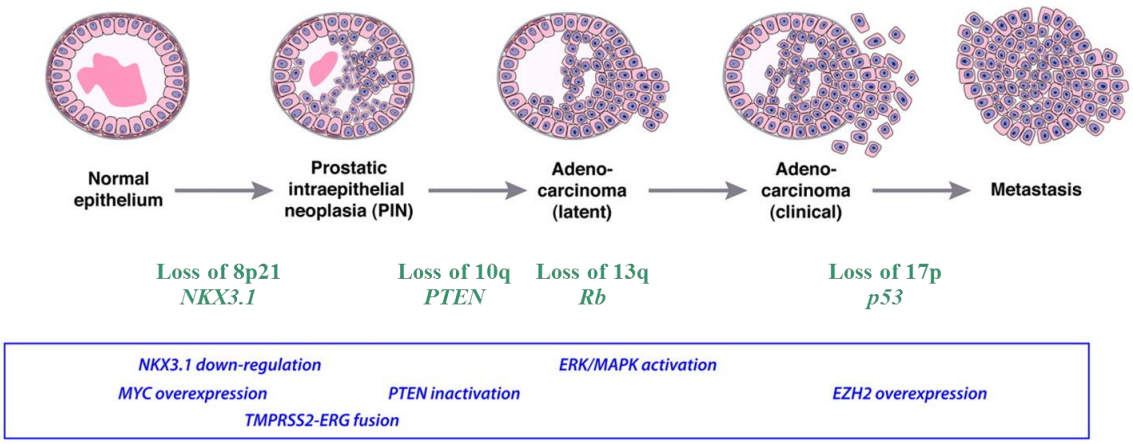

Figure 1.6. Human prostate cancer progression.

A schematic illustration of the stages of progression from normal prostate epithelium, through to prostatic intraepithelial neoplasia (PIN), invasive carcinoma and ultimately to metastatic prostate cancer. Stages of progression correlate with loss of specific chromosome regions and tumour suppressor genes. Adapted from (Shen and Abate-Shen, 2010).

1.2.4.1. Prostate cancer incidence and mortality

Prostate cancer is the most common cancer in men in the UK (Cancer Research UK, 2011). There are over 40,000 new cases of prostate cancer diagnosed every year, which accounts for 25% of all new cases of cancers in males. The incidence of prostate cancer is strongly related to age, and its highest rate of 800 per 100,000 men is in the 75-79 age group (Figure 1.7).

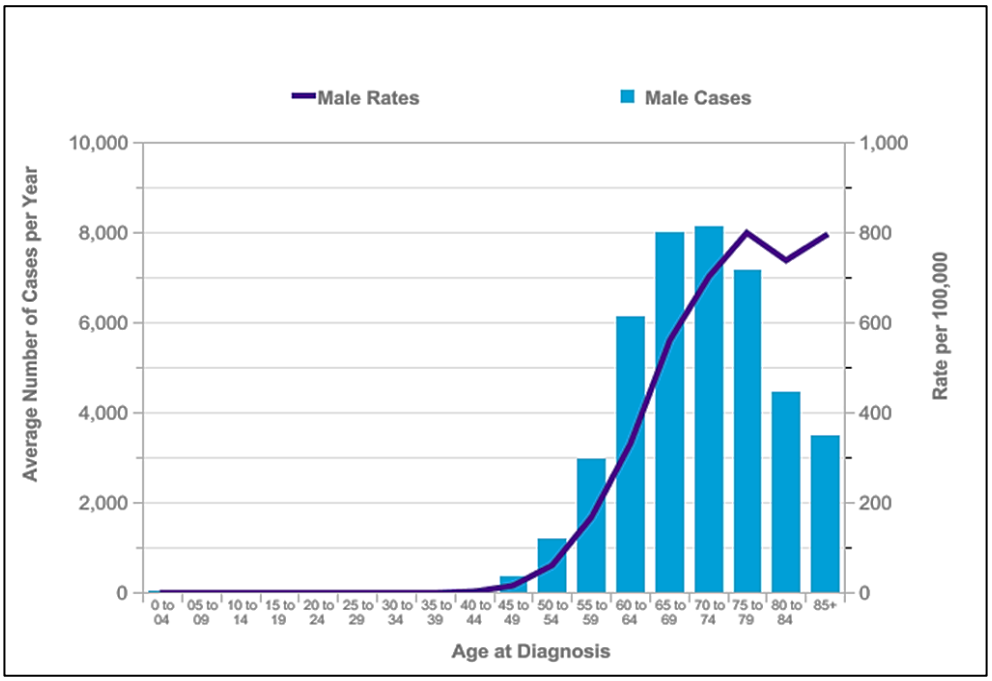

Figure 1.7. Incidence of prostate cancer.

The average number of new cases per year and age-specific incidence rates of prostate cancer in the UK between 2009 and 2011. Taken from (Cancer Research UK).

Prostate cancer is the second most common cause of cancer death in men in the UK (Cancer Research UK, 2011). The mortality rate of prostate cancer is strongly related to age; it rises sharply from age 50 and its highest rates are observed in the 85+ age group (Figure 1.8).

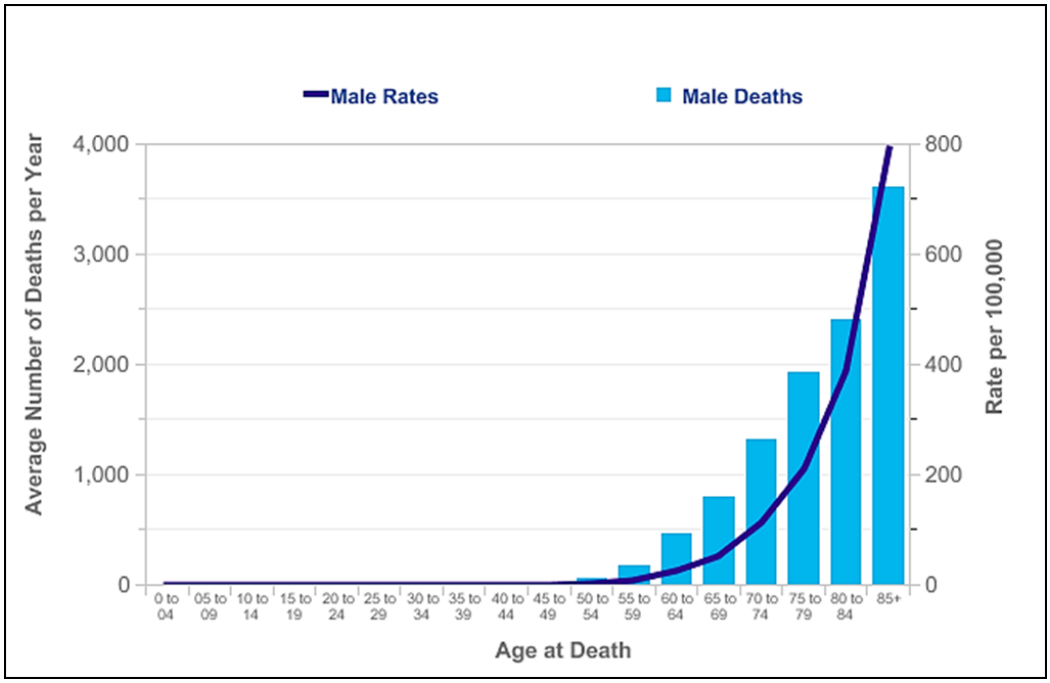

Figure 1.8. Mortality of prostate cancer.

Average number of deaths per year and age-specific mortality rates of prostate cancer in the UK between 2010 and 2012. Taken from (Cancer Research UK).

1.2.4.2. Diagnosis of prostate cancer

The diagnosis of prostate cancer is currently based on the quantification of prostate specific antigen (PSA) levels in serum (Stampfer et al., 2014, Placer and Morote, 2011). In the normal prostate, PSA functions as a serine protease and is responsible for maintaining the fluidity of seminal fluid (Lilja and Abrahamsson, 1988). A PSA concentration of less than 4 ng/ml is considered to be normal, whereas PSA of more than 4 ng/ml usually requires further investigation, which involves a biopsy and digital rectal examination (DRE). However, PSA test might give false-positive or false-negative result. A false-positive test result occurs when a man's PSA level is elevated but cancer is not present. A false-negative test result occurs when detected PSA level is low but the patient actually has prostate cancer. Majority of men with an elevated PSA level do not have prostate cancer; increased PSA level might also be a result of prostatitis or urinary tract infection. Only about 25% of men undergoing prostate biopsy due to elevated PSA level turn out to have prostate cancer (National Cancer Institute).

During prostate cancer progression, the characteristic morphology of the gland begins to degrade and the basement membrane is eventually destroyed (Gleason, 1966). Following biopsy, the prostate tissue is histologically analysed and graded according to the Gleason tumour grading system (Figure 1.9) (Gleason, 1966). The Gleason grading system is based on the degree of glandular differentiation and 5 grades are identified; grade 1 represents normal, differentiated histology and grade 5 represents the least differentiated pattern. The Gleason grading system was recently updated and it has been proposed that Gleason grades 2 + 4 should be rarely diagnosed on needle biopsy and should be replaced with 3 + 3 (Epstein, 2010).

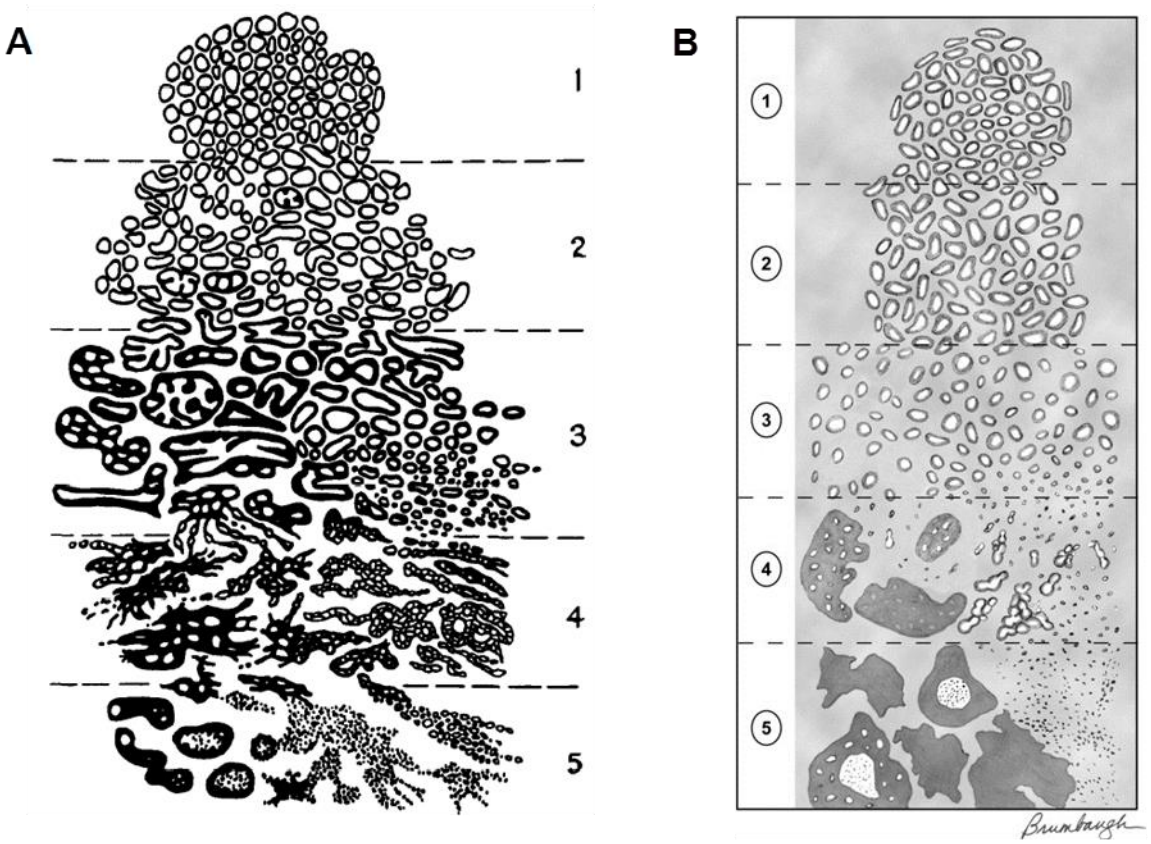

Figure 1.9. Gleason grading system for prostatic adenocarcinoma.

The original (A) and modified (B) Gleason grading system describing architectural features divided into 5 histological patterns of decreasing differentiation, with pattern 1 representing the most differentiated and pattern 5 being the least differentiated. Adapted from (Gleason, 1966, Epstein, 2010).

1.2.4.3. Current strategies for treatment of prostate cancer

The treatment strategy for patients with prostate cancer depends on the stage of disease at the time of the diagnosis and most importantly whether the cancer is confined to the prostate or it has spread. The different treatment options can include:

- Watchful waiting
- active surveillance
- Radical prostatectomy
- Radiotherapy
- Androgen deprivation therapy (ADT)
- Chemotherapy

1.2.4.3.1. Organ-confined prostate cancer

Patients diagnosed with small volume, low Gleason grade tumours, which are still confined to the prostate can be offered active surveillance rather than aggressive treatment options.

However, the most common treatment for organ-confined tumours is total surgical removal of the prostate – radical prostatectomy. It has been shown that this method of treatment reduces disease-specific mortality, risk of metastasis and local progression (Bill-Axelson et al., 2005). Although radical prostatectomy is a most common treatment for early stage prostate cancer, there are potential side effects, including urinary impotence and sexual dysfunction (Catalona et al., 1999). The risk of those side effects was reduced after introduction of nerve-sparing surgery (Walsh, 2007).

An additional treatment option for localised prostate cancer is radiotherapy, which involves applying ionising radiation directly to the tumour (brachytherapy) or indirectly by using external beam radiotherapy (Duchesne, 2011). Brachytherapy involves implantation of small radioactive seeds, which allows direct targeting of the cancerous tissue while surrounding healthy tissue only gets a small amount of radiation.

1.2.4.3.2. Metastatic prostate cancer

The treatment of prostate cancer, which has spread outside the prostate gland, usually involves androgen deprivation therapy (ADT). ADT blocks testosterone-driven proliferation of prostate cancer cells, which induces apoptosis in the majority of cancer cells. Prostate tumours initially respond well to androgen ablation therapy and a reduction of tumour volume is observed. However, in most cases, ADT ultimately fails and castration resistant prostate cancer (CRPC) emerges, which is inevitably fatal (Feldman and Feldman, 2001). The median survival for patients with CRPC is approximately 18 – 24 months (Tannock et al., 2004, Taichman et al., 2007).

There is evidence to suggest that the mechanisms of resistance to ADT can be acquired via:

- Point mutations in the AR ligand binding domain (Veldscholte et al., 1992)
- Amplification of the AR gene and consequent overexpression (Visakorpi et al., 1995)
- Activation of the IL-6 pathway (Hobisch et al., 1998)
- Changes in AR co-activators (Culig and Santer, 2012)
- Crosstalk with the PI3K/AKT pathway (Carver et al., 2011)
- Autonomous intratumoural androgen biosynthesis (Chang et al., 2011)
- Altered expression of AR transcriptional cofactors such as FOXA1 (Gerhardt et al., 2012)
- AR splice variants lacking the ligand binding domain (Sun et al., 2010)

Recently novel therapeutic agents, such as abiraterone and enzalutamide have demonstrated improved overall survival in metastatic castration-resistant prostate cancer (Esch et al., 2014). A summary of the most recent treatment strategies for prostate cancer is presented in Table 1.1.

Table 1.1. A list of new treatments for CRPC prostate cancer. (Adapted from Maitland N.J., Prostate cancer. Diagnosis and clinical management; 2014).

Treatment	Disease stage	Median / Mean survival [months]	Placebo / Standard of Care (SOC) comparator [months]	Therapeutic advantage [months]
Docetaxel +prednisone +ADT	1st line mPC	57.6	44	13.6
Docetaxel	1st line mCRPC	18.9	16.4	2.5
Abiraterone	CRPC	14.8	11.2	3.6
Provenge	CRPC	25.8	21.7	4.1
MDV3100 (Enzalutamide)	1st line mCRPC	32.4	30.2	2.2
MDV3100 (Enzalutamide)	2nd line mCRPC	18.4	13.6	4.8
Radium-223 chloride	mCRPC (Bone metastasis)	14	11	3

mPC – metastatic prostate cancer

mCRPC – metastatic castration resistant prostate cancer

1.2.4.4. Prostate cancer stem cells

The origin of prostate cancer is still controversial. It has been suggested that the initiating cell of a prostate cancer would be a luminal cell, because terminally differentiated luminal cells constitute the majority of cells in the tumour bulk (Signoretti et al., 2000). However, evidence has been accumulating to support the cancer stem cell theory of tumour initiation. A cancer stem cell (CSC) is defined as a cell within the tumour that is able to self-renew and initiate tumour development in immunocompromised mice (Li et al., 2009). Additional characteristics of cancer stem cells include:

- Resistance to chemotherapy and radiotherapy
- Ability to regenerate the tumour after treatment
- Asymmetrical division
- Quiescence or slow proliferation
- Extensive proliferative potential
- Cell colony formation *in vitro*
- Matrix invasion

(Tindall, Reya et al., 2001, Vogelstein and Kinzler, 1993).

Cancer stem cells have been identified in a number of cancers, including acute myeloid leukaemia (Bonnet and Dick, 1997), breast (Al-Hajj et al., 2003), brain (Singh et al., 2003), multiple myeloma (Matsui et al., 2004), lung (Eramo et al., 2008) and many others.

Human prostate stem-like cells have been identified and isolated from prostate cancer biopsies based on the expression of cell surface markers $CD44^{+}\alpha_2\beta_1^{hi}CD133^{+}$ (Collins et al., 2005). The prostate CSCs have been shown to constitute a small cell population (0.1%) within the tumour, which have a basal phenotype and do not express the androgen receptor (Collins et al., 2005). Moreover, under differentiating conditions, luminal cells expressing androgen receptor (AR), cytokeratin 18 (CK18) and prostatic acid phosphatase (PAP) can be derived from prostate CSCs. It has also been shown that fewer than 100 cells were required to initiate tumour growth in immunocompromised

mice, indicating that this basal phenotype fraction of cells has indeed very high tumour initiation potential (Maitland et al., 2011).

1.2.5. Models of prostate cancer

1.2.5.1. Prostate epithelial cell lines

Prostate epithelial cell lines are the most commonly used model for studying prostate cancer. Using cell lines in research has several advantages, including easy maintenance and manipulation as well as extended potential to proliferate in culture. The most commonly used prostate cancer cell lines include LNCaP cells, derived from lymph node metastasis (Horoszewicz et al., 1983), PC3 derived from bone metastasis (Kaighn et al., 1979) and DU-145 from brain metastasis (Stone et al., 1978).

However, cell lines do not accurately represent human tumours. Additionally, it has been shown that long-term culture of cells in media with the addition of serum, is very likely to induce chromosomal changes (Izadpanah et al., 2008). Therefore, different models, such as primary cultures derived from patient biopsies should be considered.

1.2.5.2. Primary prostate epithelial cultures

Primary cultures derived from prostate cancer tumours and from benign prostatic hyperplasia more accurately represent the heterogeneity and complexity of the human disease. Moreover, growing primary cells on collagen I-coated plates and in the presence of feeder cells mimics the tumour-matrix/stroma interactions. However, primary cultures' limited lifespan *in vitro* can be a serious limiting factor for performing experiments.

1.2.5.3. Mouse models

The significant role of PTEN loss in prostate cancer progression has influenced the development of genetically engineered mice models based on *PTEN* gene inactivation

(De Velasco and Uemura, 2012). However, it has been shown that homozygous deletion of PTEN is embryonic lethal, whereas heterozygous PTEN knock-out mice develop PIN, but do not progress to malignant adenocarcinoma (Di Cristofano et al., 1998, Podsypanina et al., 1999). This indicated that inactivation of one allele of PTEN was sufficient to induce tumorigenesis, but not prostate cancer progression.

Several animal models have shown evidence of collaboration between *PTEN* haploinsufficiency and inactivation of other tumour suppressor genes in promoting prostate cancer progression (Kwabi-Addo et al., 2001).

Development of conditional gene targeting by the Cre-LoxP system has expanded the opportunities for transgenic mouse modelling research. The main advantage of the system is that in the conditional knock-out mice a genetic mutation can be induced in specific tissue without affecting other cell types (De Velasco and Uemura, 2012, Anton and Graham, 1995, Kanegae et al., 1995) .

Two of the most frequently used inducible promoters for conditional targeting of the mouse prostate include $PSA^{CreERT2}$ and $Nkx3.1^{CreERT2}$ and are both inducible with tamoxifen (Ratnacaram et al., 2008). Importantly, it has been demonstrated that prostate-specific conditional *PTEN* knock-out mice show many similar features to human prostate cancer, including histopathological and molecular similarities (Berquin et al., 2005)

1.3. The PI3K/AKT/mTOR pathway over-activation in human cancers

The phosphatydidyl inositol-3-OH kinases (PI3Ks) are a family of proteins involved in many cellular processes including: growth, metabolism, proliferation and glucose homeostasis. There are three classes in the family: class I, which is divided in to IA and IB, class II and class III (Cantley, 2002). Members of class IA are heterodimers consisting of a regulatory subunit, with three isoforms: p85α, p85β and p55γ, and a catalytic subunit p110 also with three isoforms: α, β and δ. Class IB are also heterodimers which consist of p101 – regulatory subunit and a p100γ catalytic subunit (Chalhoub and Baker, 2009). PI3K IA are activated by receptor tyrosine kinases (RTKs) and PI3K IB, by

G-protein-coupled receptors (GPCRs), which generate lipid second messenger phosphatidylinositol (3-5)-triphosphate (PIP_3) from phosphatidylinositol 4,5-biphosphate (PIP_2) (Figure 1.10) (Carracedo and Pandolfi, 2008, Meric-Bernstam and Gonzalez-Angulo, 2009). PTEN directly opposes the activity of PI3Ks by dephosphorylating PIP_3 into PIP_2 (Chalhoub and Baker, 2009). PIP_3 recruits proteins, containing pleckstrin homology (PH) domains, such as AKT and phosphoinositide-dependent kinase 1 (PDK1), to the cell membrane. After conformational change AKT gets phosphorylated by constitutively active PDK1 at Threonine 308 and by mammalian target of rapamycin complex 2 (mTORC2) at Serine 473 leading to its full activation (Sarker et al., 2009). Following activation, AKT translocates from the cell membrane to the cytoplasm and the nucleus and phosphorylates downstream targets, including the glycogen synthase kinase 3 β (GSK3 β), the tuberous sclerosis 2 (TSC2) tumour suppressor, FKHR and FKHRL transcription factors and many others (Vanhaesebroeck et al., 2012, Sarker et al., 2009). AKT signalling results in inhibition of apoptosis through phosphorylation of pro-apoptotic proteins, such as BAD, MDM2 and proteins from the Forkhead family, it also activates proliferation through inactivation of p27 and GSK3 (del Peso et al., 1997, Brunet et al., 1999, Carracedo and Pandolfi, 2008, Sano et al., 2003). Additionally, AKT regulates growth, protein translation (through regulation of mTORC1) and metabolism (by increasing rate of glucose catabolism) (Sano et al., 2003, Cross et al., 1995).

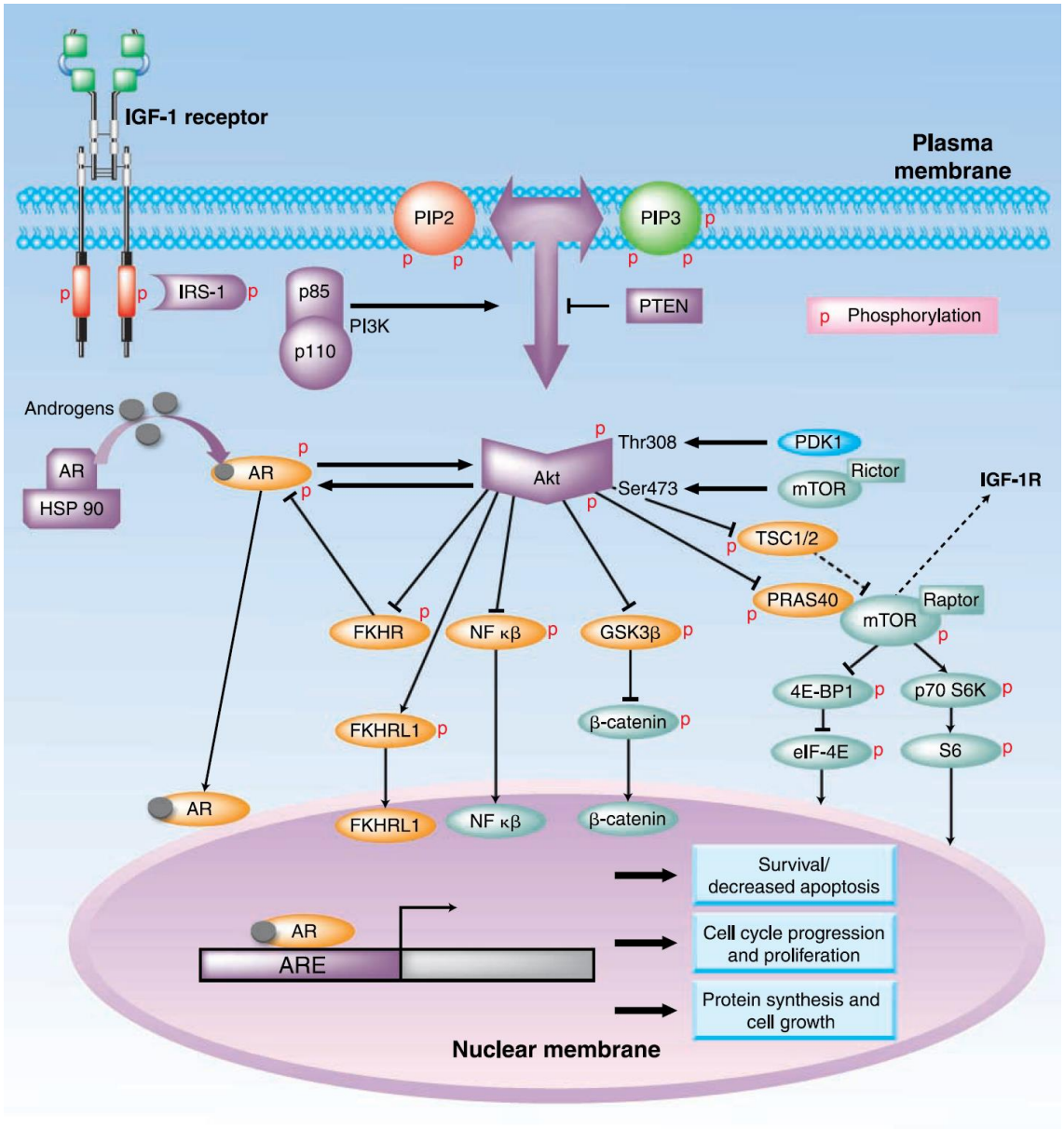

Figure 1.10. The PI3K/AKT/mTOR signalling network.

Activation of the PI3K pathway leads to phosphorylation of AKT and activates a cascade of phosphorylation events which result in increase of survival, proliferation and inhibition of apoptosis. Additionally, PI3K/AKT pathway interacts with androgen receptor (AR) signalling; upon binding of androgens, AR (which is normally bound to heat shock protein 90 (HSP-90) in the cytoplasm) dissociates from HSP-90, which allows phosphorylation of AR at multiple sites. AR-androgen complex translocates to the nucleus, binds to androgen response elements on promotors of target genes, leading to transcription. Arrows represent activation and bars represent inhibition. Taken from (Sarker et al., 2009).

The PI3K pathway has been found to be up-regulated in many human cancers, including glioblastoma, breast, ovarian, lung and prostate cancer (Vivanco and Sawyers, 2002, Engelman, 2009, Courtney et al., 2010). PI3K can get activated at the cell membrane by a number of receptor tyrosine kinases, such as epidermal growth factor receptor (EGFR), insulin-like growth factor receptor (IGFR) and platelet derived growth factor receptor (PDGFR) (Rameh and Cantley, 1999).

The PI3K pathway is constitutively activated, and aberrant PI3K signalling is estimated to be present in >30% of human cancers (Shaw and Cantley, 2006). It has been proposed by Carnero et al (Carnero et al., 2008) that possible biological events leading to PI3K pathway increased activation include:

- amplification of receptor tyrosine kinases
- amplification of PI3K
- activating mutations in the *PIK3CA* gene coding the p110α catalytic subunit
- overexpression of AKT
- loss or inactivating mutations of the tumour suppressor gene *PTEN*
- constitutive recruitment and activation of mutant forms of the *Ras* oncogene

Additionally, it has been shown that in prostate cancer the PI3K and androgen receptor signalling pathways regulate each other by reciprocal negative feedback, such that inhibition of one activates the other (Carver et al., 2011). Prostate cancer is dependent of androgens such as testosterone which activates AR signalling. The AR is a member of the steroid hormone receptor family which in the absence of androgens is predominantly inactive and localized in the cytoplasm bound to heat shock proteins (Figure 1.10). Upon ligand binding AR undergoes conformational changes, dimerization and translocates into the nucleus. In the nucleus, AR binds to androgen response

elements on promotors of target genes, leading to transcription (Bennett et al., 2010, Knudsen and Penning, 2010, Sarker et al., 2009).

There is evidence indicating that AR signalling continues to contribute to progression of CRPC after failure of ADT treatment despite low levels of androgen. A variety of possible mechanisms have been proposed to explain this phenomenon (see page 35). However, it has also been shown that activation of the PI3K pathway occurs in prostate tumours with repressed androgen signalling, which might be responsible for castrate-resistant phenotype (Carver et al., 2011). Carver and colleagues have demonstrated that inhibition of the PI3K pathway restores AR signalling in PTEN-deficient prostate cells trough a relief of negative feedback to HER kinases. They have also shown that a blockade of AR relieves feedback inhibition of AKT through reduced levels of FKBP5 which decrease stability of the phosphatase PHLPP. They have demonstrated that a combined inhibition of both pathways using an AR blocker MDV3100, that impairs AR translocation at the nucleus and binding to DNA and a PI3K/mTOR inhibitor BEZ235 resulted in a decrease in cell number and activation of apoptosis in PTEN-negative LNCaP cells (Carver et al., 2011).

However, prostate basal cells, unlike luminal cells, do not express high levels of AR and are not dependent on androgens for survival (Maitland et al., 2011, Lilja and Abrahamsson, 1988, Sar et al., 1990, Kyprianou and Isaacs, 1988, Bonkhoff and Remberger, 1993). Therefore androgen signalling was not investigated in this study.

1.3.1. PTEN

The tumour suppressor gene PTEN, which negatively regulates AKT, is the second (after p53) most frequently mutated gene in human cancers (Yilmaz and Morrison, 2008). PTEN has been implicated in multiple cancers through mutation, homozygous deletion, loss of heterozygosity, or epigenetic loss of expression (Mehrian-Shai et al., 2007). It has been shown that PTEN mutations consist of 49% frameshift mutations, 30% missense mutations and 15% nonsense mutations. Among the cancers most commonly affected by PTEN abnormalities are glioblastoma, prostate and endometrial tumours, with frequencies approaching 50% (Sulis and Parsons, 2003).

A cluster of six phosphorylation sites (Thr366, Ser370, Ser380, Thr382, Thr383 and Ser385), involved in PTEN tumour suppressor function, modulating stability and subcellular distribution, has been identified at the C-terminus of PTEN (Figure 1.11 A). It has been shown that mutation of the Ser380, Thr382 and Thr383 destabilizes PTEN and increases its phosphatase activity, compared to wild-type PTEN (Vazquez et al., 2000). PTEN is tightly regulated at the transcriptional level, and can be activated by EGR1, IGF2, PPARγ, p53 and inhibited by NFκB activation. PTEN mRNA is post-transcriptionally regulated by miRs (miR21, miR221/222 and miR25) (Figure 1.11). PTEN protein is regulated by post-translational modifications, including phosphorylation and ubiquitination (Figure 1.11 B) (Zhang and Yu, 2010, Salmena et al., 2008, Wang and Jiang, 2008, Carracedo and Pandolfi, 2008). It has been proposed that PTEN is normally maintained in a phosphorylated, inactive state and that its activation can be mediated through dephosphorylation of Ser380, Thr382 and Thr383 (Salmena et al., 2008). PTEN biological function includes PIP_3 dephosphorylation in the membrane, regulation of the cell cycle through CHK1 and maintaining chromosomal stability by association with centromeres in the nucleus (Figure 1.11 B) (Zhang and Yu, 2010).

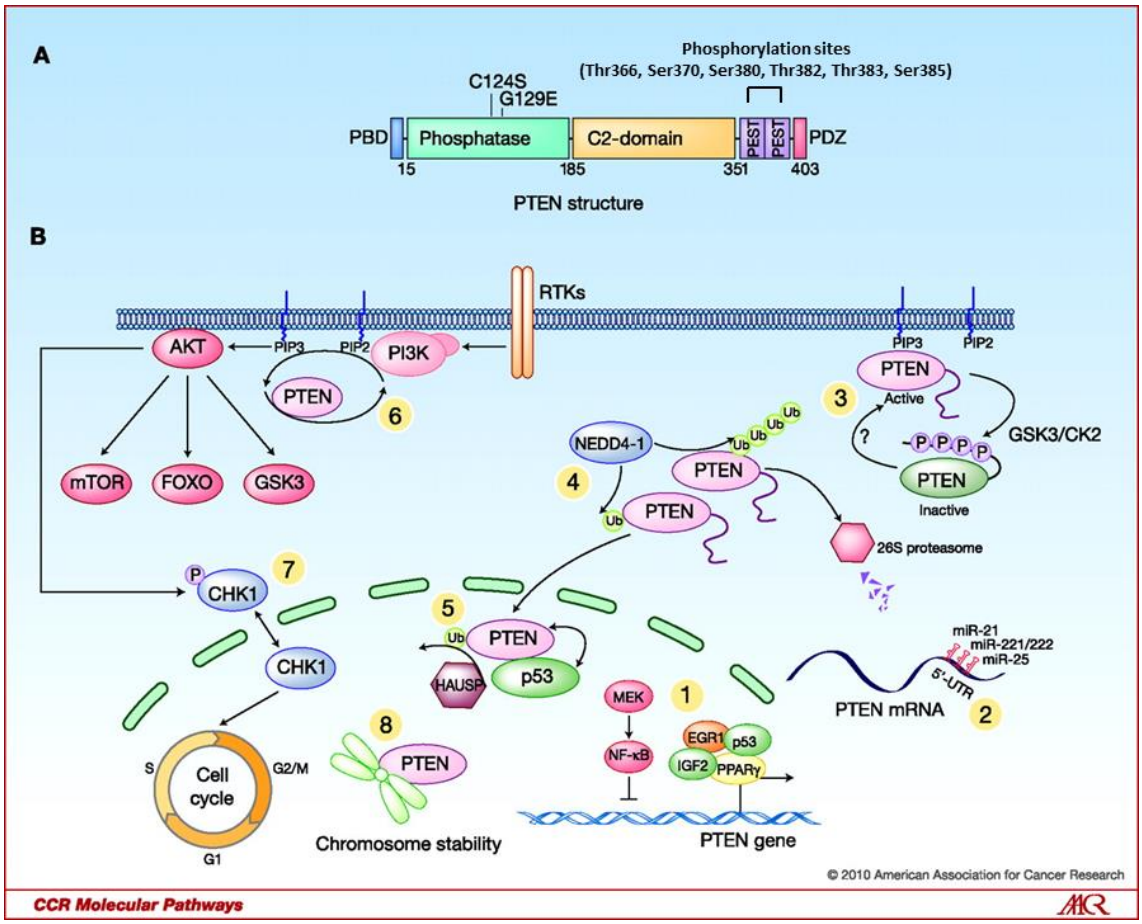

Figure 1.11. Structure and regulation of PTEN.

Schematic representation of PTEN structure (A), function and regulation (B). 1 – PTEN transcription is activated by EGR1, IGF2, p53 etc. and inhibited by MEK-mediated NF-κB activation; 2 – PTEN is post-transcriptionally regulated by miRs, including miR21, niR221/222 and miR25; 3 – phosphorylation of C-terminal domains of PTEN lead to 'closed' state of the protein and therefore influencing its activity and stability ; 4 – NEDD4-1 is an E3 ligase of PTEN, which mediates its mono- and poly-ubiquitination; 5 – HAUSP de-ubiquitinates PTEN in the nucleus and leads to PTEN nuclear exclusion; 6 – at the cell membrane PTEN dephosphorylated PIP3 and subsequently inhibits PI3K pathway; 7 – PTEN regulates cell cycle; 8 – PTEN associates with centromeres in the nucleus and maintains chromosome stability. Taken from (Zhang and Yu, 2010).

1.3.1.1. PTEN haploinsufficiency in prostate cancer

It is estimated that pathway up-regulation occurs in 30-50% of primary prostate cancers, and its aberrant signalling has also been detected in prostate cancer cell lines and xenografts (Morgan et al., 2009). The PTEN gene encodes a dual-specificity phosphatase that has activity against lipid and protein substrates (Vivanco and Sawyers, 2002). Its tumour suppressive property is attributed to its lipid phosphatase activity against phosphatidylinositol (3-5)-triphosphate (PIP3). PTEN dephosphorylates PIP3, which inhibits activation of the downstream effector AKT, leading to inhibition of cell survival and proliferation (Mehrian-Shai et al., 2007).

It has been shown by Kremer et al (2006), in immunohistochemistry experiments, on prostate tissue that the level of PTEN expression was lower in prostate intraepithelial neoplasia (PIN) and prostate cancer compared to normal prostate tissue (Kremer et al., 2006). Decreased levels of PTEN have also been found to be significantly associated with prostate cancer progression. Kinkade and colleagues (2008) investigated the expression of PTEN in BPH, PIN, low and high Gleason score prostate cancers. They found that levels of PTEN protein were reduced during prostate cancer progression in 59% of cases (Kinkade et al., 2008).

It has been shown by Sharrard and Maitland (2000) that there are several splice variants of PTEN present in prostate cell lines, mostly involving deletions from the full-length coding sequence (Figure 1.12) (Sharrard and Maitland, 2000).

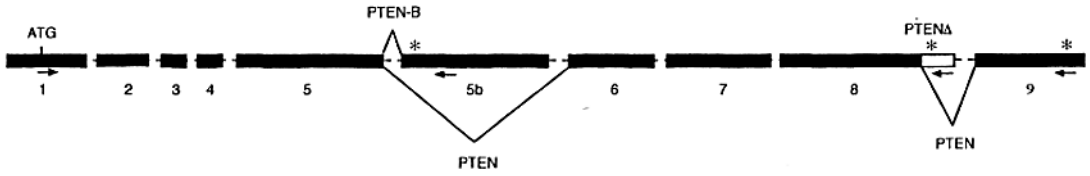

Figure 1.12. Partial genomic structure of PTEN gene.

The exons are shown to scale as solid boxes. An open box at the end of exon 8 indicates an alternatively spliced segment of intron H forming the 3' end of PTEN- Δ. The in-frame stop codons are marked by asterisks. Taken from (Sharrard and Maitland, 2000);

Two of the model cell lines for metastatic prostate cancer, LNCaP and PC3, were shown to lack expression of the PTEN protein; LNCaP cells have a two-base pair deletion in codon 6, and PC3 cells have a deletion at the 3' end of the gene (Sharrard and Maitland, 2007).

1.3.2. AKT kinase

There are three members of the AKT family: AKT1, AKT2 and AKT3, which are broadly expressed in most tissues (Zinda et al., 2001). AKT1 (also called protein kinase B) is one of the downstream effectors of PIP3, activated by phosphorylation at threonine 308 by phosphoinositide-dependent kinase 1 (PDK1) and at serine 473 by the rapamycin-insensitive mTOR complex (mTORC2) (Guertin et al., 2009). Activated AKT moves from the cell membrane to the cytoplasm and the nucleus, and phosphorylates a number of downstream targets, including Forkhead family of transcription factors (FOXO), glycogen synthase kinase 3 (GSK3) and many other proteins involved in cell survival, proliferation and cellular growth (Figure 1.13) (Jiang and Liu, 2008).

AKT-mediated phosphorylation can also modulate cell function by enhancing the activity of proteins such as MDM2, which promotes degradation of the tumour-suppressor p53 and the nuclear factor-kappa B (NF-κB) (Chalhoub and Baker, 2009).

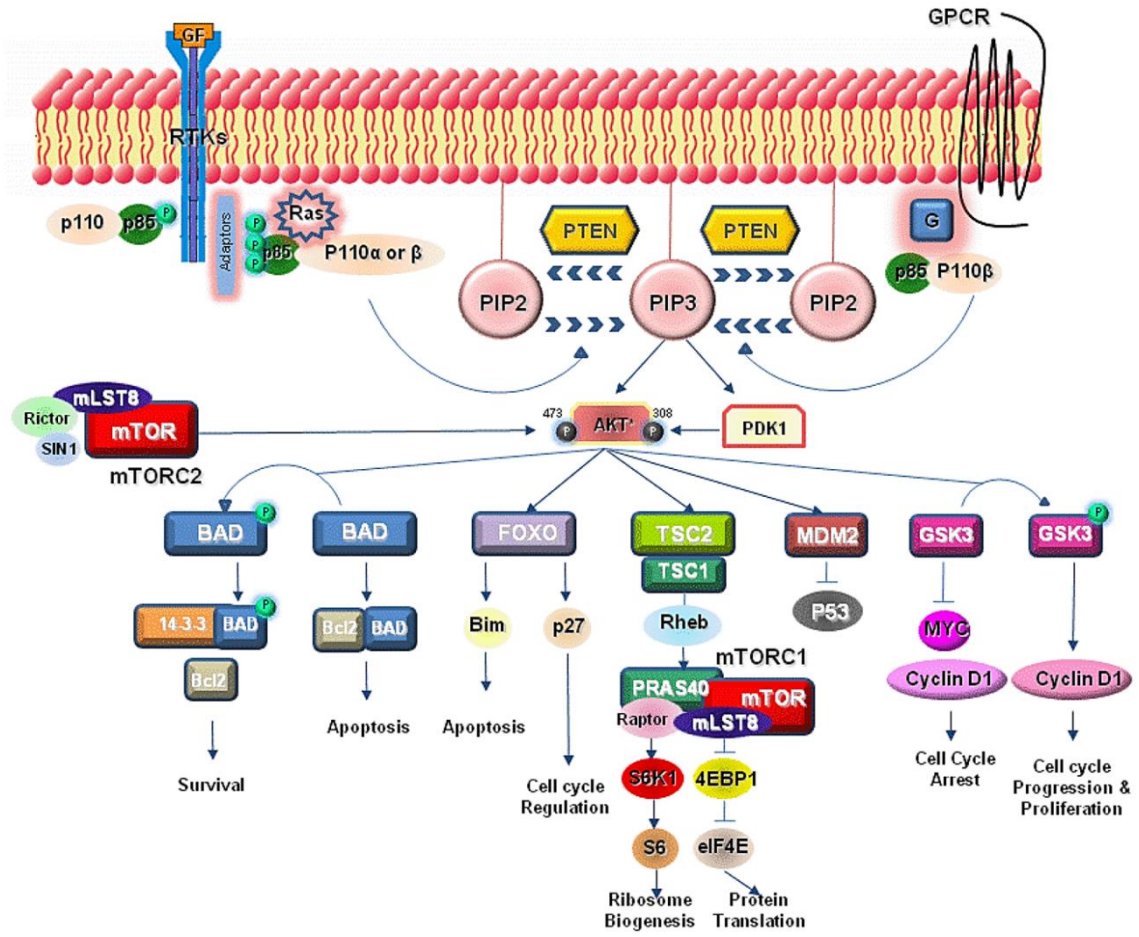

Figure 1.13. AKT kinase signalling.

Upon activation of the PI3K pathway AKT kinase gets phosphorylated at Thr308 by PDK1 and at Ser473 by mTORC2. Fully active AKT phosphorylates multiple downstream substrates including pro-apoptotic proteins BAD and BAX protecting cells from apoptosis, GSK3 which leads to activation of glycogen synthase and cyclin D1. AKT phosphorylates TSC1 and TSC2, tumour suppressors, which are negative regulators of mTORC1 complex leading to increased ribosome biogenesis and protein translation. The main outcomes of AKT activity are increase in survival and proliferation, inhibition of apoptosis and cell cycle progression (Sarris et al., 2012).

1.3.3. mTOR kinase

Mammalian target of rapamycin (mTOR) is a serine-threonine kinase that exists in two distinct intracellular complexes, mTOR complex 1 (mTORC1) and 2 (mTORC2) (Engelman, 2009). Both mTOR complexes have distinct functions and are activated in response to different stimuli (Figure 1.14) (Laplante and Sabatini, 2012).

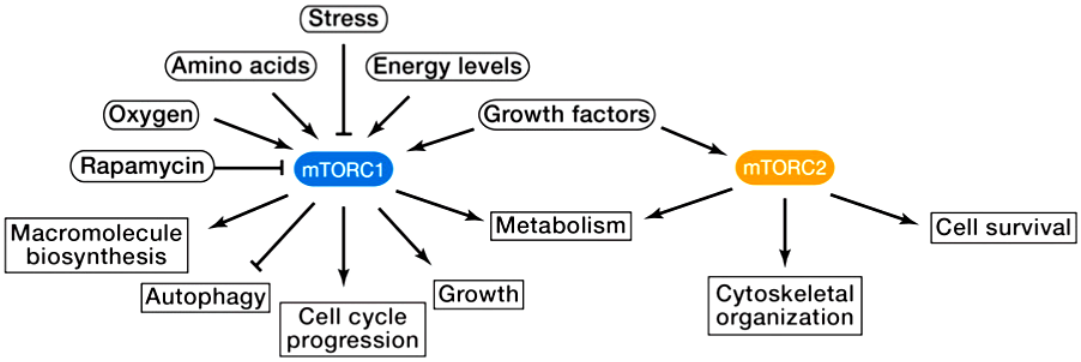

Figure 1.14. Activation and function of mTORC1 and mTORC2.

The mTORC1 responds to a range of intracellular and extracellular signals, including: growth factors, amino acids, stress and energy levels. It controls protein and lipid synthesis and autophagy. mTORC2 is mainly responsive to growth factors and its major function is to regulate cell survival downstream from AKT. Adapted from (Laplante and Sabatini, 2012).

It has been shown that many cancer-promoting lesions activate the mTORC1 pathway (Sabatini, 2006). In response to growth factors and nutrients, mTORC1 regulates cell growth through downstream effectors, such as the regulators of translation, namely eukaryotic translation initiation factor 4E binding protein 1 (4EBP1) and ribosomal S6 kinase 1 (S6K1). Several negative feedback loops have been detected within the PI3K pathway, for example S6K1 represses the PI3K/AKT pathway by inhibiting insulin receptor substrate 1 (IRS1) and 2 (IRS2), therefore an active mTORC1 pathway can suppress PI3K/AKT signalling (Sparks and Guertin, 2010, Sabatini, 2006). S6K1 is also responsible for inhibition of platelet-derived growth factor receptor (PDGFR), which similarly to IRS1 and IRS2 also signals through PI3K, thus creating functionally similar feedback loop (Zhang et al., 2007). Moreover, it has been shown that inhibition of mTORC1 also leads to MAPK pathway activation through a PI3K-dependent feedback loop (Carracedo et al., 2008, Efeyan and Sabatini, 2010). The importance of negative

feedback loops has been demonstrated in clinical trials with rapamycin; it has been shown that mTORC1 inhibitor, rapamycin, increases AKT activation in certain cancers including prostate, breast and colorectal carcinoma (O'Reilly et al., 2006). mTORC1 has been also shown to promote cell growth by inhibition of autophagy and to negatively regulate the biogenesis of lysosomes, which have the ability to degrade a majority of cellular components (Laplante and Sabatini, 2012).

Complex mTORC2 consists of mTOR, GβL, rictor (rapamycin-insensitive companion of mTOR) and mSin1 (mitogen-activated-protein-kinase-associated protein 1) and it has been shown that it directly phosphorylates AKT at serine 473 (Sarbassov et al., 2006b). mTORC2 does not respond to the nutritional status of the cell, but it is activated in response to growth factors such as insulin (Laplante and Sabatini, 2012).

It has been reported by Kremer and colleagues (2006) that the mTOR pathway is activated in advanced prostate cancer. The results of their investigation showed that expression of mTOR signalling markers increased in PIN and prostate cancer in comparison to normal prostate (Kremer et al., 2006). Additionally, it has been shown by Guertin et al (2009) that the development of invasive prostate cancer, induced by PTEN loss in mice requires mTORC2 activity. They have also shown that rictor, which is involved in mTORC2 complex, was required for PC3 cells to form tumours as xenografts (Guertin et al., 2009). These studies emphasise mTORC2's role in promoting tumourigenesis, therefore indicating that mTOR might be a good target for anti-cancer therapy (Laplante and Sabatini, 2012).

1.4. Ras/MEK/ERK pathway

The Ras/MEK/ERK pathway is responsible for regulation of many cellular processes including proliferation, differentiation, development, survival and also apoptosis (Shaul and Seger, 2007). The ability to regulate such variety of cellular processes is achieved through a range of mechanisms directing MEK-ERK signals to appropriate downstream locations. Integration and direction of signals is mediated through changes in subcellular localization, strength and length of signals, interaction with specific scaffolds and presence of multiple members of the pathway cooperating in

transduction of the signals (Shaul and Seger, 2007, Torii et al., 2004, Yoon and Seger, 2006).

The pathway signalling is usually initiated by activation of small G proteins, such as Ras. Transmission of signals continues through recruitment to the plasma membrane and activation of Raf kinases, followed by activation of MAPK/ERK kinases (MEKs) (Wellbrock et al., 2004, Ahn et al., 1991). There are three highly homologous isoforms of MEK kinases: MEK1, its alternatively spliced inactive form MEK1b and MEK2. MEKs are activated by phosphorylation of two serine (Ser) residues in their activation loop (Alessi et al., 1994). However, MEKs' activity is also regulated by additional phosphorylation and dephosphorylation processes. For example phosphorylation of Ser386 of MEK1 (by ERKs) can either inhibit or activate ERKs activity. Downregulation of MEKs activity is achieved by rapid dephosphorylation of phospho-Ser218 (pSer218) and pSer222 by the protein Ser/Thr phosphatase PP2A (Sontag et al., 1993). Activated MEKs phosphorylate the regulatory tyrosine (Tyr) and threonine (Thr) residues the ERK proteins, ERK1 and ERK2, which leads to their activation (Seger et al., 1992). ERK1 and ERK2 proteins are evolutionary conserved products of the two genes erk1 and erk2 (Boulton et al., 1991). The inactivation of ERKs is achieved by dephosphorylation of one or both regulatory Tyr and Thr residues, which can be mediated by either protein Ser/Thr phosphatases such as PP2A, protein Tyr phosphatases or dual specificity phosphatases MAPK phosphatases (MKPs) (Alessi et al., 1995b, Pulido et al., 1998). Additionally, ERKs' activity is also mediated through their involvement in multiple feedback loops including inhibitory phosphorylation of the upstream exchange factor SOS, Rafs and MEKs (Dougherty et al., 2005, Shaul and Seger, 2007). It has been shown that upon stimulation, ERKs phosphorylate large number of substrates, which are localized in cytoplasm and also in the nucleus (Yoon and Seger, 2006). It has also been demonstrated that ERKs phosphorylate and activate several transcription factors including p53, Ets1/2, c-Fos and Elk1 (Shaul and Seger, 2007).

ERK1 and ERK2 are very similar proteins with about 70% similarity between them (Boulton et al., 1991). They are both expressed in all types of tissues, they share cellular localization, substrates and similar activation kinetics, indicating similar functions of the two isoforms (Shaul and Seger, 2007, Boulton et al., 1991). However, it

has been demonstrated that differences exist between ERK1 and ERK2. It has been shown that ERK1 participates in MEKs signalling during G2M phase and ERK2 seems to be essential during the G1 phase of the cell cycle (Shaul and Seger, 2007, Liu et al., 2004). Moreover, ablation of ERK1 has been shown to promote cell proliferation in Ras-dependent proliferation in fibroblasts, whereas ERK2 knockdown has been shown to block this effect, which indicates that ERK1 and ERK2 are not functionally redundant molecules (Vantaggiato et al., 2006).

1.5. Cross-talk between the PI3K/AKT/mTOR and the Ras/MEK/ERK pathway in prostate cancer

The PI3K/AKT/mTOR and the RAS/MEK/ERK pathways are the two most frequently over-activated pathways, with mutated components, that promote cancer progression by increasing survival of the cancer cells (Yuen et al., 2012).

The RAS/MEK/ERK signalling cascade has been shown to be frequently activated in advanced prostate cancer, which is often coordinated with aberrant activity of PI3K/AKT/mTOR signalling (Gioeli et al., 1999, Kinkade et al., 2008). It has been demonstrated that combinatorial inhibition of these pathways inhibits CRPC in *Nkx3.1;Pten* mutant mice (Kinkade et al., 2008).

The PI3K and the ERK pathways are known to interact at multiple points, which can lead to cross-activation or cross-inhibition as well as pathway convergence (Figure 1.15) (Mendoza et al., 2011).

In case of cross-activation, a member of one pathway positively regulates an upstream component of another pathway resulting in increased activity of that pathway. For example, Ras-GTP can directly bind and allosterically activate PI3K; an over-activated ERK can also phosphorylate TSC2 at sites distinct from those phosphorylated by AKT, leading to increased activation of mTORC1 (Rodriguez-Viciana et al., 1994, Zoncu et al., 2011).

Cross-inhibition takes place when a member of one pathway negatively regulates an upstream component of another pathway, thereby inhibiting the other pathway's

signalling. For example, during strong IGF1 stimulation, AKT is able to inhibit ERK activation by phosphorylating inhibitory sites of the regulatory domain of RAF (Zimmermann and Moelling, 1999).

A phenomenon of pathway convergence takes place when members of two or more signalling pathways act directly on the same protein or complex. For example, the AGC kinases, namely RSK, AKT and S6K often phosphorylate the same substrates, which include FOXO3A and c-Myc transcription factors, BAD and GSK3, to promote cell survival, proliferation and motility (Yang et al., 2008, Manning and Cantley, 2007).

Inhibition of only one pathway has proven not to be sufficient for treatment of cancer due to the existence of feedback loops and cross-talk between pathways (Grant, 2008, Turke et al., 2012, Yuen et al., 2012). Single agent inhibition of PI3K or MEK kinase in tumours driven by activated or amplified RTKs results in a compensatory increase in activity of ERK or AKT, respectively (Turke et al., 2012). Therefore a combined targeting of the PI3K/AKT/mTOR and the Ras/MEK/ERK pathways has been proposed as an alternative approach to target tumour cells, in a range of different cancers, including multiple myeloma (MM), melanoma and prostate cancer (Steinbrunn et al., 2012, Gioeli et al., 2011, Kinkade et al., 2008).

In multiple myeloma inhibition of the PI3K pathway alone was shown to induce apoptosis in cell lines and in primary MM samples. However, a combined blockade of PI3K and MAPK pathway resulted in significantly enhanced cell death in the majority of primary samples (Steinbrunn et al., 2012). Moreover, combination of the mTOR inhibitor, rapamycin and MEK inhibitor, PD325901, induced growth inhibition of androgen-responsive (CWR22Rv1 and CASP 2.1) and androgen-independent (CASP 1.1) prostate cancer cell lines (Kinkade et al., 2008, Gioeli et al., 2011).

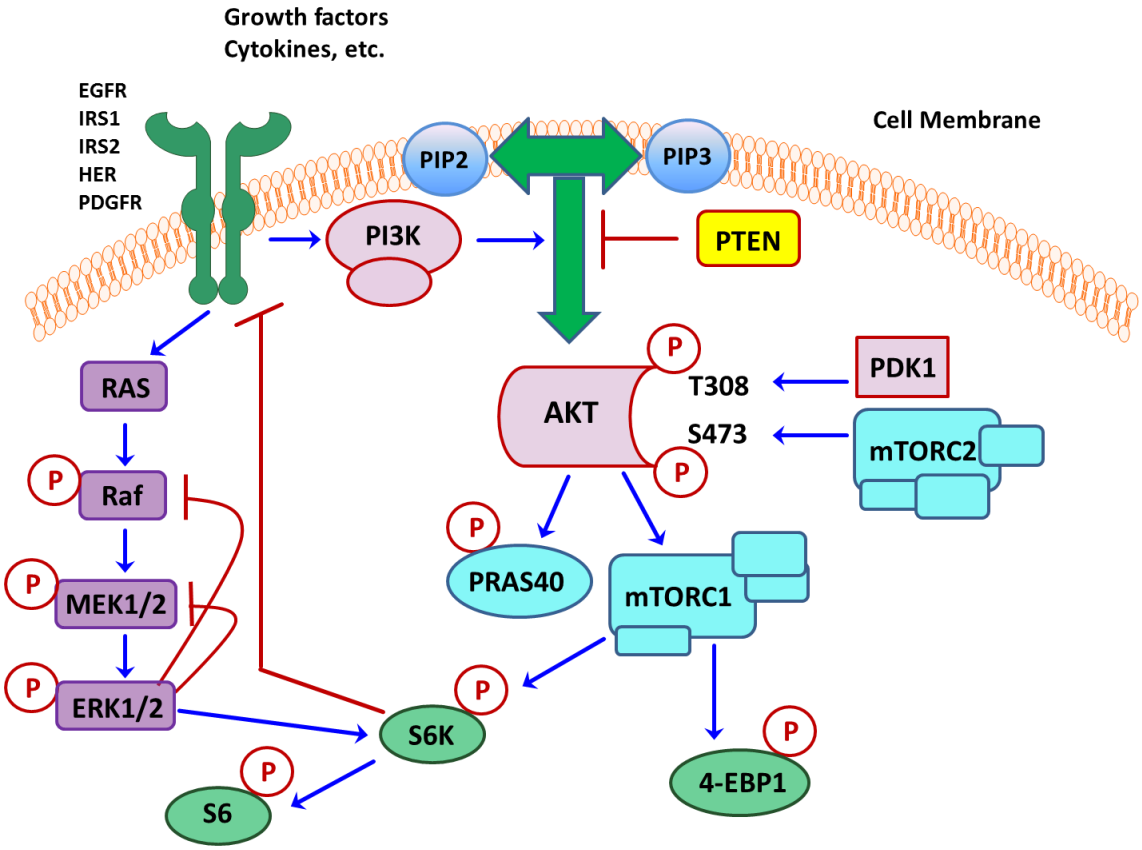

Figure 1.15. The PI3K/AKT/mTOR and Ras/MEK/ERK pathways interactions.

Activated receptor tyrosine kinases (RTKs) recruit and activate PI3K, which leads to membrane recruitment and activation of PDK1 and AKT. PDK1 together with mTORC2 phosphorylate AKT, which in turn triggers a downstream cascade of phosphorylation events. The mammalian target of rapamycin is present in two distinct complexes: mTORC1 and mTORC2. Activated RTKs can also activate Ras and subsequently Raf, MEK1/2 and ERK1/2. ERK1/2 can in turn phosphorylate a number of transcription factors and other signalling proteins leading to increased cell survival. Inhibition of mTORC1, and subsequently S6K, can lead to a relief of inhibitory activity of S6K on RTKs therefore increasing signalling through PI3K or Ras.

1.6. Development of the PI3K/AKT/mTOR and the Ras/MEK/ERK pathway inhibitors

The main negative regulator of PI3 kinase activity is the tumour suppressor PTEN, which dephosphorylates PIP_3 to PIP_2. In advanced prostate cancer, PTEN is frequently lost and therefore the PI3K signalling pathway becomes over-activated. The first generation of pan-PI3K inhibitors: LY294002 and wortmannin, which inhibit the p110 catalytic subunit, were shown to be active in prostate cancer cell lines. However, because of their high toxicity and poor pharmaceutical properties they have been restricted to preclinical studies (Yap et al., 2008). Treatment of LNCaP, PC3 and DU145 cells with LY294002 caused cell cycle arrest, decreased invasive properties and sensitized the cells to radiation (Shukla et al., 2007, Gottschalk et al., 2005). Wortmannin, which is a fungicide originally isolated from soil, is an irreversible inhibitor of PI3K (Powis et al., 1994). It has been demonstrated that treatment of LNCaP and PC3 cells decreased phospho-AKT levels, and also induced apoptosis and radiosensitized DU145 cells (Lin et al., 1999, Seol et al., 2005).

1.6.1.1. AKT kinase inhibitors

AKT kinase phosphorylates up to 100 substrates and is involved in regulating many cellular processes, such as proliferation (by inhibition of GSK3 and p27), apoptosis (by inhibiting of FOXO proteins and pro-apoptotic proteins BAD and MDM2), metabolism and survival (Crowell et al., 2007, Carracedo and Pandolfi, 2008). AKT-specific inhibitors include:

- agents that target plekstrin homology domain

- the ATP-binding pocket molecules

- allosteric inhibitors

- pseudosubstrates (Crowell et al., 2007)

Perifosine is a plekstrin homology domain inhibitor, which has been shown to inhibit growth and induce cell cycle arrest of PC3 cells and also differentiation of PC3 and

LNCaP cells through activation of the GSK3β pathway (Floryk and Thompson, 2008). GSK690693 is an example of an ATP competitive kinase domain inhibitor, which prevents substrate phosphorylation by AKT. It has been demonstrated that GSK690693 inhibits proliferation of PC3 and DU145 cells *in vitro* and also inhibits growth of LNCaP tumours *in vivo* (Rhodes et al., 2008). However, due to lack of oral bioavailability it was withdrawn from development in phase I trials. MK-2206 is an allosteric inhibitor of AKT that binds to the region, which interacts with the PH and kinase domains, and prevents translocation of AKT to the cell membrane and its activation. It has been shown that MK-2206 in combination with RTK inhibitors (erlotinib and lapatinib) inhibited cell proliferation in breast cancer cell lines and caused tumour regression in xenograft models of breast and ovarian cancer (Hirai et al., 2010). Moreover, a combination of MK-2206 with different chemotherapeutic agents such as topoisomerase inhibitors (doxorubicin, camptothecin), antimetabolites (gemcitabine, 5-fluorouracil), anti-microtubule agents (docetaxel) and DNA cross-linker (carboplatin) resulted in induction of apoptosis and reduced levels of phospho-S6 in breast cancer cell line HCC70 (Hirai et al., 2010).

1.6.1.2. mTOR kinase inhibitors

The first generation of mTOR inhibitors are derivatives of rapamycin – "rapalogs" that specifically inhibit the mTORC1 complex, examples include RAD001 (everolimus), CCI-779 (temsirolimus) and ridaforolimus (Meric-Bernstam and Gonzalez-Angulo, 2009). The mechanism of action of rapamycin involves FK506-binding protein (FKBP12) which targets the FKBP12-rapamycin-binding domain adjacent to the catalytic site of the mTOR protein (Choi et al., 1996). A number of studies have shown that mTORC2 is rapamycin insensitive, however, it has also been shown that long-term exposure to rapamycin can also inhibit mTORC2 and that it is tissue specific (Sarbassov et al., 2006a). Rapamycin treatment decreased levels of phosphorylated substrates of mTOR (S6K and 4EBP1) and also induced cell cycle arrest in PC3 and DU145 cells (Gao et al., 2003). It has been demonstrated that temsirolimus and everolimus both inhibited the growth of PC3 and DU145 cells in a dose-dependent manner *in vitro,* and reduced tumour volumes in PC3 and DU145 xenografts (Wu et al., 2005).

The second generation of mTOR inhibitors targeting the ATP site of the kinase domain of mTOR, are able to block both mTORC1 and mTORC2 complexes (Vilar et al., 2011). Some of these second generation compounds have dual activity against PI3K and mTOR, which is due to the fact that their catalytic domains are structurally similar (Courtney et al., 2010). Dual PI3K-mTOR inhibitors disable both inputs to AKT: PI3K-PDK1 and mTORC2, and may bypass feedback loops. An example of dual PI3K-mTOR inhibitors is NVP-BEZ235. NVP-BEZ235 has been shown to reversibly block the p110α catalytic subunit of PI3K and mTOR (Maira et al., 2008). Treatment with NVP-BEZ125 has resulted in a significant decrease in phosphorylation levels of mTORC1 substrates, S6K1 and 4E-BP1, and mTORC2 target AKT, and higher antiproliferative effect than everolimus in BT474 breast cancer cells and in xenografts derived from them (Serra et al., 2008). However, this broad inhibition can also be toxic to normal cells (Janes et al., 2010).

1.6.1.3. MEK inhibitors

A number of MEK inhibitors have been developed and are currently being tested for the treatment of cancer (clinicaltrials.gov). Both MEK1 and MEK2 have unique inhibitor binding sites located on a hydrophobic pocket adjacent to the ATP-binding site, which allows a design of highly specific compounds (Ohren et al., 2004). Additionally, specific targeting of MEK1/2 is possible due to the fact that ERK1 and ERK2 are the only well-described downstream targets (Chappell et al., 2011).

The first MEK inhibitor to enter clinical trials was PD-184352. However, despite being able to inhibit phospho-ERK in patients, phase II clinical trials performed on patients with wide range of solid tumours did not show expected efficacy, which was probably due to its high metabolism (Sebolt-Leopold, 2008). An improved MEK inhibitor, PD0325901, showed higher bioavailability and increased potency against MEK as well as greater metabolic stability (Sebolt-Leopold, 2008, McCubrey et al., 2012a).

Selumetinib (AZD6244) has been shown to be a potent, selective and ATP-uncompetitive inhibitor of MEK1/2 kinases (Davies et al., 2007). It has been suggested that binding of the AZD6244 inhibitor may lock MEK1/2 kinases in an inactive

conformation, which would not prevent binding of ATP and substrate. However, it has been confirmed that despite increased phospho-MEK1/2 levels, the activity of ERK remained at comparable level to vehicle control (Davies et al., 2007).

It has been shown that MEK1/2 inhibitor, AZD6244, induced G1/S cell cycle arrest in colon and melanoma cell lines and also increased caspase-3 and caspase-7 expression (McCubrey et al., 2012a). Importantly, it has been demonstrated that AZD6244 showed higher efficiency in suppressing the tumour growth of pancreatic cancer in immunocompromised mice than standard chemotherapeutic drug, gemcitabine. However, once the treatment was discontinued, the tumours reappeared (McCubrey et al., 2012b).

1.6.2. Preclinical assessment of the candidate compounds

The development of successful treatment strategy for advanced prostate cancer has been challenging due to heterogeneity of the disease. A large number of prospective therapeutics are currently being tested in clinical trials. However, in order to identify and validate an effective drug, relevant preclinical models of prostate cancer are needed (De Velasco and Uemura, 2012).

A combined approach of cell culture *in vitro* and animal studies is essential in predicting the efficacy of novel anti-cancer treatments in human clinical trials (HogenEsch and Nikitin, 2012). The use of well characterised cell lines enables determination of the efficacy, pharmacodynamics and mechanism of action of novel drugs in highly controlled, reproducible conditions. However, it has been demonstrated in a number of studies that gene expression and DNA methylation patterns in cancer cell lines are significantly different from human primary tumours and xenografts derived from them (Houshdaran et al., 2010, Hennessey et al., 2011).

It has been reported by pharmaceutical companies that less than 1% of drugs entering drug development process succeeds in achieving drug approval (Kola and Landis, 2004, De Velasco and Uemura, 2012). The drug development process (Figure 1.16) consists of:

- Drug research
- Preclinical assessment based on cell cultures and animal studies
- Clinical trials:
    - Phase I, healthy volunteers
    - Phase II, determining drug safety and dosing in patients
    - Phase III, testing efficacy and adverse events in patients
- Evaluation and approval
- Phase IV studies

The process of drug approval takes on average 12 years and costs over 1 billion pounds. The most common reason for drug failure is lack of efficacy in Phase II and Phase III trials, which has been attributed to unpredictable preclinical models (De Velasco and Uemura, 2012, Suggitt and Bibby, 2005).

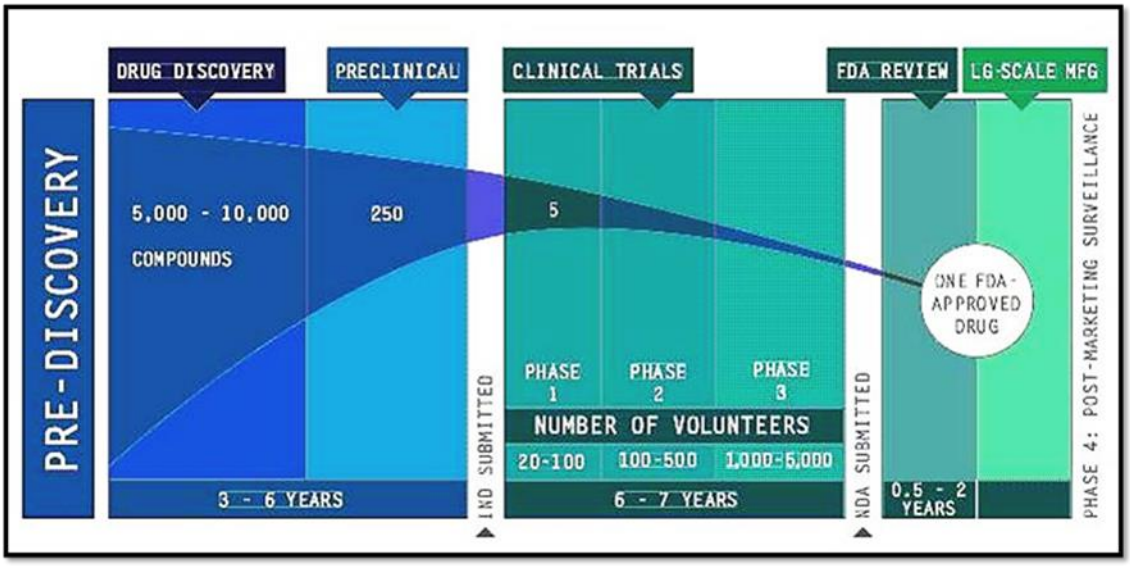

Figure 1.16. Drug development process.

A schematic representation of an approval process of a new drug. Taken from (http://venture-pharmaceuticals.com/what-is-drug-development/olddrugs2/).

1.7. Compounds used in this study

The inhibitors used in this study include AKT inhibitor AZD7328 (AKTi), mTOR inhibitor Ku-0063794 (mTORi), MEK1/2 inhibitor AZD6244 (MEKi) and an additional MEK1/2 inhibitor RO-5126766 (RO-512). AKT and mTOR inhibitors are pro-compounds, which have not been tested in the clinical trials. Whereas, both MEK1/2 inhibitors are currently undergoing clinical assessment in either Phase I (RO-512) or Phase II (MEKi).

Table 1.2. A list of inhibitors used in this study.

Compound	Target	Type of inhibition	Clinical Trial	References
AKT inhibitor AZD7328	AKT1 AKT2 AKT3	ATP-competitive	N/A	(Dickstein et al., 2012)
mTOR inhibitor Ku-0063794	mTORC1 mTORC2	ATP-competitive	N/A	(Garcia-Martinez et al., 2009)
MEK1/2 inhibitor AZD6244	MEK1 MEK2	Non-ATP competitive	Currently in Phase II	(Davies et al., 2007)
MEK1/2 inhibitor RO-5126766	MEK1 MEK2	Non-ATP competitive	Phase I study completed	(Ishii et al., 2013)

1.8. Aims of research

There is no effective cure for advanced prostate cancer. Current treatment strategies based on androgen deprivation therapy and chemotherapy fail in the majority of prostate cancer patients. Therefore, there is an urgent need for new therapeutic approaches. A number of studies have demonstrated that the PI3K/AKT/mTOR signalling pathway is over-activated in advanced prostate cancer and its activity is correlated to enhanced tumour growth and emergence of castration resistant prostate cancer (CRPC) (Kinkade et al., 2008, McMenamin et al., 1999). Therefore targeting of the pathway might be an effective treatment for patients with advanced prostate cancer and potentially for patients with CRPC.

The main aim of this project was to investigate the PI3K/AKT/mTOR signalling in prostate cancer and to determine the effect of novel small molecule inhibitors on the signal transduction within the pathway.

The objectives of the research were to:

- determine the PI3K/AKT/mTOR pathway activity in prostate cell lines in comparison to clinical tumour samples from prostate cancer patients

- explore the effect of inhibition of AKT and mTOR kinase on proximal and distal signalling molecules of the pathway in prostate cell lines and in primary prostate cultures

- determine cell fate of cancer stem-like cells following therapeutic intervention in primary tumour cultures

- investigate the role of the PI3K/AKT/mTOR pathway activity on tumour outgrowth and tumour initiation frequency using 'near-patient' xenograft models of prostate cancer

Chapter 2

Materials and methods

2. MATERIALS AND METHODS

2.1. Mammalian cell culture

2.1.1. Maintenance of cell lines

Human prostate cell lines used in the experiments included: BPH1, P4E6, LNCaP and PC3 cells (Table 2.1). All cell lines were purchased from American Type Culture Collection (ATCC, USA), or the European Collection of Animal Cell Culture (ECACC, UK), except for P4E6, which were derived in our laboratory (Maitland et al., 2001). BPH1 and LNCaP cells were cultured in Roswell Park Memorial Institute-1640 (RPMI) (Invitrogen) supplemented with 5% or 10% Foetal Calf Serum (FCS) (PAA), respectively, and 2 mM L-Glutamine (Invitrogen). PC3 cells were cultured in Ham's F-12 medium (Lorza) supplemented with 7% FCS and 2 mM L-Glutamine. P4E6 cells were cultured in Keratinocyte Serum-Free Medium (KSFM) (Invitrogen) supplemented with 2% FCS, 2 mM L-Glutamine, 5 ng/ml Epidermal Growth Factor (EGF), 50 µg/ml bovine pituitary extract (Invitrogen). All cell lines were cultured in T25 or T75 cell culture flasks (Corning) at 37°C in 5 % CO_2.

Table 2.1. Human prostate cell lines.

Cell line	Description	Growth medium	Reference
BPH1	Derived from Human benign prostate hyperplasia immortalised with SV-40	RPMI + 5% FCS	(Hayward et al., 1995)
P4E6	Human prostatic cell line derived from early stage, well differentiated prostate cancer; Immortalised with retrovirus HPV16 E6	KSFM + 2% FCS	(Maitland et al., 2001)
LNCaP	Androgen-dependent human prostate cancer cell line, derived from lymph node metastasis	RPMI + 10% FCS	(Horoszewicz et al., 1983)
PC3	Androgen-independent human prostate cancer cell line, derived from bone metastasis	HAMS F12 + 7% FCS	(Kaighn et al., 1979)

2.1.2. Isolation and culture of primary epithelial cells

Prostate tissue was obtained from patients undergoing radical prostatectomy or transurethral resection of the prostate, with informed patient consent and approval from the York Research Ethics Committee. All patient samples were anonymized.

Patient tissues were chopped with a disposable scalpel (Swann Morton) and digested with 200 IU/mg collagenase (Lorne Laboratories) dissolved in 2.5 ml Keratinocyte Serum-Free Medium (KSFM with 5 ng/ml human EGF and 50 µg/ml bovine pituitary extract supplements (Invitrogen)) and 5 ml Roswell Park Memorial Institute-1640 medium (RPMI, Invitrogen), supplemented with 100 IU/ml antibiotic/antimycotic solution containing 100 IU/ml Penicillin, 100 µg/ml Streptomycin, and 0.25 µg/ml Fungizone (ABM, Invitrogen) and 2 mM L-Glutamine (Invitrogen) overnight at 37°C, with shaking at 80 RPM. The digested tissue was then triturated by passing through a 5 ml pipette and 21G blunt needle (Kendall Tyco Healthcare) and centrifuged at 2000 RPM for 10 min to sediment cells. Two washing steps with PBS were performed to wash out the collagenase; the supernatant was removed, 10 ml PBS was added, the cell pellet was re-centrifuged at 2000 RPM for 10 min and the procedure repeated. Organoids were separated from the stromal cells by differential centrifugation at 800 RPM for 1 minute. The pellet consisting of the acini-containing epithelial cells were treated with 5 ml 0.05% trypsin-EDTA for 30 min at 37°C in an orbital shaker at 80 RPM. Trypsin-EDTA was inactivated with R10 medium, and epithelial cells centrifuged at 1500 RPM for 3 min.

2.1.2.1. Isolation of subpopulations from primary prostate epithelial cells

Primary prostate epithelial cultures were grown on collagen I-coated plates and then harvested using 0.05% trypsin-EDTA. Collagen I-coated 10 cm dishes were blocked with 0.3% bovine serum albumin (BSA) in PBS, (denatured by heating at 80°C for 5 minutes) for 1 hour at 37°C before the cell suspension was added. To isolate CB cells ($40min^{+}$

fraction) a suspension of cells was incubated (on the blocked plates) for 40 minutes at 37°C and the non-adherent cells collected by washing the plates with PBS. The adherent cells (stem cells and TA cells) were collected by 0.05% trypsin-EDTA. Trypsin was neutralized with R10 or D10 medium, and the suspension of cells was washed in PBS before resuspending in stem cell medium. Stem cells were then isolated by selecting for CD133 by MACS cell sorting according to the manufacturer's instructions (Miltenyi Biotec). Briefly, the cells were resuspended in 300 µl magnetic-activated cell sorting (MACS) buffer (2 mM EDTA, 0.5% (v/v) FCS in PBS), 100 µL FcR blocking reagent (Miltenyi Biotec) and 100 µL CD133 beads (Miltenyi Biotec) at 4°C for 30 min. Cells were then washed with MACS buffer, centrifuged at 1500 RPM for 5 minutes, resuspended in 500 µl MACS buffer and added to a pre-prepared MS column. The column was washed three times with 3 ml MACS buffer to collect the $CD133^-$ fraction, followed by collection of $CD133^+$ cells which were eluted from the beads with a plunger. To increase the purity of the $CD133^+$ population from 70-75% to 95%, the procedure was repeated by passing the CD133+ cells over a second MS column. Three populations of cells were isolated: $\alpha_2\beta_1^{low}$ cells (committed basal), $\alpha_2\beta_1^{high}$ $CD133^-$ (transit amplifying) and $\alpha_2\beta_1^{high}$ $CD133^+$ (stem cells) and resuspended in SCM for further use.

2.1.3. Preparation of feeder cells by Irradiation

Mouse STO fibroblasts were trypsinized and centrifuged at 1500 RPM for 3 minutes, they were then resuspended in 10 ml SCM per 100 cm^2 of culture surface and treated with a radiation dose of 60 Gy. Radiation-inactivated STO cells were resuspended in KSFM medium (with 5 ng/ml human EGF and 50 µg/ml bovine pituitary extract supplements) (Invitrogen) and stored at 4°C for up to 5 days before use. This procedure was routinely performed by Mrs. Caty Hyde.

2.1.4. Determination of live cell number using a haemocytometer

Trypan Blue exclusion was used to determine viable cells by adding 0.4% Trypan Blue Stain (Sigma) to a suspension of cells in a 1:1 ratio. Total cell number (blue and non-stained cells) and live cell number (non-stained cells) were counted using a haemocytometer (Neubauer).

2.1.5. Determination of viable cell number using the Vi-Cell cell viability analyser

Trypsinized cells were centrifuged at 1500 RPM for 3 minutes and cell pellets were resuspended in 500 µl PBS and analysed on a Vi-Cell Cell Viability Analyser (Beckman Coulter). The average number of total and viable cells was determined from 50 images.

2.1.6. Determination of proliferation using MTS assay

The CellTiter 96 AQ_{ueous} Non-Radioactive Cell Proliferation Assay (Promega) was used to determine changes in the proliferation of viable cells following treatment. Cells were seeded onto 24-well plates and once plated (24 hours later) an MTS reagent (tetrazolium compound [3-(4,5-dimethylthiazol-2-yl)-5-(3-carboxymethoxyphenyl)-2-(4-sulfophenyl)-2H-tetrazolium, inner salt) was added at 70 µl per well, where it was then bioreduced by cells into a formazan product during a 2-hour incubation at 37°C at 5% CO_2. The absorbance of the formazan was measured at 490 nm directly from the plates on the microplate reader POLARstar Optima (BMG Labtech). The quantity of formazan product is directly proportional to the number of living cells in culture.

2.2. Transfection of cell lines with siRNA

DharmaFECT 2 transfection reagent (Thermo Scientific) was used to transfect cell lines with scrambled (Ambion, ID:4390843), PTEN (Cell Signaling Technology, #6538) and GAPDH-Cy3 conjugated siRNA (Life Technologies, ID:AM4649). BPH1 and P4E6 cells were seeded onto 6-well plates 24 hours prior to transfection. A 50 µM working stock

siRNA solution was prepared in RNase-free double distilled water (ddH_2O). In separate tubes siRNA (tube 1) and DharmaFECT 2 (tube 2) were diluted into OptiMEM reduced serum medium (Fisher Scientific Ltd) in a polystyrene tube, gently pipetted to mix and incubated at room temperature for 5 min. Tubes 1 and 2 were combined, gently mixed by pipetting and incubated at room temperature for 20 min. R10 (BPH1) or K2 (P4E6) culture medium was added to the mix and the mixture was added to the cells. The final concentration of siRNA was 20 nM. The cells were incubated with siRNA solution for 72 h and 96 h, and then they were collected for mRNA and protein analysis.

2.3. Treatment of mammalian cells with inhibitors

2.3.1. Treatment of cell lines with AKT and mTOR inhibitors

Cell lines were seeded onto 6-well plates or 10 cm dishes 24 hours prior to treatment. Cells were treated with increasing concentrations (0.01 µM to 50 µM) of AKT and mTOR inhibitors dissolved in dimethyl sulfoxide (DMSO) either alone or in combination for up to 72 hours. The vehicle control was made up in DMSO and did not exceed 0.5%.

2.3.2. Treatment of primary cultures with AKT, mTOR and MEK inhibitors

Primary cells were seeded onto collagen I-coated 10 cm dishes, 24 hours prior to treatment. Cells were treated with increasing concentrations (0.1 µM to 50 µM) of AKT, mTOR or MEK inhibitors either alone or in combination: AKT + MEK and AKT + mTOR for up to 72 hours. Control cells were treated with DMSO, as above.

2.4. Isolation and analysis of cell RNA

2.4.1. RNA extraction

RNA extraction was performed using RNeasy Mini kit (Qiagen) according to the manufacturer's protocol. Cells were resuspended in 350 µl RTL buffer and the lysate

was added onto a Shredder column and centrifuged at 13 000 RPM for 2 minutes to remove cell debris. An equal volume of 70% ethanol was added to the flow through and the suspension was added to a binding column. RNA was eluted from the binding column by washing three times with RNase-free water. RNA concentration was measured using a Nanodrop spectrophotometer and the RNA stored at -80°C.

2.4.2. cDNA synthesis

Total RNA (~1 µg) was reverse transcribed using 1 µl RNase OUT (Invitrogen) and 1 µl Oligo $(dT)_{12-18}$ (Invitrogen) in a total volume of 9.5 µl and heated to 70°C for 10 min. The Reaction mix, consisting of 4 µl, 5 x First strand buffer (Invitrogen), 2 µl of 0.1 M DTT (Invitrogen), 2 µl of 10 mM dNTPs (Invitrogen), 0.5 µl RNase OUT and 1 µl of Superscript II enzyme (Invitrogen), was added to the mixture and incubated at 45°C for 2 hours. Complementary DNA (cDNA) was purified by ethanol (EtOH) precipitation, by the addition of 15 µl of 3 M NaCl and 120 µl of 100% EtOH and stored at -80°C, for 30 min. Samples were centrifuged at 13,000 RPM for 10 min in a benchtop centrifuge and the supernatant removed. The pelleted cDNA was washed in 100 µl of 70% EtOH and re-centrifuged at 13,000 RPM for 5 min. The supernatant was removed; the pellet was dried and then resuspended in 30 µl DEPC-treated ddH_2O. Synthesized cDNA was stored at -20°C.

2.4.3. Reverse Transcription polymerase chain reaction (RT-PCR)

Reverse transcription polymerase chain reaction (RT-PCR) was performed using a 1 in 10 dilution of cDNA synthesized using the method described in section 2.4.2. PTEN primers, forward: 5' GAGGATGGATTCGACTTAGA 3' and reverse: 5' CCTTTTTGTCTCTGGTCCTTAC 3', flanking the region between exon 1 and 5 of the PTEN coding sequence were previously described in (Sharrard and Maitland, 2007). cDNA was added to a PCR reaction mix containing: 2.5 µl 10 µM forward and reverse primers, 1.5 µl 25 mM $MgCl_2$ (Promega), 0.2 µl 25 mM dNTPs, 5 µl 5 x Go Taq Buffer (Promega), 0.2 µl 5 U/µl GoTaq polymerase (Promega). cDNA integrity was confirmed

using GAPDH primers, forward: 5' CCTCCCGCTTCGCTCTCT 3' and reverse: 5' GCTGGCGACGCAAAAGA 3'. The standard PCR programme was used:

94°C for 2 minutes

94°C for 30 seconds
60°C for 30 seconds
72°C for 30 seconds
} 25 cycles

72°C for 2 minutes

The reaction was carried out using a GeneAmp PCR System 9700 thermal cycler (Applied Biosystems).

PCR products were visualized on a 1% (w/v) agarose (Invitrogen) gel together with a 100 base pair (bp) marker (Invitrogen) to assess product sizes using GeneGenious UV transilluminator (Syngene).

2.4.4. Quantitative RT- PCR (qRT-PCR)

RNA was extracted from cells as described in section 2.4.1. and cDNA synthesis was performed as described in section 2.4.3. Quantitative RT-PCR was performed in a total volume of 20 µl per well using 2 µl 1 in 10 dilution cDNA, 1 x TaqMan PCR mastermix (AB Applied Biosystems), 1 x TaqMan gene expression assay (AB Applied Biosystems). Samples were run in triplicate on a C1000 Thermal Cycler (CFX96 Real Time System, Biorad). Gene expression levels were normalized to the housekeeping gene human ribosomal protein, large, P0 (RPLP0).

2.5. Protein expression analysis

2.5.1. SDS-PAGE and Western blotting

2.5.1.1. Preparation of whole cell lysates

Adherent and non-adherent cells were harvested, centrifuged at 1500 RPM for 3 minutes and resuspended in 120 µl Cytobuster protein extraction reagent (Novagen) with the addition of protease inhibitor cocktail (Roche) and phosphatase inhibitor cocktail (Roche). The cells were incubated at room temperature for 5 minutes, then centrifuged at 13 000 RPM for 5 minutes and the supernatant was collected and stored at -80°C for further analysis.

2.5.1.2. Determination of protein concentration using the Bicinchoninic acid (BCA) assay

Whole cell protein lysates were quantified using the Bicinchoninic acid assay (BCA) protein assay kit (Thermo Scientific), according to manufacturer's instructions. Briefly, 10 µl of BSA standards, or unknown samples, were pipetted in triplicate into a 96 well plate. 200 µl working reagent was added to each well, and the plate was incubated at 37°C for 30 min. The absorbance was read at 562 nm on a POLARstar OPTIMA microplate reader (BMG Labtech). A standard curve of BSA samples was prepared to determine the protein concentration of the test samples.

2.5.1.3. SDS-PAGE gel electrophoresis

20 µg protein lysate (in a volume of 30 µl) was added to 4 x SDS loading buffer (10% (v/v) glycerol, 62.5 mM Tris-HCl pH 6.8, 1% (w/v) SDS, 65 mM DTT and bromophenol blue to colour), and heated to 100°C for 10 min in a Grant QBD2 heating block (Grant). The samples were then centrifuged for 15 seconds to collect the contents. Samples were loaded onto 10% Tris-SDS acrylamide gels using the mini-PROTEAN Tetra Cell system (Biorad). Precision plus kaleidoscope (Biorad) and biotinylated (Cell Signaling Technology) protein markers were used to determine molecular weights of the separated proteins. Gels were run at 80 volts (V) for approximately 2 hours in SDS running buffer (25 mM Tris, 0.19 M Glycine, 3.5 mM SDS).

2.5.1.4. Western blotting

Resolved proteins were immediately transferred onto Immobilon-P membrane (Millipore) pre-treated with methanol at 60 V for 2 hours (or 40 V overnight at 4°C) in transfer buffer (48 mM Tris, 39 mM Glycine, 10% (v/v) Methanol). Membranes were air-dried for storage, re-wet using methanol and washed three times with 0.1% Tris-buffered saline – Tween 20 (TBS-T: 150 mM NaCl, 50 mM Tris/HCl, pH 7.5, 0.1% (v/v) Tween20). Membranes were then blocked with 10% blocking reagent (Roche) prepared in TBS-T for 1 hour at room temperature, followed by incubation with primary antibodies (Table 2.2) at 4°C for 2 hours or overnight. Membranes were washed three times with TBS-T, then blocked with 10% blocking reagent for 30 minutes, followed by incubation with peroxide-labelled secondary antibodies for 1 hour at room temperature. Membranes were washed three times with TBS-T and chemiluminescent detection was performed using the BM Chemiluminescence Blotting Substrate (POD) system (Roche). Labelled proteins were visualised using ECL Hyperfilm (Amersham) and manually processed using Kodak GBX developer and fixer solutions (SLS).

Table 2.2. List of antibodies used in western blotting experiments.

Antibody	Clone	Species/ Isotype	Working dilution	Manufacturer	Catalogue number
AKT (pan)	C67E7	Rabbit IgG	1:1000	Cell Signaling Technology	4691
Phospho-AKT (Thr308)	C31E5E	Rabbit IgG	1:1000	Cell Signaling Technology	2965
Phospho-AKT (Ser473)	D9E XP™	Rabbit IgG	1:2000	Cell Signaling Technology	4060
Cleaved caspase – 3 (Asp175)	N/A	Rabbit polyclonal	1:1000	Cell Signaling Technology	9661
Cleaved PARP (Asp214)	N/A	Rabbit polyclonal	1:1000	Cell Signaling Technology	9541
4E-BP1	N/A	Rabbit polyclonal	1:1000	Cell Signaling Technology	9452
Phospho-4E-BP1 (Thr37/46)	236B4	Rabbit IgG	1:1000	Cell Signaling Technology	2855
LC3 B	N/A	Rabbit polyclonal	1:3000	abcam	ab51520
p44/42 MAPK (ERK 1/2)	137F5	Rabbit IgG	1:1000	Cell Signaling Technology	4695
Phospho-p44/42 MAPK (ERK 1/2) (Thr202/Tyr204)	D13.14.4E XP™	Rabbit IgG	1:2000	Cell Signaling Technology	4370
PRAS40	D23C7 XP™	Rabbit IgG	1:1000	Cell Signaling Technology	2691

Phospho-PRAS40 (Thr246)	C77D7	Rabbit IgG	1:1000	Cell Signaling Technology	2997
PTEN	D4.3 XP™	Rabbit IgG	1:1000	Cell Signaling Technology	9188
S6 Ribosomal Protein	5G10	Rabbit IgG	1:1000	Cell Signaling Technology	2217
Phospho-S6 Ribosomal Protein (Ser235/236)	N/A	Rabbit polyclonal	1:1000	Cell Signaling Technology	2211
β – actin	AC-40	Mouse IgG	1:5000	Sigma	A4700
Anti-rabbit IgG HRP linked	N/A	N/A	1:5000	Cell Signaling Technology	7074
Sheep – anti – mouse IgG POD	N/A	N/A	1:5000	Boehringer	1500686

2.5.1.5. Stripping western blots

The membranes were stripped in stripping buffer (20 mM Tris-HCl pH 6.8, 0.1% (w/v) SDS and 20 mM DTT) for 30 min at 55°C, with shaking and washed three times in 0.1% TBS-T. The membranes were blocked and re-stained, as detailed above, with β-actin antibody as an internal control to ensure equal loading of protein and to obtain quantitative protein expression intensities using Image J software (National Institutes of Health, http://rsbweb.nih.gov/ij/).

2.5.2. Flow cytometry

2.5.2.1. Detection of intracellular antigens

For detection of intracellular antigens either primary prostate cells or tumour cells from xenografts were used. Primary cells were harvested after treatment with the inhibitors using 0.05% Trypsin-EDTA and tumour xenografts were firstly depleted of mouse cells using the method described in section 3.1.3.1. Harvested cells were washed once with MACS buffer and stained with 1:1000 LIVE/DEAD Fixable Violet Dead Cell Stain (Invitrogen, L34955) for 15 to 30 minutes at 4°C. Cells were then fixed in 4% PFA (w/v) for 10 minutes at 37°C followed by permeabilisation with ice-cold 100% Methanol while vortexing to prevent clustering of cells. After 30 minutes' incubation on ice, cells were washed with 0.5% BSA, centrifuged at 1500 RPM for 3 minutes and then labelled with primary antibodies (Table 2.3) for 1 hour at room temperature. Cells were then washed with 0.5% BSA and incubated with secondary antibody for 30 minutes at room temperature. Following staining, cells were washed once with MACS buffer, resuspended in 1 ml and analysed on the Cyan ADP flow cytometer (Dako Cytomation). Results were analysed using Summit v4.3 software.

Table 2.3. List of antibodies used in flow cytometry experiments.

Antibody	Clone	Species / Isotype	Working dilution	Manufacturer	Catalogue number
CD24-PE	32D12	Mouse IgG1	1:10	Miltenyi Biotec	130-098-861
CD44-FITC	DB105	Mouse IgG1	1:10	Miltenyi Biotec	130-098-210
Phospho-AKT (Ser473)	D9E XP™	Rabbit IgG	1:100	Cell Signaling Technology	4060
Phospho-S6 (Ser235/236)	N/A	Rabbit IgG	1:50	Cell Signaling Technology	2211
Phospho-ERK1/2 (Thr202/Tyr204)	D13.14.4E XP™	Rabbit IgG	1:200	Cell Signaling Technology	4370
Anti-Rabbit Alexa Fluor 488	N/A	Goat	1:300	Invitrogen	A-11034
Cytokeratin 18 FITC conjugated (CK-18)	CY-90	Mouse IgG	1:10	Sigma	C8541

The staining was analysed using the following gates: 1) FSlin/SSlin dot plot which depicts granularity and cell size, 2) pulse width to exclude doublets and cell debris and 3) Violet 1 log histogram to exclude dead cells which were labelled with LIVE/DEAD stain. Additional gates were set to the secondary only control and the fluorescence was measured using FITC log histogram on the FITC (488nm) channel.

2.5.2.2. Cell cycle analysis

Cell lines and primary prostate cells were used for cell cycle analysis following treatment. Cells were trypsinized, centrifuged and resuspended in 0.5 ml PBS. To fix cells, 2.5 ml ice-cold 70% Ethanol was added drop wise to the cell suspension while vortexing, to prevent clustering of cells. Cells were incubated on ice for 30 minutes, then centrifuged, washed with 5 ml PBS and centrifuged again before resuspending the cells in 400 µl PBS. 50 µl RNase A (1 mg/ml final concentration) and 50 µl propidium iodide (PI; 400 µg/ml final concentration) was added and cells were incubated at 37°C for 30 min. Cells were then placed on ice, analysed on a CyAn ADP flow cytometer (Dako Cytomation) and PI fluorescence was recorded in the PE channel. To prevent bleaching of the fluorescence, cells were protected from light where possible during the procedure.

The results were analysed using the Summit v4.3 software. To select the cell population of interest a gate was set in an FSlin/SSlin (R1) histogram, which allowed exclusion of cell debris. Additional gates were set up in the PE channel and these included: cells in G0/G1 phases (R2), S phase (R3), G2M phases (R4) and also apoptotic cells (R5). For statistical significance, at least 20,000 events were collected.

2.5.3. Immunofluorescence

Immunofluorescence was performed in BD-Biocoat collagen I-coated 8-well chamber slides (BD Bioscience). Primary prostate cells were seeded at a density of 7.5×10^4 per well and incubated at 37°C at 5% CO_2 for 24 hours before treatment. Cells were washed twice with PBS and fixed with 4% (w/v) PFA for 15 minutes at room temperature. Cells were washed twice with ice-cold PBS and then permeabilised with 0.25% Triton X-100 in PBS for 10 minutes. Cells were washed a further three times with PBS, and then incubated with blocking buffer (10% (v/v) (goat) serum diluted in PBS containing 0.3 M glycine) for 30 minutes to block nonspecific binding of the secondary antibodies. Following blocking, the cells were incubated with primary antibody in blocking buffer at 4°C overnight (Table 2.4).

Cells were washed three times with PBS, incubated in blocking buffer for 30 minutes at room temperature and then incubated with a secondary antibody diluted in blocking buffer, for 1 hour at room temperature, and protected from light. After a final three washes with PBS, the chambers were removed from the slides, mounted in Vectashield containing DAPI (Vector laboratories) and glass cover slips added. Cover slips were sealed with clear nail varnish and stored at 4°C until analysis on a Nikon Eclipse TE300 fluorescent microscope (Nikon). Secondary only antibodies, where the primary antibody was replaced with PBS, were used as controls.

Table 2.4. List of antibodies used in Immunofluorescence

Antibody	Clone	Species / Isotype	Working dilution	Manufacturer	Catalogue number
LC3 B	N/A	Rabbit polyclonal	1:2000	abcam	ab51520
Cytokeratin 18 FITC conjugated (CK-18)	CY-90	Mouse IgG	1:100	Sigma	C8541
Anti-Rabbit Alexa Fluor 488	N/A	Goat	1:300	Invitrogen	A-11034

2.5.4. β-Galactosidase assay staining

Cells were seeded onto 10 cm dishes and following treatment a β-Galactosidase assay (Cell Signaling, #9860) was performed as an indicator of senescence. Briefly, cells were washed once with PBS and fixed for 15 minutes at room temperature, washed twice with PBS, and then incubated with β-Galactosidase staining solution, at pH 6.1, overnight at 37°C in a dry incubator. The staining results were analysed using an Evos XL transmitted light microscope (AMG) at 10x and 20x magnification.

2.6. Functional analysis

2.6.1. Wound healing assay

Following treatment of semi-confluent cells, a scratch was created in the cell monolayer with a 1 ml pipette tip. The cells were then washed with PBS and fresh medium was added to the wells. Cell migration into the wound was monitored over time and 10 x images were taken on an Evos XL transmitted light microscope (AMG) at 0 hours, 2 hours and 10 hours after wounding and the percentage of wound closure was calculated. The width of the wound at 0 and 10 hours was measured, the average (of 10 points) taken and the relative percentage wound closure at 10 hours with respect to 0 hours was calculated.

2.6.2. Clonogenic recovery assay

Primary prostate cancer cells were treated with AKTi and mTORi as described in section 2.3.2. Following treatment, the cells were selected for $\alpha_2\beta_1^{hi}/CD133^+$ (SC), $\alpha_2\beta_1^{hi}/CD133^-$ (TA) and $\alpha_2\beta_1^{low}$ (CB) cells as described in section 2.1.2.1. The sorted fractions were subsequently plated at 100 cells per well, diluted in 2 ml SCM, in a 6 well collagen-I coated plate, in triplicate. Irradiated STOs were added (to a concentration that resulted in a confluent monolayer) and plates were incubated at 37°C in 5% CO2. The number of STOs was evaluated following plating so that a confluent monolayer was achieved. Medium was changed every 2 days and STOs were added when required. When colonies greater than 32 cells (5 population doublings) started to appear, medium was removed and cells were washed with 1 ml PBS. The cells were then fixed with 2 ml crystal violet stain (1% (w/v) crystal violet, 10% (v/v) ethanol and 89% (v/v) PBS) and the number of colonies counted visually under the 10 x objective of a Leica DM IL LED microscope (Leica Microsystems). The percentage colony forming efficiency (CFE) was calculated, by dividing the number of colonies by the number of cells plated and multiplying by 100.

2.7. In vivo studies

2.7.1. Generation and maintenance of xenografts

Tissue from serially-transplantable Xenografts of primary prostate cancer, derived in our laboratory, was used in these experiments. Immune-compromised $RAG2^{-/-}\gamma C^{-/-}$ mice were used to generate the xenografts.

2.7.1.1. Depletion of mouse endothelial and lineage positive blood cells

15 mm^3 tumours were removed from humanely euthanized mice and placed in transport medium (R10 + ABM + 10 nM DHT). The tumour was then placed in a Petri dish, washed with PBS, and digested in 200 IU/ml collagenase. The collagenase was dissolved in 7.5ml of R10 and was filter sterilised prior to use. Tumour was finely chopped with a disposable scalpel and the tissue suspension was placed in an Erlenmeyer flask for digestion overnight in an orbital shaker at 37°C at 80 RPM. After overnight digestion, the cell suspension was transferred into a universal and further triturated by passing through a 21G blunt needle, followed by centrifugation at 1200 RPM for 2 minutes. Collected cells were washed with 10 ml PBS and centrifuged for a further 2 minutes at 1200 RPM. The pellet was resuspended in 10 ml 0.05% Trypsin/EDTA and incubated at 37°C for 30 minutes, after which R10 was added to inactivate trypsin and cells were centrifuged at 1300 RPM for 5 minutes. The cell pellet was resuspended in 15 ml R10 and passed through a 40 µm cell strainer (BD Biosciences). In order to further separate viable cells from dead cells and tissue debris, density centrifugation was performed using Ficoll-Paque Plus (MP Biomedicals). 15 ml of Ficoll-Paque solution was slowly placed underneath the cell suspension and centrifuged at 1800 RPM for 30 minutes with the brake turned off. The cells at the interface of the Ficoll-Paque Plus and cell dissociation buffer were collected, an equal volume of R10 was added and the cell suspension centrifuged at 1300 RPM for 10 minutes. The cell pellet was resuspended in 80 µl MACS buffer, 20 µl anti-mouse biotin antibody cocktail (Miltenyi Biotec), and 5 µl CD31 biotin antibody (AbD serotec) and incubated at 4°C for 10 minutes using MACSmix Tube Rotator. After the incubation, 60

µl MACS buffer and 40 µl anti-biotin Microbeads (Miltenyi Biotec) were added and cells were further incubated at 4°C for 15 minutes on the rotator. The cell suspension was washed with 4 ml MACS buffer, resuspended in 500 µl MACS buffer and added onto a pre-wetted LS column. The column was washed three times with 3 ml MACS buffer and the elute of LIN^-CD31^- cells was collected for further use.

2.7.1.2. *Ex vivo* treatment and re-engraftment of prostate tumour cells

Xenograft tumours were depleted of mouse endothelial and lineage positive blood cells as described in section 2.7.1.1. LIN^-CD31^- tumour cells were resuspended in D10 medium placed into 10 cm collagen I – dishes and treated. Following treatment, the cells were counted and limiting dilutions prepared (10 000 cells to 1 cell). The required cell number was placed into a 1.5 ml Eppendorf tube and 2 x 10^5 irradiated STO cells were added. The cell suspension was centrifuged at 2000 RPM for 2 minutes. The cell pellet was resuspended in 50 µl Ice-cold Matrigel basement membrane complex (BD Biosciences) and kept on ice. The cells were injected subcutaneously, using a 1 ml insulin syringe (27G) (BD Biosciences) into both flanks of a $Rag2^{-/-}\gamma C^{-/-}$ mouse. The surgical procedures were carried out under general anaesthesia (2.5% Isoflurane (Abbott)) and prior to surgery mice were administered 4.5 mg/kg Rimadyl (Pfizer) as a local anaesthetic. Mice were monitored weekly for tumour growth. Once the tumours were detectable they were measured every 2-3 days using a digital calliper (Duratool DC150). Tumour volume (mm^3) was calculated using the ellipsoidal formula: (length x $width^2$)/2. Tumour initiation frequency was calculated using Extreme Limiting Dilution Analysis software available online at (http://bioinf.wehi.edu.au/software/elda/), which provided an estimate of frequency with 95% confidence intervals and includes the Pearson's chi-square test for pairwise analysis to determine differences between treatment groups.

2.7.2. Preparation of Xenograft tumour tissue blocks and sections

Prostate tissue from xenografts was fixed in 10% (v/v) formalin for at least 24 hours and then transferred to 70% ethanol. The tissue was then placed in an embedding cassette (Cell Path+ address) and submerged in fresh 70% ethanol for 10 minutes, followed by incubation in absolute ethanol for 10 minutes, which was repeated two more times. The cassette was then submerged into fresh isopropanol for two x 10 minutes and submerged in fresh xylene (Fisher Scientific) for four times 10 minutes, after that the excess xylene was removed. The cassette was placed into Histoplast Paraffin at 60 - 65˚C (Thermo Scientific) for four x 15 minutes, followed by embedding in moulds with molten wax. The samples were allowed to set on a cold plate at -10˚C. Paraffin-embedded sections of tissues were prepared using APES-coated (2% (3'aminopropyl triehoxysilane) (v/v) (Sigma) in acetone) SuperFrost Plus slides (Merck), sections were cut using a microtome to a thickness of 5 µM. These procedures were carried out by Mrs. Caty Hyde.

2.7.3. Haematoxylin & eosin (H&E) staining

Tumour tissue sections embedded in paraffin, as described in section 3.7.4. dewaxed in xylene for two x 10 minutes and two x 1 minute, followed by rehydration with absolute ethanol at three x 1 minute and then one x 1 minute with 70% ethanol.

Chapter 3

Results I

3. RESULTS I

3.1. PTEN expression in human prostate cell lines

The phosphatase and tensin homologue gene (PTEN) codes for a negative regulator of the PI3K/AKT/mTOR pathway and is the most frequently deleted tumour suppressor gene in prostate cancer (Bitting and Armstrong, 2013).

PTEN expression was determined at the mRNA level in several human prostate cell lines including BPH1 (derived from benign prostatic hyperplasia), P4E6 (from well differentiated prostate cancer), LNCaP and PC3 (from metastatic prostate cancer). The results showed expression of PTEN in all cell lines apart from PC3 (Figure 3.1 A and B), suggesting that the PI3K axis might be over-activated in only those cells. However, western blotting, to determine protein expression, showed that PTEN is expressed in BPH1 and P4E6, but not in the metastatic cell lines, LNCaP and PC3 (Figure 3.1 C).

To determine the PI3K/AKT/mTOR pathway activity in prostate cell lines, western blotting, of selected phospho-biomarkers, was performed. Phosphorylation levels of AKT (at Ser473) and ribosomal protein S6 (at Ser235/236) (indicative of AKT kinase and mTOR kinase activity, respectively) were analysed, as well as total AKT and total S6 protein levels (Figure 3.1 C). As expected, the results demonstrate higher expression of phospho-AKT in the PTEN-negative cell lines in comparison to BPH1 and P4E6, suggesting higher activity of the PI3K/AKT pathway. Additionally, the presence of a double band in PC3 cells may indicate phosphorylation of AKT kinase at both Thr308 and Ser473. However, phospho-S6 was mainly expressed in BPH1 and PC3 cells, indicating that mTOR kinase activity does not directly correlate with PTEN expression. Levels of total S6 varied between the cell lines, with the lowest expression in P4E6 and LNCaP, unlike total AKT, which was comparable across all analysed cell lines.

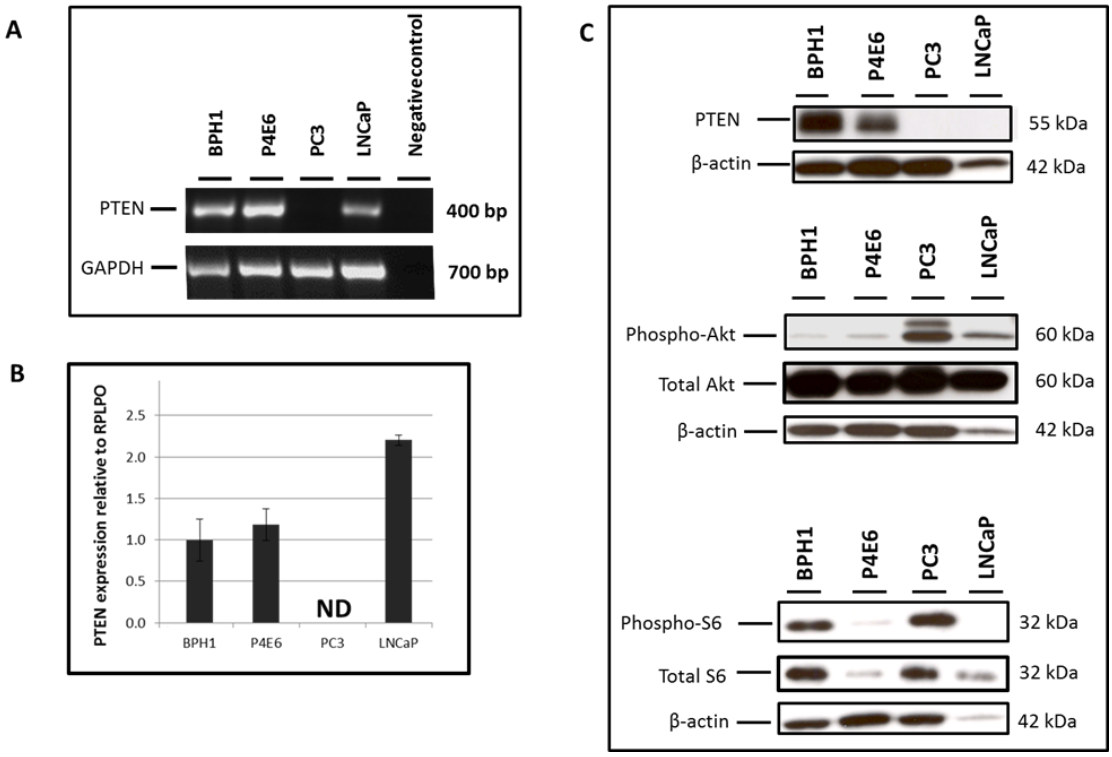

Figure 3.1. Expression of PTEN, AKT and S6 in human prostate cell lines.

mRNA expression of PTEN was measured using RT-PCR (A) and qRT-PCR (B). Total RNA was extracted, followed by reverse transcriptase PCR and cDNA synthesis. GAPDH expression was assessed to confirm cDNA integrity. Protein expression of PTEN, phospho-AKT (S473), total AKT, phospho-S6 (S235/236) and total S6 was determined using western blotting (C). Whole cell lysates were prepared and 20 µg of protein was loaded per lane onto a 10% SDS gel, electrotransferred onto PVDF membranes and stained for the biomarkers indicated. Staining for β-actin was used as a loading control. ND – not detected.

3.2. Knock down of PTEN using siRNA

To determine if the PI3K/AKT/mTOR pathway can be activated following knock down of PTEN expression, siRNAs to PTEN were used in the cell lines BPH1 and P4E6. PTEN knock down was confirmed at both the mRNA (Figure 3.2 A), by qRT-PCR, and protein level (Figure 3.3), by western blotting. Transfection efficiency for PTEN siRNA, determined by cy3-conjugated GAPDH siRNA, used at the same concentration (of 20 nM), was 80-90% (Figure 3.2B). The results show that 24-hour treatment with siRNA resulted in approximately 70% knock-down of PTEN expression, in BPH1 cells and approximately 88% in P4E6 cells. The level of PTEN decreased further and reached over 85% knock down after 96 hours, relative to non-selective siRNA, in both cell lines (Figure 3.2 A).

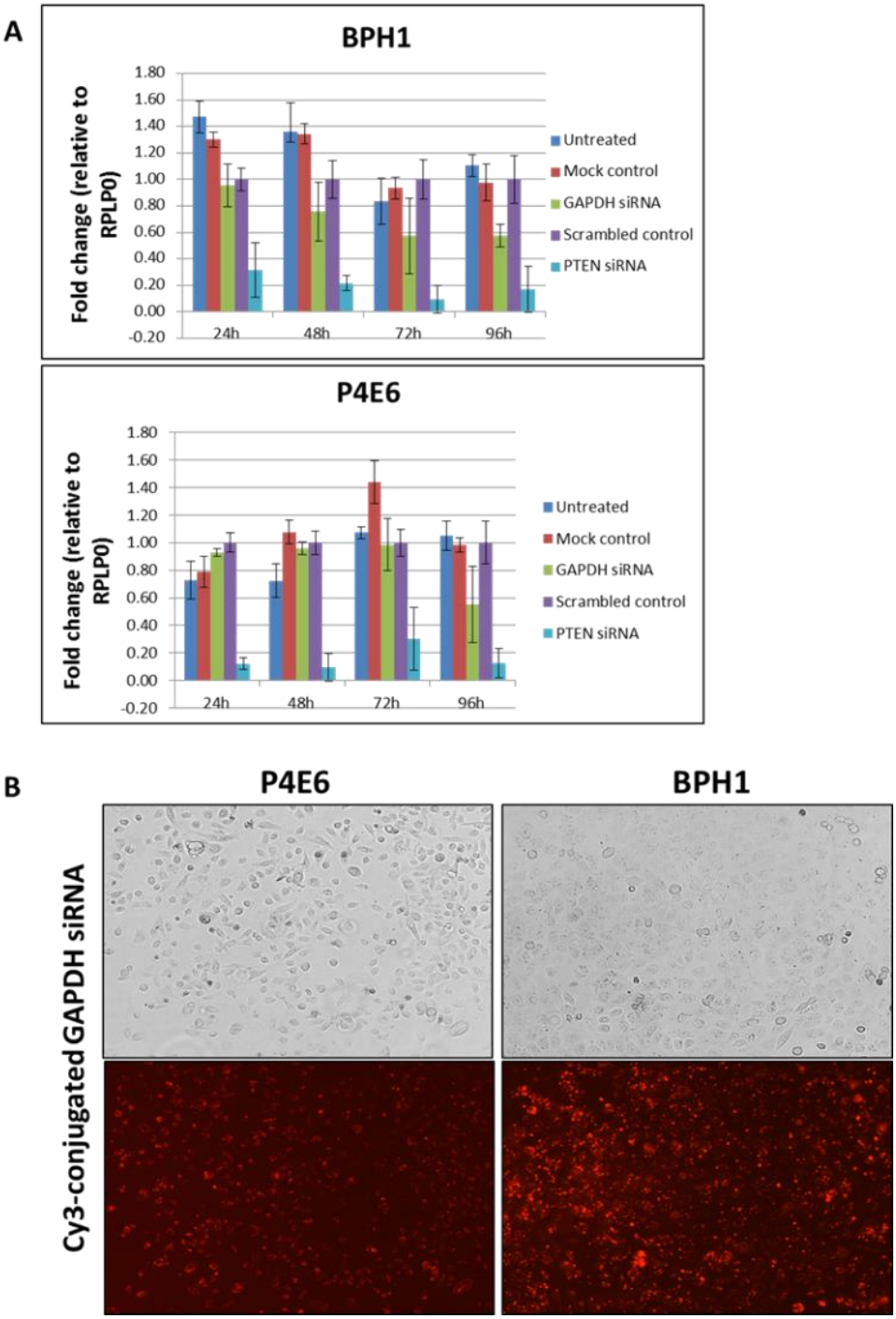

Figure 3.2. PTEN knock down in human prostate cell lines.

BPH1 and P4E6 cells were treated with PTEN siRNA at 20nM or a scrambled control for up to 96 hours. Subsequently total RNA was extracted, reverse transcribed and subjected to qRT-PCR and PTEN mRNA levels were determined (A). Transfection efficiency was determined using GAPDH cy3-conjugated siRNA at 20nM. (B) Phase contrast images (top panel) and immunofluorescent images (bottom panel) were taken at x40 magnification and show P4E6 and BPH1 cells transfected with Cy3-conjugated GAPDH siRNA.

3.2.1. Phospho-AKT expression is increased following PTEN down regulation

In order to determine if PTEN knock down was sufficient to activate the PI3K/AKT/mTOR pathway, expression of PTEN, phospho-AKT (Ser473) and phospho-S6 (Ser235/236) proteins was determined by western blotting. The results showed a decrease in PTEN expression at 72h and 96h in BPH1 (89% and 99.8%, respectively) and P4E6 (87.3% and 97.4%, respectively) cells relative to controls (Figure 3.3 A and B). Moreover, a dramatic increase in expression of phospho-AKT was observed in both cell lines in response to PTEN knock down. In BPH1 cells phospho-AKT levels increased by 97.9% at 72h and by 99.1% at 96h, and in P4E6 cells by 98.3% at 72h and by 91.8% at 96h.

Following PTEN knock down, the levels of phosphorylated ribosomal protein S6 decreased in BPH1 cells by 38.3% (after 72h) and 70.7% (after 96h) and in P4E6 cells by 88.7% and 100% after 72 and 96h, respectively (Figure 3.3 B).

This result demonstrates that knock down of PTEN was sufficient to activate the PI3K pathway signalling.

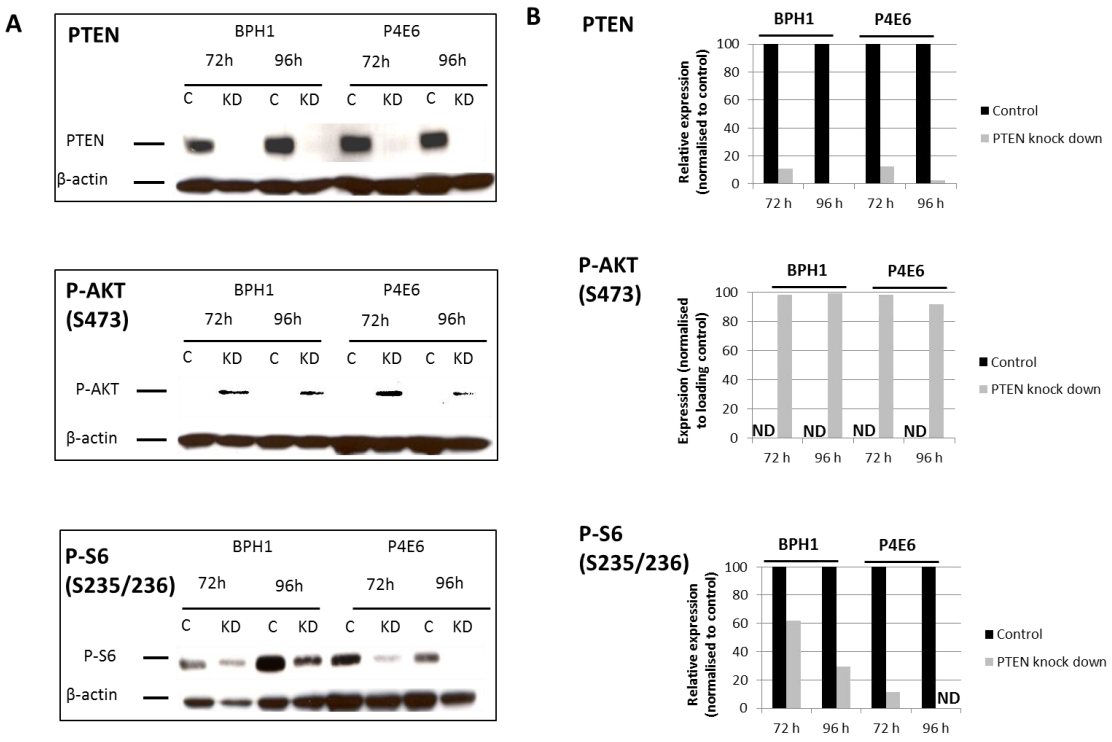

Figure 3.3. Knock down of PTEN protein in BPH1 and P4E6 cells.

BPH1 and P4E6 cells were treated with 20nM of PTEN siRNA (or a scrambled control) for up to 96 hours; cell pellets were subsequently collected at four time points: 24h, 48h, 72h and 96h. Whole cell lysates were prepared, quantified and subjected to western blotting. Activation of the PI3K pathway was determined by analysis of phospho-AKT (Ser473) and phospho-S6 (Ser235/236) expression following 72-hour and 96-hour incubation with PTEN siRNA (A). Quantification of protein expression was determined and was normalized to β-actin (B); ND – non detectable protein levels, C – control, KD – knock down;

3.2.2. Knock down of PTEN increases cell migration

A wound healing assay was performed using PTEN siRNA-treated BPH1 cells in order to determine if knock down of PTEN influenced cell migration. Confluent monolayers of cells were wounded and the process of healing observed under phase contrast microscopy at x10 magnification. The width of the wound was measured at the beginning of the experiment (T_0), after 2 hours and at the end of experiment – after 10 hours of healing (T_{10}). The rate of migration was calculated using the following equation $(1-T_{10}/T_0) \times 100$.

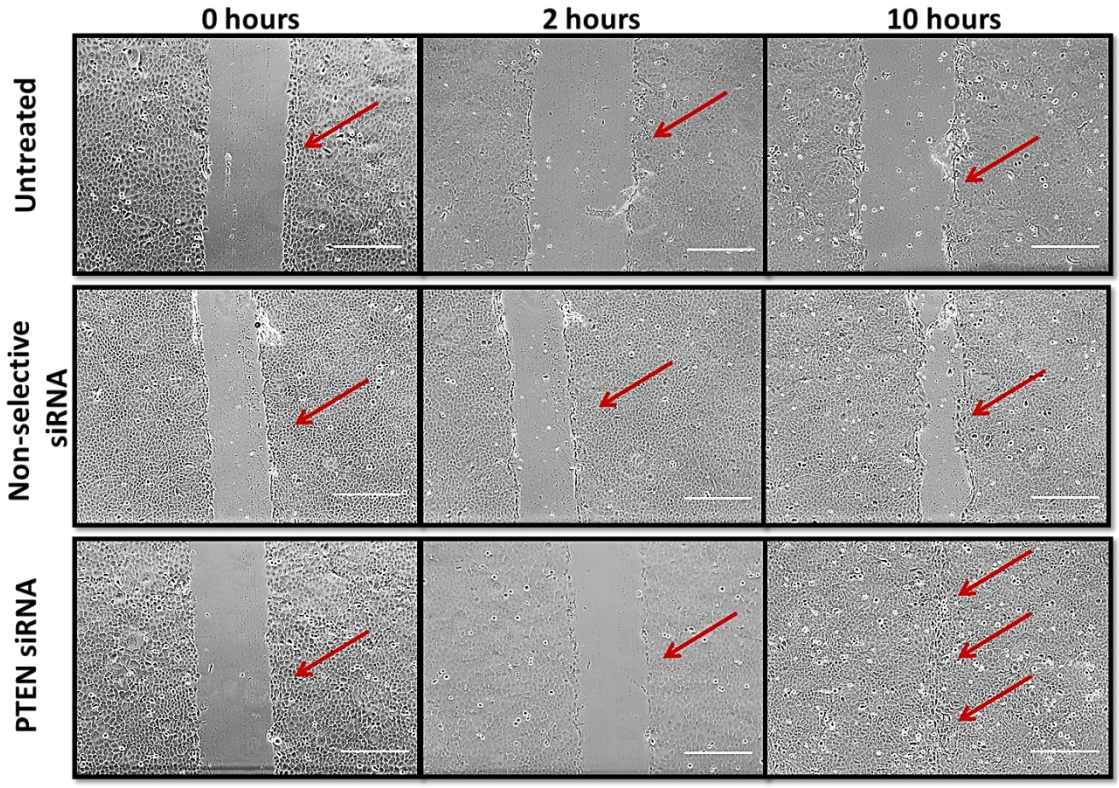

Figure 3.4. Wound healing assay following a PTEN knock-down in BPH1 cells.

BPH1 cells were treated with a 20nM PTEN siRNA and non-selective (scrambled) siRNA for 72 hours. The monolayer was then scratched and left to recover. Phase contrast images were taken at 0, 2 and 10 hours and the migration rate calculated. Single red arrows point at the wound and three arrows indicate where the wound used to be before it healed. The scale bar represents 400µm.

There was a significant difference ($p = 7.8 \times 10^{-9}$) in wound healing process between the scrambled control, where only 28.8% increase in wound closure was observed, and PTEN siRNA with nearly complete wound closure (98.8%) 10 hours after wounding. The result of the assay indicates that cells treated with PTEN siRNA have an increased rate of migration (by 3.4 fold) relative to control cells (non-selective siRNA) (Figure 3.4).

3.3. Treatment of cell lines with the AKT and mTOR inhibitors

The efficacy of the AKT kinase inhibitor (AKTi) and the mTOR kinase inhibitor (mTORi), two ATP-competitive small molecule inhibitors, was tested in human prostate cell lines (BPH1, P4E6, LNCaP and PC3) over a wide range of concentrations (0.01 – 30 µM) and for up to 72 hours. Morphological and density changes following treatment with an AKT inhibitor and mTOR inhibitor were determined.

Two PTEN-positive (BPH1 and P4E6) and two PTEN-negative (LNCaP and PC3) cell lines were treated with increasing concentrations of AKTi and mTORi. Phase contrast images were taken after 72 hours' treatment, to determine the effect on morphology and density of the cells.

A concentration of 10 µM of AKTi did not affect BPH1, P4E6 or PC3 cell morphology (Figure 3.5 and Figure 3.6), but a decrease of approximately 10% in PC3 cell density was observed (Figure 3.6). In contrast, changes in cell morphology were observed in LNCaP cells (following AKTi treatment at 1 µM) from an elongated to rounded shape (Figure 3.6). Following treatment with 10 µM AKTi almost all of the LNCaP cells detached from the dish (Figure 3.6, top panel - enlarged image).

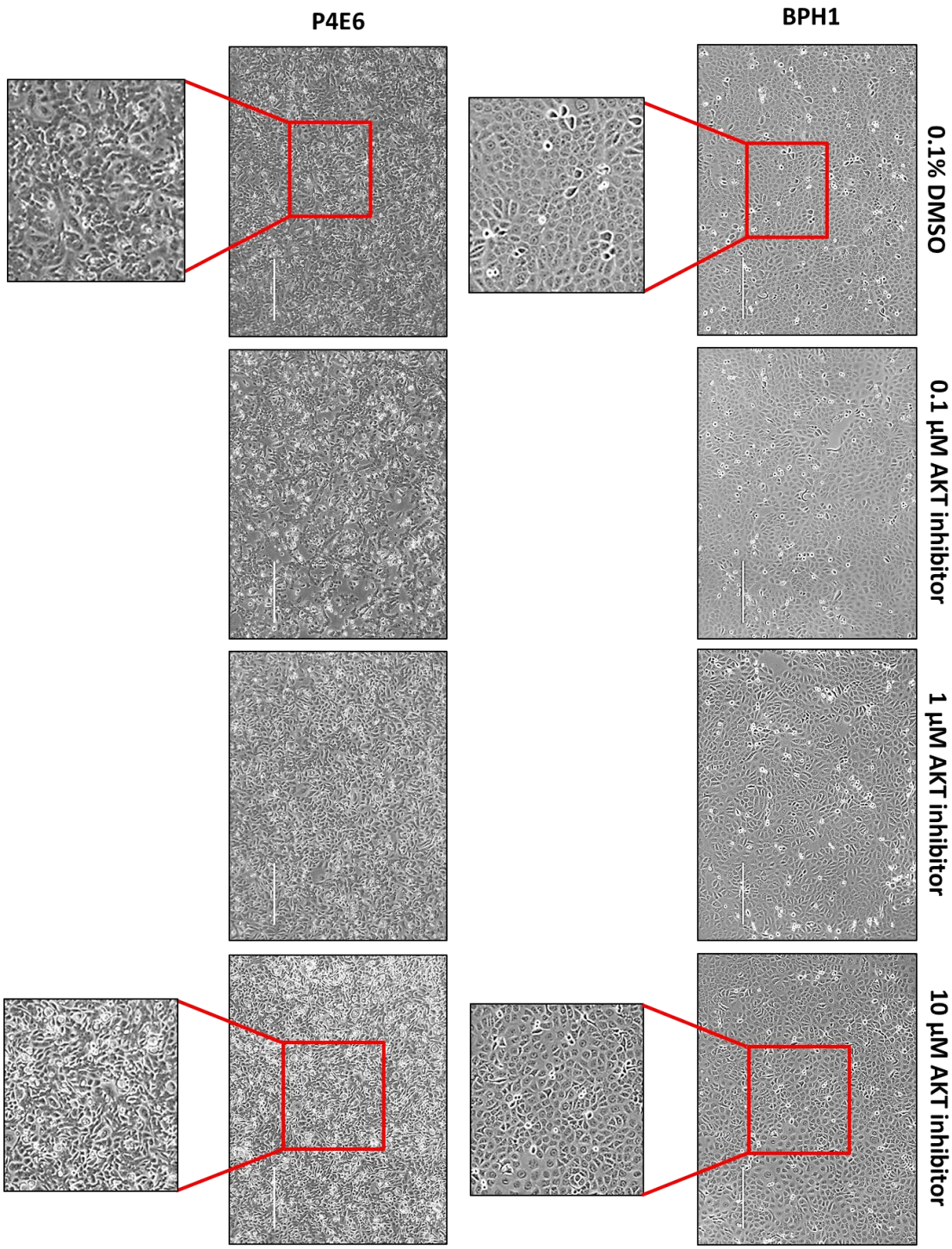

Figure 3.5. Cell morphology and density changes after treatment with AKTi of BPH1 and P4E6 cells.

Phase contrast images showing BPH1 (right) and P4E6 cells (left) treated with 0.1, 1 or 10 µM of the AKT inhibitor for 72 hours. Vehicle control cells were treated with 0.1% DMSO. The scale bar represents 400 µm.

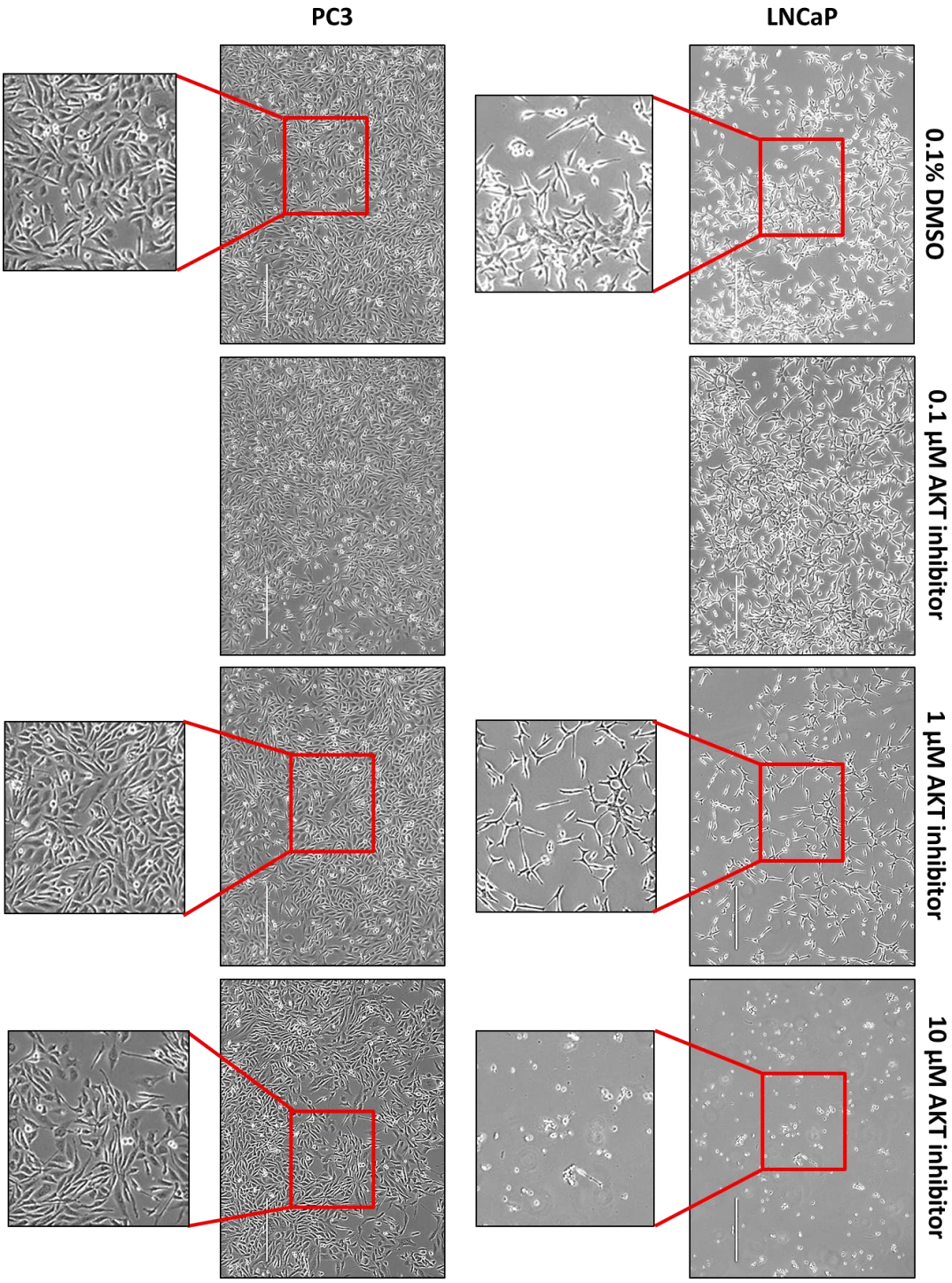

Figure 3.6. Cell morphology and density changes after treatment with AKTi of LNCaP and PC3 cells.

Phase contrast images showing LNCaP (right) and PC3 cells (left) treated with 0.1, 1 or 10 µM of the AKT inhibitor for 72 hours. Vehicle control cells were treated with 0.1% DMSO. The scale bar represents 400 µm.

Treatment with 10 µM mTORi (for 72 hours) resulted in a decrease in cell density in all cell lines analysed (Figure 3.7 and Figure 3.8). The highest drop in density was observed in LNCaP cells. Additionally, LNCaP cells were the only cell line which showed changes in morphology (from elongated to round shape) and detached from the dish (Figure 3.8, enlarged image). PC3 cells were also affected by treatment, but less so than LNCaP whereas BPH1 and P4E6 were the least affected - around 20-30% decrease in cell density, when treated with 10 µM mTOR inhibitor (Figure 3.7 and Figure 3.8). Concentrations of 0.1 and 1 µM of the compound did not affect morphology or density of any analysed cell lines.

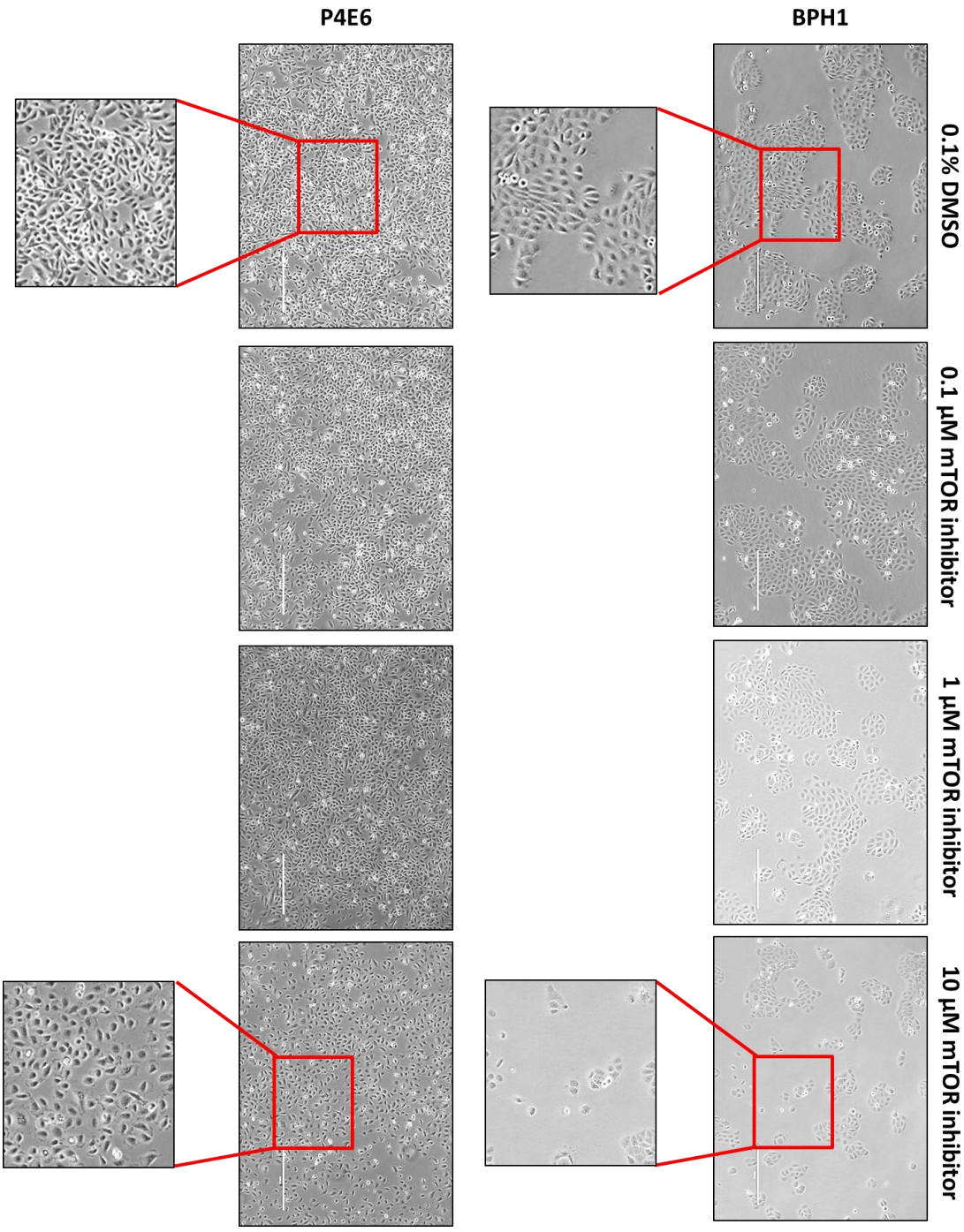

Figure 3.7. Cell morphology and density changes after treatment with mTORi of BPH1 and P4E6 cells.

Phase contrast images showing BPH1 (right) and P4E6 cells (left) treated with 0.1, 1 or 10 µM of the mTOR inhibitor for 72 hours. Vehicle control cells were treated with 0.1% DMSO. The scale bar represents 400 µm.

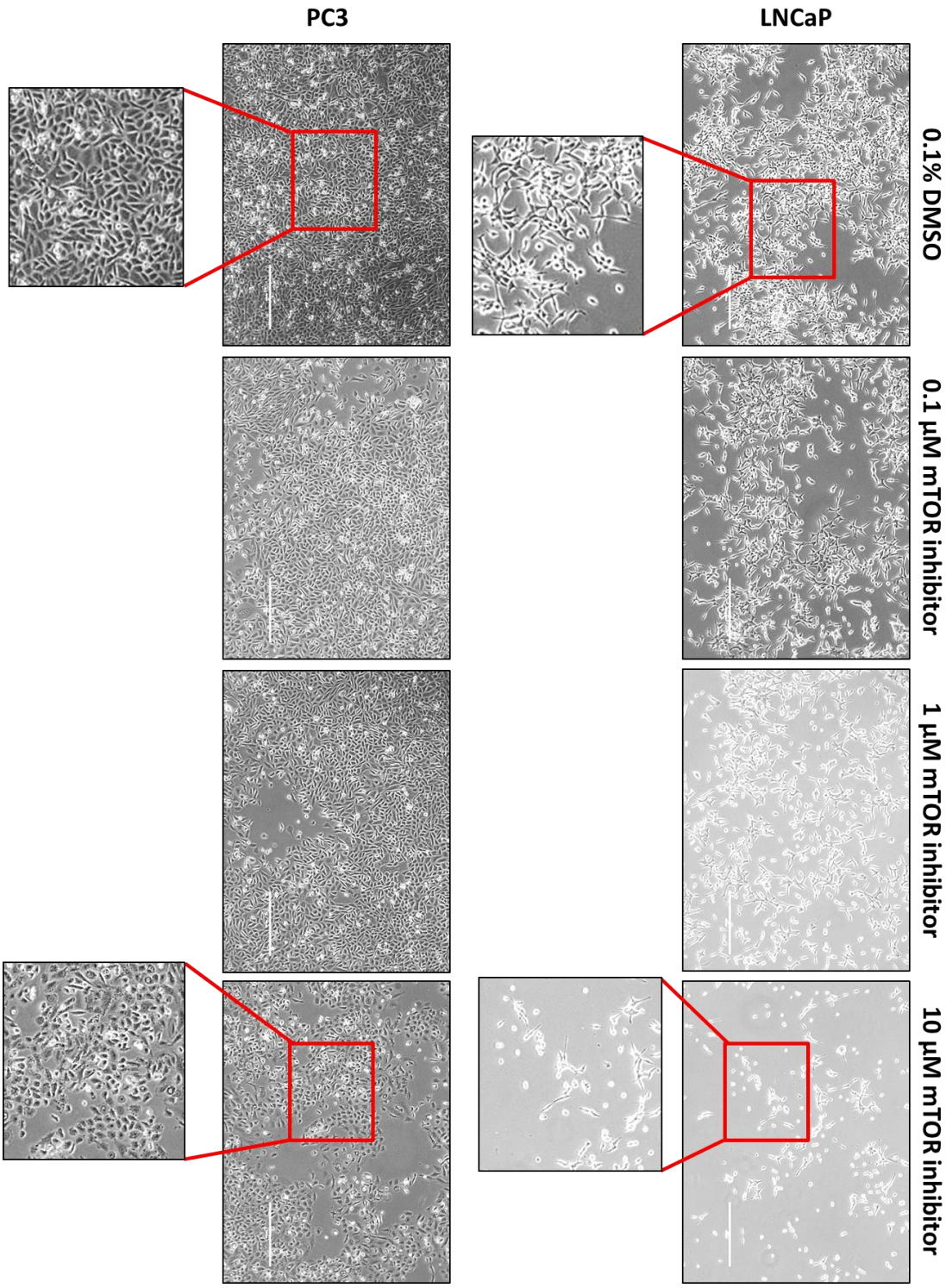

Figure 3.8. Cell morphology and density changes after treatment with mTORi of LNCaP and PC3 cells.

Phase contrast images showing LNCaP (right) and PC3 cells (left) treated with 0.1, 1 or 10 µM of the mTOR inhibitor for 72 hours. Vehicle control cells were treated with 0.1% DMSO. The scale bar represents 400 µm.

3.3.1. AKTi and mTORi affects the viability of cell lines

The AKT and mTOR kinases are crucial regulators of cell growth, proliferation and survival. An MTS assay, which gives an indication of a cells metabolic activity, which is indirectly proportional to cell number, was performed to investigate if AKTi and mTORi affect cell viability.

Two PTEN-positive (BPH1 and P4E6) and two PTEN-negative (LNCaP and PC3) cell lines were treated with increasing concentrations (0.01 – 30 µM) of AKTi and mTORi, for up to 48 hours. Cell viability was assessed at 24 hours and 48 hours after treatment. The results showed a dose-dependent decrease in cell viability in all analysed cell lines (Figure 3.9). LNCaP cells were the most sensitive, to both inhibitors with an EC_{50} (50% viability effective concentration) of 0.5 µM (AKTi) and 0.9 µM (mTORi) (Figure 3.9 B). Although PC3 cells showed a similar sensitivity to the mTORi, they were 30 fold less sensitive to the AKTi (15.2 µM) (Figure 3.9 B).

A

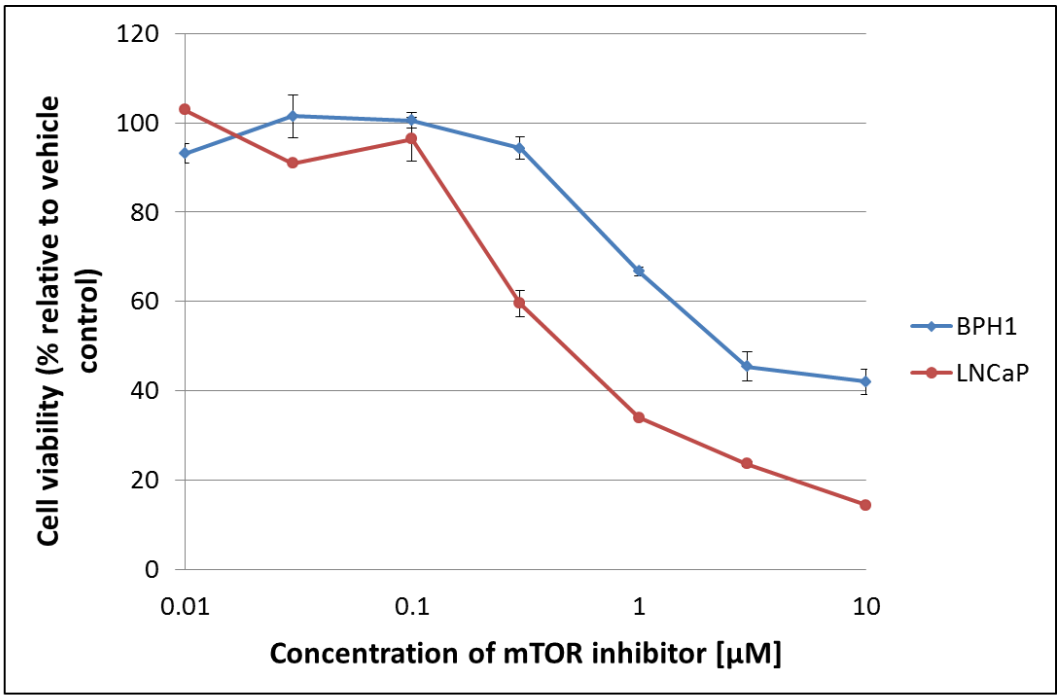

B

Cell line	EC_{50} [µM]	
	AKT inhibitor	mTOR inhibitor
BPH1	N/A*	4.7
P4E6	N/A*	6.5
LNCaP	0.5	0.9
PC3	15.2	0.6

* N/A – 50% growth inhibition was not reached

Figure 3.9. Decrease in cell viability following incubation with AKTi and mTORi.

An MTS assay was performed on a panel of prostate cell lines including BPH1, P4E6, LNCaP and PC3 cells treated (in triplicate) with increasing concentrations of AKTi and mTORi for 48 hours. (A) The results are expressed relative to vehicle control. (B) Summary of EC_{50}s for all analysed cell lines. Vehicle cells were treated with 0.3% DMSO.

Although treatment with AKTi reduced viability of both PTEN-negative cell lines, the PTEN-positive cells lines (BPH1 and P4E6) were not affected by AKT inhibition. Moreover, the EC_{50} for the mTORi were approximately 5 – 10 fold higher for BPH1 and P4E6 in comparison to LNCaP and PC3 (Figure 3.9 B).

Taken together, these results suggest that AKTi and mTORi' ability to reduce cell viability is dependent on PTEN status.

3.3.2. Cell migration decreased after treatment with AKTi and mTORi

A wound healing assay was performed to determine if treatment with AKT and mTOR inhibitors affected cell migration. LNCaP and PC3 cells were grown in 6-well plates to confluence, and then a scratch was made in the cell monolayer and drug solutions subsequently added. Based on the EC_{50} for both cell lines, a concentration of 1 µM was chosen. Cells were treated with either 1 µM mTORi or 1 µM AKTi and control cells were treated with 0.01% DMSO. Images were taken at 0, 2, 24 and 96 hours after wounding. The rate of migration was calculated using the following equation $(1\text{-}T_{24 \text{ or } 96} /T_0) \times 100$. The data are presented as mean ± SD.

The cancer cell line LNCaP showed a slower migration rate in comparison to PC3 cells and therefore the wound was left to heal for up to 96 hours. LNCaP cells treated with 1 µM AKTi showed a 94.3% wound recovery rate relative to vehicle control, but this was not significant (p value = 0.64) (Figure 3.10 A). However, treatment with 1 µM mTORi significantly affected migration with a decrease of 23% relative to control (p value = 3.4×10^{-5}).

The wound healing process was significantly faster in PC3 cells compared to LNCaP cells. However, treatment with 1 µM AKTi did not affect cell migration (Figure 3.10 B). In contrast, the mTORi – treated cells healed significantly slower, with a reduction in the rate of healing 28% less that vehicle control (p value = 0.006).

Taken together, the results showed that 1 µM mTORi was sufficient to significantly inhibit cell migration in both cancer cell lines (Figure 3.10 C).

Figure 3.10. Migration rate of LNCaP (A) and PC3 (B) cells following incubation with AKT and mTOR inhibitors.

Cell monolayer was wounded, 1 μM solution of AKTi and mTORi were added and phase contrast images were taken at 0h, 2h, 24h and 96h. Migration rates of the cells were calculated relative to the vehicle control (set as 100%) (C). Vehicle control cells were treated with 0.1% DMSO. The scale bar represents 400 μm.

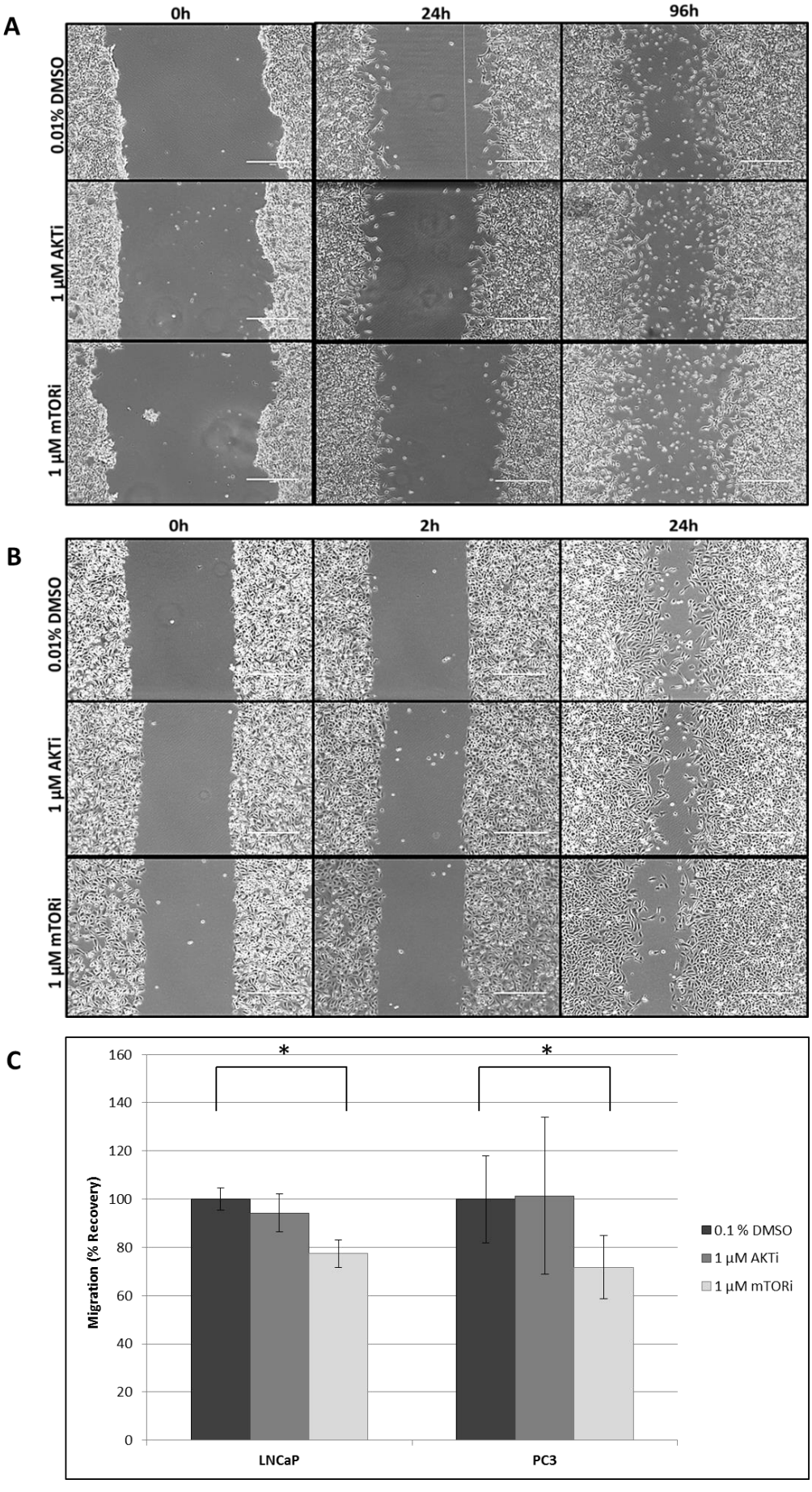
A
0h
24h
96h
0.01% DMSO
1 µM AKTi
1 µM mTORi
B
0h
2h
24h
0.01% DMSO
1 µM AKTi
1 µM mTORi
C
Migration (% Recovery)
160
140
120
100
80
60
40
20
0
*
*
LNCaP
PC3
0.1 % DMSO
1 µM AKTi
1 µM mTORi

3.3.3. Phospho-biomarker expression is decreased following treatment with AKT and mTOR inhibitors

Cell lines were treated with increasing concentrations of the mTOR inhibitor (0.01 – 10 μM) for 2, 24 and 72 hours, to determine the effect on proximal and distal biomarkers of the pathway, including AKT and S6. Phosphorylation of AKT was determined at Ser473 (mTORC2 substrate) and phosphorylation of ribosomal protein S6 was determined at Ser235/236 (an indirect substrate of mTORC1). The direct substrate of mTORC1, p70S6K, was not investigated in this analysis due to detection of nonspecific proteins by the antibody used to detect p70S6K.

Following a 2-hour exposure to the mTOR inhibitor, PC3 cells showed a dose-dependent decrease in phospho-AKT (88% inhibition at 3 μM) and phospho-S6 levels (60% inhibition at 1 μM) (Figure 3.11 A). However, when incubation with the drug was extended to 24 and 72 hours, the inhibitory effect was achieved mainly at the highest concentration (10 μM) (Figure 3.11 B and C); a 60% inhibition was observed for p-AKT at 24 hours and over 93% at 72 hours. A 50% inhibition of S6 phosphorylation was achieved at 0.1-0.3 μM concentration of the mTOR inhibitor at 24 hours and over 75% at 10μM following 72-hour incubation (Figure 3.11 C).

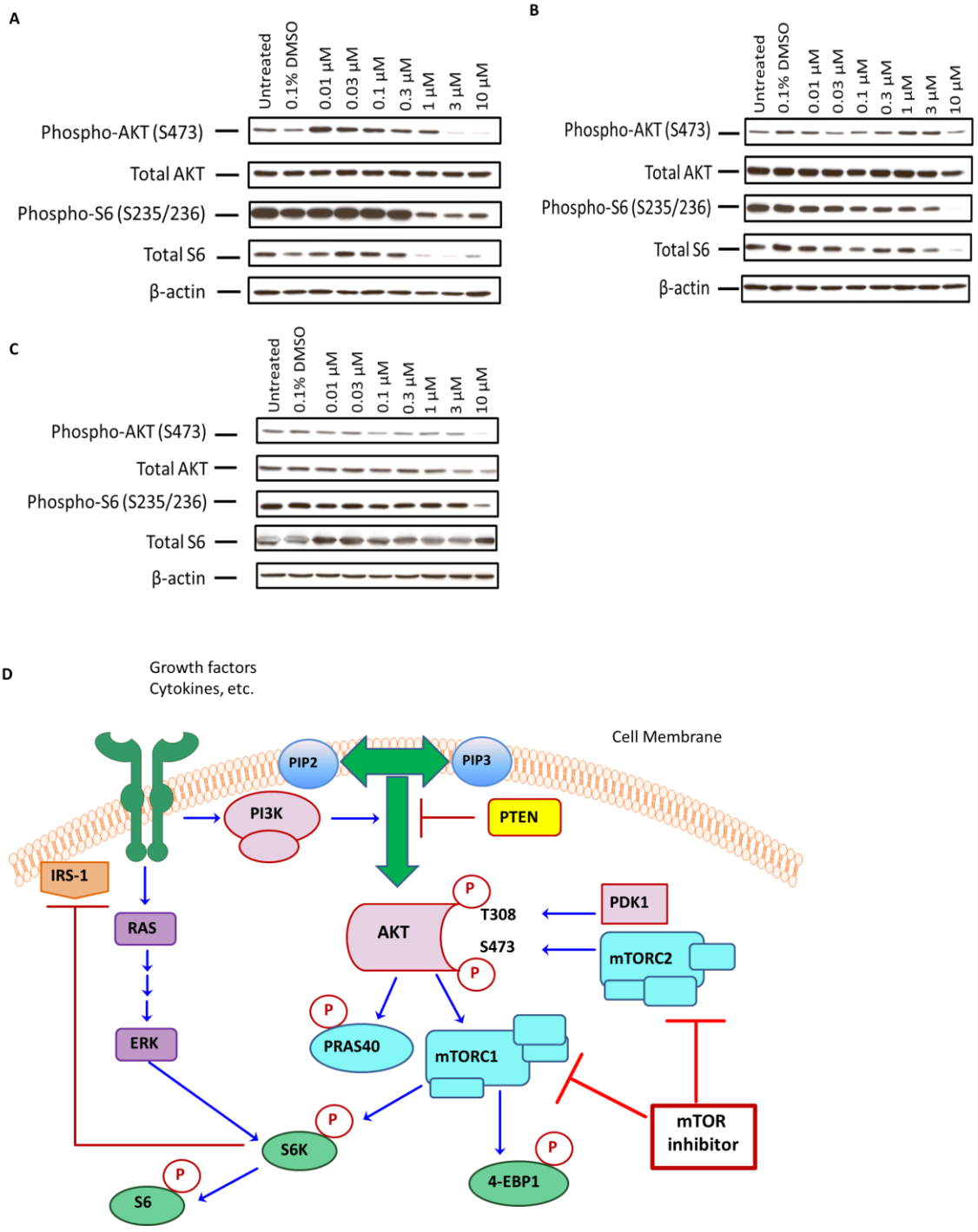

Figure 3.11. Changes in phospho-biomarker expression in PC3 cells following treatment with increasing concentrations of mTORi.

Cells were treated with 0.01 – 10 µM mTORi for 2h (A), 24h (B) and 72h (C). Whole cell lysates were subsequently prepared and 20 µg of protein was loaded per lane onto a 10% SDS gel, electrotransferred onto PVDF membranes and stained with antibodies against phospho-AKT (Ser473), total AKT, phospho-S6 (Ser235/236), total S6 and β-actin (loading control). (D) Schematic illustration of the PI3K/AKT/mTOR pathway showing mTOR inhibition.

PTEN-positive cell lines, BPH1 and P4E6, as well as LNCaP (PTEN-negative), were also treated with increasing concentrations of mTORi, for 72 hours. Expression of downstream biomarkers, phospho-AKT and phospho-S6, were determined by western blotting. The results showed a dose-dependent decrease of phospho-AKT in BPH1 and LNCaP cells following treatment. The levels of phospho-AKT (mTORC2 substrate) decreased to 58% of control levels after treatment with 0.1 µM mTORi in BPH1 cells (Figure 3.12 A). Similarly, a concentration of 0.3 µM decreased phospho-AKT levels to 47% in LNCaP cells (Figure 3.12 C). However, an unexpected dose-dependent increase in phosphorylation of S6, at Serine 235/236, was observed in P4E6 cells (Figure 3.12 B). A significant decrease in phospho-S6 expression in all of the cell lines was only observed after treatment with 10 µM mTORi.

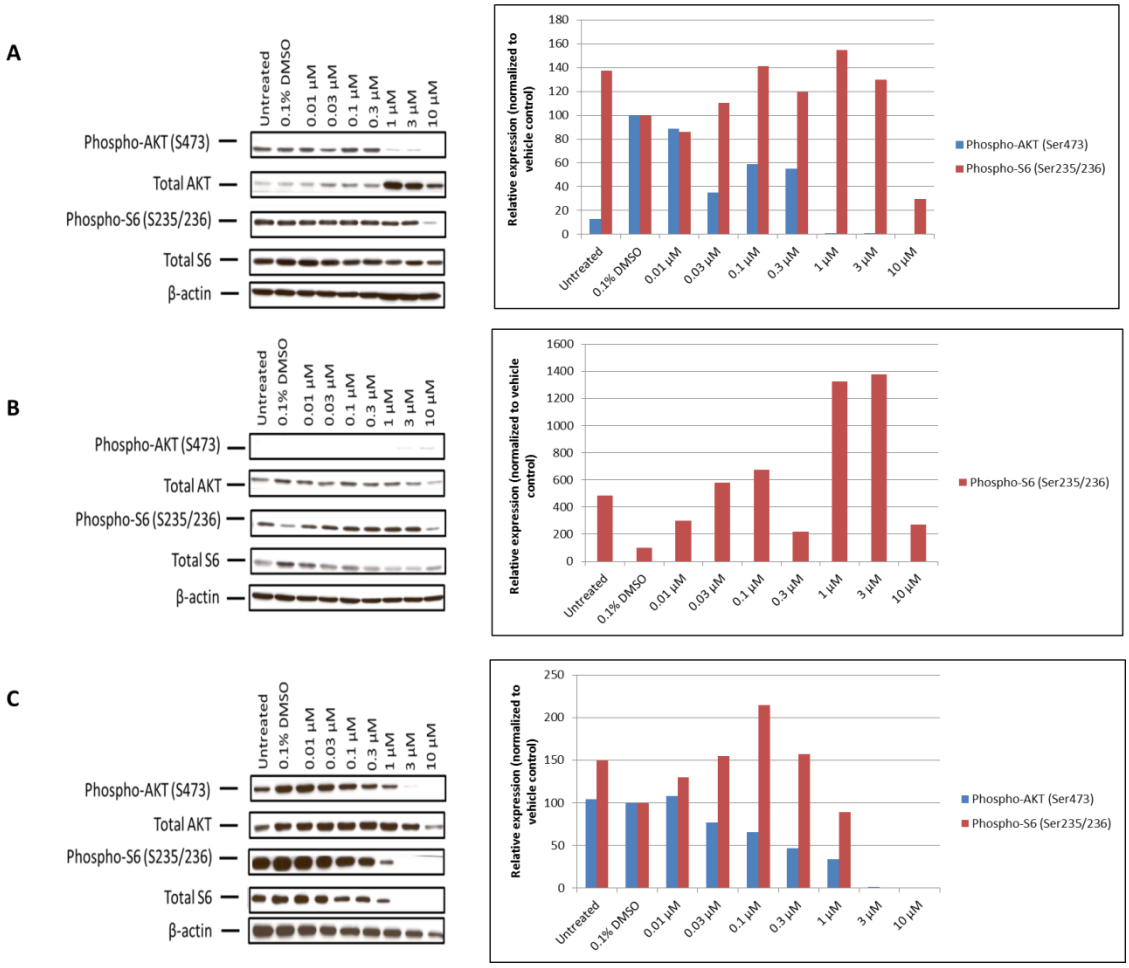

Figure 3.12. Phospho-biomarker expression following treatment with mTORi.

BPH1 (A), P4E6 (B) and LNCaP (C) cells were treated with 0.01 – 10 µM mTOR inhibitor for 72 hours. Whole cell lysates were subsequently prepared and 20 µg of protein was loaded per lane onto a 10% SDS gel, electrotransferred onto PVDF membranes and stained with antibodies against phospho-AKT (Ser473), total AKT, phospho-S6 (Ser235/236), total S6 and β-actin (loading control). Each cell line was treated at least twice and the representative blot was quantified using Image J software.

3.3.3.1. The efficacy of AKTi and mTORi differs across a panel of prostate cell lines

The efficacy of AKTi and mTORi was determined in a panel of prostate cell lines using phospho-biomarkers expression by western blotting. Following a 72-hour incubation with the AKTi, a significant increase in phosphorylation of AKT at Serine 473 was detected in all the analysed cell lines (Figure 3.13 A). Additionally, an unexpected increase in the levels of phospho-PRAS40, an indicator of AKT kinase activity, was observed in P4E6 (4 fold increase) and in LNCaP cells (2 fold increase) relative to the vehicle control (Figure 3.13 A and B).

Treatment with AKTi also resulted in a 20% decrease and 50% increase of phospho-ERK in P4E6 and LNCaP cells, respectively, whereas in PC3 phospho-ERK remained unchanged (Figure 3.13 A and B). Moreover, cleaved caspase-3, an indicator of apoptosis, was also detected in cells treated with AKTi.

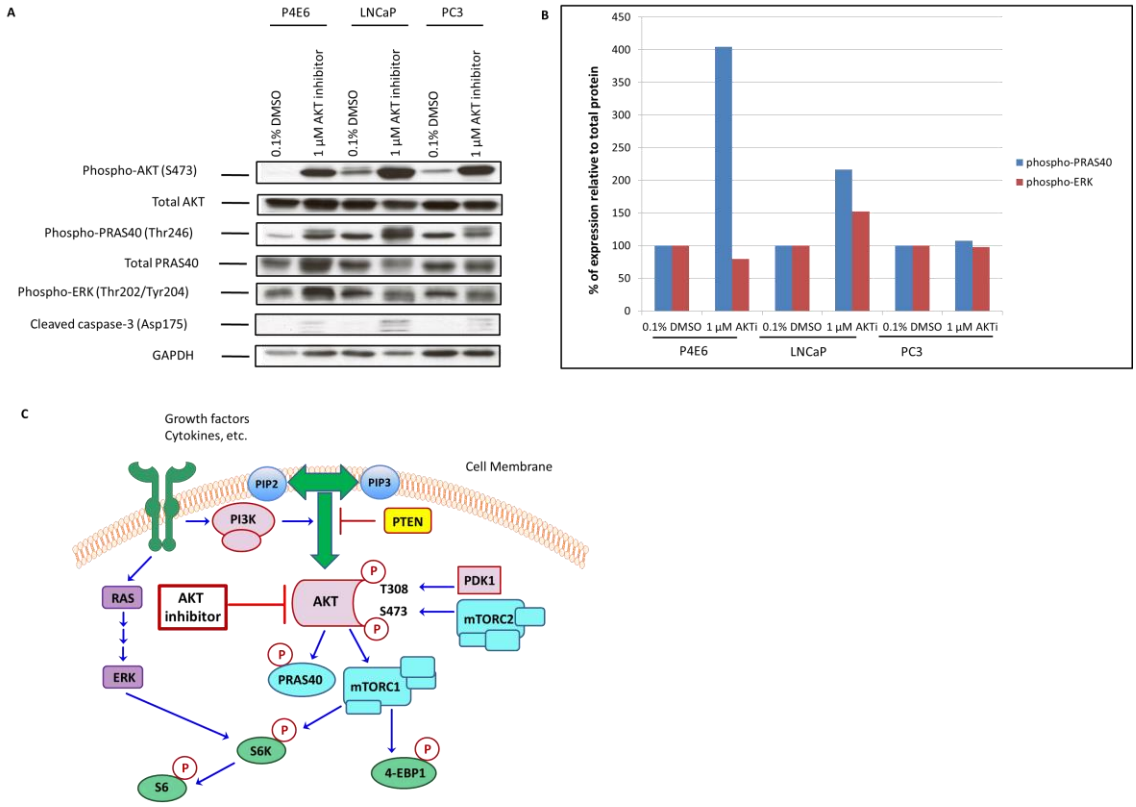

Figure 3.13. Biomarkers expression in prostate cell lines following treatment with AKTi.

P4E6, LNCaP and PC3 cells were treated with 1 μM AKTi for 72 hours. Following treatment, whole cell lysates were prepared and 20 μg of protein was loaded per lane onto a 10% SDS gel, electrotransferred onto PVDF membranes and stained with phospho-AKT (Ser473), total AKT, phospho-PRAS40 (Thr246), total PRAS40, phospho-ERK (Thr202/Tyr 204), cleaved caspase 3 (Asp 175) and GAPDH (loading control) (A). Relative expression of the phospho-biomarkers was determined and quantified against the loading control GAPDH (B). A schematic representation of the pathway illustrating AKT inhibition (C).

Treatment with 1 µM mTOR inhibitor showed a decrease in phospho-S6 of 63% and phospho-4EBP1 of 12%, biomarkers downstream from mTORC1, in LNCaP cells relative to vehicle control (Figure 3.14 A). Additionally, PC3 cells showed a decrease in phospho-4EBP1 (21%) and phospho-ERK (40%), but there was no significant change in phospho-S6 expression (Figure 3.14 A and B). However, an unexpected pattern of biomarker expression was observed in PTEN-positive P4E6 cells. The immunoblotting results showed increased levels of all analysed biomarkers following 72-hour treatment with the mTOR inhibitor.

The data shows that 1 µM concentration of the AKT and mTOR inhibitors achieved a sufficient inhibitory effect only in LNCaP cells.

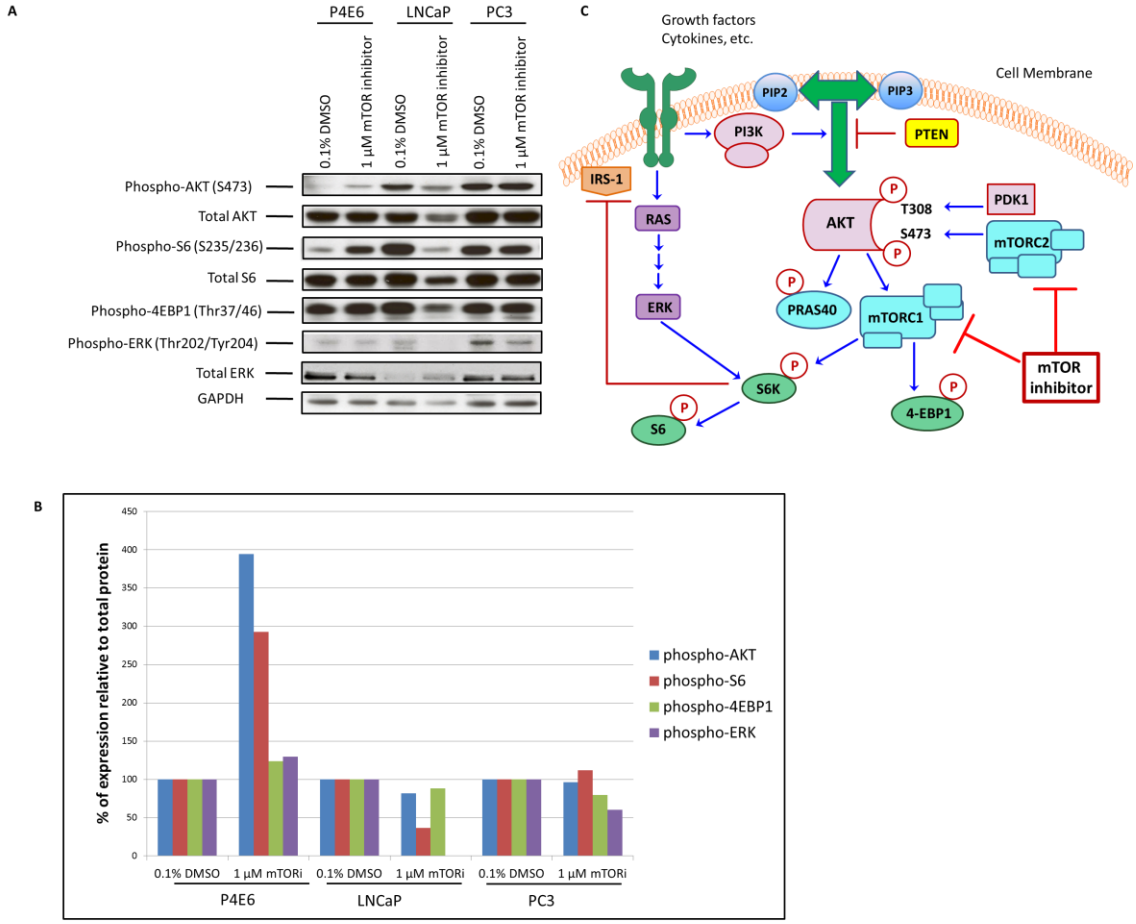

Figure 3.14. Biomarkers expression in prostate cell lines following treatment with mTORi.

P4E6, LNCaP and PC3 cells were treated with 1 µM mTOR inhibitor for 72 hours. Following treatment, whole cell lysates were prepared and 20 µg of protein was loaded per lane onto a 10% SDS gel, electrotransferred onto PVDF membranes and stained with phospho-AKT (Ser473), total AKT, phospho-S6 (Ser235/236), total S6, phospho-4EBP1 (Thr37/46), phospho-ERK (Thr202/Tyr 204), total ERK and GAPDH (loading control) (A). Relative expression of the phospho-biomarkers was determined and quantified against the loading control GAPDH (B). A schematic representation of the pathway illustrating mTOR inhibition (C).

3.3.4. LNCaP cells show G1 arrest after treatment with AKT and mTOR inhibitors

Flow cytometry analysis for cell cycle distribution was performed to test whether AKT or mTOR inhibition affected cell cycle in prostate cell lines. Cells were treated with increasing concentrations of inhibitor for up to 72 hours. The results showed that the majority of LNCaP cells (87.5%) were in G0/G1 following treatment with 1 µM mTORi compared to 67.9% for the vehicle control. Similarly, after treatment with 1 µM AKT inhibitor, 84.3% of LNCaP cells were in G0/G1 relative to 76.5% for vehicle control (Figure 3.15 A). Moreover, treatment with 3 µM of AKTi resulted in G0/G1 arrest of 96.9% of LNCaP cells (result not shown).

Cell cycle distribution of PC3 as well as the PTEN-positive P4E6 cells – did not change after treatment with either inhibitor relative to vehicle control (Figure 3.15 B and C). However, a benign prostate cell line BPH1, showed a modest increase of 7.1% and 4.1% in number of cells in S and G2M phase, respectively, after treatment with 1 µM mTORi (Figure 3.15 C). Moreover, after treatment with 3 µM AKTi, cell number in G2M phase increased by 8.6% relative to vehicle control (result not shown).

Taken together, the data shows that G0/G1 phase arrest was only induced in LNCaP cells and this was achieved by both inhibitors at 1µM relative to vehicle control.

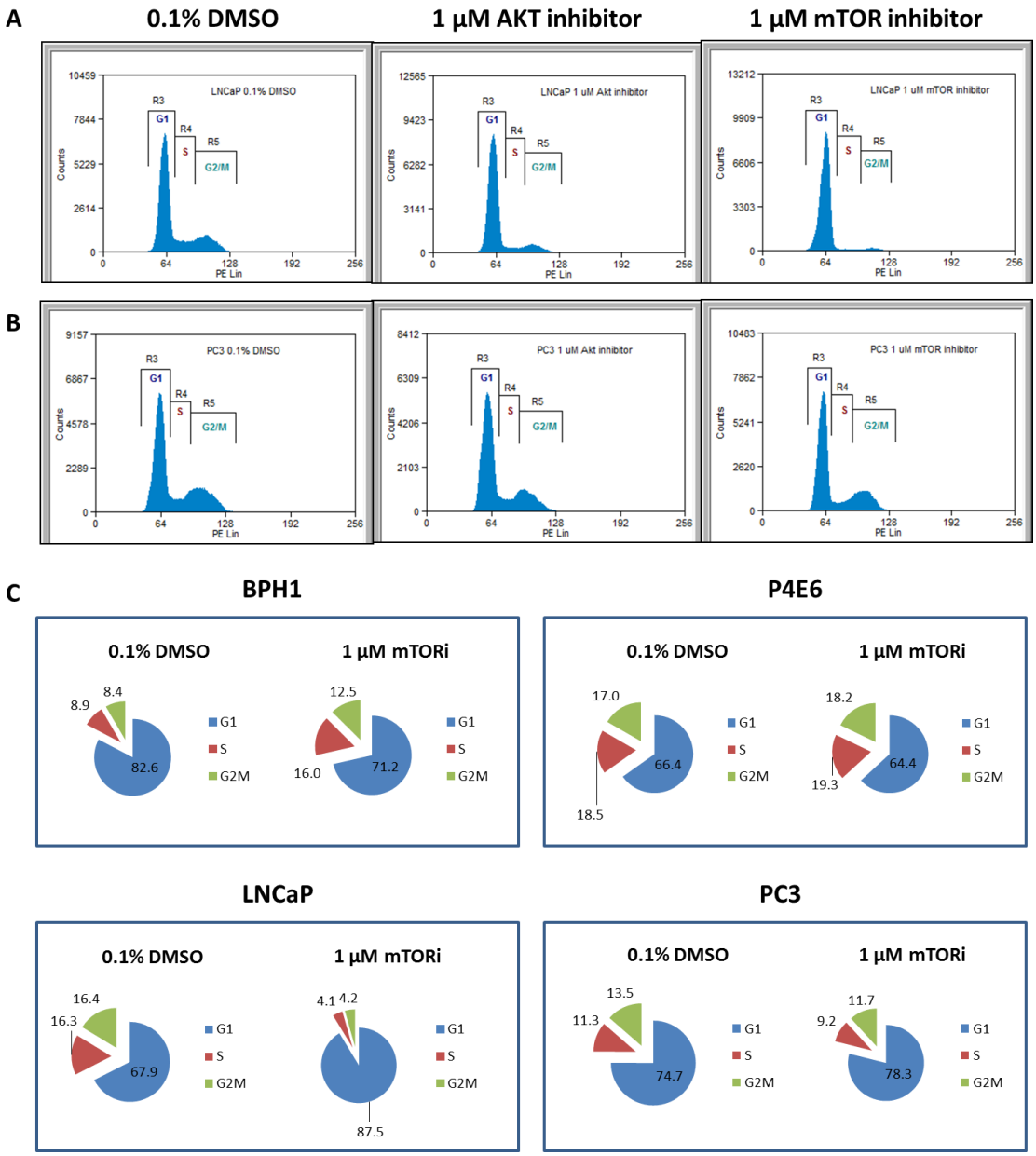

Figure 3.15. Flow cytometry cell cycle analysis using propidium iodide staining (PE) in prostate cell lines after 72 hour-treatment with AKTi and mTORi.

Cell cycle profile for LNCaP cells (A) and PC3 cells (B) treated with 1 µM AKT inhibitor and 1 µM mTOR inhibitor. (C) Pie chart summary illustrating cell cycle distribution, following treatment with 1 µM mTORi relative to vehicle control (0.1% DMSO) in BPH1, P4E6, LNCaP and PC3 cells.

Chapter 4

Results II

4. RESULTS II

4.1. PTEN expression in primary prostate cell cultures

Expression of PTEN was determined at the protein level in a number of prostate epithelial cultures. The results showed that expression of PTEN measured by western blotting varies between samples obtained from patients undergoing radical prostatectomies and does not seem to be Gleason grade dependent (Figure 4.1). The highest levels of PTEN were detected in H313/13 (BPH), H240/12 R (GL7) and H330/13 (GL7) in comparison to the PTEN-positive BPH1 cell line. Surprisingly, the lowest expression of PTEN was detected in H278/13 (GL6) as well as in H359/13 (GL9) and H363/13 (GL9).

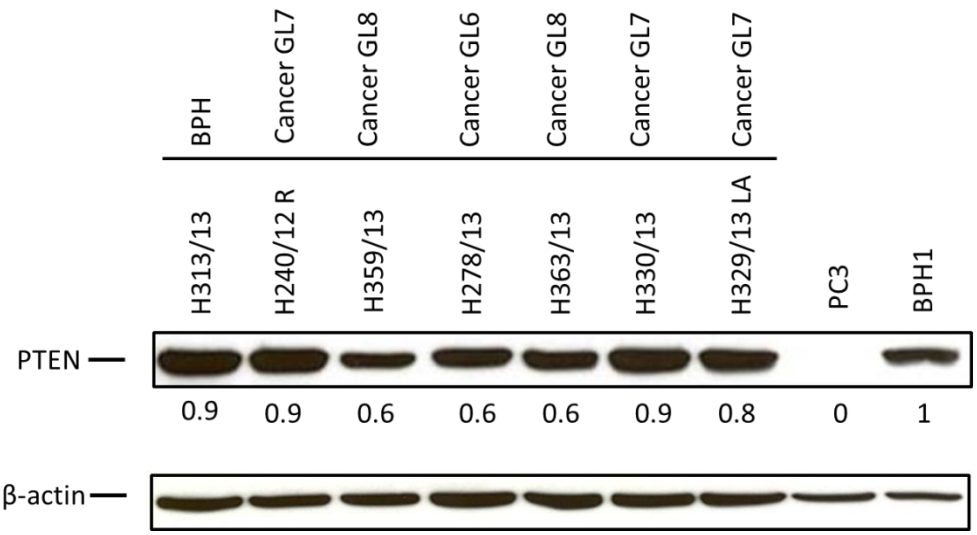

Figure 4.1. PTEN expression in primary prostate cultures.

PTEN expression was measured in prostate epithelial cultures using western blotting. Whole cell lysates were prepared and 20 µg of protein was loaded per lane onto a 10% SDS gel, electrotransferred onto PVDF membranes and stained for PTEN. Cell lines PC3 and BPH1 were negative and positive control, respectively. Intensity of staining was measured using Image J software and normalized to β-actin (loading control).

4.2. Treatment of primary cell cultures with inhibitors

Prostate epithelial cultures were treated with increasing concentrations of the AKT inhibitor (AKTi) and the mTOR inhibitor (mTORi) for up to 72 hours.

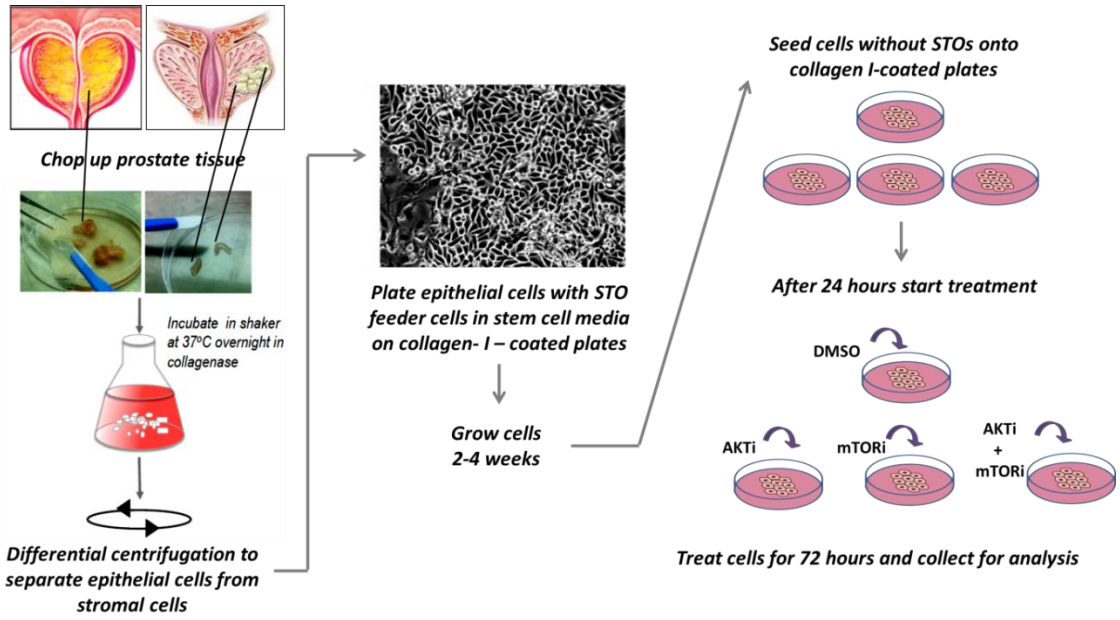

Figure 4.2. Culture and treatment schedule of primary prostate epithelial cells.

Prostate benign and malignant tissue was chopped with a scalpel and then digested with collagenase overnight in order to obtain a single cell suspension. This was followed by differential centrifugation to separate epithelial cells from stromal cells. The epithelia were cultured on collagen I-coated plates with inactivated STO feeder cells. Cultures were grown for 2-4 weeks to reach confluence, when they were seeded onto fresh dishes without STOs, and treated 24 hours later with the inhibitors. Following 72 hours incubation with the inhibitors, cells were collected for analysis. Adapted from (Frame and Maitland, 2011)

4.2.1. Cell morphology changes following treatment with high concentrations of AKTi and mTORi

The efficacy of the AKT and mTOR inhibitors was tested in prostate epithelial cultures including BPH, cancer and castration resistant prostate cancer (CRPC) (Figure 4.2). Cell cultures were treated with up to 25 µM concentrations of each inhibitor, for up to 72 hours. Phase contrast images were taken after 72 hours' treatment to determine the effect on the morphology and density of the cells.

A concentration of 5 µM AKTi did not affect the cell morphology of H277/13 (BPH), H282/13 (GL7) or H271/13 (CRPC), but a decrease of approximately 15% in cell density was observed in H271/13 cells (Figure 4.3). However, a combined treatment of 5 µM AKTi with 5 µM mTORi reduced cell density by 10 to 15% in all treated cultures. Additionally, a small increase in a number of cells detached from the dish was observed in H271/13 following treatment with 5 µM mTORi in comparison to the vehicle control cells (Figure 4.3).

There was no difference in BPH and cancer cell cultures' susceptibility to the inhibitors over this concentration range.

Figure 4.3. Morphology and density of prostate epithelial cultures following treatment with AKTi and mTORi.

A BPH (H277/13) (top row), cancer GL7 (H282/13) (middle row) and a CRPC (H271/13) cells (bottom row) were treated with 5 μM AKTi or mTORi as single agents or in a combination of 5 + 5. Phase contrast images of the cells were taken after 72 hour-treatment. Vehicle control cells were treated with 0.1% DMSO. Scale bar represents 400 μm.

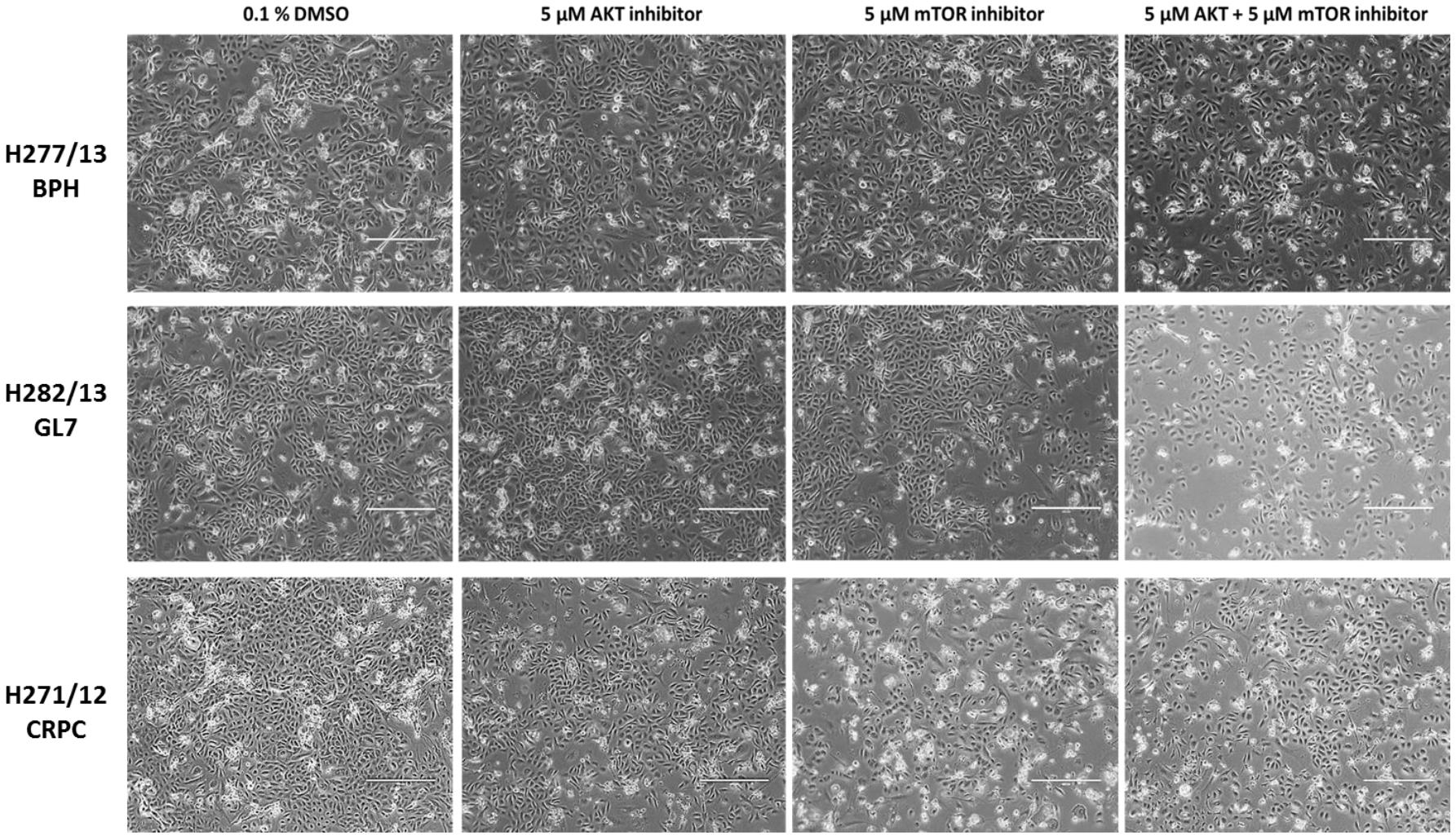
0.1 % DMSO
5 µM AKT inhibitor
5 µM mTOR inhibitor
5 µM AKT + 5 µM mTOR inhibitor
H277/13
BPH
H282/13
GL7
H271/12
CRPC

Treatment with higher concentrations of the inhibitors (10 – 50 µM) caused dramatic morphological changes which were very specific for each inhibitor (Figure 4.4). Following a 72-hour exposure to 25 µM of AKTi, increased vacuolation of a Gleason 7 primary culture (H282/12) was observed, suggestive of autophagy (Figure 4.4, left panel). In contrast, following treatment of the same cells with 25 µM of mTORi, membrane blebbing, indicative of apoptosis, was observed in a number of cells (Figure 20, middle panel). Vehicle control cells (treated with 0.5% DMSO) did not show any morphological changes (Figure 4.4, right panel).

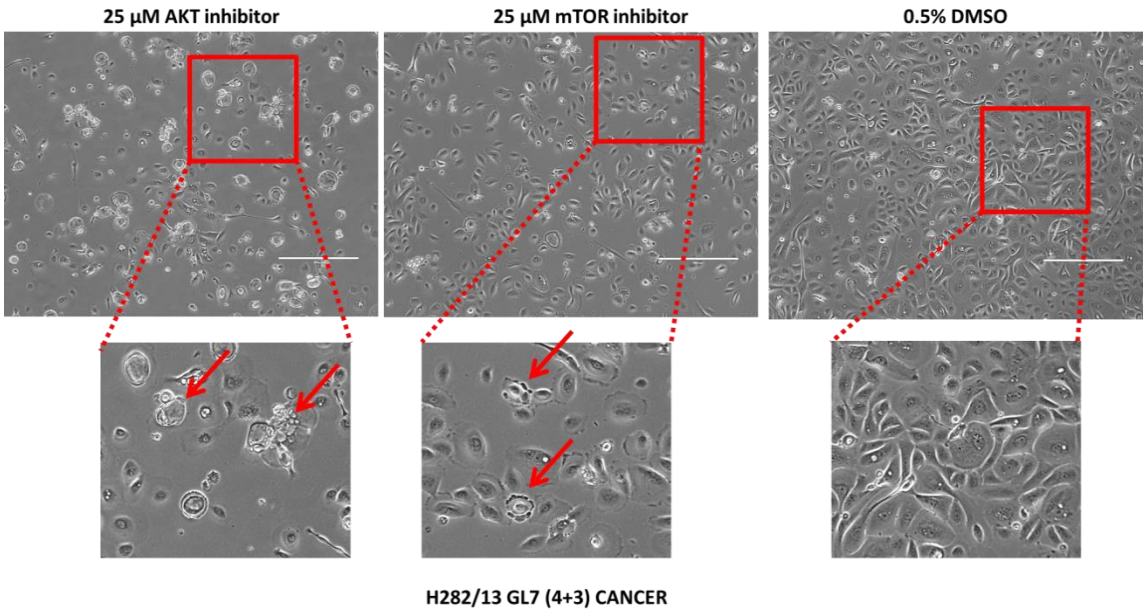

Figure 4.4. Cell morphology after exposure to high concentrations of AKTi and mTORi.

Phase contrast images of primary cells (H282/12) from a Gleason 7 (4+3) prostate cancer, treated with 25 µM AKT inhibitor (left panel) and 25 µM mTOR inhibitor (middle panel) for 72 hours. Increased vacuolization of AKTi-treated cells and membrane blebbing of mTORi-treated cells were observed (arrows). Control cells were treated with 0.5% DMSO. Scale bar represents 400 µm.

Taken together, treatment with low concentrations (up to 5 µM) of the inhibitors did not change cell morphology, whereas high concentrations (25 µM) of AKTi and mTORi caused distinct morphology changes. Membrane blebbing might be an indication of apoptosis, whereas vacuolization might suggest an induction of autophagy which was investigated further (see section 4.2.3.).

4.2.2. Cell viability is reduced in BPH and cancer after treatment with AKTi and mTORi

A number of primary cells (derived from patients with BPH and cancer) were treated with increasing concentrations of AKTi and mTORi, either alone or in combination, to determine the effect on cell viability. The majority of samples showed a decrease in viability of approximately 30-40% following treatment with 3 µM of either inhibitor, whereas a decrease of up to a 50% was observed following treatment with a combination of 3 µM AKTi and 3 µM mTORi (Table 4.1 and Figure 4.5).

Table 4.1. Summary of primary samples viability following treatment with AKTi and mTORi.

	Sample	Treatment	% Viability (relative to vehicle control)
24h	H233/12 L - Benign	3 µM AKTi	65%
		3 µM mTORi	58%
		3 µM AKTi + 3 µM mTORi	57%
	H240/12 - GL7 (3+4)	3 µM AKTi	75%
		3 µM mTORi	72%
		3 µM AKTi + 3 µM mTORi	51%
	H233/12 - GL8 (3+5)	3 µM AKTi	105%
		3 µM mTORi	101%
		3 µM AKTi + 3 µM mTORi	102%
	H236/12 - GL8 (4+4)	3 µM AKTi	58%
		3 µM mTORi	58%
		3 µM AKTi + 3 µM mTORi	47%
	H239/12 - GL9 (4+5)	3 µM AKTi	137%
		3 µM mTORi	84%
		3 µM AKTi + 3 µM mTORi	45%
48h	H237/12 - GL7 (3+4)	3 µM AKTi	82%
		3 µM mTORi	76%
		3 µM AKTi + 3 µM mTORi	71%
	H240/12 - GL7 (3+4)	3 µM AKTi	102%
		3 µM mTORi	70%
		3 µM AKTi + 3 µM mTORi	59%
	H239/12 - GL9 (4+5)	3 µM AKTi	80%
		3 µM mTORi	62%
		3 µM AKTi + 3 µM mTORi	44%
72h	H240/12 - GL7 (3+4)	3 µM AKTi	40%
		3 µM mTORi	27%
		3 µM AKTi + 3 µM mTORi	20%

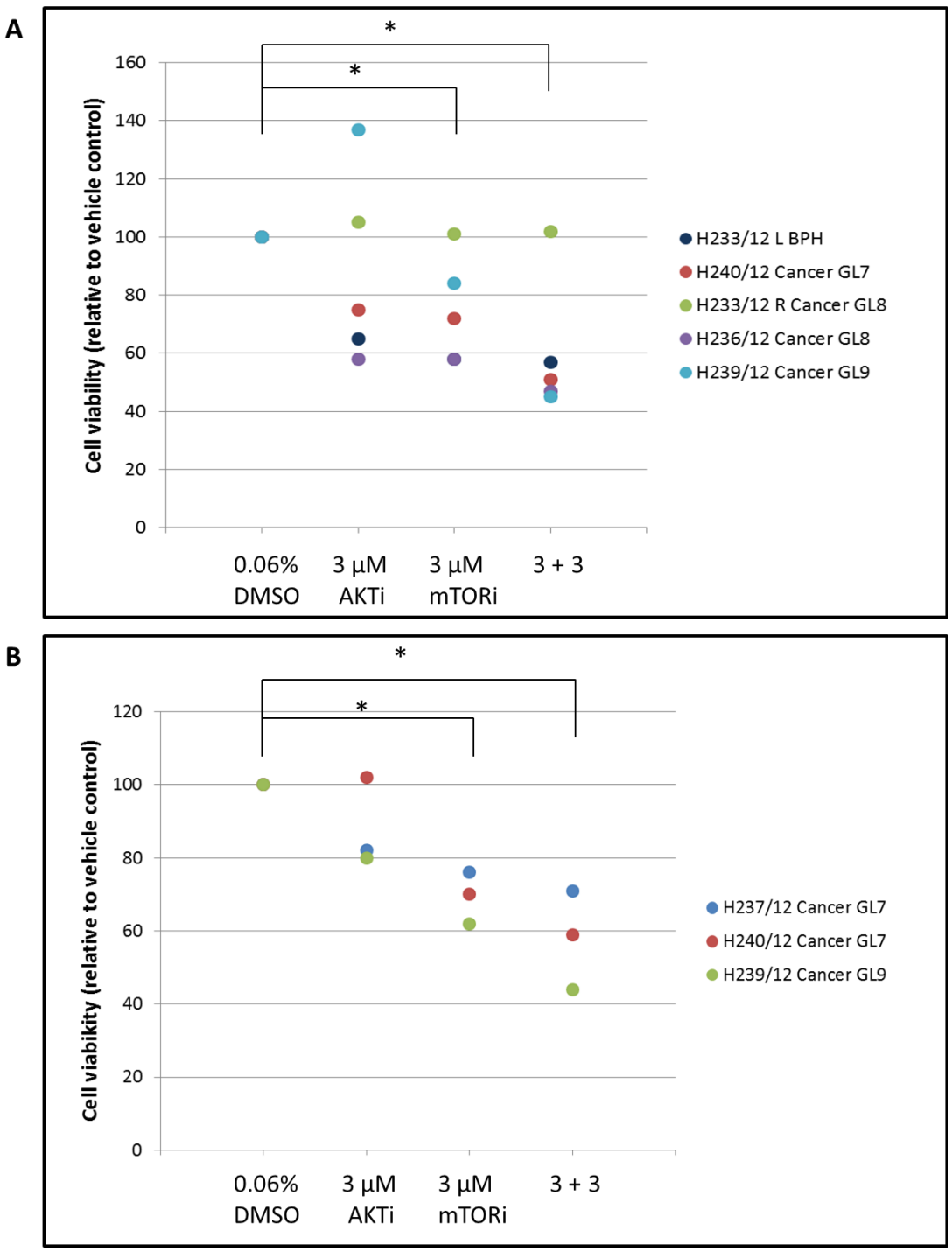

Figure 4.5. Cell viability following treatment with AKTi and mTORi.

Primary cultures derived from BPH and cancer were treated with either 3 µM AKTi, 3 µM mTORi or a combination of 3 µM AKTi + 3 µM mTORi for 24 hours (A) and 48 hours (B). Following treatment, the cells were harvested, stained with Trypan blue and counted. Percentage of viable cells was calculated relative to the vehicle control (0.04% DMSO). Significant differences (p value < 0.05) in cell viability are indicated on the graphs.

However, there was variability in the response and some patients did not respond. This variability was observed with a matched normal and cancer sample (H233/12) in which the primary cells from the cancer biopsy showed little effect in contrast to the normal matched control (Figure 4.6).

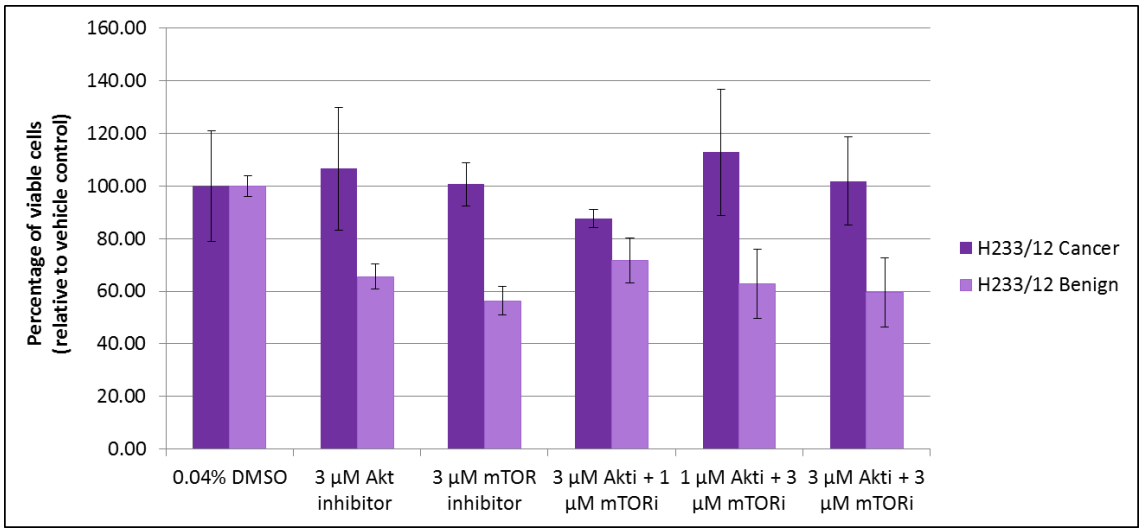

Figure 4.6. Cell viability of matched benign and cancer cells after treatment with AKTi and mTORi.

A primary cancer H233/12 (GL7 (4+3)) and matched benign cells were treated with either 3 µM AKTi, 3 µM mTORi or a combination of 3 µM AKTi + 1 µM mTORi or 1 µM AKTi + 3 µM mTORi or 3 µM AKTi + 3 µM mTORi for 24 hours. Following treatment, the cells were harvested, stained with Trypan blue and counted. The percentage of viable cells was calculated and the results normalised to the vehicle control (0.04% DMSO). Error bars represent the standard error of the mean (SEM).

In order to determine whether an extended incubation time had an effect on cell viability, a primary cancer culture H240/12 was treated with AKTi and mTORi alone or in combination for up to 72 hours. The results showed a decrease of 40 to 50% in cell viability after 24 and 48 hours respectively. However, 72-hour incubation decreased cell viability even further; up to 80% when treated with a combination of 3 µM AKTi + 3 µM mTORi (Figure 4.7).

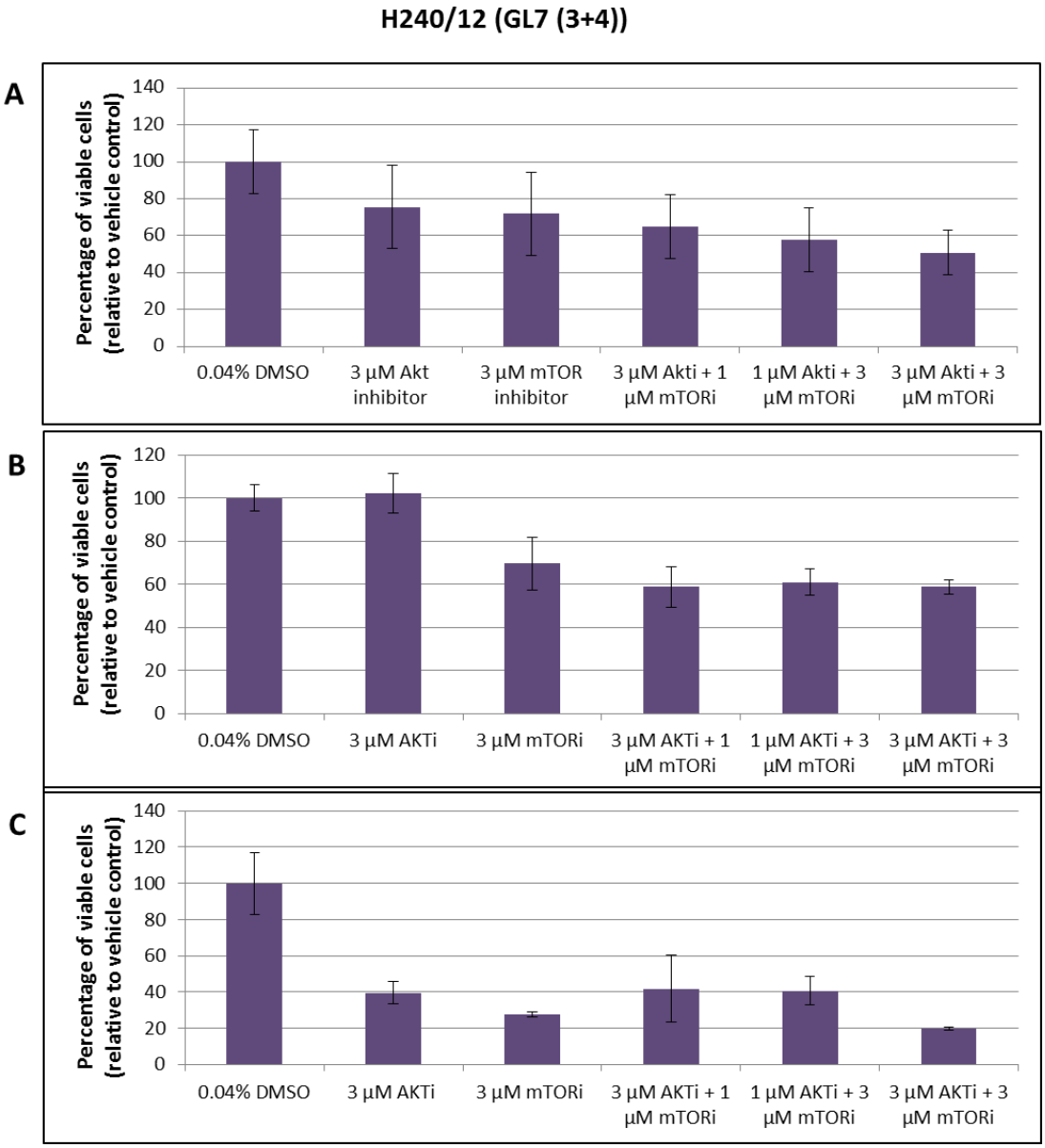

Figure 4.7. Viability of H240/12 (GL7) cells following treatment with AKTi and mTORi.

Primary prostate cancer sample H240/12 (GL7) was treated with either 3 µM AKTi,3 µM mTORi or a combination of 3 µM AKTi + 1 µM mTORi, 1 µM AKTi + 3 µM mTORi or 3 µM AKTi + 3 µM mTORi, for 24h (A), 48h (B) and 72h (C). Cell viability was determined using Trypan blue exclusion. Percentage of cell viability was calculated relative to the vehicle control (0.04% DMSO). Error bars represent standard error of the mean (SEM).

In addition to trypan blue exclusion cell viability assessment, an MTS assay was also performed, which gives an indication of cells' metabolic activity following treatment. Primary cell cultures H313/13 (BPH) and H315/13 (Cancer, GL7) were treated with increasing concentrations (5 – 50 µM) of AKTi and mTORi for 72 hours and an MTS assay performed. The results showed that both cultures responded similarly to each inhibitor, with up to 50% decrease in cell viability when treated with 50 µM AKTi or 50 µM mTORi (Figure 4.8 A and B). Additionally, there was a greater than 27-fold difference in response to treatment with mTORi between a primary cancer culture H315/13 and the prostate cancer cell line LNCaP, with an EC_{50} of 25 µM and 0.9 µM for H315/13 and LNCaP respectively (Figure 4.8 B).

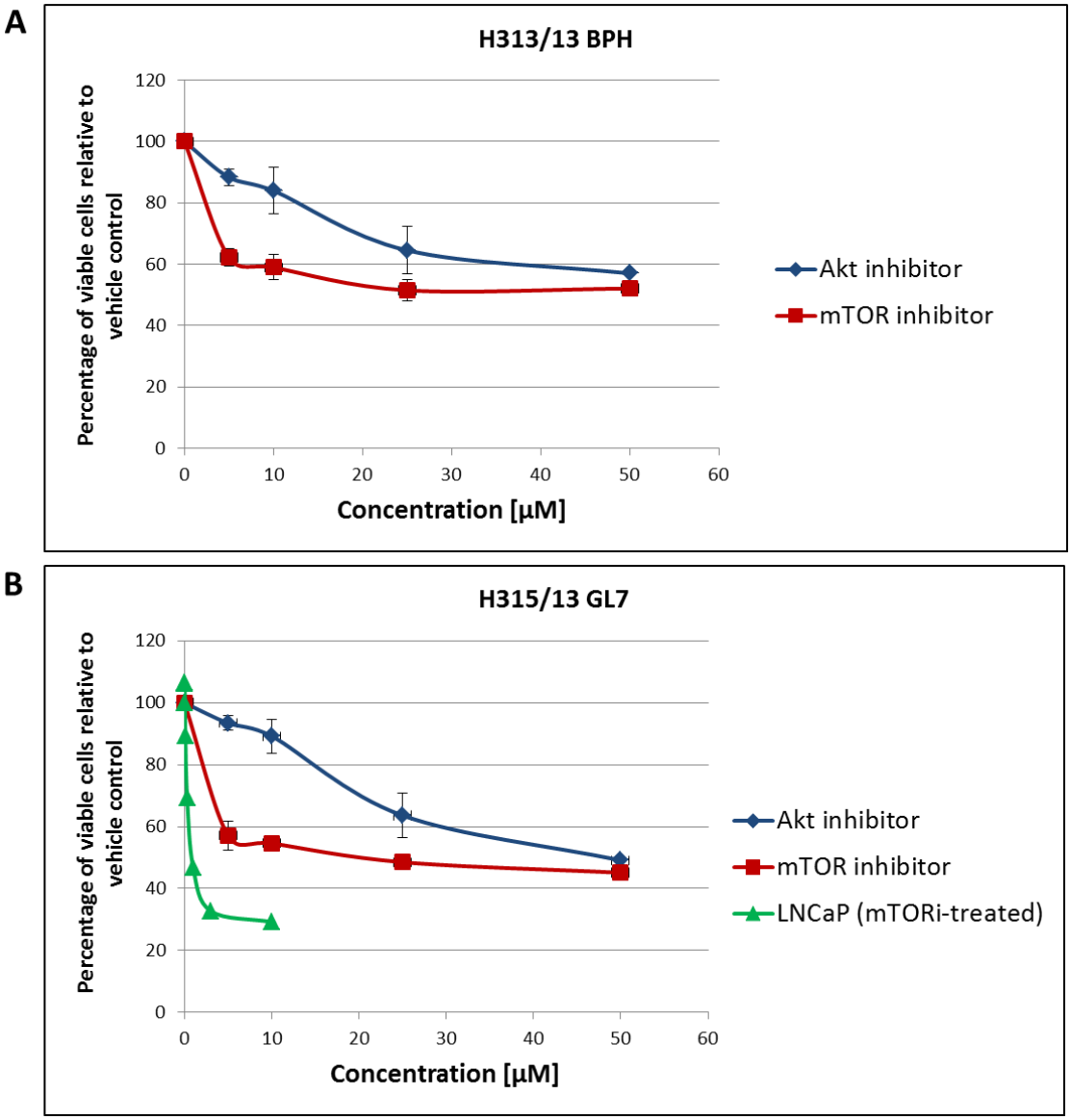

Figure 4.8. MTS viability assay following treatment with AKTi and mTORi.

An MTS assay was performed with H313/13 (BPH) (A) and H315/13 (GL7) (B) primary prostate cultures treated (in triplicate) with increasing concentrations of AKT and mTOR inhibitors, for 72 hours. Cell viability was calculated relative to the vehicle control (0.5% DMSO). LNCaP viability following treatment with up to 10 µM mTORi (green line) was inserted for comparison purposes (B). Error bars represent standard error of the mean, n=3 (SEM).

4.2.2.1. Viability of primary cells subpopulations following treatment with AKTi and mTORi

Due to the heterogeneity of primary prostate cultures, the effect of treatment on cell viability was also assessed in subpopulations of cancer samples. A range of cancer cultures (GL7-GL9) were treated with either 3 µM AKTi, 3 µM mTORi or a combination of 3 µM AKTi + 3 µM mTORi for 72 hours. The cell subpopulations consisting of Stem Cells (SC), Transit Amplifying (TA) and Committed Basal (CB) cells were isolated (as described in section 2.1.2.1.) following treatment and subsequently counted using Trypan blue.

Treatment with 3 µM AKTi reduced the number of stem cells in 3 out of 4 cancer samples with the highest reduction of 78% in H149/12 (GL9), (Figure 4.9 A). A similar decrease in SCs was observed following treatment with 3 µM mTORi in H149/12 cells. However, in one sample (H163/12) a surprising increase of over 50% in SC number was observed following treatment with AKTi (Figure 4.9 A). Treatment with a combination of 3 µM AKTi + 3 µM mTORi resulted in a decrease of SC by 63% and 55% in two GL9 samples, H149/12 and H135/11, respectively (Figure 4.9 A).

An increase of 55% in the number of TA cells, and up to 69% of CB cells was observed following treatment with both inhibitors either as a single agent or in combination in H252/12 (GL7) and H135/11 (GL9) (Figure 4.9 B and C). In contrast, a decrease of up to 62% in TAs and CBs was observed, relative to the vehicle controls, in H163/12 and H149/12 cells (Figure 4.9 B and C).

Figure 4.9. Viability of selected subpopulations of primary prostate cancer samples following treatment with AKTi and mTORi.

Primary prostate cancer samples H252/12 (GL7), H163/12 (GL8), H149/12 (GL9) and H135/11 (GL9) were treated with 3 µM AKTi, 3 µM mTORi or a combination of 3 µM AKTi + 3 µM mTORi for 72 hours. Following treatment, the cells were harvested, sorted into committed basal (CB), transit amplifying (TA) and stem cells (SC) and counted using Trypan blue exclusion. Percentage of viable cells was calculated relative to the vehicle control (0.06% DMSO).

A

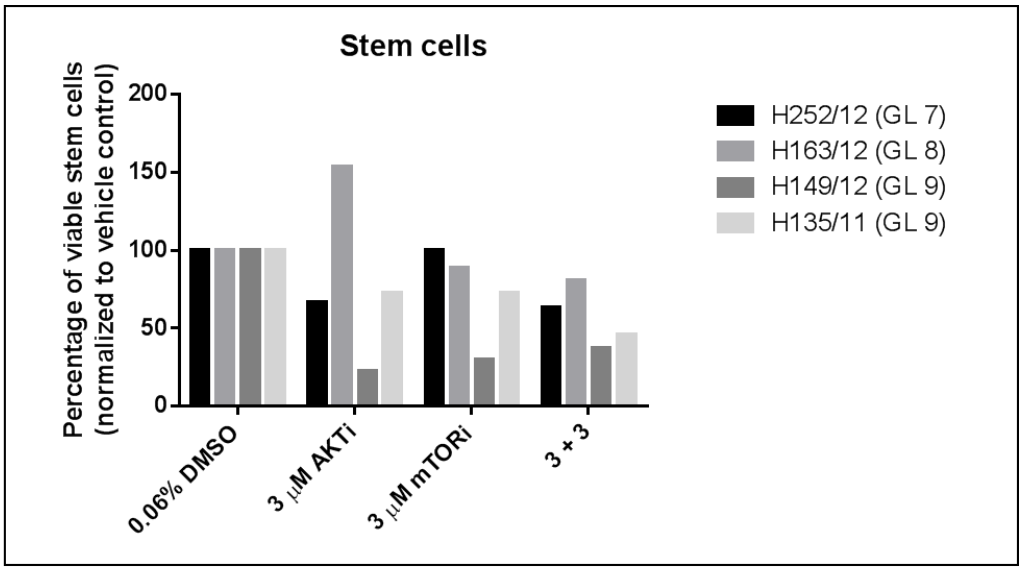
Stem cells
Percentage of viable stem cells (normalized to vehicle control)
200
150
100
50
0
0.06% DMSO
3 μM AKTi
3 μM mTORi
3 + 3
H252/12 (GL 7)
H163/12 (GL 8)
H149/12 (GL 9)
H135/11 (GL 9)

B

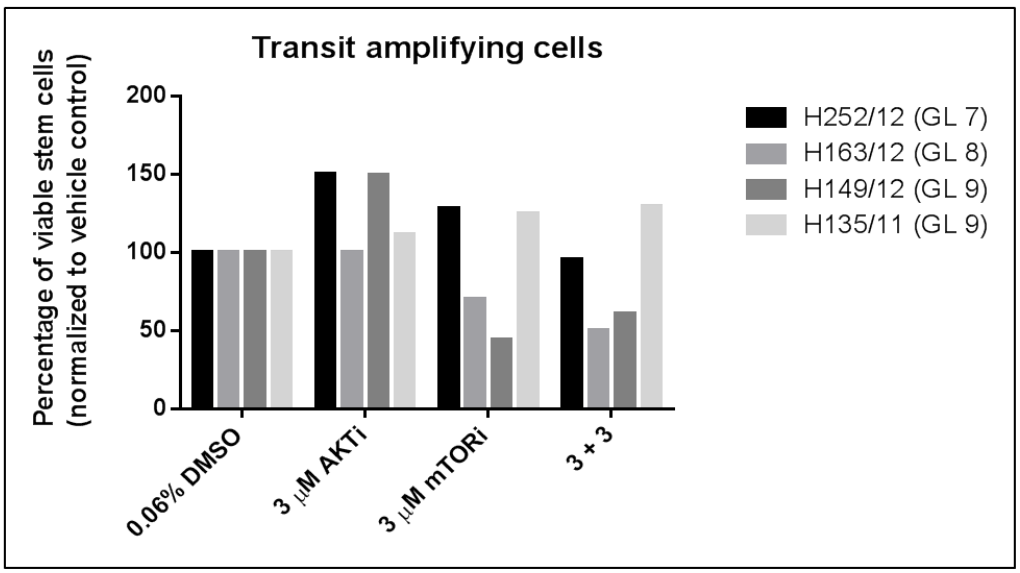
Transit amplifying cells
Percentage of viable stem cells (normalized to vehicle control)
200
150
100
50
0
0.06% DMSO
3 μM AKTi
3 μM mTORi
3 + 3
H252/12 (GL 7)
H163/12 (GL 8)
H149/12 (GL 9)
H135/11 (GL 9)

C

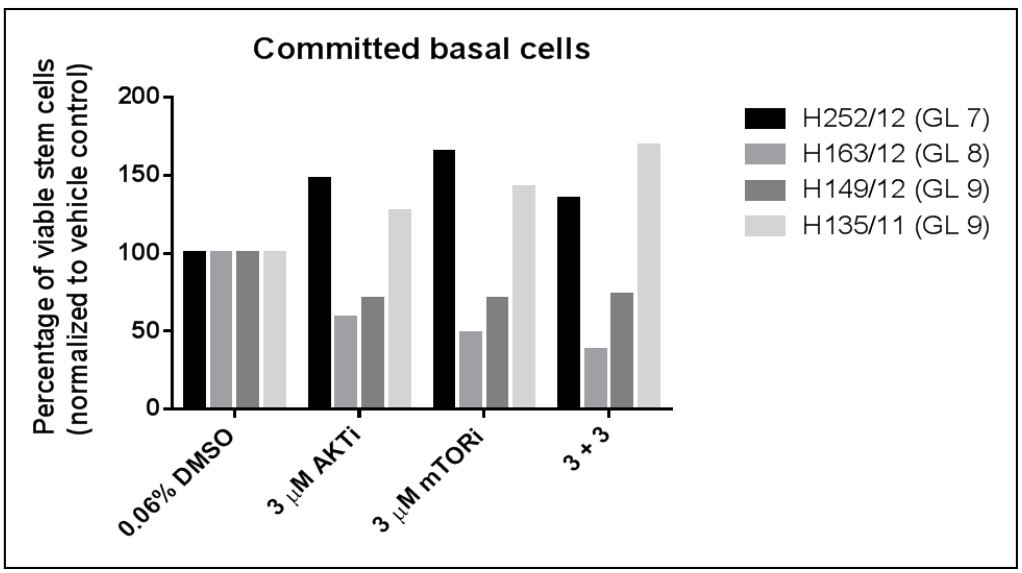
Committed basal cells
Percentage of viable stem cells (normalized to vehicle control)
200
150
100
50
0
0.06% DMSO
3 μM AKTi
3 μM mTORi
3 + 3
H252/12 (GL 7)
H163/12 (GL 8)
H149/12 (GL 9)
H135/11 (GL 9)

The effect of treatment with AKTi and mTORi on stem-like cells population was also determined using flow cytometry. A prostate cancer culture H317/12 (GL7) was treated with 10 µM AKTi, 10 µM mTORi and a combination of 10 + 10 for 72 hours. The results showed an increase of 50% in a number of CD133-positive cells following treatment with mTORi and with a combination of 10+10 (Figure 4.10). However, after treatment with AKTi, a decrease of 37.5% in stem-like cells population was observed, relative to the vehicle control. Moreover, an increase in non-viable CD133-positive cells was evident following treatment with either inhibitor alone or a combination (Figure 4.10, bottom panel).

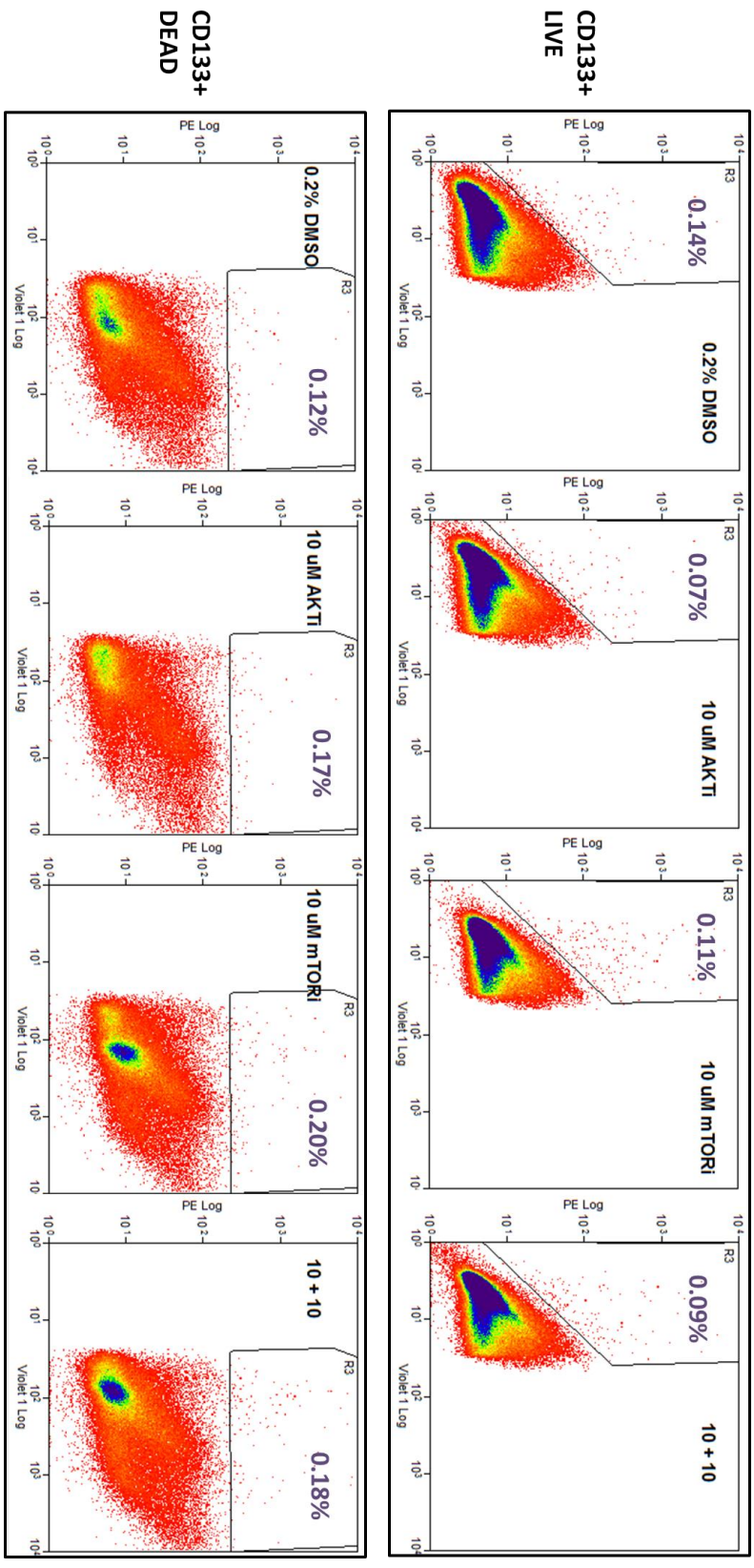

Figure 4.10. Influence of treatment with AKTi and mTORi on stem-like cell population.

Prostate cancer cells (H317/13) were treated with 10 µM AKTi, mTORi or a combination of 10 + 10 for 72 hours. The cells were then collected and stained with anti-CD133 antibody and analysed on a flow cytometer. Vehicle control cells were treated with 0.2% DMSO.

Taken together, the cell viability data showed a patient-specific variability in primary cultures' response to treatment which was not dependent on Gleason grade. However, a 72-hour incubation with the inhibitors significantly decreased cell viability in comparison to 24-hour treatment. Moreover, primary prostate cancer cultures showed much lower susceptibility to AKTi and mTORi than prostate cancer cell lines, for example LNCaP, which had a 27-fold higher EC_{50}.

4.2.3. Autophagy is activated in cells treated with the AKT inhibitor

To follow up the observation of changes in cell morphology and to determine the effect on cell fate following treatment with the inhibitors, expression of an apoptosis marker (cleaved PARP) and an autophagy marker (LC3 B) were assessed by western blotting. A prostate cancer culture H278/13 (GL7) was treated with increasing concentrations (10 – 50 μM) of AKTi and mTORi either alone or in combination.

The results showed that there was no increase in expression of cleaved PARP, suggesting that the cells had not undergone apoptosis following treatment with either compound (Figure 4.11). However, there was a dose-dependent increase in LC3 B after treatment with the AKTi, indicating that the cells had activated autophagy; which is primarily a survival mechanism allowing cells to avoid death (Figure 4.11).

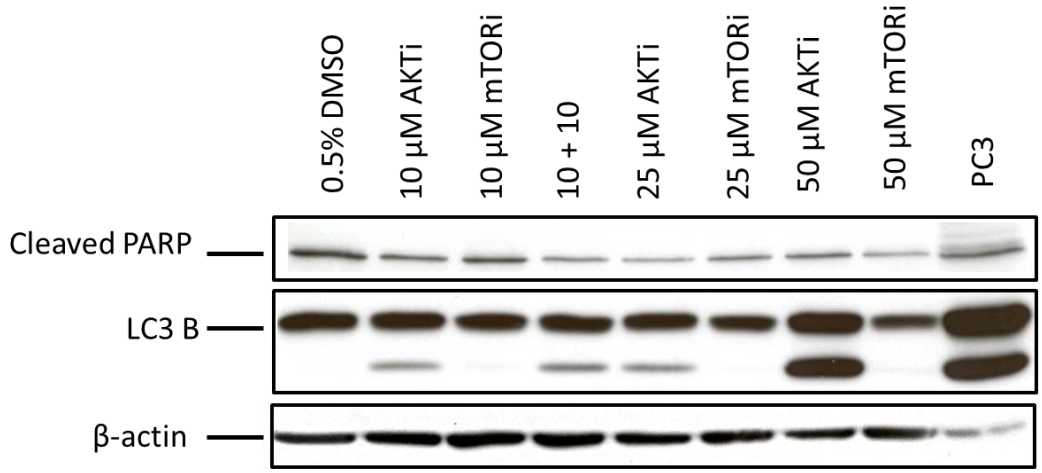

Figure 4.11. Expression of an apoptosis and an autophagy marker following treatment with AKTi.

A primary prostate culture H278/13 (GL7) was treated with up to 50 µM concentration of either AKTi or mTORi or a combination of 10 µM AKTi + 10 µM mTORi for 72 hours. Following the treatment, expression of an apoptosis marker, cleaved PARP, and an autophagy marker, LC3 B, were determined using western blotting. Whole cell lysates were prepared and 20 µg of protein was loaded per lane onto a 10% SDS gel, electrotransferred onto PVDF membranes and stained. Lysate of PC3 cells was a positive control for expression of LC3 B. Staining with β-actin antibody was used as a loading control.

In order to confirm whether treatment with AKTi induces autophagy, cancer H310/13 cells were treated with 25 µM AKTi or 25 µM mTORi for 96 hours and expression of LC3 B analysed by immunofluorescence.

The results showed an increase in vacuolisation of the cells treated with AKTi, but not with mTORi (Figure 4.12 A), which correlated with expression of the autophagy marker in those cells (Figure 4.12 B).

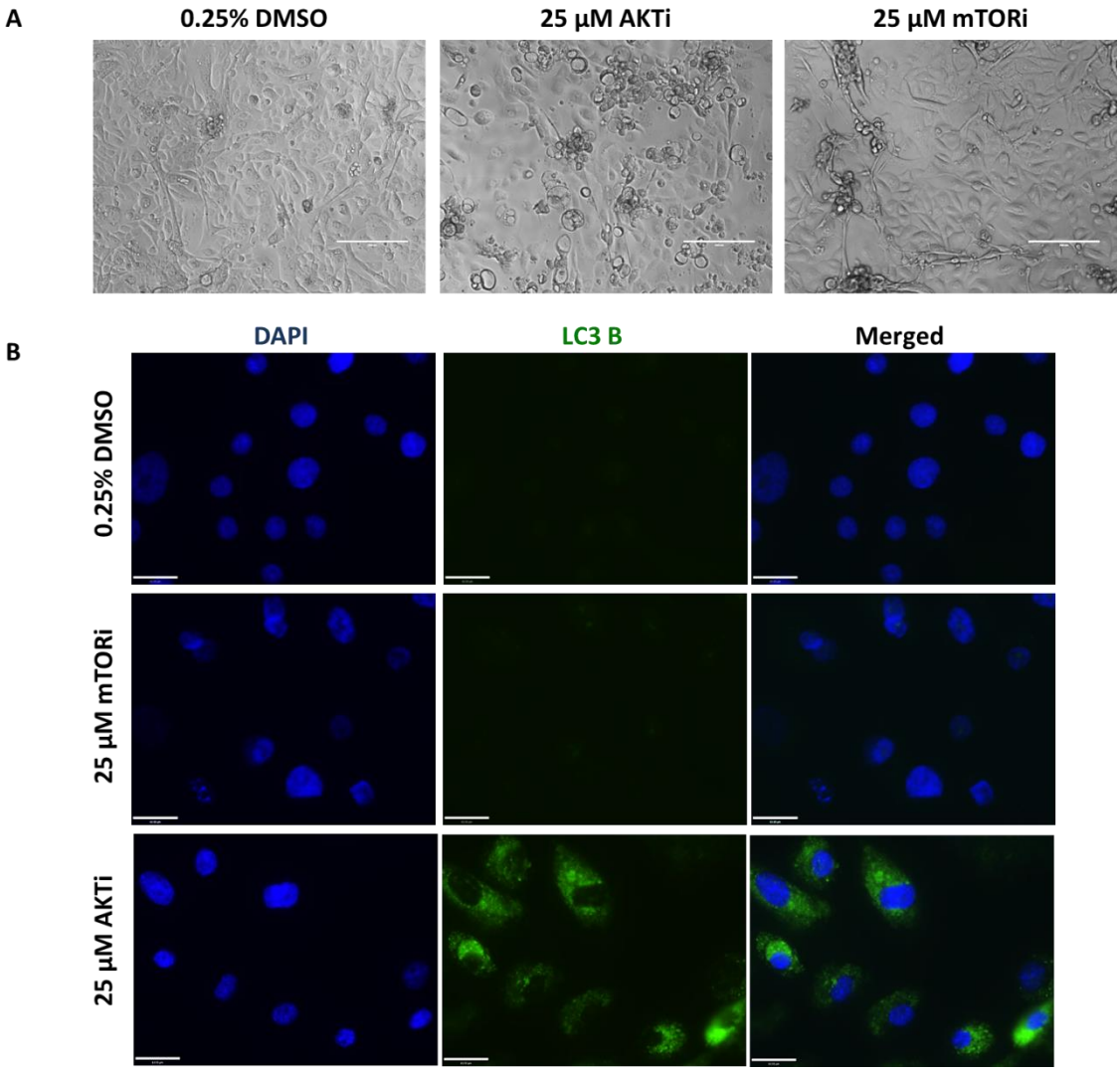

Figure 4.12. LC3 B expression in H310/13 (GL7) cells following treatment with AKTi and mTORi.

Primary prostate cancer H310/13 (GL7) cells were treated with 25 µM AKTi or 25 µM mTORi for 96 hours. Phase contrast images were taken following the treatment (A). Expression of an autophagy marker, an LC3 B, was determined using Immunofluorescence (B). The cells were seeded into collagen I-coated 8-well chamber slides and treated with either 25 µM AKTi or 25 µM mTORi for 96 hours and then fixed in 4% PFA. The cells were then permeabilised with 0.25% Triton-100, washed with PBS, blocked with 10% goat serum and incubated with an LC3 B antibody overnight. Following staining with primary antibody, the cells were washed with PBS, incubated with secondary goat-anti-rabbit antibody for 1 hour, washed with PBS and mounted with mounting solution containing DAPI. Control cells were treated with 0.25% DMSO. Scale bar on the phase contrast images represents 200 µm and on the fluorescent images 63 µm.

4.2.4. Phosphorylation status of selected biomarkers downstream from AKT and mTOR following treatment

The number of cells expressing phospho-AKT and phospho-S6 (biomarkers downstream of AKT and mTOR kinases), was determined by flow cytometry following 72-hour treatment with increasing concentrations of inhibitors of the pathway.

A primary prostate culture H317/13 (GL7) was treated with either 10 µM AKTi, 10 µM mTORi or a combination of 10 + 10 for 72 hours. The phosphorylation status of AKT and S6 was determined following treatment. The results showed an increase of 58.4% in the number of cells expressing phospho-AKT following treatment with 10 µM AKTi (Figure 4.13 A). In contrast, a decrease of 11.1% in phospho-AKT was observed after treatment with 10 µM mTORi. Moreover, treatment with a combination of 10 + 10 resulted in an increase of phospho-AKT of 41.2% relative to the vehicle control, which was a decrease of 17.2% in comparison to AKTi-treated cells (Figure 4.13 A).

Expression of phospho-S6, an indirect substrate of mTORC1, increased by 3.5% and 2% following treatment with 10 µM AKTi and 10 µM mTORi, respectively (Figure 4.13 B). However, there was a 5.5% decrease in phospho-S6 expression after treatment with a combination of 10 + 10, relative to the vehicle control (Figure 4.13 B).

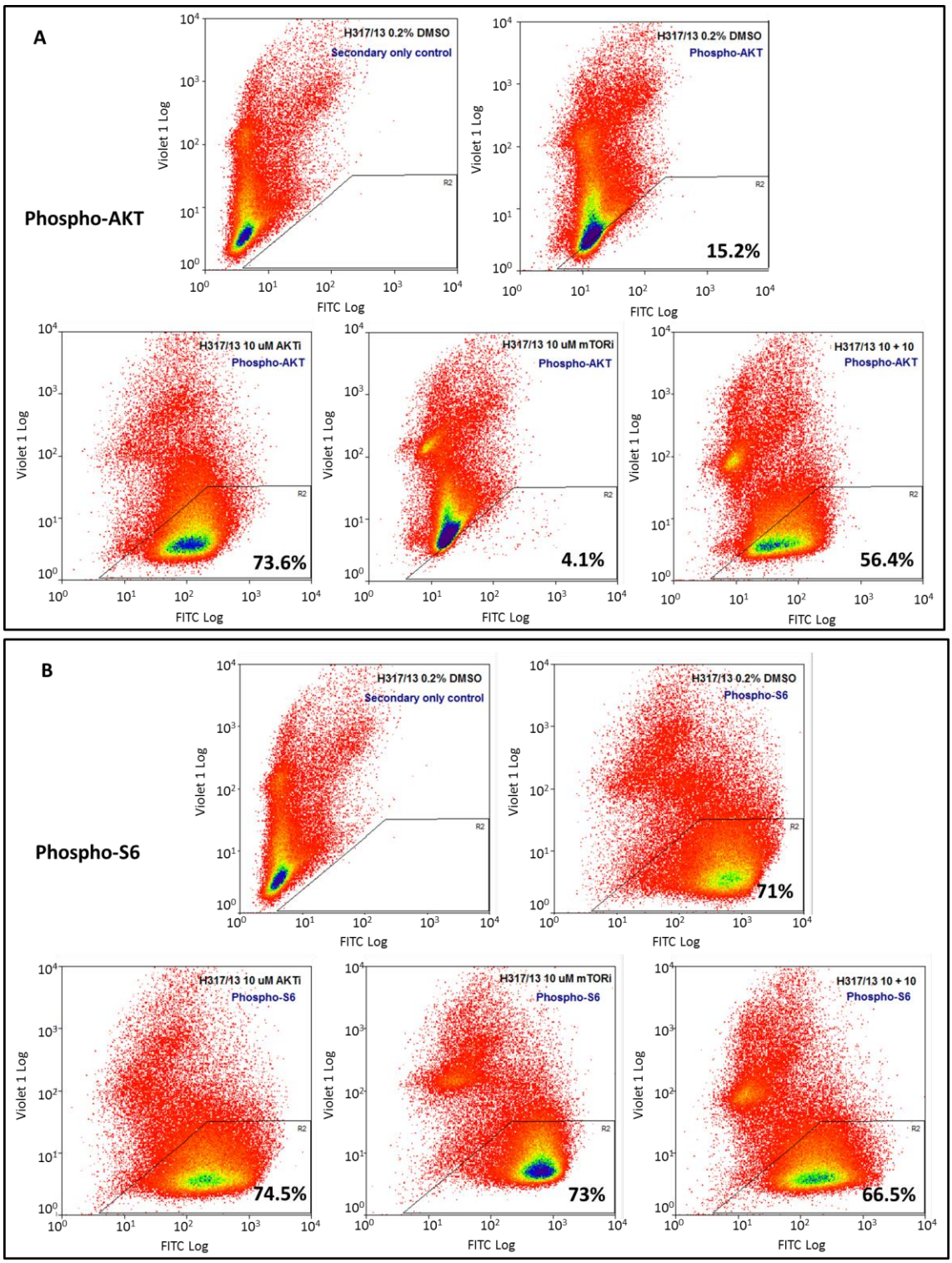

Figure 4.13. Biomarkers expression following treatment with AKTi and mTORi.

Primary prostate cancer cells H317/13 (GL7) were treated with 10 µM AKTi, 10 µM mTORi or a combination of 10 + 10 for 72 hours. Following treatment cells were harvested, fixed with 4% PFA, permeabilised with methanol and stained with phospho-AKT (Ser473) and phospho-S6 (Ser235/236) antibodies; negative control cells were stained with FITC-conjugated secondary goat anti-rabbit antibody. Vehicle control cells were treated with 0.1% DMSO.

4.2.4.1. Biomarker expression following withdrawal of the inhibitors

Next, the effect of inhibitors' withdrawal on the phosphorylation of the biomarkers was tested to determine whether therapeutic effect was reversible, which is clinically relevant. Patients receiving treatment, for example chemotherapy which is toxic to cancer cells and to normal cells, need breaks in drugs delivery for recovery. It is important to establish whether after inhibitors' withdrawal activity of the pathway increases. This was assessed using western blotting. A primary cancer culture H210/12 (GL7) was treated with 1 µM AKTi or 1 µM mTORi for 5 days, after which fresh media (without inhibitors) was added and the cells were incubated for a further 48 hours (Figure 4.14 A).

The results showed a 26-fold increase in phospho-AKT and a 9.4-fold increase in phospho-PRAS40 after 5 days treatment with AKTi. However, after withdrawal of the inhibitor, phospho-AKT decreased to 12.5-fold and phospho-PRAS40 to 3.6-fold in comparison to the control (Figure 4.14 B).

Five-day treatment with 1 µM mTORi decreased both phospho-AKT and phospho-S6 levels down to 0.6-fold, relative to the vehicle control. Interestingly, a withdrawal of mTORi increased phospho-AKT expression by 2 fold above the vehicle control level, but phospho-S6 expression remained at a comparable level (Figure 4.14 B).

The results suggest that inhibitory activity of AKTi and mTORi is reversible.

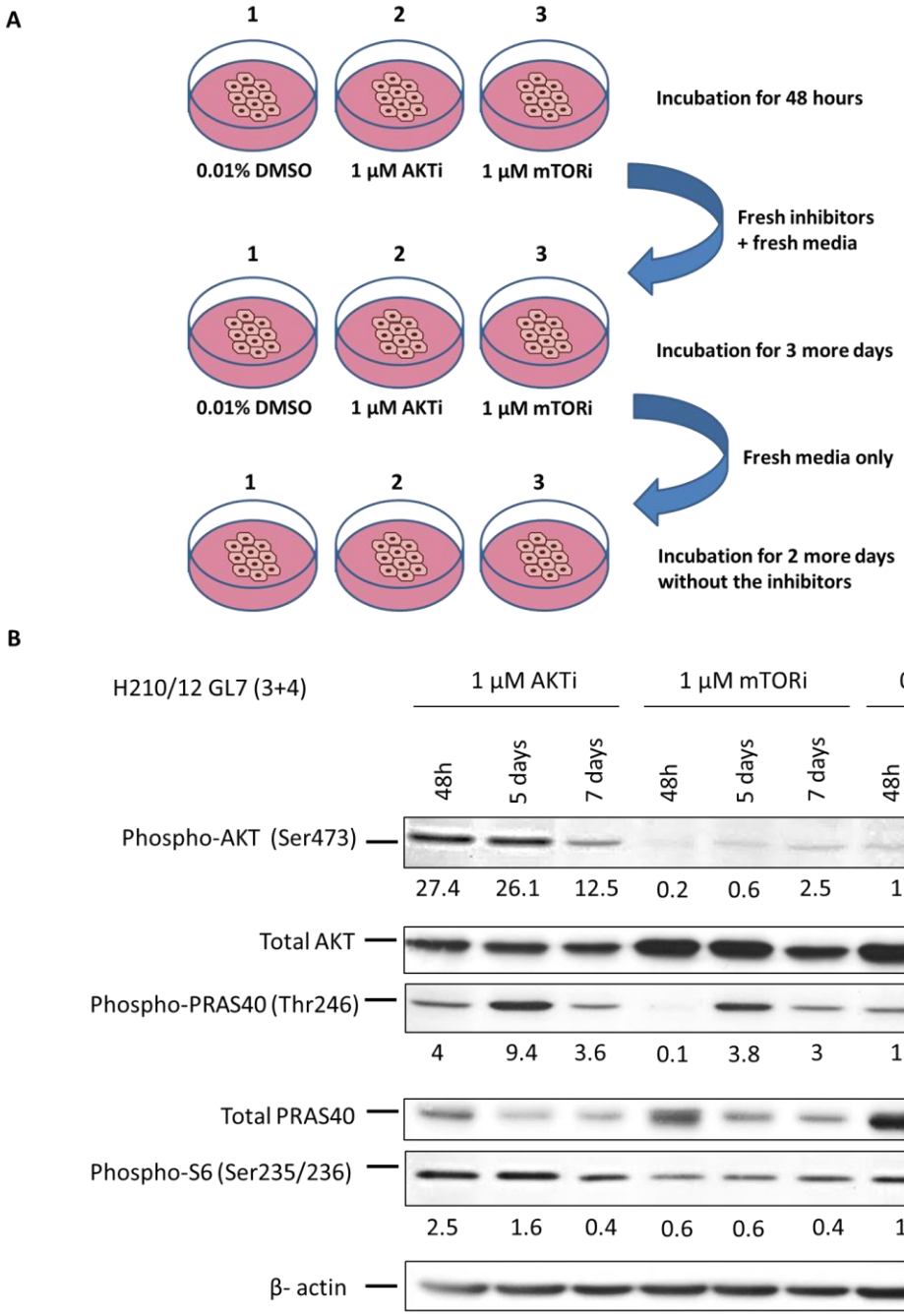

Figure 4.14. Expression of the phospho-biomarkers following treatment and withdrawal of the inhibitors.

Prostate cancer cells H210/12 were seeded 24 hours before the treatment with 1 µM AKTi or 1 µM mTORi for 5 days followed by inhibitors' withdrawal (after 5th day) and replacement with fresh culture media for further 2 days (A). Treated cells were collected and whole cell lysates prepared. 20 µg of protein was loaded per lane onto a 10% SDS gel, electrotransferred onto a PVDF membrane and immunoblotted with antibodies against phospho-AKT (Ser473), total AKT, phospho-PRAS40 (Thr246), total PRAS40 and phospho-S6 (Ser235/236). Staining with β-actin antibody was used as a loading control. The bands were quantified using Image J software.

4.2.4.2. Presence or absence of EGF in medium alters biomarkers expression following treatment

The effect of EGF in the culture medium on expression of PI3K pathway biomarkers was determined in a BPH sample (H268/12) and a cancer sample (H282/13) treated with 5 µM AKTi, 5 µM mTORi or a combination of 5 + 5. This experiment was carried out to determine whether EGF, which is required for primary cell expansion, affected the outcome of treatment with the inhibitors.

The results showed that in BPH culture the presence of EGF, phospho-AKT and phospho-S6 expression increased by 2 fold compared to cells grown without EGF (Figure 4.15 A). In contrast, phospho-ERK1/2 expression was higher in the absence of EGF (2 fold, relative to β-actin) than in the presence of EGF (1.4 fold). When cells were treated with AKTi a 9-fold increase in phospho-AKT was observed in the presence of EGF whereas in the absence of EGF a 12.1-fold increase in expression was observed relative to the vehicle control (Figure 4.15 A). Phosphorylation of ERK1/2 increased by 2.8-fold following treatment with AKTi (in the presence of EGF) and by 1.2 in the absence of EGF. However, phosphorylation of S6 remained at a comparable level following treatment either in the presence or absence of EGF (Figure 4.15 A). In cancer culture phospho-ERK1/2 levels were higher when cells were treated in the presence of EGF in comparison to cells treated in the absence of EGF (Figure 4.15 B). However, levels of cleaved PARP and LC3B were similar in cultures treated in the presence and in the absence of EGF. The difference in bands quantification values was mainly due to understated β-actin level in the first lane of the blot (Figure 4.15 B).

Taken together, the data shows that there is a difference in biomarker expression when cells are cultured with EGF, but this effect was not significant ($p=0.22$ for phospho-AKT, $p=0.08$ for phospho-ERK1/2 and $p=0.62$ for phospho-S6). In subsequent experiments, EGF was included in the culture of primary cells.

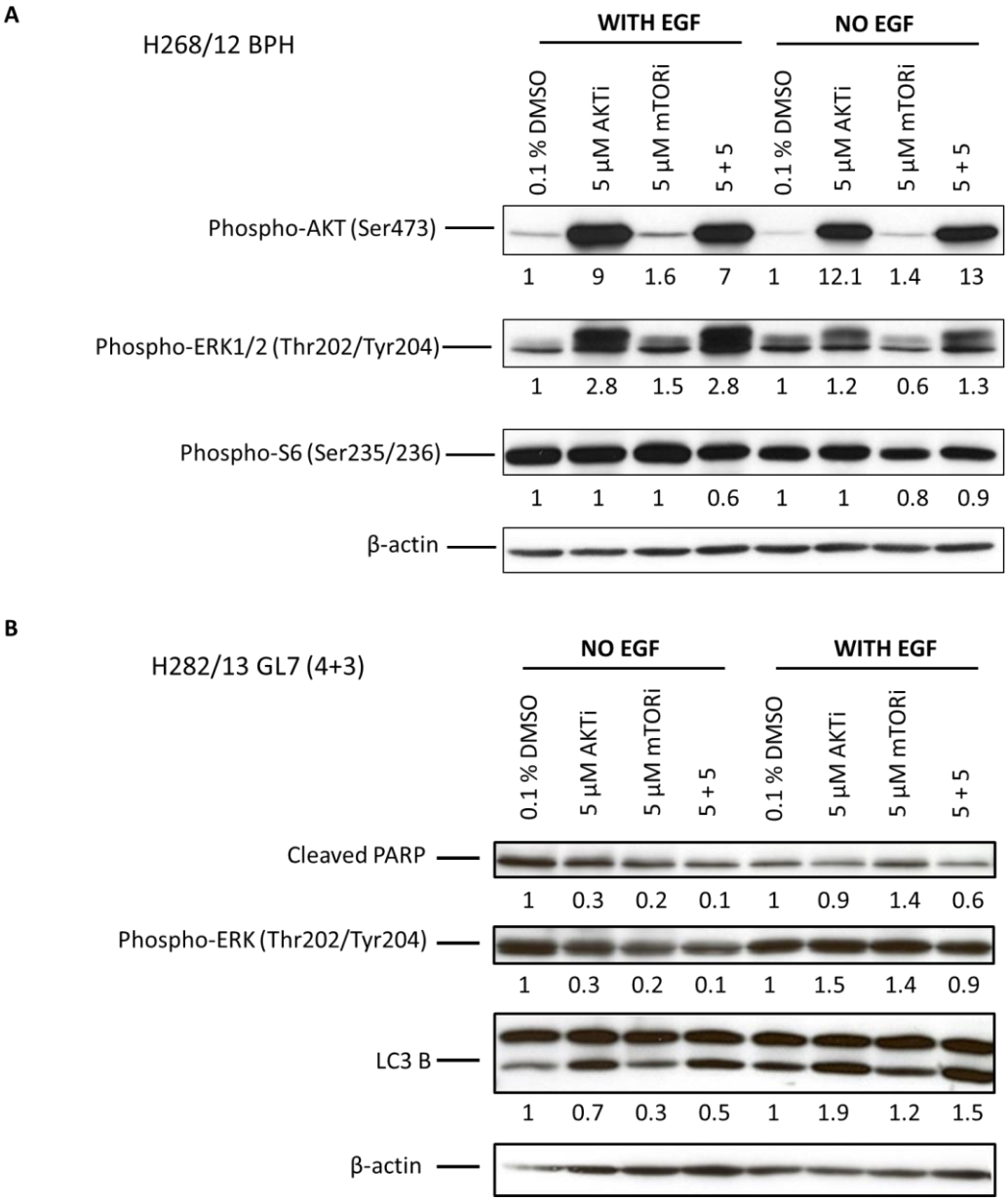

Figure 4.15. Phospho-biomarker expression analysis following treatment with AKTi and mTORi in presence or absence of EGF in culture media.

A BPH (H268/12) (A) and a cancer (H282/13) (B) cultures were treated with either 5 µM of AKTi or 5 µM mTORi alone or in a combination of 5 + 5 for 72 hours. Cells were subsequently collected, whole cell lysates prepared and quantified. 20 µg of protein was loaded per lane, electrotransferred to PVDF membrane and stained with antibodies against phospho-AKT (Ser473), phospho-ERK1/2 (T202/Tyr204) phospho-S6 (Ser235/236), cleaved PARP and LC3 B. Staining with β-actin antibody was used as a loading control. The bands were quantified using Image J software and the expression levels normalized to the vehicle control.

4.2.5. Changes in colony forming efficiency after treatment with AKTi and mTORi

In order to establish whether prostate stem-like cells are dependent on the PI3K/AKT/mTOR pathway for survival, an ability of the stem-like cells and progenitor cells to form colonies was tested following treatment with AKTi and mTORi.

Cells derived from patients with cancer Gleason 9 (H149/12) and CRPC (H271/13) were treated with either 3 µM or 5 µM of AKTi or mTORi alone or with a combination of 3 + 3 or 5 + 5. The cells were treated for 72 hours after which they were sorted into stem cells (SC), transit amplifying (TA) and committed basal (CB) cells (as described in section 2.1.2.1.). The cells were then plated and incubated without the inhibitors and colony forming efficiency (CFE) determined.

AKTi treatment increased the number of colonies founded by stem cells, but the effect was only significant in 1 of 2 cultures examined and with the higher concentration of AKTi. A similarly significant increase in CFE of stem cells was observed with mTORi. However, this increase was abolished with a higher concentration of mTORi. A combination of both inhibitors had little effect on CFE of stem cells (Figure 4.16).

In contrast, transit amplifying cells showed a decrease in colony forming ability following treatment, down to approximately 79% and 73% (of control) in H271/13 and H149/12, respectively, when treated with AKTi alone (Figure 4.16 A and B, middle row). Treatment with mTORi alone decreased number of colonies to around 82-83% relative to vehicle control, in both patients. However, simultaneous treatment with both inhibitors showed only modest decreases: down to approximately 93% in H271/13 and 83% in H149/12, in comparison to vehicle control (Figure 4.16 A and B, middle row).

Although committed basal cells' potential to form colonies is lower than SCs and TAs, treatment with either inhibitor alone or a combination reduced CFE. Indeed no colonies were observed from H271/13 following treatment with 5 µM AKTi or 5 + 5 (Figure 4.16 B, bottom row).

In summary, a surprising increase in CFE was observed in stem cells of both cultures, which was significant in mTORi-treated H149/12 cells (p value=0.03) and in AKTi-treated H271/13 cells (p value=0.05), relative to the vehicle control. In contrast, a decrease in CFE of TA cells was observed, which was significant in H149/12 cells treated with 3 µM AKTi (p value= 0.01), relative to the vehicle control.

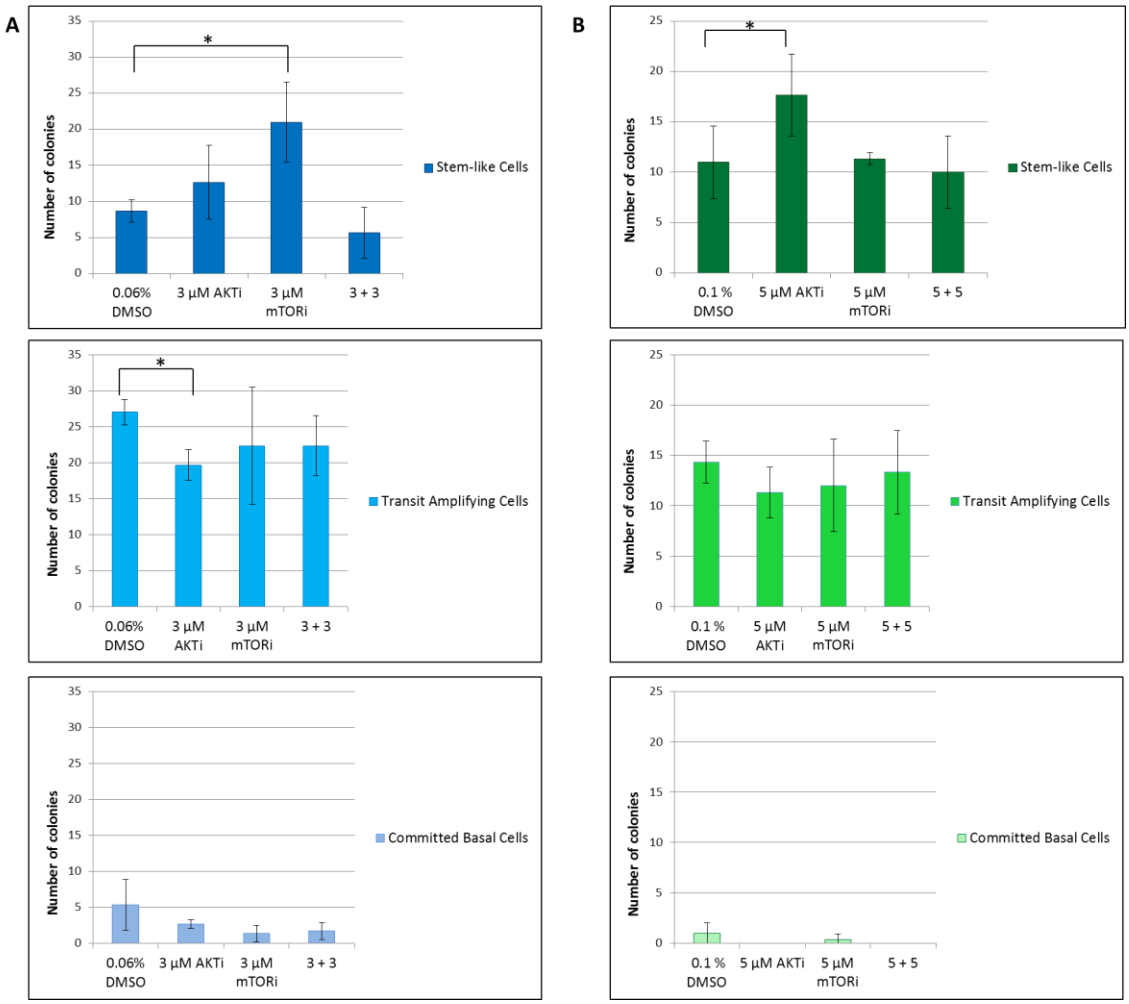

Figure 4.16. Colony forming efficiency (CFE) after treatment with AKTi and mTORi.

Primary cancer cultures H149/12 (GL9) (A) and H271/13 (CRPC) (B) were treated with 3 µM or 5 µM AKTi or mTORi alone or with a combination of 5 + 5 or 10 + 10. Following 72-hour' treatment, the cell cultures were sorted for stem cells (SC), transit amplifying (TA) and committed basal (CB) cells. The sorted cells were then plated, in triplicate, onto collagen I-coated 35 mm-dishes, at a density of 100 cells per dish in the presence of irradiated STO feeder cells. The cells were incubated for 10 to 14 days and colonies of >32 cells (5 population doublings) were counted.

4.2.6. Cell cycle distribution remains unaffected after treatment with both inhibitors as single agents or in combination

To determine whether the inhibitors affected the cell cycle, primary cells were treated for 72 hours, with 5 µM AKTi, 5 µM mTORi, and a combination of 5 + 5. The cells were subsequently stained with propidium iodide and cell cycle distribution was determined by flow cytometry. The results showed no significant change between vehicle controls (0.1% DMSO) and cells treated with either inhibitor or with a combination of 5 µM AKTi and 5 µM mTORi (Figure 4.17). However, in 1 out of 3 samples, H278/13 cancer cells, an increase of 8% in cells in G1 phase and 9% of cells in G2M phase was observed following treatment with AKTi and a combination of 5 µM AKTi + 5 µM mTORi, respectively (Figure 4.17 B).

Taken together, the results show that treatment with AKTi and mTORi, either alone or in combination, does not induce growth arrest in primary prostate cultures at this concentration range.

Figure 4.17. Cell cycle distribution after treatment with inhibitors.

Cell cycle distribution analysis was performed after 72-hour treatment with 5 µM AKTi, 5 µM mTORi and 5 + 5 combination on primary cultures in H277/13 (BPH) (A), H282/13 (cancer GL7) (B) and in H271/12 (CRPC) (C). Following treatment cells were harvested, fixed with 70% ice-cold ethanol, and stained with propidium iodide and analysed by flow cytometry. Control cells were treated with 0.1% DMSO.

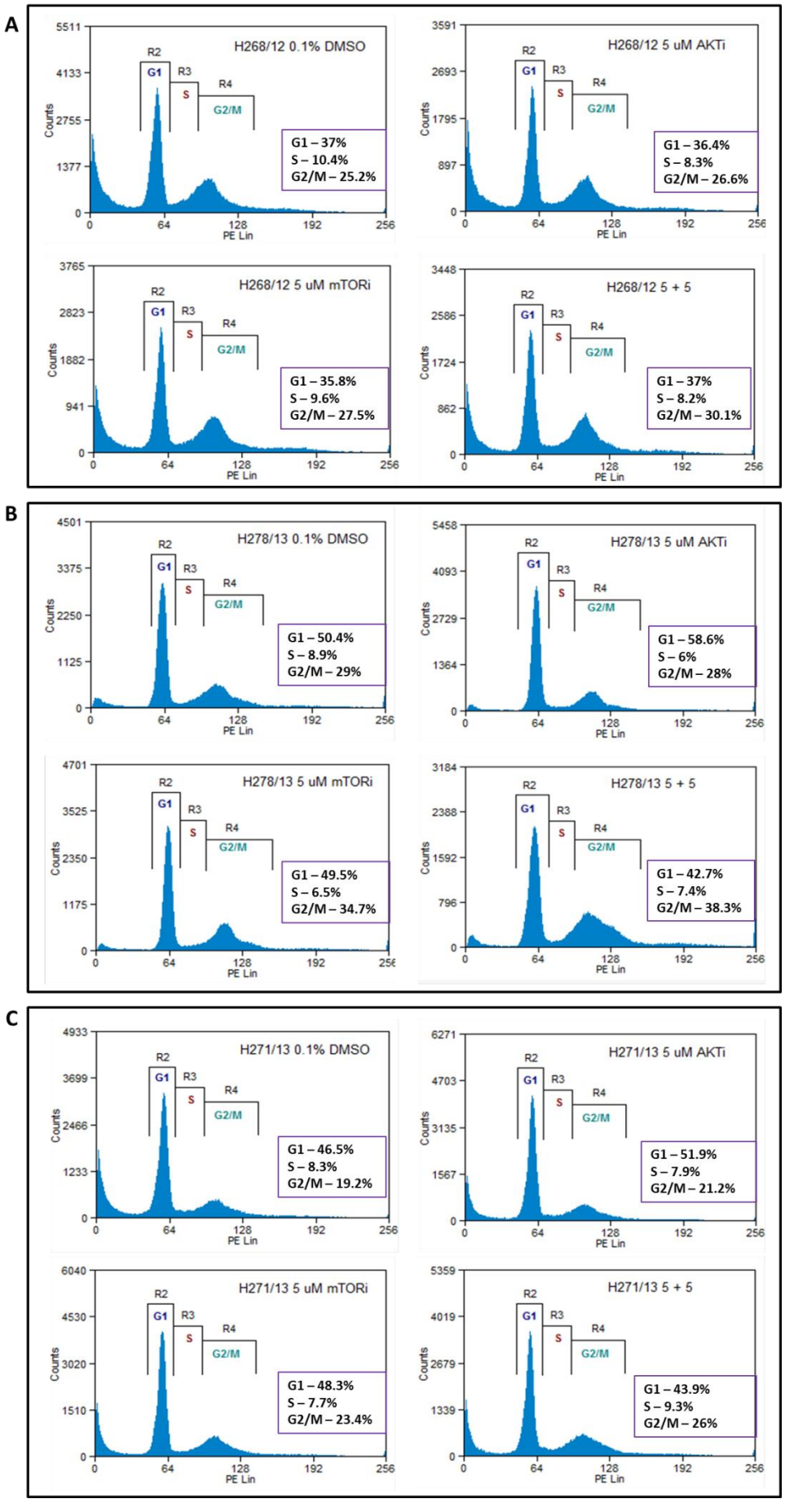
A
H268/12 0.1% DMSO
G1 – 37%
S – 10.4%
G2/M – 25.2%
H268/12 5 uM AKTi
G1 – 36.4%
S – 8.3%
G2/M – 26.6%
H268/12 5 uM mTORi
G1 – 35.8%
S – 9.6%
G2/M – 27.5%
H268/12 5 + 5
G1 – 37%
S – 8.2%
G2/M – 30.1%
B
H278/13 0.1% DMSO
G1 – 50.4%
S – 8.9%
G2/M – 29%
H278/13 5 uM AKTi
G1 – 58.6%
S – 6%
G2/M – 28%
H278/13 5 uM mTORi
G1 – 49.5%
S – 6.5%
G2/M – 34.7%
H278/13 5 + 5
G1 – 42.7%
S – 7.4%
G2/M – 38.3%
C
H271/13 0.1% DMSO
G1 – 46.5%
S – 8.3%
G2/M – 19.2%
H271/13 5 uM AKTi
G1 – 51.9%
S – 7.9%
G2/M – 21.2%
H271/13 5 uM mTORi
G1 – 48.3%
S – 7.7%
G2/M – 23.4%
H271/13 5 + 5
G1 – 43.9%
S – 9.3%
G2/M – 26%
Counts
PE Lin
R2
R3
R4
G1
S
G2/M

4.3. Cross-talk between PI3K/AKT/mTOR and Ras/MEK/ERK pathway

4.3.1. Phospho-ERK1/2 levels are increased following treatment with AKTi

In order to determine whether inhibition of the PI3K/AKT/mTOR pathway affects the activity of the MAP kinase pathway, the phosphorylation status of ERK1/2 was assessed following a 72-hour treatment (of primary prostate cultures) with AKT and mTOR inhibitors.

Western blotting performed on a BPH (H277/13) and a cancer sample (H278/13, GL7) showed an increase in phospho-ERK1/2 following treatment with the AKTi, but not the mTORi. However, treatment of cells with a combination of both inhibitors increased phospho-ERK1/2 expression (Figure 4.18 A). An increase in phospho-ERK1/2 also correlated with increased expression of an autophagy biomarker (LC3 B).

To follow up this observation, another primary cancer sample (H282/13; GL7) was treated with higher concentrations (10-50 μM) of both inhibitors (for 72 hours) to assess if the increase in MAPK activity was dose-dependent. The results showed a dose-dependent increase in phosphorylation levels of ERK1/2 when the cells were treated with AKTi, but not with mTORi (Figure 4.18 B). This indicates that a cross-talk exists between the PI3K/AKT/mTOR and the MAPK pathway in human prostate primary epithelial cells, and that inhibition of the PI3K pathway alone might not be sufficient to treat prostate cancer.

Figure 4.18. Phospho-biomarkers expression in prostate primary cultures following treatment with AKTi and mTORi.

Primary BPH (H277/13) and cancer cells (H278/13) (A) and H282/13 cancer cells (B) were treated for 72 hours with increasing concentrations of AKTi and mTORi or a combination of both. Whole cell lysates were subsequently prepared and 20 µg of protein was loaded per lane onto a 10% SDS gel, electrotransferred onto PVDF membranes and stained for the biomarkers indicated (phospho-AKT, total AKT, phospho-ERK1/2, total ERK1/2, phospho-S6, total S6, cleaved PARP and LC3 B). Vehicle control cells were treated with 0.1% DMSO (A) or 0.5% DMSO (B). Staining with β-actin antibody was used as a loading control. The bands were quantified using Image J software and the expression normalized to the vehicle control (A) or to β-actin (B).

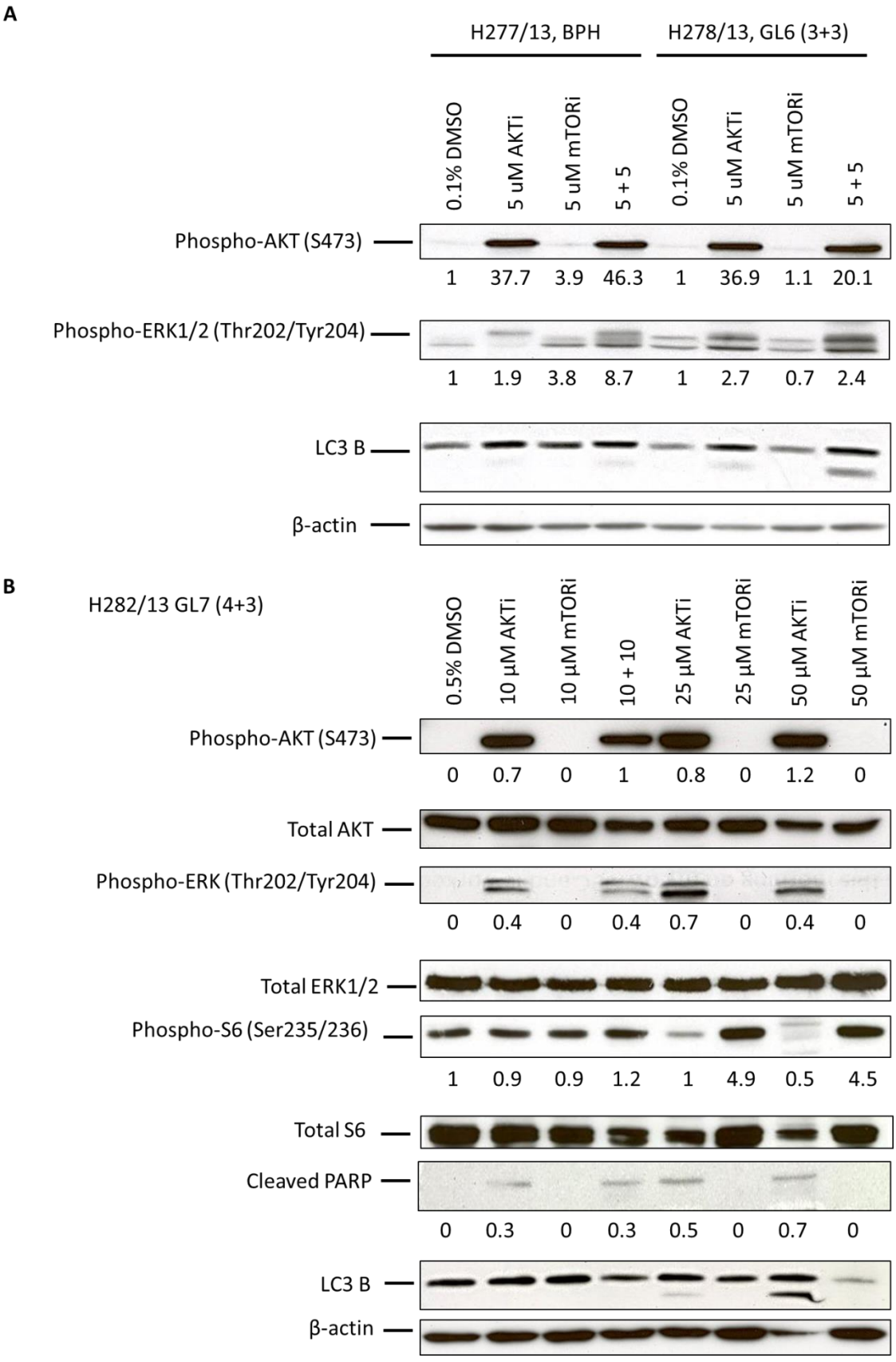
A
H277/13, BPH
H278/13, GL6 (3+3)
0.1% DMSO
5 uM AKTi
5 uM mTORi
5 + 5
0.1% DMSO
5 uM AKTi
5 uM mTORi
5 + 5
Phospho-AKT (S473)
1 37.7 3.9 46.3 1 36.9 1.1 20.1
Phospho-ERK1/2 (Thr202/Tyr204)
1 1.9 3.8 8.7 1 2.7 0.7 2.4
LC3 B
β-actin
B
H282/13 GL7 (4+3)
0.5% DMSO
10 µM AKTi
10 µM mTORi
10 + 10
25 µM AKTi
25 µM mTORi
50 µM AKTi
50 µM mTORi
Phospho-AKT (S473)
0 0.7 0 1 0.8 0 1.2 0
Total AKT
Phospho-ERK (Thr202/Tyr204)
0 0.4 0 0.4 0.7 0 0.4 0
Total ERK1/2
Phospho-S6 (Ser235/236)
1 0.9 0.9 1.2 1 4.9 0.5 4.5
Total S6
Cleaved PARP
0 0.3 0 0.3 0.5 0 0.7 0
LC3 B
β-actin

4.3.2. Treatment of primary cultures with a combination of AKT and MEK1/2 inhibitors

4.3.2.1. A combination of AKTi with MEKi further increases phospho-ERK1/2 expression

In order to determine whether MEK1/2 inhibitor (MEKi) showed any activity in primary prostate cultures, selected cancer samples were treated with increasing concentrations (0.1 – 25 μM) of a MEKi for 72 hours.

Phase contrast images were then taken to determine the effect on morphology and density of the cells. At a concentration ≥ 1 μM a decrease of approximately 30-40%, in cell density was observed. Cell morphology was also changed; the cells appeared larger and their shape was more elongated comparing to vehicle controls (Figure 4.19 A).

The phosphorylation status of ERK1/2, which is downstream of MEK1/2, as well as phospho-AKT and LC3 B, was determined following treatment using western blotting (Figure 4.19 B). The results showed a dose-dependent decrease in phospho-ERK1/2 expression after treatment with the MEKi. A concentration of 1 μM was sufficient to completely abolish expression of phospho-ERK1/2. However, an increase in phospho-AKT levels (2.8-fold at 0.5 μM MEKi) was observed at the lower concentration range (0.1 - 1 μM) of MEKi, which might indicate an increase in activity of the PI3K pathway in response to inhibition of the MAPK signalling.

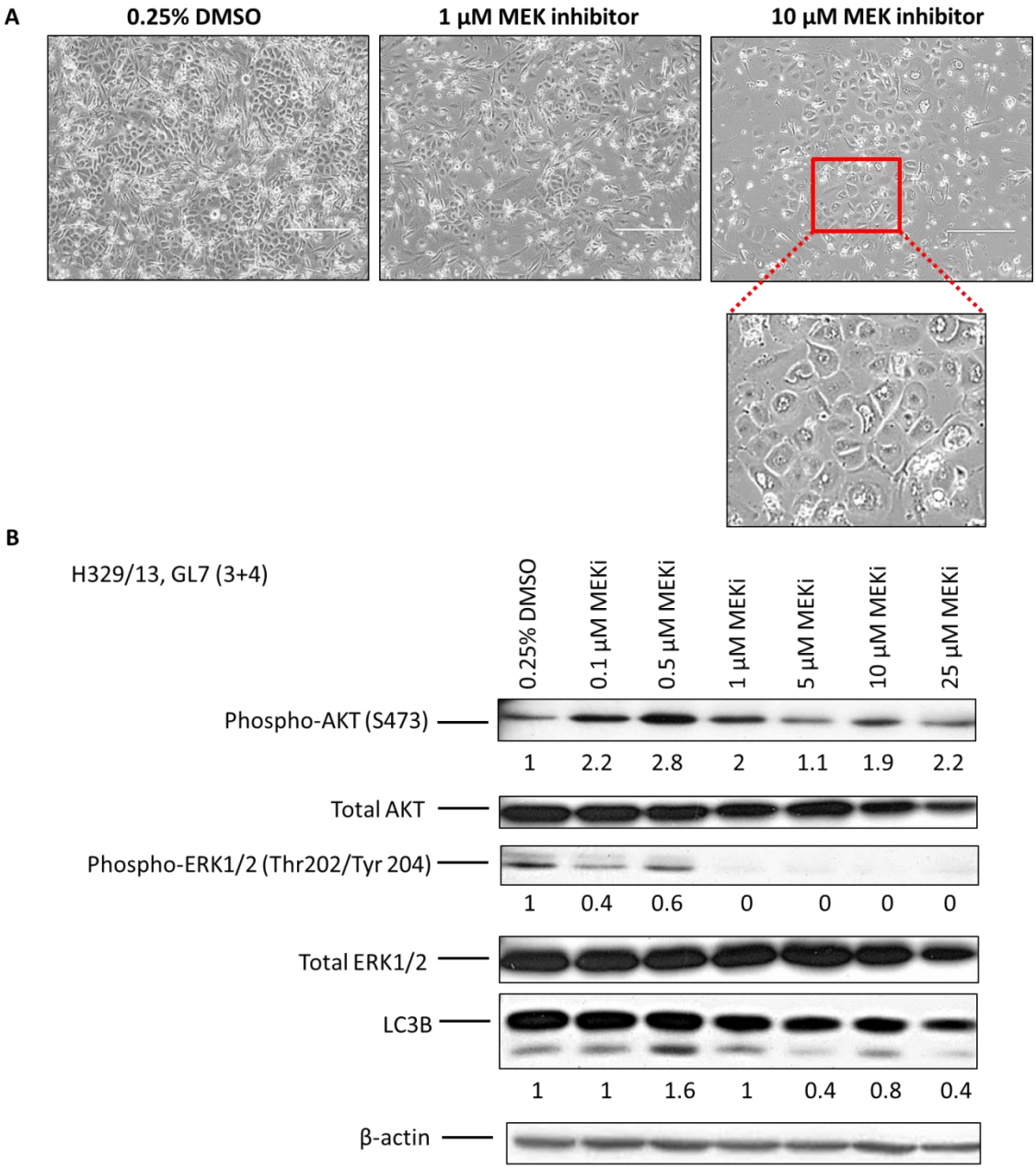

Figure 4.19. Cell morphology and biomarker expression following treatment with MEKi.

Primary cancer cells H135/11 (GL9) (A) and H329/13 (GL7) (B) were treated with increasing concentrations (0.1 - 25µM) of MEK1/2 inhibitor for 72 hours. Phase contrast images were taken and cell morphology assessed following treatment (A). Whole cell lysates were prepared after treatment of H329/13 and 20 µg of protein was loaded per lane onto a 10% SDS gel, electrotransferred onto PVDF membranes and stained for the biomarkers (phospho-AKT, total AKT, phospho-ERK1/2, total ERK1/2 and LC3 B). Vehicle control cells were treated with 0.25% DMSO. Staining with β-actin antibody was used as a loading control. Image J software was used for densitometry analysis.

To overcome the activation of the MAPK pathway following treatment with AKTi, primary cells were next treated with a combination of AKTi and MEKi. In order to determine the effectiveness of combined treatment, the phosphorylation status of specific biomarkers was determined using western blotting. Primary cancer cells H236/12 were treated with increasing concentrations of the inhibitors in three different treatment experiments (combinations):

- 1-25 μM AKTi + constant concentration of MEKi of 1 μM for 72 hours;
- 1-10 μM AKTi + matching concentration of MEKi for 72 hours;
- 1-10 μM AKTi alone for 24 hours + matching concentration of MEKi for additional 24 hours after initial treatment with AKTi;

Different treatment schedules and combinations were designed in order to test whether there was an advantage of using both inhibitors simultaneously or if subsequent treatment with MEKi following AKTi would have a better therapeutic effect. Concentration range of the inhibitors was chosen on a basis of their optimal activity determined in phospho-biomarker analysis in previous experiments.

The results showed a surprising increase, instead of a decrease in phospho-ERK1/2 levels, following treatment with a combination of AKTi and MEKi in all three experiments (Figure 4.20 A, representative result shown). Moreover, treatment of cancer H282/13 (GL7) cells with a higher concentration of 25 μM of AKTi and MEKi, increased phospho-ERK1/2 levels even further (Figure 4.20 B). Interestingly, autophagy was not induced in cells treated with MEKi alone, only in AKTi-treated cells or in a combination of AKTi + MEKi (Figure 4.20 B).

This result indicates that treatment with a combination of AKTi and MEKi does not inhibit phosphorylation of ERK1/2. Moreover, addition of MEKi to AKTi-treated culture increases phospho-ERK1/2 even further.

Figure 4.20. Phospho-biomarkers expression following treatment with a combination of AKTi and MEKi.

Primary cancer cells H236/12 (GL7) (A) were treated with 1 μM, 5 μM and 10 μM AKTi for 24 hours, after which matching concentrations of MEKi were added, and treatment continued for further 24 hours (sequential treatment). An additional cancer culture H282/13 was treated with up to 25 μM concentration of AKTi, MEKi or a combination of AKTi + MEKi for 72 hours (B) (simultaneous treatment). Adherent and non-adherent cells were collected and whole cell lysates prepared. 20 μg of protein was loaded per lane onto a 10% SDS gel, electrotransferred onto PVDF membranes and stained for the biomarkers indicated (phospho-AKT, total AKT, phospho-ERK1/2, total ERK1/2 and LC3 B). Vehicle control cells were treated with 0.2% DMSO (A) or 0.5% DMSO (B). Staining with β-actin antibody was used as a loading control. Image J software was used for densitometry analysis.

A

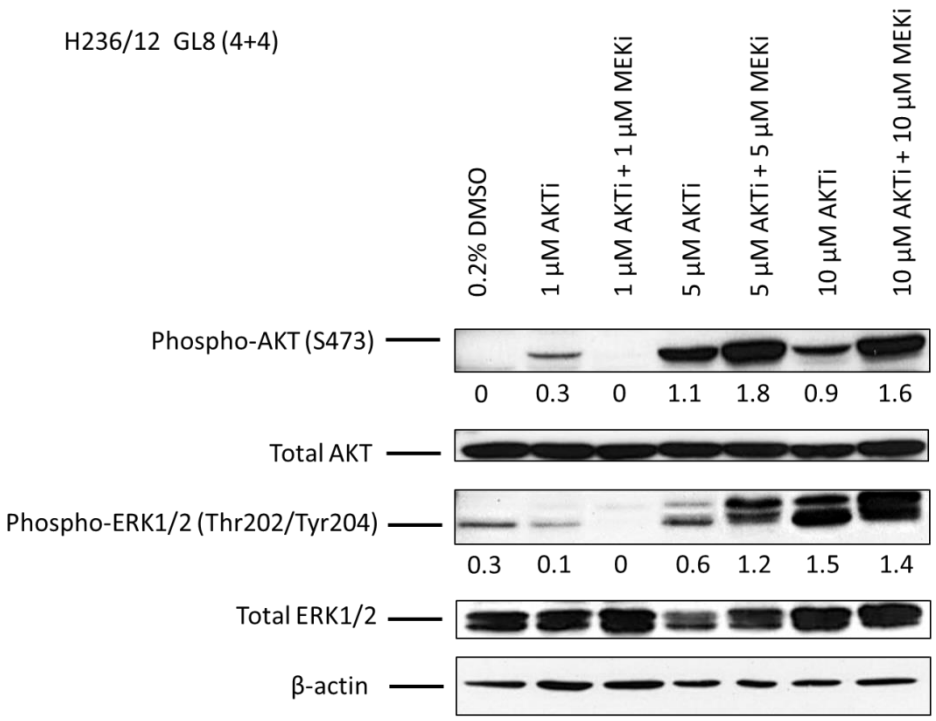
H236/12 GL8 (4+4)
0.2% DMSO
1 µM AKTi
1 µM AKTi + 1 µM MEKi
5 µM AKTi
5 µM AKTi + 5 µM MEKi
10 µM AKTi
10 µM AKTi + 10 µM MEKi
Phospho-AKT (S473)
0 0.3 0 1.1 1.8 0.9 1.6
Total AKT
Phospho-ERK1/2 (Thr202/Tyr204)
0.3 0.1 0 0.6 1.2 1.5 1.4
Total ERK1/2
β-actin

B

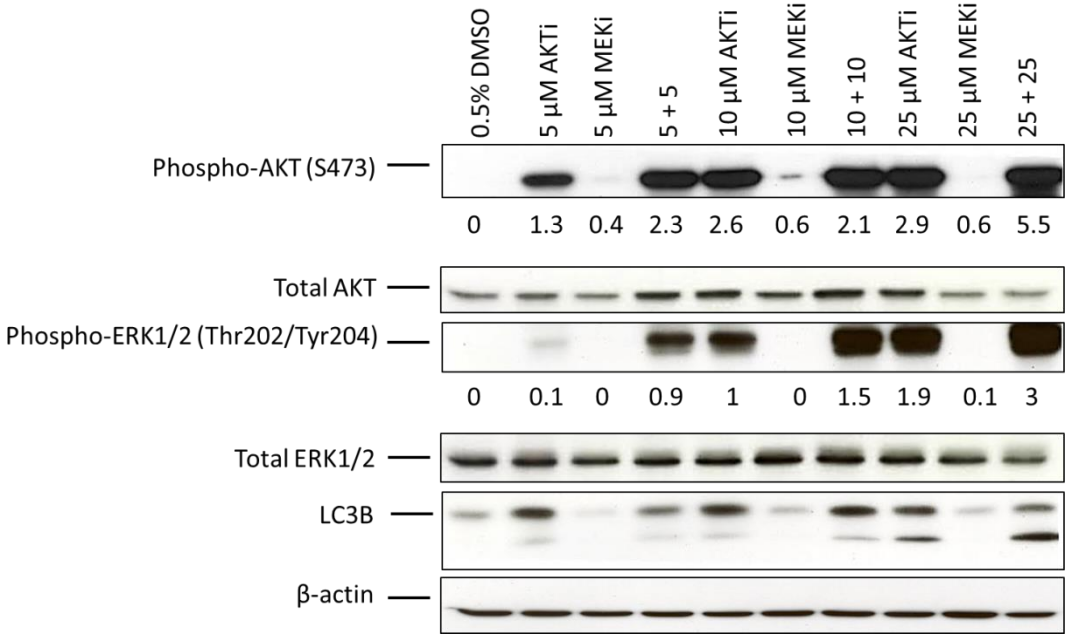
H282/13 p4, GL7 (3+4)
0.5% DMSO
5 µM AKTi
5 µM MEKi
5 + 5
10 µM AKTi
10 µM MEKi
10 + 10
25 µM AKTi
25 µM MEKi
25 + 25
Phospho-AKT (S473)
0 1.3 0.4 2.3 2.6 0.6 2.1 2.9 0.6 5.5
Total AKT
Phospho-ERK1/2 (Thr202/Tyr204)
0 0.1 0 0.9 1 0 1.5 1.9 0.1 3
Total ERK1/2
LC3B
β-actin

4.3.2.2. Treatment with AKTi and RO-512 induces senescence, but not differentiation in primary prostate cells

Activity of an additional MEK1/2 inhibitor (RO-512) was tested in primary cultures with the aim of overcoming the compensatory effect of MAPK pathway activation.

A BPH (H313/13) and a cancer (H240/12) sample were treated with increasing concentrations (0.1 – 10 μM) of RO-512 alone in order to test the effect of treatment on biomarker expression. The results showed a complete inhibition of MEK1/2 activity with just 0.1 μM RO-512 in H313/13 and with 1 μM in H240/12 cells (Figure 4.21). Interestingly, an increase in phospho-S6 following treatment with 0.1 μM RO-512 was observed in BPH cells, but not in cancer. Moreover, a transient increase in phospho-AKT expression was observed in BPH cells treated with 1 μM RO-512. This was not observed in the cancer sample.

Additionally, an apoptosis marker, cleaved PARP, was detected in BPH and cancer cells following treatment with 0.1 μM and 1 μM RO-512 (Figure 4.21).

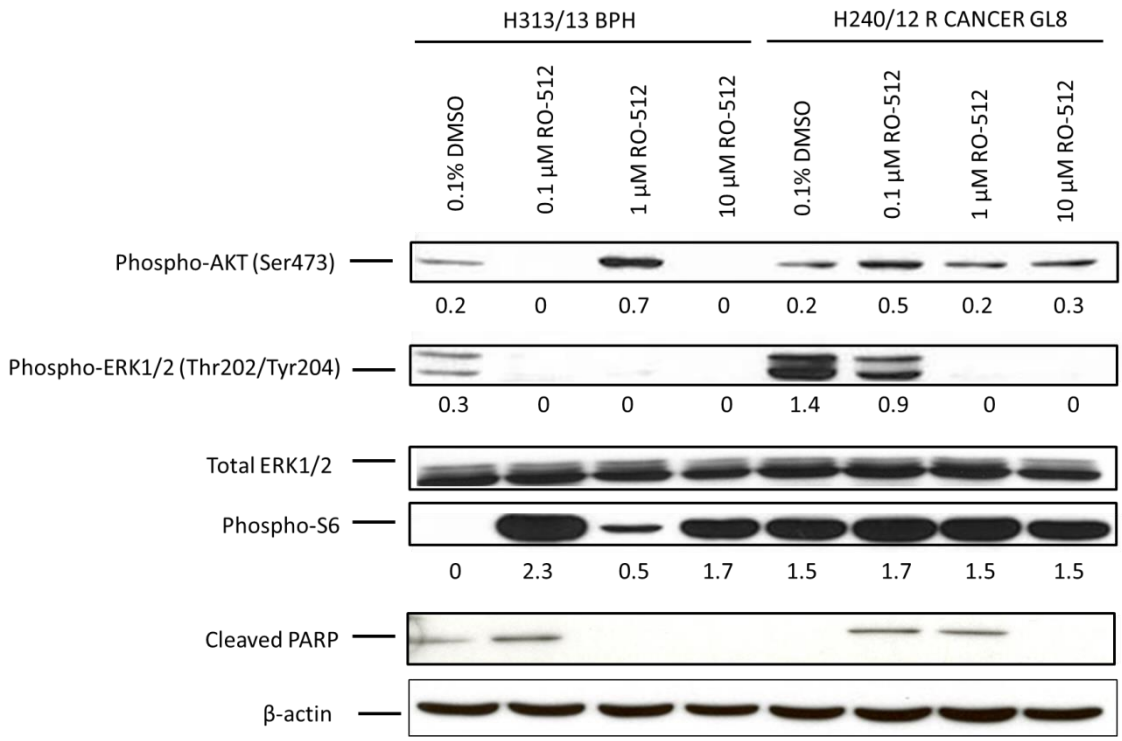

Figure 4.21. RO-512 effect on phospho-biomarker expression.

A primary BPH H313/13 and cancer H240/12 (GL8) cells were treated with increasing concentrations of MEK1/2 inhibitor RO-512 for 72 hours. Whole cell lysates were then prepared for western blotting analysis of biomarker expression. 20 µg of protein was loaded per lane onto a 10% SDS gel, electrotransferred onto PVDF membranes and stained for the biomarkers indicated (phospho-AKT, phospho-ERK1/2, total ERK1/2, phospho-S6 and cleaved PARP). Vehicle control cells were treated with 0.1% DMSO. Staining with β-actin antibody was used as a loading control. Image J software was used for densitometry analysis.

After confirmation of inhibitory activity of RO-512 in prostate epithelial cultures, a combination treatment with AKTi + RO-512 was performed in a BPH sample (H377) and a cancer sample H363/13 (GL8). The effect of a 72-hour treatment was determined using western blotting. The results showed a decrease in phospho-ERK1/2 in BPH cells when treated with RO-512 alone (Figure 4.22 B). However, in both BPH and cancer cells, the expression of phospho-ERK increased after treatment with a combination of AKTi + RO-512, even when treated with a high concentration of 5 + 5 or 10 + 10 with AKTi (Figure 4.22). This suggests that despite confirmed inhibitory activity against MEK1/2 kinase, RO-512 inhibitor is not capable of preventing ERK1/2 phosphorylation following compensatory activation of MAPK pathway.

Figure 4.22. Expression of phospho-biomarkers following treatment with AKTi and RO-512.
A primary BPH H377/13 and cancer culture H363/13 (GL8) were treated with up to 10 μM of AKTi and RO-512, either alone or in a combination for 72 hours. Whole cell lysates were subsequently prepared and 20 μg of protein was loaded per lane onto a 10% SDS gel, electrotransferred onto PVDF membranes and stained for the biomarkers indicated (phospho-AKT, total AKT, phospho-ERK1/2, total ERK1/2, phospho-S6, total S6 and cleaved PARP). Vehicle control cells were treated with 0.2% DMSO (A) or 0.1% DMSO (B). Staining with β-actin antibody was used as a loading control. Image J software was used for densitometry analysis.

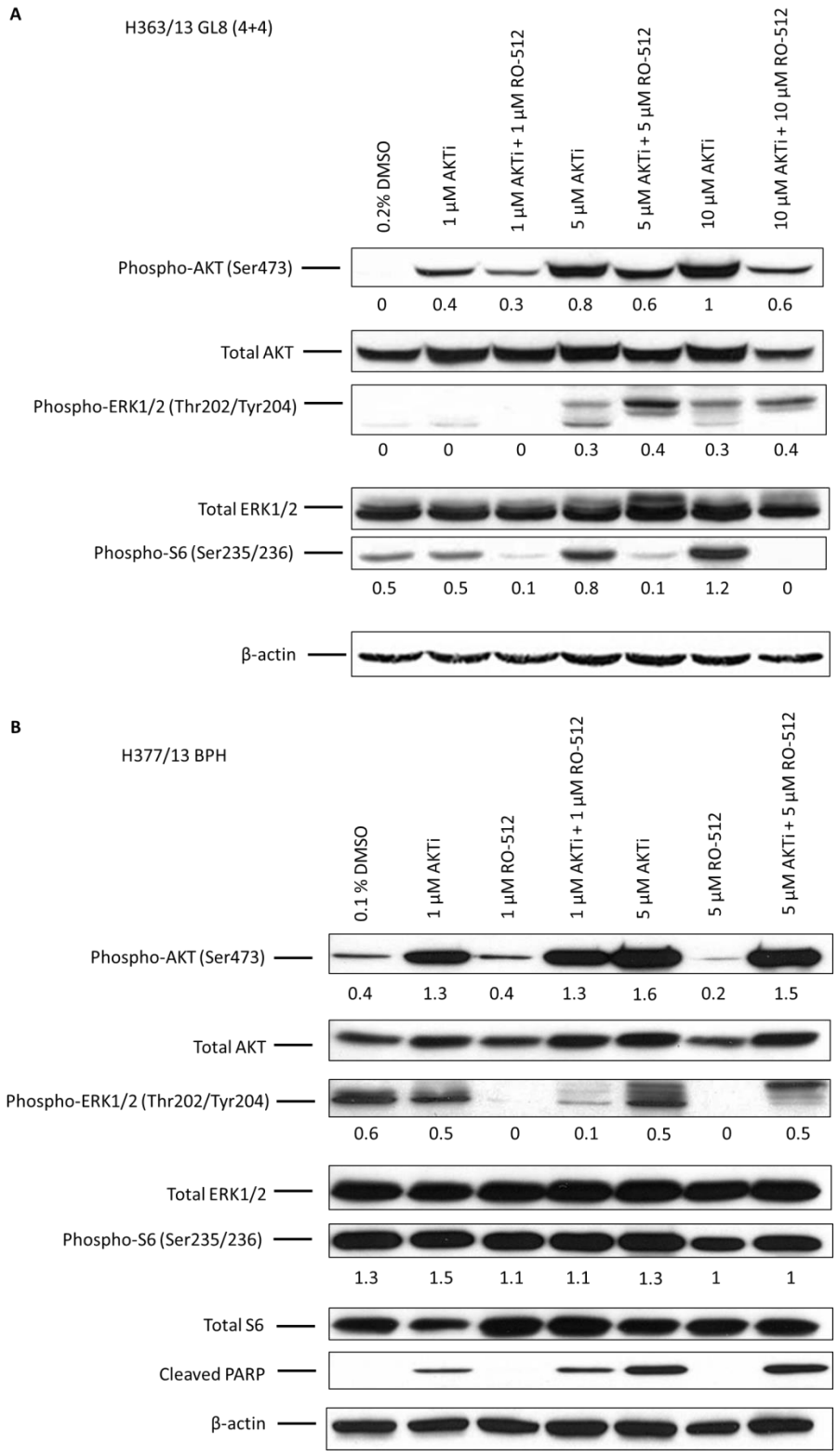
A
H363/13 GL8 (4+4)
0.2% DMSO
1 µM AKTi
1 µM AKTi + 1 µM RO-512
5 µM AKTi
5 µM AKTi + 5 µM RO-512
10 µM AKTi
10 µM AKTi + 10 µM RO-512
Phospho-AKT (Ser473)
0 0.4 0.3 0.8 0.6 1 0.6
Total AKT
Phospho-ERK1/2 (Thr202/Tyr204)
0 0 0 0.3 0.4 0.3 0.4
Total ERK1/2
Phospho-S6 (Ser235/236)
0.5 0.5 0.1 0.8 0.1 1.2 0
β-actin
B
H377/13 BPH
0.1 % DMSO
1 µM AKTi
1 µM RO-512
1 µM AKTi + 1 µM RO-512
5 µM AKTi
5 µM RO-512
5 µM AKTi + 5 µM RO-512
Phospho-AKT (Ser473)
0.4 1.3 0.4 1.3 1.6 0.2 1.5
Total AKT
Phospho-ERK1/2 (Thr202/Tyr204)
0.6 0.5 0 0.1 0.5 0 0.5
Total ERK1/2
Phospho-S6 (Ser235/236)
1.3 1.5 1.1 1.1 1.3 1 1
Total S6
Cleaved PARP
β-actin

Metabolic inhibitors can induce a wide range of cytotoxic effects, but in a stem cell context, they can equally induce differentiation (Kroon et al., 2013).

In order to verify whether treatment with AKTi and MEK1/2 inhibitors could be inducing differentiation in prostate epithelial cultures, flow cytometry of cytokeratin 18 (CK18) expression was performed. A primary cancer sample H366/13 (GL7) was treated with either 1 µM RO-512, 1 µM MEKi or a combination of 1 µM RO-512 + 1 µM AKTi or 1 µM MEKi + 1 µM AKTi for 72 hours.

The results showed that treatment with RO-512 affected the number of cells expressing CK18. The number of viable CK18 cells reduced by 50% suggesting that the inhibitor did not induce differentiation but affected the viability of the $CK18^{+}$ fraction. However, a comparable level of CK18 expression was observed after treatment with RO-512 and MEKi either as a single agent or in a combination with AKTi (Figure 4.23). This suggests that neither of the inhibitors induces differentiation in primary prostate cultures at this concentration range.

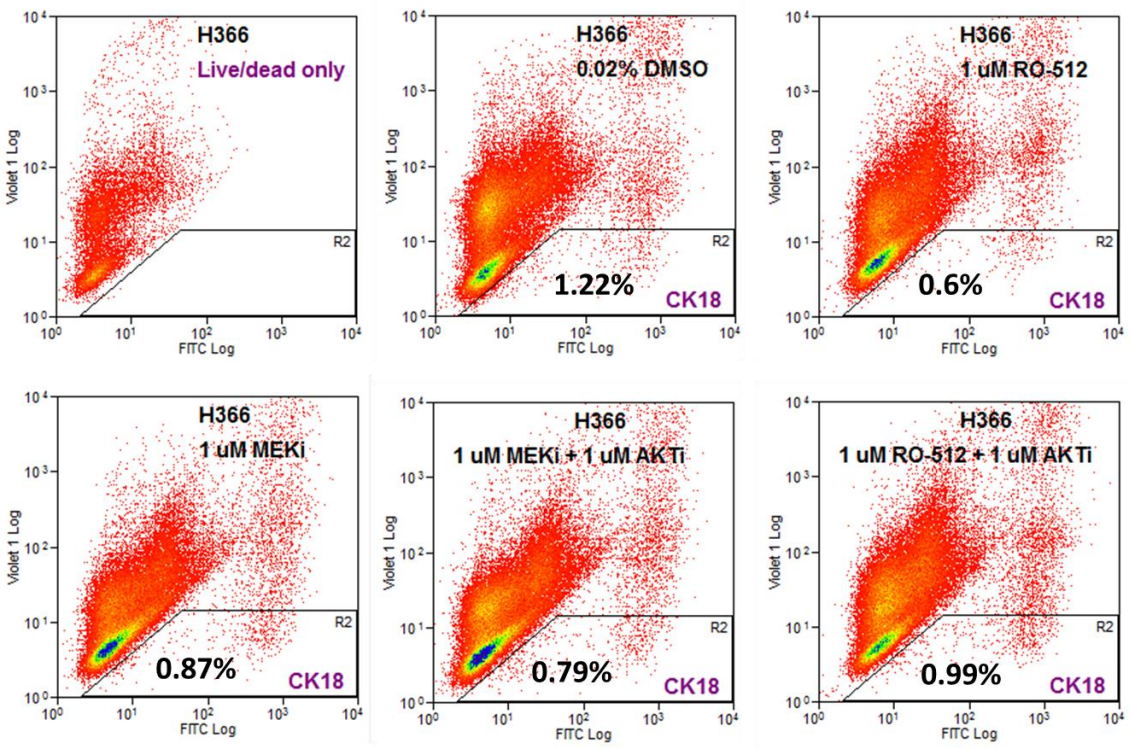

Figure 4.23. Cytokeratin 18 expression following treatment with AKTi and MEK1/2 inhibitors. Primary prostate cancer cells H366/13 (GL7) were treated with 1 µM RO-512, 1 µM MEKi or a combination of 1 µM RO-512 + 1 µM AKTi or 1 µM MEKi + 1 µM AKTi for 72 hours. Following treatment, adherent and non-adherent cells were collected, fixed in 4% PFA, permeabilised with methanol and stained with antibody against Cytokeratin 18 (CK18). Vehicle control cells were treated with 0.02% DMSO.

In order to test whether treatment with AKTi and MEK1/2 inhibitors can induce senescence, β-galactosidase staining was performed. A BPH culture (H373/13) was treated with MEKi or RO-512 either as a single agent or in combination with AKTi for 72 hours (Figure 4.24).

The result showed a striking increase in β-galactosidase – positive cells after treatment with a combination of 1 µM AKTi + 1 µM MEKi and also with 1 µM AKTi + 1 µM RO-512. Moreover, treatment with RO-512 in combination with AKTi induced senescence in all of the treated cells (Figure 4.24).

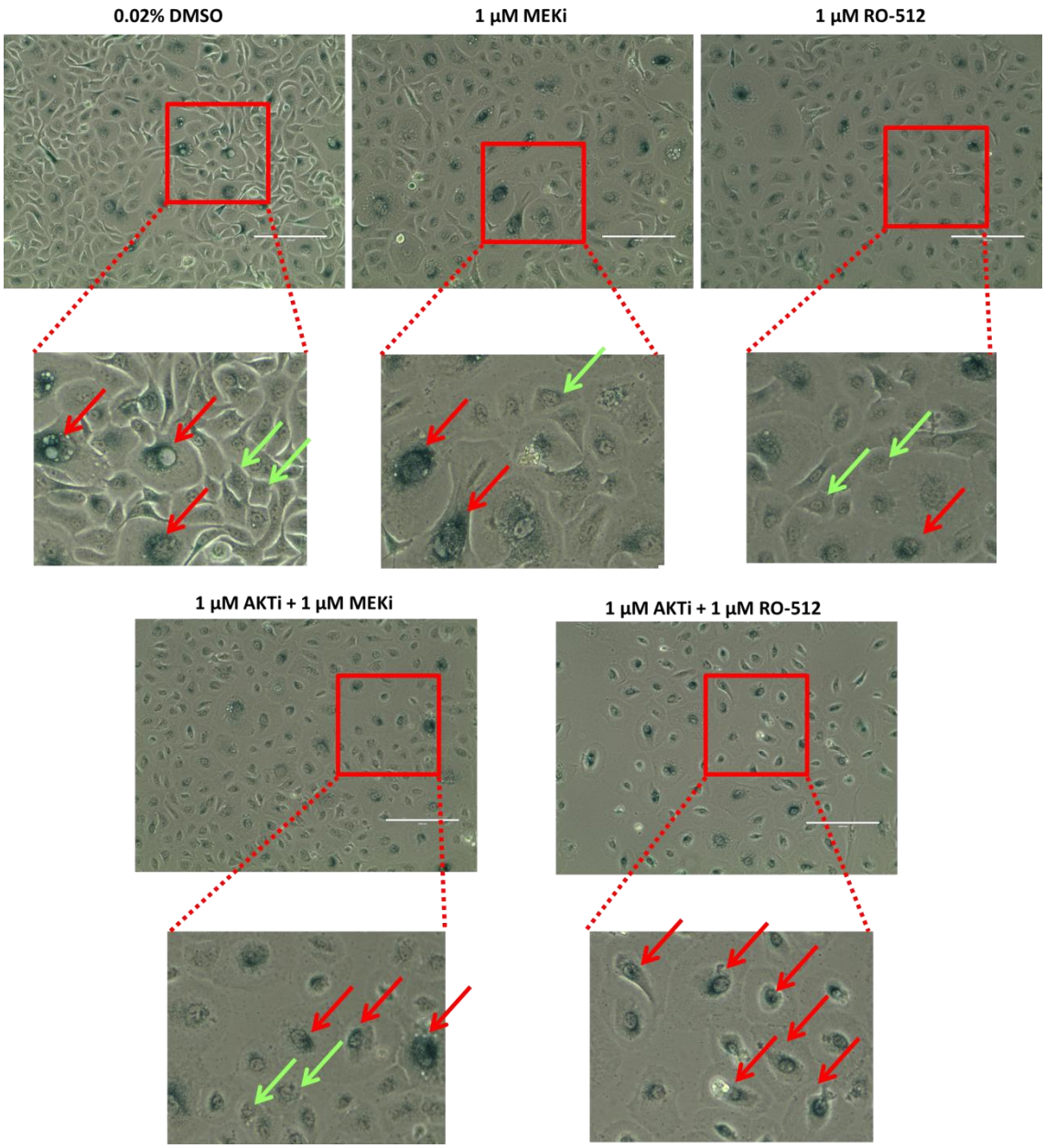

Figure 4.24. β-galactosidase staining following treatment with AKTi and MEK1/2 inhibitors.

A primary BPH culture H373/13 was treated with either 1 µM MEKi, 1 µM RO-512 or a combination of 1 µM MEKi + 1 µM AKTi or 1 µM RO-512 + 1 µM AKTi for 72 hours. Following treatment cells were fixed and stained according to the manufacturer's instructions and phase contrast images were taken. β-galactosidase – positive cells were observed (red arrows) as well as β-galactosidase negative cells (green arrows). Scale bar represents 400 µm.

Taken together, the data shows that a combined treatment of AKTi with RO-512 inhibitor induces irreversible growth arrest in primary prostate epithelial cultures, but it does not induce differentiation.

4.4. The effect of inhibiting the PI3K/AKT/mTOR pathway on tumour outgrowth

The effect of inhibiting the PI3K/AKT/mTOR pathway on tumour outgrowth was determined. A human prostate cancer xenograft (Y042/07), which was derived from a patient with hormone-naïve Gleason 7 disease, was first depleted of mouse blood lineage and endothelial cells before treating (*ex vivo*) with 3 µM and 10 µM of AKTi and mTORi either alone or in combination. Cell viability was assessed by counting live cells using trypan blue exclusion, following treatment after 24, 48 and 72 hours, in order to select the optimal treatment time and concentration of the inhibitor to be used for subsequent *in vivo* experiments (Figure 4.25).

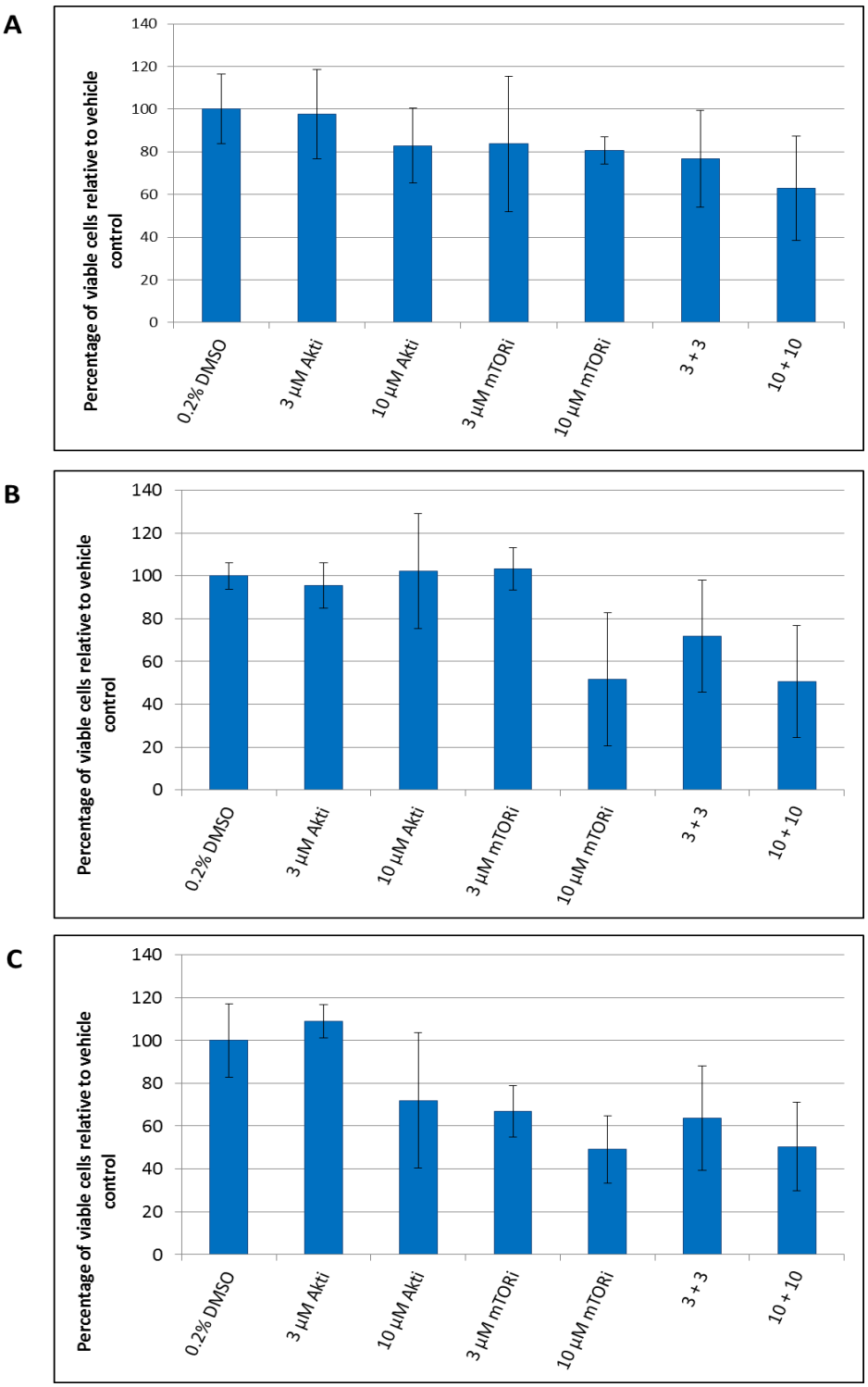

Figure 4.25. Y042 xenograft viability following treatment with AKTi and mTORi.

Y042 xenograft cells were treated with 3 µM, 10 µM, a combination of 3+3 and 10+10 of AKT and mTOR inhibitors for 24 hours (A), 48 hours (B) and 72 hours (C). Cell viability was determined using Trypan blue exclusion. The percentage of viable cells was calculated and expressed as relative to vehicle control (0.2% DMSO). Error bars represent the standard error of the mean.

The results showed that a decrease of approximately 50% in cell viability was achieved at a 10 µM concentration of the mTOR inhibitor alone and in combination with 10 µM AKTi (10+10), following 72 hours treatment (Figure 4.25 C). However, treatment with AKTi alone (at a concentration of 10 µM) only caused a 30% decrease in viability.

From these observations, the optimal treatment conditions for the tumour outgrowth experiment was decided; 10 µM concentrations of both inhibitors and a combination of 10 + 10, for a period of 72 hours.

4.4.1. Effect of AKT and mTOR inhibition on tumour outgrowth

In order to determine the effect of AKT and mTOR inhibitors on tumour initiating frequency, limiting dilution experiment was performed with xenograft Y042. The Y042 tumour is maintained in vivo and is serially transplantable in Rag2-/-GC-/- mice. Single tumour cells (Lin-/CD31-) were derived following the protocol outlined in section 2.7.1.1. Resultant human tumour cells (Lin-/CD31-) were treated *ex vivo* with 10 µM AKTi, 10 µM mTORi and a combination of 10 + 10, for 72 hours. Following treatment, live cells were counted using trypan blue exclusion and serial dilutions of cells were prepared (10,000 – 1 cell) and the cells injected subcutaneously into both flanks of Rag2-/-GC-/- mice (Table 4.2).

The results showed that xenograft tumour cells were still able to initiate tumours after treatment with either inhibitor or the combination.

The tumour initiation frequency was approximately 26 fold lower (relative to the vehicle control) (1:434; confidence intervals 1:94 – 1:2008) following treatment with a combination of AKTi and mTORi and over 2 fold lower (1:44; confidence intervals 1:10 – 1:201) when treated with AKTi alone (Table 4.2). Treatment with mTOR inhibitor alone did not show any advantage over treatment with DMSO. A pairwise test for differences in tumour initiation frequencies between treatment groups showed a significant advantage of combination treatment over DMSO and mTORi alone (p value=0.00954) (Table 4.3). The difference between combination treatment and AKTi

alone was not significant (p value=0.0714), similarly, DMSO versus AKTi alone and AKTi versus mTORi (p value=0.443).

An additional effect of treatment with a combination of the inhibitors was an 8-day delay in the tumour latency compared to vehicle control (38 days and 30 days, respectively). There was no difference in the tumour latency following treatments with either inhibitor alone, relative to a vehicle control.

Table 4.2. Tumour initiation frequency is lower in xenograft cells treated with a combination of AKT and mTOR inhibitor.

	10 000 cells per injection	1000 cells per injection	100 cells per injection	10 cells per injection	1 cell per injection	Tumour initiation frequency (95% CI)
0.2% DMSO	2/2	2/2	2/2	1/2	0/2	16.6 (98.9-3.16)
10 µM AKTi	2/2	2/2	2/2	0/2	0/2	43.8 (201.1-9.84)
10 µM mTORi	2/2	2/2	2/2	1/2	0/2	16.6 (98.9-3.16)
10 +10 Combination	2/2	2/2	0/2	0/2	0/2	434.6 (2008.4-94.36)

Table 4.3. Pairwise tests for differences in tumour initiation frequencies.

Group 1	Group 2	p value
AKTi	Combination	0.0714
AKTi	DMSO	0.443
AKTi	mTORi	0.443
Combination	DMSO	0.00954
Combination	mTORi	0.00954
DMSO	mTORi	1

4.4.2. Flow cytometry analysis of biomarkers in xenograft tumours

Expression of selected biomarkers downstream from AKT and mTOR was determined by flow cytometry in Y042 tumours retrieved from mice following *ex vivo* treatment with AKTi and mTORi. The results showed a decrease of 14.2% and 16.6% in phospho-S6 in tumours pre-treated with 10 µM AKTi and 10 µM mTORi, respectively, in comparison to the vehicle control. However, the cells treated with a combination of AKTi + mTORi showed only a modest decrease of 4.8%, relative to control (Figure 4.26). Expression of phospho-AKT and phospho-ERK1/2 were comparable to the vehicle control cells in all tumours.

Interestingly, the proportion of dead cells (violet – positive) differed between the treatment groups, with the lowest level in 0.2% DMSO-treated cells and highest in AKTi-treated cells (Figure 4.26).

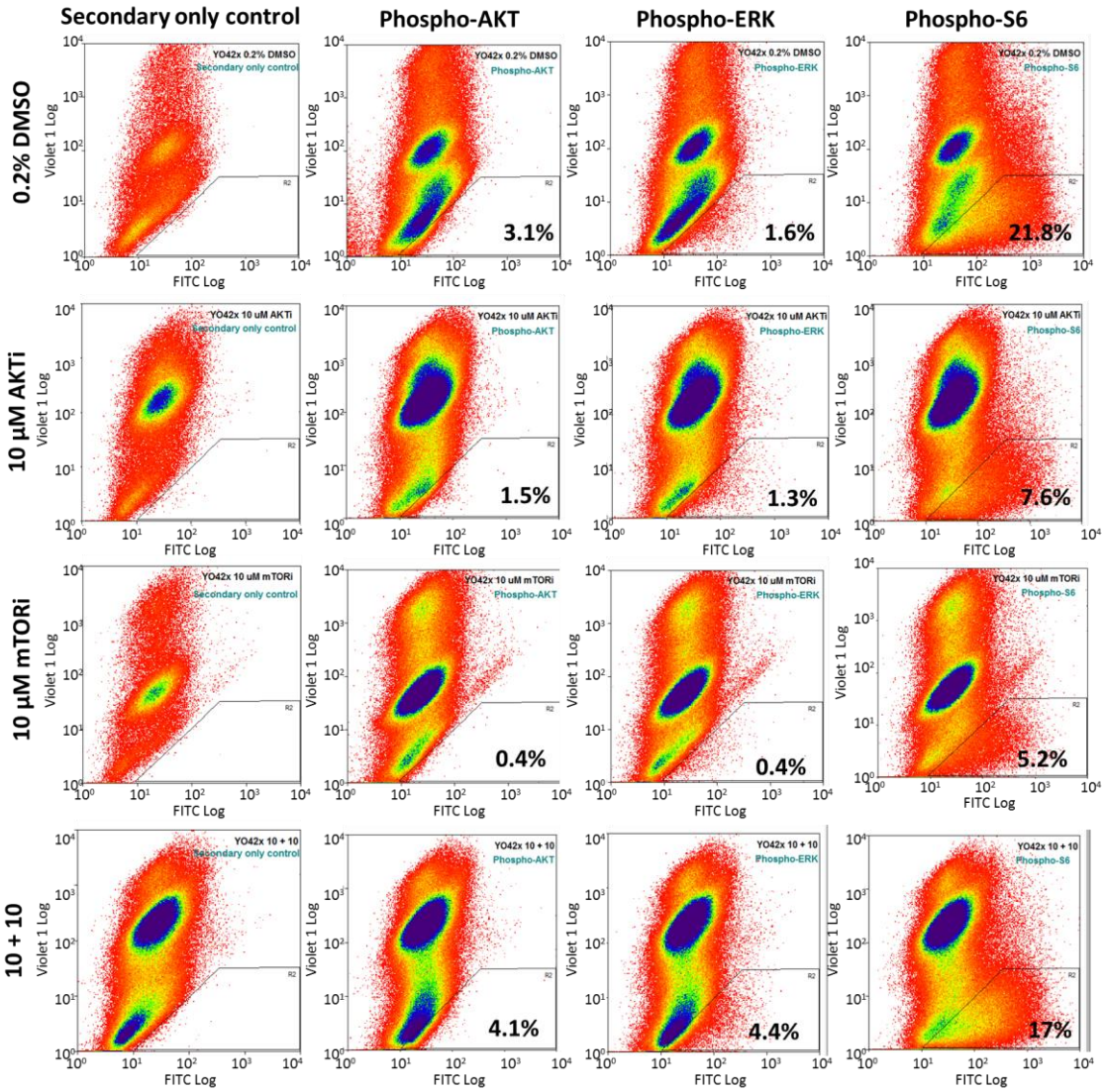

Figure 4.26. Biomarkers expression in *ex vivo* treated Y042 xenograft.

The YO42 tumours retrieved from mice following an ex vivo treatment, were depleted of mouse cells and the resultant human fraction (Lin-/CD31-) was analysed by flow cytometry. The cells were fixed in 4 % PFA, permeabilised with methanol, and stained with antibodies against: phospho-AKT, phospho-ERK1/2 and phospho-S6.

Chapter 5

Discussion

5. DISCUSSION

The aim of this study was to determine the importance of the PI3K/AKT/mTOR pathway in human prostate cancer. This was performed by targeting the pathway with AKT and mTOR inhibitors in prostate cancer cell lines, primary cell cultures and 'near-patient' xenografts. Targeting of the PI3K/AKT/mTOR pathway has been investigated in a number of studies as an alternative treatment method for patients with over-activation of the pathway (Cheng et al., 2005, Engelman, 2009). Inhibitors against selected elements of the pathway have been designed, including small molecule inhibitors against AKT and mTOR kinases, and their activity has been tested in different types of tumours (Davies et al., 2012, Garcia-Martinez et al., 2009).

5.1. PTEN expression and PI3K pathway activity in prostate cancer cell lines and primary cultures

The PTEN gene is the second most frequently mutated tumour suppressor gene after p53 and its role in human cancer development and progression has been widely investigated (Chalhoub and Baker, 2009, Leslie et al., 2008). It is estimated that around 70% of metastatic prostate cancers have genomic alterations in the PI3K signalling pathway, due to mutations, deletions or epigenetic silencing via methylation of the PTEN gene (Blanco-Aparicio et al., 2007, Cairns et al., 1997). PTEN negatively regulates the PI3K/AKT/mTOR pathway and its frequent loss in cancer leads to over-activation of the pathway (Yoshimoto et al., 2007, Kwabi-Addo et al., 2001, Cairns et al., 1997, El Sheikh et al., 2008). It has been demonstrated that AKT activation, due to PTEN loss, induces resistance to inhibitors of receptor tyrosine kinases, anti-hormonal therapies in prostate cancer and also to chemotherapy (Kim et al., 2005, Wendel et al., 2004). A number of studies have shown that the PTEN tumour suppressor activity is lost in primary and metastatic prostate cancer. Published reports have demonstrated that biallelic deletion of *PTEN* correlates with disease-specific mortality and is associated with over-activation of the PI3K/AKT/mTOR pathway (Yoshimoto et al., 2007, Suzuki et al., 1998, Lotan et al., 2011).

It has been shown, by Li and co-workers, that loss of PTEN in the prostate cancer cell line LNCaP is due to a 2 bp deletion in exon 6 of the PTEN sequence resulting in a frameshift mutation (Li et al., 1997). Similarly, the absence of detectable expression of PTEN in PC3 cells is the result of deletion of the 3' end of the *PTEN* gene (Sharrard and Maitland, 2000). The analysis reported in this study verified that both PC3 and LNCaP do not express PTEN at the protein level. However, PTEN is expressed at the RNA level in LNCaP cells.

PTEN loss also resulted in increased activity of the pathway, as the highest levels of phospho-AKT and phospho-S6 were observed in PC3 cells. However, detected levels of phospho-S6 did not directly correlate with PTEN status as both PC3 and BPH1 cells had more phospho-S6 than either P4E6 or LNCaP cells.

To confirm if loss of PTEN would increase activity of AKT and mTOR kinases, siRNA knock down of PTEN was carried out in PTEN expressing cell lines. As expected, the results showed an increased activity of AKT kinase. This result is in agreement with other studies, which showed that PTEN siRNA knock down in DU145 and 22Rv1 cells resulted in increased PI3K/AKT/mTOR pathway activity (Kim et al., 2014). However, PTEN knock down also resulted in a significant decrease in phospho-S6 levels indicating a decrease in mTORC1 activity. Masiello and co-workers have shown that a combinatorial treatment with rapamycin and receptor tyrosine kinase antagonists (PD16839 and imatinib) dramatically decreased phospho-S6 and that it was independent of phospho-AKT (Masiello et al., 2007). They have also demonstrated a paradoxical activation of p70 S6 kinase and its downstream target S6, in LNCaP cells, following treatment with either of the RTK antagonist alone (Masiello et al., 2007). An unexpected increase in phospho-S6 could be a result of an activation of a negative feedback mechanism, possibly involving MAPK signalling as it has been shown that S6 kinase can be phosphorylated by both mTORC1 and ERK (Steelman et al., 2011).

In contrast to prostate cancer cell lines, PTEN expression was observed in all primary cells investigated, including Gleason 8 tumours. Although there was variability in PTEN expression, none of the cultures showed a loss of PTEN. This might have been due to the presence of non-malignant cells (PTEN-positive) contaminating the cultures. However, the majority of cultures were derived from patients with early stage disease,

whereas it has been reported that PTEN is most frequently lost in advanced prostate cancer. Mithal et al reported that only 12% of radical prostatectomy samples showed complete loss of *PTEN* (Mithal et al., 2014). It is also possible that western blotting may not be sufficient to address a question of PTEN activity and capability of counteracting the PI3 kinase activity. Therefore an additional analysis of PTEN sequence regarding possible mutations and loss of heterozygosity (LOH) in *PTEN* gene is currently being investigated in our laboratory.

It was first demonstrated by Di Cristofano and Pandolfi (2000) that PTEN is involved in cell migration. They observed that reintroduction of *PTEN* into the glioblastoma cell line U-87MG led to inhibition of integrin-mediated cell spreading and migration as a consequence of direct dephosphorylation of focal adhesion kinase (FAK) (Di Cristofano and Pandolfi, 2000). The involvement of PTEN in cell adhesion and migration could provide a rationale for the frequent loss of the gene observed in late-stage metastatic prostate cancer. In this study the results of a wound healing assay showed an increased migration rate in cells treated with PTEN siRNA. Moreover, a significant decrease in cell migration rate was observed following treatment with mTORi in both PTEN-negative cell lines, LNCaP and PC3. However, treatment with an AKTi did not show a significant effect on cell migration in either of those cell lines.

5.2. The effect of treatment with AKTi and mTORi on cell viability and morphology

Pre-clinical testing of new anti-cancer drugs in cancer cell lines alone has its limitations. Although the use of cell lines allows testing drugs under highly controlled and reproducible conditions, it does not represent the complexity of primary tumours, their heterogeneous populations or phenotypic variability (HogenEsch and Nikitin, 2012). Therefore, in this study, a wide range of primary clinical samples of prostate cancer and benign prostatic hyperplasia (BPH) as well as 'near patient' prostate tumour xenografts were used to determine the effect of AKT and mTOR inhibitors.

It has been reported in the literature that the allosteric mTORC1 inhibitor rapamycin and its analogues did not show a satisfactory efficacy in prostate cancer, which is most

likely due to lack of clinical activity against mTORC2 complex, leading to activation of AKT kinase (Sarbassov et al., 2006b, Sarbassov et al., 2005). Additionally, an activation of receptors, such as AR or RAS can also contribute to treatment resistance. Therefore improved dual mTORC1/2 inhibitors were designed showing greater efficacy than mTORC1 compounds in prostate cancer. Hsieh et al demonstrated that dual mTORC1/2 inhibitor (MLN0128) prevented prostate cancer invasion and metastasis and was also able to induce apoptosis (Hsieh et al., 2012). A study with another dual mTORC1/2 inhibitor, AZD8055, has been shown to inhibit cell proliferation and tumour growth *in vitro* in lung cancer cell lines and in a broad range of human tumour xenografts (Chresta et al., 2010). However, the loss of S6K-mediated negative feedback loop might still lead to activation of the PI3K/AKT/mTOR pathway via activation of the receptor tyrosine kinases (Bitting and Armstrong, 2013).

In this study the results of treatment with up to 10 µM of both inhibitors, AKTi and mTORi, showed a relatively small decrease in cell density and minor changes in morphology, which were mainly observed in LNCaP cells. This suggested that out of four cell lines tested, LNCaP cells were the most susceptible to both inhibitors, which was further confirmed by an MTS viability assay. The results showed that only LNCaP cells had EC_{50} lower than 1 µM for AKTi and mTORi. Similarly, treatment of primary cultures (derived from patients with BPH and cancer) with up to 5 µM of AKTi and mTORi showed a limited effect on cell density and cell morphology. The results of cell viability assessment, following treatment, showed that there is variability in response between samples, even if they have been diagnosed with the same Gleason grade. Cell viability was also measured by an MTS assay and the results showed a comparable susceptibility of primary cultures to both inhibitors. However, when compared to a cancer cell line LNCaP, prostate primary cultures were more resistant to treatment; with ~27-fold higher EC_{50}.

Additionally, treatment of a matched cancer and normal culture showed different susceptibilities to the inhibitors, where only normal control responded. This difference in response might have been caused by the presence (or higher expression) of ABC transporters in the cancer cells resulting in efflux of the inhibitors from the cells. It has been demonstrated that tyrosine kinase inhibitor resistance is mediated by the

presence of ABC transporters in a range of human cancers, including breast, prostate, head and neck and also leukaemia (Anreddy et al., 2014). It has been also shown by Suzuki and co-workers that a significant degree of mutational heterogeneity in PTEN was found in different metastatic sites from the same patient (Suzuki et al., 1998). Moreover, it is also possible that the presence of pre-existing mutations in the PI3K pathway in cancer cells might influence the response to specific inhibitors. Susceptibility of cancer cells to PI3K/AKT/mTOR pathway inhibitors has been shown to depend on specific mutations, for example Carver and colleagues demonstrated that inhibition of the PI3K pathway in PTEN-negative prostate cancer cells led to activation of androgen receptor through feedback signalling to the receptor tyrosine kinase HER2/HER3 (Carver et al., 2011). Additionally, there is a positive correlation between the presence of PI3K mutations and susceptibility to an AKT inhibitor (AZD5363), as well as between the presence of RAS mutations and resistance to AZD5363 (Davies et al., 2012).

Despite the limited effects of the inhibitors on primary cell cultures' viability, dramatic morphological changes, such as vacuolation of cells and membrane blebbing were observed following treatment with high concentrations (≥ 25 μM) of AKT and mTOR inhibitors, respectively. Membrane blebs are spherical outgrowths of the plasma membrane that occur upon membrane detachment from the underlying cytoskeleton, which is indicative of apoptosis (Norman et al., 2010). However, there was no increase in cleaved PARP expression observed with mTOR inhibitor treatment. This could be due to the small numbers of cells showing such features, and therefore being undetectable by western blotting. Increased vacuolation of cells following treatment with the AKT inhibitor could indicate an activation of autophagy and formation of autophagosomes. Autophagy is a cellular catabolic degradation process in response to starvation or stress, in which cellular organelles, proteins and cytoplasm are digested and recycled to maintain metabolism (Mathew et al., 2007). Autophagy activation following treatment with AKTi was further confirmed as there was a clear increase in the LC3 B marker expression demonstrated by western blotting and immunofluorescence. It has been previously shown by others that treatment with the ATP-competitive AKT inhibitor (AZD7328) can induce autophagy in human bladder cancer cell lines, and that this can be overcome by treating cells with the autophagy

inhibitor chloroquine (Dickstein et al., 2012). However, there is evidence that autophagy can also prevent tumourigenesis, therefore acting as a tumour suppressor (Chen et al., 2013). It has been reported that mice with systemic mosaic deletion of autophagy genes *atg5* and liver-specific *atg7*$^{-/-}$ developed hyperproliferative liver adenomas (Takamura et al., 2011). Although it has also been shown that ATG deficiency is responsible for increasing tumour cell proliferation in vivo, the mechanism of this is unclear.

Interestingly, Chen and colleagues have uncovered that accumulation of the autophagy substrate p62/SQSTM1 was sufficient to activate the MAPK pathway and to increase cell proliferation in PI3K-expressing mammary 3D structures (Chen et al., 2013). They emphasised that increased cell proliferation and MAPK activation due to inhibition of autophagy was only evident in 3D culture conditions and not in cells grown in a monolayer (Chen et al., 2013). In this study the cells treated with AKTi showed an increase in autophagy as well as in the MAPK pathway activity.

5.3. Phospho-biomarkers response to the inhibition of the PI3K/AKT/mTOR pathway

The efficiency of the inhibitors was also tested by determining biomarker expression using western blotting. The results showed that the majority of cell lines responded to treatment as the phosphorylation levels of the biomarkers reduced. However, the immediate response of cells to inhibitors can be different to the response following prolonged treatment such as the activation of a feedback mechanism, which is often observed after 24 hours exposure or even later (Kholodenko, 2006). Therefore the effect of prolonged incubation with inhibitors was tested. In cell lines, the results of a 72-hour treatment showed a reduced inhibitory effect. Phosphorylation levels of biomarkers following treatment were comparable to vehicle controls and only treatment with the highest concentration (10 μM) of mTORi decreased levels of phospho-biomarkers. Additionally, a dose-dependent increase in phospho-S6 was observed in P4E6 cells following 72h treatment with mTORi. This implies that during an extended incubation with the inhibitors, the cells become more resistant and perhaps

activate a mechanism to overcome the inhibition by subsequently activating another node of the signalling network.

Additionally, the question of reversible inhibition is clinically relevant, as with any treatment, the dosing of inhibitors in patients will probably not be continuous. Therefore, it is essential to establish what possible consequences might arise following withdrawal of the inhibitors. Therefore, the effect of treatment withdrawal was determined in primary prostate cultures to test whether inhibition of the PI3K/AKT/mTOR pathway is reversible. A Gleason 7 cancer culture was treated for 5 days, treatment was stopped and phospho-biomarker levels were subsequently determined. Upon treatment with the AKT inhibitor, a surprising increase in phospo-PRAS40 was observed, suggesting elevated activity of AKT kinase, which has not been reported before. Interestingly, an increase in phosphorylation of AKT (Ser473) upon treatment with ATP-competitive AKT inhibitors has been shown previously and it is due to the protein being held in a hyper-phosphorylated (but inactive) form as a consequence of compound binding (Okuzumi et al., 2009, Davies et al., 2012). This suggests that either hyper-phosphorylated AKT has not totally lost its activity or there is another kinase which can phosphorylate PRAS40. However, following the withdrawal of AKTi the levels of phospho-AKT and phospho-PRAS40 decreased. Interestingly, treatment with the mTORi confirmed its inhibitory activity against both mTORC1 and mTORC2 by decreasing phospho-S6 and phospho-AKT, respectively. Additionally, after 48-hour treatment with mTORi a decrease in phospho-PRAS40 was observed, followed by an approximate 4-fold increase after treatment was extended to 5 days. However, a withdrawal of the mTOR inhibitor did not significantly alter phospho-S6. In contrast, phospho-AKT levels increased. This might suggest that release of mTOR inhibition could potentially cause a paradoxical increase in the pathway activity and will have to be investigated further.

The PI3K/AKT/mTOR and Ras/MEK/ERK signalling pathways can become activated via EGF – induced activation of the epidermal growth factor receptor (EGFR). Therefore it was important to assess whether the presence of EGF in the culture medium affected treatment with the inhibitors. A BPH culture was treated with the inhibitors either in the presence or absence of EGF. The results showed that in the presence of EGF, the

levels of phospho-AKT and phospho-ERK were not significantly altered. Therefore an EGF-supplemented media was used throughout the experiments with primary prostate cultures.

5.4. The effect of treatment on prostate cancer stem-like cells

In order to verify whether selected subpopulations of primary cultures responded in a similar way to cell lines, a range of primary cultures was used. The results showed that there was variability between patients. Viability either decreased with treatment or an increase in stem cell content was observed. Despite this variability, viable cells were present following treatment suggesting that a subpopulation of CD133-positive cells is probably dependent on additional factors, such as PTEN expression, pre-existing mutations in PI3K or other signalling molecules of the pathway. This heterogeneity in response is highlighted by the colony forming assay in which stem-like cells, resistant to treatment, were capable of enhanced CFE. In contrast, the CFE of the TA cells decreased with treatment. This might suggest that stem-like cells are dependent on the PI3K signalling and that inhibition of the pathway affects their survival.

It has been previously shown by Dubrovska and co-workers that the PI3K/AKT/FOXO3a signalling plays a critical role in maintenance and viability of tumour initiating cells ($CD133^+/CD44^+$) in prostate cancer cell lines (Dubrovska et al., 2009). Their study has demonstrated that inhibition of the PI3K pathway led to a decrease in the stem-like cell population and in their clonogenic potential (Dubrovska et al., 2009). Furthermore, they have also shown that a combination treatment with PI3K/mTOR inhibitor (BEZ235) and chemotherapeutic drug Taxotere eliminated stem-like progenitor cells and led to a significant tumour regression in a DU145-derived prostate cancer xenograft model (Dubrovska et al., 2010). However, they have also shown that, in the relapsed DU145 tumours, an expansion of cancer progenitors with a PTEN E91D missense mutation was observed, which was the cause of the combination therapy resistance (Dubrovska et al., 2010).

Moreover, it has also been shown in another study that loss of PTEN and therefore an increase in the PI3K pathway activity, increased the stem-like properties of the cells,

including sphere-forming ability, epithelial-mesenchymal transition-related gene expression and multi drug resistance efflux transport ATP-binding cassette sub-family G (ABCG2) expression (Kim et al., 2014). This could provide a rationale for targeting the PI3K/AKT/mTOR pathway.

The results reported in the literature regarding targeting the PI3K/AKT/mTOR pathway in order to eliminate cancer stem cells are very encouraging. Ke and co-workers reported that treatment of anaplastic thyroid cancer with a PI3K inhibitor, LY294002, attenuated self-renewal of cancer stem cells and induced cell differentiation (Ke et al, 2014). Similar findings were also reported in acute myeloid leukaemia and in breast cancer stem cells, where it was shown that the PI3K/AKT/mTOR pathway was critical for cancer stem cells' proliferation and survival (Martelli et al., 2006, Dillon et al., 2007). Moreover, it has recently been shown by Vassilopoulos and colleagues that following treatment with a chemotherapeutic drug cisplatin, there was a significant increase in breast cancer stem cells number, which was partially attributed to the activation of the PI3K/AKT/mTOR pathway (Vassilopoulos et al., 2014). However, they have also shown that combined treatment with cisplatin and mTOR inhibitor rapamycin, synergistically inhibited cancer stem cells-mediated primary and metastatic cancer growth (Vassilopoulos et al., 2014). Those recent findings emphasise the need for testing of combination treatments, which might be a more successful approach in targeting cancer stem cells. Frame and Maitland have summarised the potential effects of different prostate cancer treatments on the stem cell population (Figure 5.1).

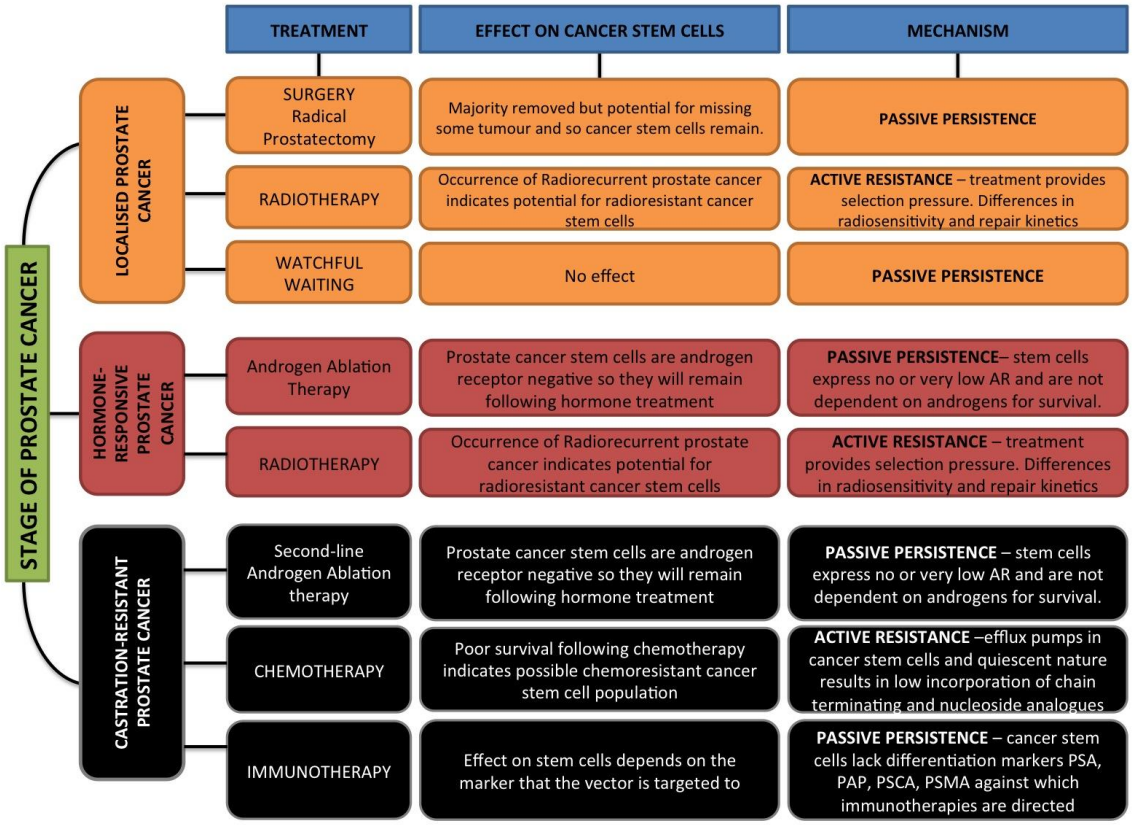

Figure 5.1: Figure 5.1. Effect of traditional therapies on stem-like cells.

Summary of treatment options related to prostate cancer stage and proposed effect on cancer stem cell population. (Taken from: Frame F.M. and Maitland N.J. (2013) Cancer stem cells provide new insights into the therapeutic responses of human prostate cancer (Chapter 4). In 'Stem Cells and Prostate Cancer'. S. Cramer, ed. (Springer Science + Business Media, LLC).

A Xenograft model of prostate cancer was next used to determine if treatment with AKTi and mTORi had any effect on tumour frequency and tumour latency. The results showed a significant advantage of *ex vivo* treatment with a combination of AKTi and mTORi relative to the vehicle control.

It has been demonstrated in the literature that combination of the PI3K pathway inhibitors targeting AKT or PI3Kbeta/delta with androgen deprivation therapy resulted in long-lasting tumour regression in PTEN-negative PC346C xenografts (Marques et al., 2014). It has also been reported by Zhang and colleagues that co-targeting of mTOR and AKT in prostate cancer with ridaforolimus/MK-8669 and M1K02206, respectively, showed additive anti-tumour effects *in vivo* in comparison to single agents (Zhang et al., 2012).

A number of studies with PI3K/AKT/mTOR pathway inhibitors have reported growth inhibition, G1 cell cycle arrest, induction of apoptosis and an increase in cells' sensitivity to radiation (Shukla et al., 2007, Gottschalk et al., 2005, Gao et al., 2003). In this study, treatment with AKT and mTOR inhibitor showed growth arrest in the G1 phase in LNCaP cells, but not in BPH1, P4E6 or PC3 cells (Figure 3.15). However, treatment of primary cultures, including BPH, hormone naïve cancer and CRPC, did not affect cell cycle distribution. This result highlights the difference in susceptibility of primary cultures compared to cell lines in their response to the different inhibitors. In particular, the requirement for a 5-fold higher concentration of the inhibitors in the treatment of primary cells.

5.5. Cross-talk between the PI3K/AKT/mTOR and the Ras/MEK/ERK pathways

It has previously been shown by Carver and co-workers that PI3K pathway inhibition activates androgen receptor signalling by relieving feedback inhibition of HER kinases. Conversely, AR inhibition leads to activation of AKT by reduction of AKT phosphatase PHLPP expression (Carver et al., 2011).

The PI3K/AKT/mTOR and the Ras/MEK/ERK pathways are the two major hyper-activated pathways, which promote cell proliferation, survival and metastasis in

human cancer (Yuen et al., 2012). Activation of the MAPK pathway has been implicated in resistance to the PI3K/AKT/mTOR signalling inhibition (Ihle et al., 2009) and significant activation of this pathway has been observed in primary and in metastatic prostate cancer (Mulholland et al., 2012). Therefore a simultaneous targeting of both pathways in prostate cancer could be highly beneficial for patients with advanced stage disease (Figure 5.2).

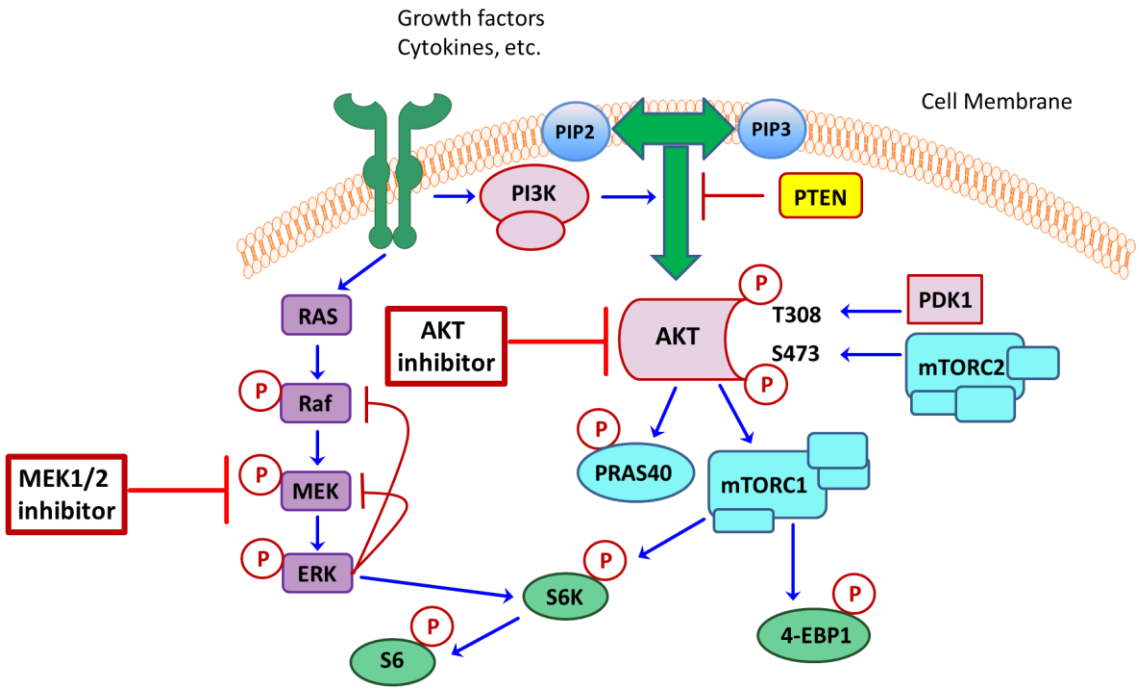

Figure 5.2. Combined inhibition of AKT and MEK1/2 kinase.

A schematic representation of the PI3K/AKT/mTOR and the Ras/MEK/ERK pathways interaction and simultaneous inhibition. Growth factor receptor activation results in activation of both signalling pathways via Ras and PI3 kinase. AKT can phosphorylate and inhibit the effects of TSC2 and PRAS40, which results in mTORC1 activation. ERK can interact with mTORC1 signalling via p70S6K. ERK is also involved in negative regulation of MEK1/2 and RAF. Simultaneous inhibition of AKT and MEK1/2 is proposed to overcome the compensatory activation of ERK signalling following inhibition of AKT.

In this study, increased levels of phospho-ERK1/2 were observed in a number of primary prostate cancer and BPH cultures following treatment with AKTi, but not mTORi. Additionally, a surprising 'switch' between phosphorylated ERK1 (AKTi treated) and ERK2 (mTORi treated) was revealed. However, a combination treatment of AKTi + mTORi increased phosphorylation of both ERK1 and ERK2 by approximately 9 fold. In contrast, treatment of primary cancer cultures with mTORi did not increase phospho-ERK1/2 levels, even when treated with very high concentrations (50 µM) of inhibitor. However, treatment with > 25 µM of AKTi resulted in a decrease of phospho-S6, a downstream target of mTORC1. Therefore, any increase in phospho-ERK1/2 levels in those cells could be due to mTORC1 inhibition as well as inhibition of AKT. This result indicates that the MAPK pathway activity increases in order to compensate for loss of activity of the PI3K pathway.

A cross-talk between the Ras/MEK/ERK and the PI3K/AKT/mTOR pathways has been previously reported in prostate cancer (Carracedo et al., 2008, Kinkade et al., 2008). However, in the studies mentioned above, activation of the MAPK pathway was mainly observed in response to inhibition of mTORC1 with rapamycin or its derivatives, rapalogs, in breast, prostate and colon cancer (Carracedo et al., 2008). Based on the results, Carracedo and colleagues proposed that mTORC1 inhibition increases RTK/IRS-1/PI3K activity towards Ras/MAPK, and promotes activation of both AKT and ERK, in what constitutes a dual feedback mechanism (Carracedo et al., 2008, Carracedo and Pandolfi, 2008). This suggests that a combined inhibition of the PI3K/AKT/mTOR pathway and the MAPK pathway might be required to improve therapeutic outcome in treatment of prostate cancer.

It has been shown that phosphorylation of S6 ribosomal protein is an indication of mTORC1 activation, which is due to AKT inhibitory phosphorylation of tuberous sclerosis complex 2 (Tee et al., 2002). In this study a surprising increase of approximately 5-fold in phospho-S6 was revealed following treatment with mTORi. A similar result was observed in another primary cancer sample in which 72-hour incubation with 10 µM mTORi showed no reduction in phospho-S6. This is in contrast to the effect observed in cell lines, where following treatment with mTORi, a significant reduction of phospho-S6 was evident. An inhibitory activity of mTORi

against mTORC1 and mTORC2 has been previously demonstrated by Garcia-Martinez and co-workers in HEK-293, HeLa and mouse embryonic fibroblasts (MEFs) (Garcia-Martinez et al., 2009). The study has shown that mTORi was a potent and highly specific inhibitor with an IC_{50} of ~ 10 nM (Garcia-Martinez et al., 2009). Additionally, an ATP-competitive mTOR inhibitor, AZD8055, structurally similar to mTORi, has been shown to be an orally bioavailable, potent and selective inhibitor with an IC_{50} of ~ 0.8 nM (Chresta et al., 2010). However, all the experiments testing mTOR inhibitors mentioned above, were performed in cancer cell lines or xenografts derived from them. In this study only a modest effect, or lack of mTORi inhibitory effect was observed in primary prostate cancer cultures derived from prostate tumours, which represent a different model of the disease, perhaps more accurate for testing new drugs. Moreover, a problem of prostate cancer heterogeneity and its' influence on treatment outcome is also represented better in primary cultures than in cell lines.

To follow up the observation of the MAPK pathway activation in cultures treated with AKTi, two MEK inhibitors, AZD6244 (MEKi) and RO-512, were tested in primary prostate cultures. In order to verify whether MEK1/2 inhibitors are effective in prostate cells, selected primary cultures (with high levels of phospho-ERK1/2) were treated with both MEK1/2 inhibitors. Treatment with MEKi has shown a dramatic decrease in phospho-ERK1/2 at 1 µM concentration, therefore confirming its inhibitory activity in prostate primary cells. There was no evidence of activation of autophagy in treated cells despite treatment with high concentrations of MEKi. However, a small increase of around 2-fold in phospho-AKT was observed, which could be an effect of regulatory feedback between the PI3K and the MAPK pathways. Next, a combination treatment with AKTi and MEKi was tested in order to determine whether activation of the MAPK pathway following treatment with AKTi can be overcome. Different treatment schedules were tested, including treatment with AKTi alone and subsequent addition of MEKi, as well as simultaneous treatment of cell cultures with both inhibitors at matching concentrations. However, the results were similar and showed a surprising increase, instead of a decrease, in phospho-ERK1/2 in all analysed samples. Moreover, a combined treatment with AKTi and MEKi AZD, with up to 25 µM concentration of each, resulted in an increased phosphorylation of ERK1/2 to even greater levels than treatment with AKTi alone. Additionally, a small increase in the

autophagy marker, LC3B, was also observed, suggesting activation of survival mechanism in cells treated with AKTi or a combination of AKTi and MEKi.

Davies and colleagues have previously demonstrated activity and efficiency of the MEKi (AZD6244) in a large panel of human cancer cell lines as well as in xenografts derived from them (Davies et al., 2007). It has been revealed that a majority of cell lines with a mutation in *KRAS*, *NRAS* or *BRAF* genes showed a significant increased sensitivity to MEK inhibition resulting in cell growth inhibition and induction of apoptosis (Davies et al., 2007). In another study it was shown that a combination treatment of the MEKi and a chemotherapeutic agent - docetaxel resulted in enhanced tumour growth inhibition in comparison to monotherapy in human colon carcinoma xenograft HCT-116 (Holt et al., 2012). However, the rate of mutations in Ras/MEK/ERK pathway in clinical prostate cancer is very low; up to 7% of clinical samples have activating point mutations of Ras and around 4 % are positive for BRAF, the most common activating mutation of RAF (Santarpia et al., 2012).

Following a disappointing lack of inhibitory activity of MEKi in AKTi-treated cultures, an additional MEK1/2 inhibitor RO-512 was tested to try to overcome the compensatory ERK1/2 phosphorylation. The RO-512 inhibitor has been shown to bind to MEK1/2, which in turn forms a complex with RAF, preventing phosphorylation of ERK1/2 and also its self-regulatory feedback loop (Beloueche-Babari et al., 2013). An initial assessment of RO-512 inhibitor activity in primary prostate cancer cultures showed an excellent inhibitory efficacy with phospho-ERK1/2 completely abolished at a concentration of 0.1 µM or 1 µM, in a BPH and a cancer culture, respectively. However, an unexpected increase in phospho-AKT was observed following treatment with 1 µM RO-512 in BPH culture, whereas in cancer cells phospho-AKT remained unaltered. Additionally, a surprising variation of phospho-S6 (downstream target of mTORC1) was also observed in the BPH cells, but not in cancer. The differences in treatment responses of BPH and cancer cells might be due to their differential reliance on mTORC1 signalling. Western blotting results showed that in the BPH culture phospho-S6 was undetectable in vehicle control cells and mTORC1 activity only became apparent when cells were treated with RO-512.

Similarly to the treatment with MEKi, a combination treatment of BPH and cancer primary cultures with AKTi and RO-512 showed no decrease, but rather a small increase in phosphorylation levels of ERK1/2. However, a combination of the drugs at 1 µM concentration decreased phospho-ERK1/2 in both BPH and cancer cultures. Interestingly, a 'switch' between phospho-ERK1 and phospho-ERK2 became apparent following treatment with AKTi alone and a combination with RO-512, and a dose-dependent decrease in phospho-S6 was observed after treatment with a combination of AKTi and RO-512 in a cancer sample, but not in BPH, which might suggest differential regulation of both pathways in BPH and cancer cells.

Both Ras/MEK/ERK pathway and the PI3K/AKT/mTOR have been shown to be over-activated in many human cancers (McCubrey et al., 2012b). It has been demonstrated that Ras/MEK/ERK signalling activity is essential for the maintenance of the growth and viability of many tumours, including breast and prostate cancer and most importantly, that its increased activity is associated with a poor prognosis (Steelman et al., 2011). It has been shown that MEK inhibitors' ability to inhibit ERK activity might be limited by their toxicity and also by relief of ERK-dependent feedback inhibition of RAF, which leads to an increase in phosphorylation of MEK (Alessi et al., 1995a). A novel allosteric inhibitor of MEK1/2, CH5126766 (RO-512) has been shown to decrease phospho-ERK1/2 levels, but does not enhance MEK phosphorylation (Ishii et al., 2013). Its efficacy has been demonstrated in a number of human cancer cell lines and also in the HCT-116 xenograft model, regardless of the mutational status of the Ras/MEK/ERK pathway in those cells (Ishii et al., 2013). However, in this study neither of MEK1/2 inhibitors was able to overcome the compensatory ERK1/2 activation caused by inhibition of AKT. It is not clear why a combination treatment of AKTi with MEKi did not reduce activity of ERK. However, a 'switch' between phospho-ERK1 and phospho-ERK2, which was observed in BPH and cancer cultures following treatment with either AKTi alone or with a combination with MEK1/2 inhibitor, could indicate that different targets of ERK might be activated downstream from ERK depending on the treatment. It has been demonstrated that ERK2, but not ERK1 signalling was necessary for Ras-induced epithelial-to-mesenchymal transition (EMT) (Shin et al., 2010, Shin and Blenis, 2010). The study has shown that overexpression of ERK2 was sufficient to induce EMT.

Interestingly, it has also been suggested that ERK1 and ERK 2 are not functionally redundant molecules (Shin et al., 2010).

Taken together, differential phosphorylation of ERK1 and ERK2 following treatment with AKTi or a combination of AKTi with MEKi might indicate that the functional outcome of treatment will probably depend on dominant isoform of ERK.

It has been suggested that inhibition of the MEK/ERK signalling and therefore reduction of the activity of anti-apoptotic proteins such as Bcl-2 and Mcl-2, could be helpful in decreasing the threshold for induction of apoptosis (Holt et al., 2012). Additionally, it has been demonstrated that chronic dosing of MEKi resulted in morphological changes to a more differentiated phenotype in a colon carcinoma SW-620 xenograft (Davies et al., 2007).

Changes in cell morphology were also observed in this study and to follow up this observation, an analysis of differentiation markers was performed on primary cultures treated with MEK1/2 inhibitors (MEKi and RO-512) either alone or in a combination with AKTi. The results showed that the expression of prostate differentiation marker CK18 did not increase following treatment, therefore indicating that primary cells are not undergoing differentiation after treatment.

However, a β-galactosidase staining of treated cultures has revealed that the cells became senescent after treatment with a combination with AKTi and MEKi. In the literature it has been presented that senescence was frequently triggered in tumours in response to chemotherapy and radiotherapy treatment in tumour samples from cancer patients (Nardella et al., 2011, Roninson, 2003). It has been demonstrated that PTEN-loss-induced cellular senescence inhibits tumorigenesis *in vivo* in a human xenograft model of prostate cancer (Alimonti et al., 2010), and that induction of senescence in cancer cells could indeed be a good therapeutic strategy for treatment of prostate cancer (Alimonti et al., 2010).

5.6. Conclusions

This work has provided evidence that pharmacological inhibition of the PI3K/AKT/mTOR pathway with AKT and mTOR inhibitors in human prostate cancer is not sufficient. A compensatory Ras/MEK/ERK pathway activation was observed in all analysed patient tissues.

This study also highlights the importance of using patient-derived tumour cells in preclinical assessment of new drugs rather than relying on cancer cell lines alone. In this work, treatment with AKTi and mTORi of prostate cancer cell line LNCaP showed a significant therapeutic advantage when targeting the PI3K pathway. However, those results were not confirmed in primary prostate cultures. Moreover, primary prostate cells activated autophagy as well as a compensatory survival pathway in response to treatment. Surprisingly, treatment with a combination of AKT and MEK1/2 inhibitors did not inhibit ERK signalling in primary prostate cultures, but an irreversible growth arrest was observed.

The majority of preclinical screening is routinely performed in panels of cell lines and xenografts derived from them. Drug development research based on those models is frequently unsuccessful in patients and new drugs ultimately fail in clinical trials. In contrast, many potentially beneficial therapies are discontinued when they fail to show efficacy in cell lines (Daniel et al., 2009). Therefore it is crucial to invest in more accurate models of human cancers for preclinical testing.

Future work should focus on determining the functional consequences of combined pharmacological targeting of the PI3K/AKT/mTOR and the Ras/MEK/ERK pathways, especially in cancer stem-like cells. This would verify whether induction of senescence could potentially offer a successful novel strategy for the treatment of prostate cancer.

APPENDICES

Appendix 1: Patient primary sample details

	Patient ID	Diagnosis	Age	Operation
1	H135/11	Cancer Gleason 9 (5+4) on hormones	56	Channel TURP
2	H149/12	Cancer Gleason 9 (4+5) on hormones	78	Channel TURP
3	H163/12	Cancer Gleason 8 (4+4) on hormones	65	Channel TURP
4	H209/12	Cancer Gleason 7 (4+3)	64	Radical prostatectomy
5	H210/12	Cancer Gleason 7 (3+4)	69	Radical prostatectomy
6	H217/12	Cancer Gleason 7 (3+4)	72	Radical prostatectomy
7	H224/12	Cancer Gleason 9 (4+5), castration resistant	76	Channel TURP
8	H233/12 RA	Cancer Gleason 7 (4+3)	61	Radical prostatectomy
9	H233/12 L	Normal control	61	Radical prostatectomy
10	H236/12	Cancer Gleason 8 (4+4)	61	Radical prostatectomy
11	H237/12 LA	Cancer Gleason 7 (3+4)	66	Radical prostatectomy
12	H239/12 RB	Cancer Gleason 9 (4+5)	50	Radical prostatectomy
13	H240/12 RA + RB	Cancer Gleason 7 (3+4)	66	Radical prostatectomy
14	H252/12	Cancer Gleason 7 (3+4)	60	Radical prostatectomy
15	H268/12	BPH	62	TURP
16	H271/12	Cancer Gleason 9, castration resistant	86	Channel TURP
17	H277/13	BPH	68	TURP
18	H278/13 RA	Cancer Gleason 6 (3+3)	72	Radical prostatectomy
19	H282/13 RA+RB	Cancer Gleason 7 (4+3)	62	Radical prostatectomy

20	H304/13	Cancer Gleason 8 (4+4)	66	Radical prostatectomy
21	H308/13 R + L	Cancer Gleason 7 (3+4)	66	Radical prostatectomy
22	H310/13 R + L	Cancer Gleason 7 (3+4)	67	Radical prostatectomy
23	H313/13	BPH	65	TURP
24	H315/13	Cancer Gleason 6 (3+3)	62	Radical prostatectomy
25	H317/13 LA	Cancer Gleason 7 (3+4)	65	Radical prostatectomy
26	H329/13 LB	Cancer Gleason 7 (3+4)	53	Radical prostatectomy
27	H330/13	Cancer Gleason 7 (3+4)	58	Radical prostatectomy
28	H359/13	Cancer Gleason 8 (3+5)	64	Channel TURP
29	H363/13 R	Cancer Gleason 8 (4+4) on hormones	74	Channel TURP
30	H366/13	Cancer Gleason 7 (4+3) on hormones	67	Radical prostatectomy
31	H373/13	Cancer Gleason 7 (3+4)	82	TURP
32	H377/13	Cancer Gleason 7 (3+4)	60	Radical prostatectomy

ABBREVIATIONS

%	Percentage
4EBP1	eukaryotic translation initiation factor 4E binding protein 1
ABCG2	ATP-binding cassette sub-family G
ADP	Adenosine diphosphate
ADT	Androgen deprivation therapy
AKT	v-akt murine thymoma viral oncogene homolog
ALDH	Aldehyde dehydrogenase
APC	Allophycocyanin
APES	aminopropyltriethoxysilane
AR	Androgen receptor
ATCC	American type culture collection
B. Taurus	Bos Taurus
BAD	BCL2-associated agonist of cell death
BCA	Bicinchoninic acid
BM	Basement Membrane
bp	Base pairs
BPE	Bovine pituitary extract
BPH	Benign Prostatic Hyperplasia
BRAF	V-Raf Murine Sarcoma Viral Oncogene Homolog B
BSA	Bovine serum albumin
c-Myc	v-myc avian myelocytomatosis viral oncogene homolog
CaP	Prostate cancer
CB	Committed basal
cDNA	Complimentary DNA

CFE	Colony forming efficiency
CHK1	Checkpoint kinase 1
CK	Cytokeratin
Cl	Chloride
Cm	Centimetre
Cm^2	Centimetre squared
CO_2	Carbon dioxide
CPA	Carboxypeptidase
CRPC	Castrate resistant prostate cancer
CRU	Cancer research unit
CSC	Cancer stem cell
C_T	Threshold cycle
D10	DMEM + 10% FCS
DAPI	4',6-diamidino-2-phenylindole
ddH_20	Double distilled water
DEPC	Diethylpyrocarbonate
dH_2O	Distilled water
DHT	Dihydrotestosterone
DMEM	Dulbecco's modified eagle medium
DMSO	Dimethyl sulfoxide
DNA	Deoxyribonucleic acid
dNTPS	Deoxyribonucleotide triphosphate
DRE	Digital Rectal Exam
DTT	Dithiothreitol
EC50	Half maximal effective concentration
ECACC	European Collection of Animal Cell Culture

ECACC	European collection of cell cultures
ECL	Enhanced chemiluminescence
ECM	Extracellular matrix
EDTA	Ethylenediaminetetraacetic acid
EGF	Epidermal growth factor
EGFR	Epidermal growth factor receptor
EGR1	Early Growth Response 1
EMT	Epithelial-to-mesenchymal transition
ER	Endoplasmic reticulum
ERK	Extracellular signal-regulated kinases
ES	Embryonic stem
EtOH	Ethanol
FAK	Focal adhesion kinase
FCS	Fetal calf serum
FDA	Food and Drug Administration
FGF	Fibroblast growth factor
FITC	Fluorescein isothiocyanate
FOXO3A	forkhead box O3
FS	Forward scatter
g	Gram
G0	G zero phase
G1	Gap 1 phase
G2/M	Gap 2 phase/mitosis
GAPDH	Glyceraldehyde 3-phosphate dehydrogenase
GPCR	G-protein coupled receptor
GSK3	Glycogen synthase kinase 3

G_Y	Gray
H. Sapiens	Homo Sapiens
H&E	Haematoxylin and eosin
H7	Ham's F-12 medium + 7% FCS
HCl	Hydrogen chloride
HNSCC	Head and neck squamous cell carcinoma
HRPC	Hormone resistant prostate cancer
HRP	Horseradish peroxidase
HSC	Haematopoietic stem cell
IGF2	Insulin-like growth factor 2 (somatomedin A)
IGFR	Insulin-like growth factor receptor
IgG	Immunoglobulin G
IHC	Immunohistochemistry
IRS1	Insulin receptor substrate 1
IRS2	Insulin receptor substrate 2
IU	International units
kB	Kilobase
KCl	Potassium chloride
kDa	Kilo Dalton
Ki67 (MKI67)	Antigen identified by monoclonal antibody Ki-67
KSFM	Keratinocyte serum free medium
LA	Left apex
LB	Left base
LIF	Leukaemia inhibitory factor
Lin	Linear
LOH	Loss of heterozygosity

LRP	Laparoscopic radical prostatectomy
M. Musculus	Mus musculus
MACS	Magnetic-activated cell sorting
MAPK	Mitogen-activated protein kinase
MDM2	MDM2 oncogene, E3 ubiquitin protein ligase
MDR1	Multidrug resistance protein 1
MEK	MAPK/ERK kinase
MET	Mesenchymal-to-epithelial transition
$MgCl_2$	Magnesium chloride
Min	Minute
miR	micro RNA
MiRNA	micro RNA
ml	Millilitre
mm	Millimetre
mM	Millimolar
mRNA	Messenger RNA
mSin1	Mitogen-activated-protein-kinase-associated protein 1
mTORC1	mTOR complex1
mTORC2	mTOR complex 2
MTS	[3-(4,5-dimethylthiazol-2-yl)-5-(3-carboxymethoxyphenyl)-2-(4-sulfophenyl)-2H-tetrazolium, inner salt]
Mw	Molecular weight
NaCl	Sodium chloride
NaOH	Sodium hydroxide
NE	Neuroendocrine
ng	Nanogram

NKX3.1	NK3 transcription factor related, locus 1
nM	Nanomolar
ORP	Open radical prostatectomy
P53	Tumour protein 53
P63	Tumour protein 63
PAGE	Polyacrylamide gel electrophoresis
PAP	Prostatic acid phosphatase
PARP	Poly (ADP-ribose) polymerase
PBS	Phosphate-buffered saline
PCR	Polymerase chain reaction
PDGFR	Platelet derived growth factor receptor
PDK1	Phosphoinositide-dependent kinase 1
PE	Phycoerythrin
PFA	Paraformaldehyde
PH	Pleckstrin homology domain
PI	Propidium iodide
PI3K	Phosphoinositide 3-kinase
PIC	Protease inhibitor cocktail
PIN	Prostatic intraepithelial neoplasia
PIP2	phosphatidylinositol 4,5-biphosphate
PIP3	phosphatidylinositol (3-5)-triphosphate
PM	Plasma membrane
PPARγ	Peroxisome proliferator-activated receptor gamma
PSA	Prostate-specific antigen
PTEN	Phosphatase and tensin homolog
PVDF	Polyvinylidene difluoride

qPCR	Quantitative PCR
qRT-PCR	Quantitative real-time PCR
R1	Region 1
R10	RPMI + 10% FCS
R2	Region 2
R3	Region 3
R5	RPMI + 5% FCS
Radical	Radical prostatectomy
RAF	v-raf murine sarcoma 3611 viral oncogene homolog
Rag2	Recombination activating gene 2
RAS	Rat Sarcoma Viral Oncogene Homolog
Rb	Retinoblastoma
RB	Right base
rictor	rapamycin-insensitive companion of mTOR
RNA	Ribonucleic acid
RPLP0	Ribosomal protein, large, P0
RPM	Revolutions per minute
RPMI	Roswell Park Memorial Institute medium
RSK	Ribosomal s6 kinase
RT	Room temperature
RT-PCR	Reverse transcriptase PCR
RTK	Receptor tyrosine kinase
S6K	Ribosomal S6 kinase
SC	Stem cell
SCM	Stem cell medium
Scr	Scrambled siRNA

SDS	Sodium dodecyl sulphate
SEM	Standard error of the mean
siRNA	Small interfering RNA
SS	Side scatter
Stem	Stem cell
STOs	STO (Mouse embryonic fibroblast cell line)
SV40	Simian vacuolating virus 40
T25	25 cm^2 tissue culture flask
T75	75 cm^2 tissue culture flask
TA	Transit-amplifying cell
TAE	Tris base, acetic acid and EDTA buffer
Taq	Thermus aquaticus
TBS	Tris-buffered saline
TBST	Tris-buffered saline with Tween-20
TE	Tris EDTA buffer
TF	Transcription factor
tRNA	Transfer ribonucleic acid
TSA	Trichostatin A
TSC2	Tuberous Sclerosis 2
TSE	Tris, sucrose, EDTA buffer
TURP	Transurethral resection of the prostate
TX-100	Triton X-100
U/mg	Units per milligram
U/ml	Units per millilitre
UK	United Kingdom
V	Volts

v/v	Volume per volume
w/v	Weight per volume
α2β1hi	High expression of alpha 2 beta 1 integrin
α2β1lo	Low expression of alpha 2 beta 1 integrin
β-actin	Beta actin
µg	Microgram
µl	Microlitre
µm	Micrometre
µM	Micromolar

REFERENCES

ABATE-SHEN, C. & SHEN, M. M. 2000. Molecular genetics of prostate cancer. *Genes Dev,* 14**,** 2410-34.

ABRAHAMSSON, P. A. 1999. Neuroendocrine cells in tumour growth of the prostate. *Endocr Relat Cancer,* 6**,** 503-19.

AHN, N. G., SEGER, R., BRATLIEN, R. L., DILTZ, C. D., TONKS, N. K. & KREBS, E. G. 1991. Multiple components in an epidermal growth factor-stimulated protein kinase cascade. In vitro activation of a myelin basic protein/microtubule-associated protein 2 kinase. *J Biol Chem,* 266**,** 4220-7.

AL-HAJJ, M., WICHA, M. S., BENITO-HERNANDEZ, A., MORRISON, S. J. & CLARKE, M. F. 2003. Prospective identification of tumorigenic breast cancer cells. *Proc Natl Acad Sci U S A,* 100**,** 3983-8.

ALESSI, D. R., CUENDA, A., COHEN, P., DUDLEY, D. T. & SALTIEL, A. R. 1995a. PD 098059 is a specific inhibitor of the activation of mitogen-activated protein kinase kinase in vitro and in vivo. *J Biol Chem,* 270**,** 27489-94.

ALESSI, D. R., GOMEZ, N., MOORHEAD, G., LEWIS, T., KEYSE, S. M. & COHEN, P. 1995b. Inactivation of p42 MAP kinase by protein phosphatase 2A and a protein tyrosine phosphatase, but not CL100, in various cell lines. *Current Biology,* 5**,** 283-95.

ALESSI, D. R., SAITO, Y., CAMPBELL, D. G., COHEN, P., SITHANANDAM, G., RAPP, U., ASHWORTH, A., MARSHALL, C. J. & COWLEY, S. 1994. Identification of the sites in MAP kinase kinase-1 phosphorylated by p74raf-1. *EMBO J,* 13**,** 1610-9.

ALIMONTI, A., NARDELLA, C., CHEN, Z., CLOHESSY, J. G., CARRACEDO, A., TROTMAN, L. C., CHENG, K., VARMEH, S., KOZMA, S. C., THOMAS, G., ROSIVATZ, E., WOSCHOLSKI, R., COGNETTI, F., SCHER, H. I. & PANDOLFI, P. P. 2010. A novel type of cellular senescence that can be enhanced in mouse models and human tumor xenografts to suppress prostate tumorigenesis. *J Clin Invest,* 120**,** 681-93.

ANREDDY, N., GUPTA, P., KATHAWALA, R. J., PATEL, A., WURPEL, J. N. & CHEN, Z. S. 2014. Tyrosine Kinase Inhibitors as Reversal Agents for ABC Transporter Mediated Drug Resistance. *Molecules,* 19**,** 13848-13877.

ANTON, M. & GRAHAM, F. L. 1995. Site-specific recombination mediated by an adenovirus vector expressing the Cre recombinase protein: a molecular switch for control of gene expression. *Journal of Virology,* 69**,** 4600-6.

BELOUECHE-BABARI, M., JAMIN, Y., ARUNAN, V., WALKER-SAMUEL, S., REVILL, M., SMITH, P. D., HALLIDAY, J., WATERTON, J. C., BARJAT, H., WORKMAN, P., LEACH, M. O. & ROBINSON, S. P. 2013. Acute tumour response to the MEK1/2 inhibitor selumetinib (AZD6244, ARRY-142886) evaluated by non-invasive diffusion-weighted MRI. *Br J Cancer,* 109**,** 1562-9.

BENNETT, N. C., GARDINER, R. A., HOOPER, J. D., JOHNSON, D. W. & GOBE, G. C. 2010. Molecular cell biology of androgen receptor signalling. *Int J Biochem Cell Biol,* 42**,** 813-27.

BERQUIN, I. M., MIN, Y., WU, R., WU, H. & CHEN, Y. Q. 2005. Expression signature of the mouse prostate. *J Biol Chem,* 280**,** 36442-51.

BERRY, P. A., MAITLAND, N. J. & COLLINS, A. T. 2008. Androgen receptor signalling in prostate: effects of stromal factors on normal and cancer stem cells. *Mol Cell Endocrinol,* 288**,** 30-7.

BILL-AXELSON, A., HOLMBERG, L., RUUTU, M., HAGGMAN, M., ANDERSSON, S. O., BRATELL, S., SPANGBERG, A., BUSCH, C., NORDLING, S., GARMO, H., PALMGREN, J., ADAMI, H. O.,

NORLEN, B. J. & JOHANSSON, J. E. 2005. Radical prostatectomy versus watchful waiting in early prostate cancer. *N Engl J Med,* 352**,** 1977-84.

BITTING, R. L. & ARMSTRONG, A. J. 2013. Targeting the PI3K/Akt/mTOR pathway in castration-resistant prostate cancer. *Endocrine-Related Cancer*.

BLANCO-APARICIO, C., RENNER, O., LEAL, J. F. M. & CARNERO, A. 2007. PTEN, more than the AKT pathway. *Carcinogenesis,* 28**,** 1379-1386.

BONKHOFF, H. & REMBERGER, K. 1993. Widespread distribution of nuclear androgen receptors in the basal cell layer of the normal and hyperplastic human prostate. *Virchows Arch A Pathol Anat Histopathol,* 422**,** 35-8.

BONKHOFF, H., STEIN, U. & REMBERGER, K. 1995. Endocrine-paracrine cell types in the prostate and prostatic adenocarcinoma are postmitotic cells. *Hum Pathol,* 26**,** 167-70.

BONNET, D. & DICK, J. E. 1997. Human acute myeloid leukemia is organized as a hierarchy that originates from a primitive hematopoietic cell. *Nat Med,* 3**,** 730-7.

BOSTWICK, D. G., LIU, L., BRAWER, M. K. & QIAN, J. 2004. High-grade prostatic intraepithelial neoplasia. *Rev Urol,* 6**,** 171-9.

BOULTON, T. G., NYE, S. H., ROBBINS, D. J., IP, N. Y., RADZIEJEWSKA, E., MORGENBESSER, S. D., DEPINHO, R. A., PANAYOTATOS, N., COBB, M. H. & YANCOPOULOS, G. D. 1991. ERKs: a family of protein-serine/threonine kinases that are activated and tyrosine phosphorylated in response to insulin and NGF. *Cell,* 65**,** 663-75.

BRUNET, A., BONNI, A., ZIGMOND, M. J., LIN, M. Z., JUO, P., HU, L. S., ANDERSON, M. J., ARDEN, K. C., BLENIS, J. & GREENBERG, M. E. 1999. Akt promotes cell survival by phosphorylating and inhibiting a Forkhead transcription factor. *Cell,* 96**,** 857-68.

CAIRNS, P., OKAMI, K., HALACHMI, S., HALACHMI, N., ESTELLER, M., HERMAN, J. G., ISAACS, W. B., BOVA, G. S. & SIDRANSKY, D. 1997. Frequent inactivation of PTEN/MMAC1 in primary prostate cancer. *Cancer Research,* 57**,** 4997-5000.

CANTLEY, L. C. 2002. The phosphoinositide 3-kinase pathway. *Science,* 296**,** 1655-1657.

CARNERO, A., BLANCO-APARICIO, C., RENNER, O., LINK, W. & LEAL, J. F. 2008. The PTEN/PI3K/AKT signalling pathway in cancer, therapeutic implications. *Curr Cancer Drug Targets,* 8**,** 187-98.

CARRACEDO, A., MA, L., TERUYA-FELDSTEIN, J., ROJO, F., SALMENA, L., ALIMONTI, A., EGIA, A., SASAKI, A. T., THOMAS, G., KOZMA, S. C., PAPA, A., NARDELLA, C., CANTLEY, L. C., BASELGA, J. & PANDOLFI, P. P. 2008. Inhibition of mTORC1 leads to MAPK pathway activation through a PI3K-dependent feedback loop in human cancer. *J Clin Invest,* 118**,** 3065-74.

CARRACEDO, A. & PANDOLFI, P. P. 2008. The PTEN-PI3K pathway: of feedbacks and cross-talks. *Oncogene,* 27**,** 5527-41.

CARVER, B. S., CHAPINSKI, C., WONGVIPAT, J., HIERONYMUS, H., CHEN, Y., CHANDARLAPATY, S., ARORA, V. K., LE, C., KOUTCHER, J., SCHER, H., SCARDINO, P. T., ROSEN, N. & SAWYERS, C. L. 2011. Reciprocal feedback regulation of PI3K and androgen receptor signaling in PTEN-deficient prostate cancer. *Cancer Cell,* 19**,** 575-86.

CATALONA, W. J., CARVALHAL, G. F., MAGER, D. E. & SMITH, D. S. 1999. Potency, continence and complication rates in 1,870 consecutive radical retropubic prostatectomies. *J Urol,* 162**,** 433-8.

CHALHOUB, N. & BAKER, S. J. 2009. PTEN and the PI3-Kinase Pathway in Cancer. *Annual Review of Pathology-Mechanisms of Disease,* 4**,** 127-150.

CHANG, K. H., LI, R., PAPARI-ZAREEI, M., WATUMULL, L., ZHAO, Y. D., AUCHUS, R. J. & SHARIFI, N. 2011. Dihydrotestosterone synthesis bypasses testosterone to drive castration-resistant prostate cancer. *Proc Natl Acad Sci U S A,* 108**,** 13728-33.

CHAPPELL, W. H., STEELMAN, L. S., LONG, J. M., KEMPF, R. C., ABRAMS, S. L., FRANKLIN, R. A., BASECKE, J., STIVALA, F., DONIA, M., FAGONE, P., MALAPONTE, G., MAZZARINO, M. C., NICOLETTI, F., LIBRA, M., MAKSIMOVIC-IVANIC, D., MIJATOVIC, S., MONTALTO, G., CERVELLO, M., LAIDLER, P., MILELLA, M., TAFURI, A., BONATI, A., EVANGELISTI, C.,

COCCO, L., MARTELLI, A. M. & MCCUBREY, J. A. 2011. Ras/Raf/MEK/ERK and PI3K/PTEN/Akt/mTOR inhibitors: rationale and importance to inhibiting these pathways in human health. *Oncotarget,* 2**,** 135-64.

CHEN, N., ERITJA, N., LOCK, R. & DEBNATH, J. 2013. Autophagy restricts proliferation driven by oncogenic phosphatidylinositol 3-kinase in three-dimensional culture. *Oncogene,* 32**,** 2543-54.

CHENG, J. Q., LINDSLEY, C. W., CHENG, G. Z., YANG, H. & NICOSIA, S. V. 2005. The Akt/PKB pathway: molecular target for cancer drug discovery. *Oncogene,* 24**,** 7482-7492.

CHOI, J., CHEN, J., SCHREIBER, S. L. & CLARDY, J. 1996. Structure of the FKBP12-rapamycin complex interacting with the binding domain of human FRAP. *Science,* 273**,** 239-42.

CHRESTA, C. M., DAVIES, B. R., HICKSON, I., HARDING, T., COSULICH, S., CRITCHLOW, S. E., VINCENT, J. P., ELLSTON, R., JONES, D., SINI, P., JAMES, D., HOWARD, Z., DUDLEY, P., HUGHES, G., SMITH, L., MAGUIRE, S., HUMMERSONE, M., MALAGU, K., MENEAR, K., JENKINS, R., JACOBSEN, M., SMITH, G. C., GUICHARD, S. & PASS, M. 2010. AZD8055 is a potent, selective, and orally bioavailable ATP-competitive mammalian target of rapamycin kinase inhibitor with in vitro and in vivo antitumor activity. *Cancer Res,* 70**,** 288-98.

COLLINS, A. T., BERRY, P. A., HYDE, C., STOWER, M. J. & MAITLAND, N. J. 2005. Prospective identification of tumorigenic prostate cancer stem cells. *Cancer Res,* 65**,** 10946-51.

COLLINS, A. T. & MAITLAND, N. J. 2006. Prostate cancer stem cells. *Eur J Cancer,* 42**,** 1213-8.

COURTNEY, K. D., CORCORAN, R. B. & ENGELMAN, J. A. 2010. The PI3K pathway as drug target in human cancer. *J Clin Oncol,* 28**,** 1075-83.

CROSS, D. A., ALESSI, D. R., COHEN, P., ANDJELKOVICH, M. & HEMMINGS, B. A. 1995. Inhibition of glycogen synthase kinase-3 by insulin mediated by protein kinase B. *Nature,* 378**,** 785-9.

CROWELL, J. A., STEELE, V. E. & FAY, J. R. 2007. Targeting the AKT protein kinase for cancer chemoprevention. *Molecular Cancer Therapeutics,* 6**,** 2139-48.

CULIG, Z. & SANTER, F. R. 2012. Androgen receptor co-activators in the regulation of cellular events in prostate cancer. *World J Urol,* 30**,** 297-302.

DANIEL, V. C., MARCHIONNI, L., HIERMAN, J. S., RHODES, J. T., DEVEREUX, W. L., RUDIN, C. M., YUNG, R., PARMIGIANI, G., DORSCH, M., PEACOCK, C. D. & WATKINS, D. N. 2009. A primary xenograft model of small-cell lung cancer reveals irreversible changes in gene expression imposed by culture in vitro. *Cancer Res,* 69**,** 3364-73.

DAVIES, B. R., GREENWOOD, H., DUDLEY, P., CRAFTER, C., YU, D. H., ZHANG, J., LI, J., GAO, B., JI, Q., MAYNARD, J., RICKETTS, S. A., CROSS, D., COSULICH, S., CHRESTA, C. C., PAGE, K., YATES, J., LANE, C., WATSON, R., LUKE, R., OGILVIE, D. & PASS, M. 2012. Preclinical pharmacology of AZD5363, an inhibitor of AKT: pharmacodynamics, antitumor activity, and correlation of monotherapy activity with genetic background. *Molecular Cancer Therapeutics,* 11**,** 873-87.

DAVIES, B. R., LOGIE, A., MCKAY, J. S., MARTIN, P., STEELE, S., JENKINS, R., COCKERILL, M., CARTLIDGE, S. & SMITH, P. D. 2007. AZD6244 (ARRY-142886), a potent inhibitor of mitogen-activated protein kinase/extracellular signal-regulated kinase kinase 1/2 kinases: mechanism of action in vivo, pharmacokinetic/pharmacodynamic relationship, and potential for combination in preclinical models. *Mol Cancer Ther,* 6**,** 2209-19.

DE VELASCO, M. A. & UEMURA, H. 2012. Preclinical Remodeling of Human Prostate Cancer through the PTEN/AKT Pathway. *Adv Urol,* 2012**,** 419348.

DEL PESO, L., GONZALEZ-GARCIA, M., PAGE, C., HERRERA, R. & NUNEZ, G. 1997. Interleukin-3-induced phosphorylation of BAD through the protein kinase Akt. *Science,* 278**,** 687-9.

DI CRISTOFANO, A. & PANDOLFI, P. P. 2000. The multiple roles of PTEN in tumor suppression. *Cell,* 100**,** 387-90.

DI CRISTOFANO, A., PESCE, B., CORDON-CARDO, C. & PANDOLFI, P. P. 1998. Pten is essential for embryonic development and tumour suppression. *Nature Genetics,* 19**,** 348-55.

DICKSTEIN, R. J., NITTI, G., DINNEY, C. P., DAVIES, B. R., KAMAT, A. M. & MCCONKEY, D. J. 2012. Autophagy limits the cytotoxic effects of the AKT inhibitor AZ7328 in human bladder cancer cells. *Cancer Biology & Therapy,* 13**,** 1325-38.

DILLON, R. L., WHITE, D. E. & MULLER, W. J. 2007. The phosphatidyl inositol 3-kinase signaling network: implications for human breast cancer. *Oncogene,* 26**,** 1338-45.

DOUGHERTY, M. K., MULLER, J., RITT, D. A., ZHOU, M., ZHOU, X. Z., COPELAND, T. D., CONRADS, T. P., VEENSTRA, T. D., LU, K. P. & MORRISON, D. K. 2005. Regulation of Raf-1 by direct feedback phosphorylation. *Molecular Cell,* 17**,** 215-24.

DUBROVSKA, A., ELLIOTT, J., SALAMONE, R. J., KIM, S., AIMONE, L. J., WALKER, J. R., WATSON, J., SAUVEUR-MICHEL, M., GARCIA-ECHEVERRIA, C., CHO, C. Y., REDDY, V. A. & SCHULTZ, P. G. 2010. Combination therapy targeting both tumor-initiating and differentiated cell populations in prostate carcinoma. *Clin Cancer Res,* 16**,** 5692-702.

DUBROVSKA, A., KIM, S., SALAMONE, R. J., WALKER, J. R., MAIRA, S. M., GARCIA-ECHEVERRIA, C., SCHULTZ, P. G. & REDDY, V. A. 2009. The role of PTEN/Akt/PI3K signaling in the maintenance and viability of prostate cancer stem-like cell populations. *Proc Natl Acad Sci U S A,* 106**,** 268-73.

DUCHESNE, G. 2011. Localised prostate cancer - current treatment options. *Aust Fam Physician,* 40**,** 768-71.

EFEYAN, A. & SABATINI, D. M. 2010. mTOR and cancer: many loops in one pathway. *Curr Opin Cell Biol,* 22**,** 169-76.

EL SHEIKH, S. S., ROMANSKA, H. M., ABEL, P., DOMIN, J. & LALANI EL, N. 2008. Predictive value of PTEN and AR coexpression of sustained responsiveness to hormonal therapy in prostate cancer--a pilot study. *Neoplasia,* 10**,** 949-53.

ENGELMAN, J. A. 2009. Targeting PI3K signalling in cancer: opportunities, challenges and limitations. *Nat Rev Cancer,* 9**,** 550-62.

EPSTEIN, J. I. 2010. An update of the Gleason grading system. *J Urol,* 183**,** 433-40.

ERAMO, A., LOTTI, F., SETTE, G., PILOZZI, E., BIFFONI, M., DI VIRGILIO, A., CONTICELLO, C., RUCO, L., PESCHLE, C. & DE MARIA, R. 2008. Identification and expansion of the tumorigenic lung cancer stem cell population. *Cell Death and Differentiation,* 15**,** 504-14.

ESCH, L., SCHULZ, W. A. & ALBERS, P. 2014. Sequential treatment with taxanes and novel anti-androgenic compounds in castration-resistant prostate cancer. *Oncol Res Treat,* 37**,** 492-8.

FELDMAN, B. J. & FELDMAN, D. 2001. The development of androgen-independent prostate cancer. *Nat Rev Cancer,* 1**,** 34-45.

FLORYK, D. & THOMPSON, T. C. 2008. Perifosine induces differentiation and cell death in prostate cancer cells. *Cancer Lett,* 266**,** 216-26.

FRAME, F. M. & MAITLAND, N. J. 2011. Cancer stem cells, models of study and implications of therapy resistance mechanisms. *Adv Exp Med Biol,* 720**,** 105-18.

GAO, N., ZHANG, Z., JIANG, B. H. & SHI, X. 2003. Role of PI3K/AKT/mTOR signaling in the cell cycle progression of human prostate cancer. *Biochem Biophys Res Commun,* 310**,** 1124-32.

GARCIA-MARTINEZ, J. M., MORAN, J., CLARKE, R. G., GRAY, A., COSULICH, S. C., CHRESTA, C. M. & ALESSI, D. R. 2009. Ku-0063794 is a specific inhibitor of the mammalian target of rapamycin (mTOR). *Biochem J,* 421**,** 29-42.

GERHARDT, J., MONTANI, M., WILD, P., BEER, M., HUBER, F., HERMANNS, T., MUNTENER, M. & KRISTIANSEN, G. 2012. FOXA1 promotes tumor progression in prostate cancer and represents a novel hallmark of castration-resistant prostate cancer. *American Journal of Pathology,* 180**,** 848-61.

GIOELI, D., MANDELL, J. W., PETRONI, G. R., FRIERSON, H. F., JR. & WEBER, M. J. 1999. Activation of mitogen-activated protein kinase associated with prostate cancer progression. *Cancer Res,* 59**,** 279-84.

GIOELI, D., WUNDERLICH, W., SEBOLT-LEOPOLD, J., BEKIRANOV, S., WULFKUHLE, J. D., PETRICOIN, E. F., 3RD, CONAWAY, M. & WEBER, M. J. 2011. Compensatory pathways induced by MEK inhibition are effective drug targets for combination therapy against castration-resistant prostate cancer. *Molecular Cancer Therapeutics,* 10**,** 1581-90.

GLEASON, D. F. 1966. Classification of prostatic carcinomas. *Cancer Chemother Rep,* 50**,** 125-8.

GOTTSCHALK, A. R., DOAN, A., NAKAMURA, J. L., STOKOE, D. & HAAS-KOGAN, D. A. 2005. Inhibition of phosphatidylinositol-3-kinase causes increased sensitivity to radiation through a PKB-dependent mechanism. *Int J Radiat Oncol Biol Phys,* 63**,** 1221-7.

GRANT, S. 2008. Cotargeting survival signaling pathways in cancer. *J Clin Invest,* 118**,** 3003-6.

GUERTIN, D. A., STEVENS, D. M., SAITOH, M., KINKEL, S., CROSBY, K., SHEEN, J. H., MULLHOLLAND, D. J., MAGNUSON, M. A., WU, H. & SABATINI, D. M. 2009. mTOR Complex 2 Is Required for the Development of Prostate Cancer Induced by Pten Loss in Mice. *Cancer Cell,* 15**,** 148-159.

HALL, J. A., MAITLAND, N. J., STOWER, M. & LANG, S. H. 2002. Primary prostate stromal cells modulate the morphology and migration of primary prostate epithelial cells in type 1 collagen gels. *Cancer Res,* 62**,** 58-62.

HALL, P. A. & WATT, F. M. 1989. Stem cells: the generation and maintenance of cellular diversity. *Development,* 106**,** 619-33.

HAYWARD, S. W., DAHIYA, R., CUNHA, G. R., BARTEK, J., DESHPANDE, N. & NARAYAN, P. 1995. Establishment and characterization of an immortalized but non-transformed human prostate epithelial cell line: BPH-1. *In Vitro Cell Dev Biol Anim,* 31**,** 14-24.

HENNESSEY, P. T., OCHS, M. F., MYDLARZ, W. W., HSUEH, W., COPE, L., YU, W. & CALIFANO, J. A. 2011. Promoter methylation in head and neck squamous cell carcinoma cell lines is significantly different than methylation in primary tumors and xenografts. *PLoS One,* 6**,** e20584.

HIRAI, H., SOOTOME, H., NAKATSURU, Y., MIYAMA, K., TAGUCHI, S., TSUJIOKA, K., UENO, Y., HATCH, H., MAJUMDER, P. K., PAN, B. S. & KOTANI, H. 2010. MK-2206, an allosteric Akt inhibitor, enhances antitumor efficacy by standard chemotherapeutic agents or molecular targeted drugs in vitro and in vivo. *Molecular Cancer Therapeutics,* 9**,** 1956-67.

HOBISCH, A., EDER, I. E., PUTZ, T., HORNINGER, W., BARTSCH, G., KLOCKER, H. & CULIG, Z. 1998. Interleukin-6 regulates prostate-specific protein expression in prostate carcinoma cells by activation of the androgen receptor. *Cancer Res,* 58**,** 4640-5.

HOGENESCH, H. & NIKITIN, A. Y. 2012. Challenges in pre-clinical testing of anti-cancer drugs in cell culture and in animal models. *J Control Release,* 164**,** 183-6.

HOLT, S. V., LOGIE, A., ODEDRA, R., HEIER, A., HEATON, S. P., ALFEREZ, D., DAVIES, B. R., WILKINSON, R. W. & SMITH, P. D. 2012. The MEK1/2 inhibitor, selumetinib (AZD6244; ARRY-142886), enhances anti-tumour efficacy when combined with conventional chemotherapeutic agents in human tumour xenograft models. *Br J Cancer,* 106**,** 858-66.

HOROSZEWICZ, J. S., LEONG, S. S., KAWINSKI, E., KARR, J. P., ROSENTHAL, H., CHU, T. M., MIRAND, E. A. & MURPHY, G. P. 1983. LNCaP model of human prostatic carcinoma. *Cancer Res,* 43**,** 1809-18.

HOUSHDARAN, S., HAWLEY, S., PALMER, C., CAMPAN, M., OLSEN, M. N., VENTURA, A. P., KNUDSEN, B. S., DRESCHER, C. W., URBAN, N. D., BROWN, P. O. & LAIRD, P. W. 2010. DNA methylation profiles of ovarian epithelial carcinoma tumors and cell lines. *PLoS One,* 5**,** e9359.

HSIEH, A. C., LIU, Y., EDLIND, M. P., INGOLIA, N. T., JANES, M. R., SHER, A., SHI, E. Y., STUMPF, C. R., CHRISTENSEN, C., BONHAM, M. J., WANG, S., REN, P., MARTIN, M., JESSEN, K., FELDMAN, M. E., WEISSMAN, J. S., SHOKAT, K. M., ROMMEL, C. & RUGGERO, D. 2012. The translational landscape of mTOR signalling steers cancer initiation and metastasis. *Nature,* 485**,** 55-61.

IHLE, N. T., LEMOS, R., JR., WIPF, P., YACOUB, A., MITCHELL, C., SIWAK, D., MILLS, G. B., DENT, P., KIRKPATRICK, D. L. & POWIS, G. 2009. Mutations in the phosphatidylinositol-3-kinase pathway predict for antitumor activity of the inhibitor PX-866 whereas oncogenic Ras is a dominant predictor for resistance. *Cancer Res,* 69**,** 143-50.

ISHII, N., HARADA, N., JOSEPH, E. W., OHARA, K., MIURA, T., SAKAMOTO, H., MATSUDA, Y., TOMII, Y., TACHIBANA-KONDO, Y., IIKURA, H., AOKI, T., SHIMMA, N., ARISAWA, M., SOWA, Y., POULIKAKOS, P. I., ROSEN, N., AOKI, Y. & SAKAI, T. 2013. Enhanced inhibition of ERK signaling by a novel allosteric MEK inhibitor, CH5126766, that suppresses feedback reactivation of RAF activity. *Cancer Res,* 73**,** 4050-60.

IZADPANAH, R., KAUSHAL, D., KRIEDT, C., TSIEN, F., PATEL, B., DUFOUR, J. & BUNNELL, B. A. 2008. Long-term in vitro expansion alters the biology of adult mesenchymal stem cells. *Cancer Res,* 68**,** 4229-38.

JANES, M. R., LIMON, J. J., SO, L., CHEN, J., LIM, R. J., CHAVEZ, M. A., VU, C., LILLY, M. B., MALLYA, S., ONG, S. T., KONOPLEVA, M., MARTIN, M. B., REN, P., LIU, Y., ROMMEL, C. & FRUMAN, D. A. 2010. Effective and selective targeting of leukemia cells using a TORC1/2 kinase inhibitor. *Nat Med,* 16**,** 205-13.

JIANG, B. H. & LIU, L. Z. 2008. PI3K/PTEN signaling in tumorigenesis and angiogenesis. *Biochimica Et Biophysica Acta-Proteins and Proteomics,* 1784**,** 150-158.

KAIGHN, M. E., NARAYAN, K. S., OHNUKI, Y., LECHNER, J. F. & JONES, L. W. 1979. Establishment and characterization of a human prostatic carcinoma cell line (PC-3). *Invest Urol,* 17**,** 16-23.

KANEGAE, Y., LEE, G., SATO, Y., TANAKA, M., NAKAI, M., SAKAKI, T., SUGANO, S. & SAITO, I. 1995. Efficient gene activation in mammalian cells by using recombinant adenovirus expressing site-specific Cre recombinase. *Nucleic Acids Research,* 23**,** 3816-21.

KHOLODENKO, B. N. 2006. Cell-signalling dynamics in time and space. *Nat Rev Mol Cell Biol,* 7**,** 165-76.

KIM, D., DAN, H. C., PARK, S., YANG, L., LIU, Q., KANEKO, S., NING, J., HE, L., YANG, H., SUN, M., NICOSIA, S. V. & CHENG, J. Q. 2005. AKT/PKB signaling mechanisms in cancer and chemoresistance. *Front Biosci,* 10**,** 975-87.

KIM, R. J., BAE, E., HONG, Y. K., HONG, J. Y., KIM, N. K., AHN, H. J., OH, J. J. & PARK, D. S. 2014. PTEN Loss-Mediated Akt Activation Increases the Properties of Cancer Stem-Like Cell Populations in Prostate Cancer. *Oncology,* 87**,** 270-279.

KINKADE, C. W., CASTILLO-MARTIN, M., PUZIO-KUTER, A., YAN, J., FOSTER, T. H., GAO, H., SUN, Y., OUYANG, X. S., GERALD, W. L., CORDON-CARDO, C. & ABATE-SHEN, C. 2008. Targeting AKT/mTOR and ERK MAPK signaling inhibits hormone-refractory prostate cancer in a preclinical mouse model. *Journal of Clinical Investigation,* 118**,** 3051-3064.

KNUDSEN, K. E. & PENNING, T. M. 2010. Partners in crime: deregulation of AR activity and androgen synthesis in prostate cancer. *Trends Endocrinol Metab,* 21**,** 315-24.

KOLA, I. & LANDIS, J. 2004. Can the pharmaceutical industry reduce attrition rates? *Nat Rev Drug Discov,* 3**,** 711-5.

KRAMER, G. & MARBERGER, M. 2006. Could inflammation be a key component in the progression of benign prostatic hyperplasia? *Curr Opin Urol,* 16**,** 25-9.

KRAMER, G., MITTEREGGER, D. & MARBERGER, M. 2007. Is benign prostatic hyperplasia (BPH) an immune inflammatory disease? *Eur Urol,* 51**,** 1202-16.

KREMER, C. L., KLEIN, R. R., MENDELSON, J., BROWNE, W., SAMADZEDEH, L. K., VANPATTEN, K., HIGHSTROM, L., PESTANO, G. A. & NAGLE, R. B. 2006. Expression of mTOR signaling pathway markers in prostate cancer progression. *Prostate,* 66**,** 1203-12.

KRIEGER, J. N. 2004. Classification, epidemiology and implications of chronic prostatitis in North America, Europe and Asia. *Minerva Urol Nefrol,* 56**,** 99-107.

KROON, P., BERRY, P. A., STOWER, M. J., RODRIGUES, G., MANN, V. M., SIMMS, M., BHASIN, D., CHETTIAR, S., LI, C., LI, P. K., MAITLAND, N. J. & COLLINS, A. T. 2013. JAK-STAT

blockade inhibits tumor initiation and clonogenic recovery of prostate cancer stem-like cells. *Cancer Res,* 73**,** 5288-98.

KWABI-ADDO, B., GIRI, D., SCHMIDT, K., PODSYPANINA, K., PARSONS, R., GREENBERG, N. & ITTMANN, M. 2001. Haploinsufficiency of the Pten tumor suppressor gene promotes prostate cancer progression. *Proceedings of the National Academy of Sciences of the United States of America,* 98**,** 11563-11568.

KYPRIANOU, N. & ISAACS, J. T. 1988. Identification of a cellular receptor for transforming growth factor-beta in rat ventral prostate and its negative regulation by androgens. *Endocrinology,* 123**,** 2124-31.

LAPLANTE, M. & SABATINI, D. M. 2012. mTOR signaling in growth control and disease. *Cell,* 149**,** 274-93.

LESLIE, N. R., BATTY, I. H., MACCARIO, H., DAVIDSON, L. & DOWNES, C. P. 2008. Understanding PTEN regulation: PIP2, polarity and protein stability. *Oncogene,* 27**,** 5464-5476.

LI, H., JIANG, M., HONORIO, S., PATRAWALA, L., JETER, C. R., CALHOUN-DAVIS, T., HAYWARD, S. W. & TANG, D. G. 2009. Methodologies in assaying prostate cancer stem cells. *Methods Mol Biol,* 568**,** 85-138.

LI, J., YEN, C., LIAW, D., PODSYPANINA, K., BOSE, S., WANG, S. I., PUC, J., MILIARESIS, C., RODGERS, L., MCCOMBIE, R., BIGNER, S. H., GIOVANELLA, B. C., ITTMANN, M., TYCKO, B., HIBSHOOSH, H., WIGLER, M. H. & PARSONS, R. 1997. PTEN, a putative protein tyrosine phosphatase gene mutated in human brain, breast, and prostate cancer. *Science,* 275**,** 1943-7.

LILJA, H. & ABRAHAMSSON, P. A. 1988. Three predominant proteins secreted by the human prostate gland. *Prostate,* 12**,** 29-38.

LIN, J., ADAM, R. M., SANTIESTEVAN, E. & FREEMAN, M. R. 1999. The phosphatidylinositol 3'-kinase pathway is a dominant growth factor-activated cell survival pathway in LNCaP human prostate carcinoma cells. *Cancer Res,* 59**,** 2891-7.

LIU, X., YAN, S., ZHOU, T., TERADA, Y. & ERIKSON, R. L. 2004. The MAP kinase pathway is required for entry into mitosis and cell survival. *Oncogene,* 23**,** 763-76.

LOTAN, T. L., GUREL, B., SUTCLIFFE, S., ESOPI, D., LIU, W., XU, J., HICKS, J. L., PARK, B. H., HUMPHREYS, E., PARTIN, A. W., HAN, M., NETTO, G. J., ISAACS, W. B. & DE MARZO, A. M. 2011. PTEN protein loss by immunostaining: analytic validation and prognostic indicator for a high risk surgical cohort of prostate cancer patients. *Clin Cancer Res,* 17**,** 6563-73.

MAIRA, S. M., STAUFFER, F., BRUEGGEN, J., FURET, P., SCHNELL, C., FRITSCH, C., BRACHMANN, S., CHENE, P., DE POVER, A., SCHOEMAKER, K., FABBRO, D., GABRIEL, D., SIMONEN, M., MURPHY, L., FINAN, P., SELLERS, W. & GARCIA-ECHEVERRIA, C. 2008. Identification and characterization of NVP-BEZ235, a new orally available dual phosphatidylinositol 3-kinase/mammalian target of rapamycin inhibitor with potent in vivo antitumor activity. *Molecular Cancer Therapeutics,* 7**,** 1851-63.

MAITLAND, N. J., FRAME, F. M., POLSON, E. S., LEWIS, J. L. & COLLINS, A. T. 2011. Prostate cancer stem cells: do they have a basal or luminal phenotype? *Horm Cancer,* 2**,** 47-61.

MAITLAND, N. J., MACINTOSH, C. A., HALL, J., SHARRARD, M., QUINN, G. & LANG, S. 2001. In vitro models to study cellular differentiation and function in human prostate cancers. *Radiat Res,* 155**,** 133-142.

MANNING, B. D. & CANTLEY, L. C. 2007. AKT/PKB signaling: navigating downstream. *Cell,* 129**,** 1261-74.

MARQUES, R. B., AGHAI, A., DE RIDDER, C. M., STUURMAN, D., HOEBEN, S., BOER, A., ELLSTON, R. P., BARRY, S. T., DAVIES, B. R., TRAPMAN, J. & VAN WEERDEN, W. M. 2014. High Efficacy of Combination Therapy Using PI3K/AKT Inhibitors with Androgen Deprivation in Prostate Cancer Preclinical Models. *Eur Urol*.

MARTELLI, A. M., NYAKERN, M., TABELLINI, G., BORTUL, R., TAZZARI, P. L., EVANGELISTI, C. & COCCO, L. 2006. Phosphoinositide 3-kinase/Akt signaling pathway and its therapeutical implications for human acute myeloid leukemia. *Leukemia,* 20**,** 911-28.

MASIELLO, D., MOHI, M. G., MCKNIGHT, N. C., SMITH, B., NEEL, B. G., BALK, S. P. & BUBLEY, G. J. 2007. Combining an mTOR antagonist and receptor tyrosine kinase inhibitors for the treatment of prostate cancer. *Cancer Biology & Therapy,* 6**,** 195-201.

MATHEW, R., KARANTZA-WADSWORTH, V. & WHITE, E. 2007. Role of autophagy in cancer. *Nat Rev Cancer,* 7**,** 961-7.

MATSUI, W., HUFF, C. A., WANG, Q., MALEHORN, M. T., BARBER, J., TANHEHCO, Y., SMITH, B. D., CIVIN, C. I. & JONES, R. J. 2004. Characterization of clonogenic multiple myeloma cells. *Blood,* 103**,** 2332-6.

MCCUBREY, J. A., STEELMAN, L. S., CHAPPELL, W. H., ABRAMS, S. L., FRANKLIN, R. A., MONTALTO, G., CERVELLO, M., LIBRA, M., CANDIDO, S., MALAPONTE, G., MAZZARINO, M. C., FAGONE, P., NICOLETTI, F., BASECKE, J., MIJATOVIC, S., MAKSIMOVIC-IVANIC, D., MILELLA, M., TAFURI, A., CHIARINI, F., EVANGELISTI, C., COCCO, L. & MARTELLI, A. M. 2012a. Ras/Raf/MEK/ERK and PI3K/PTEN/Akt/mTOR cascade inhibitors: how mutations can result in therapy resistance and how to overcome resistance. *Oncotarget,* 3**,** 1068-111.

MCCUBREY, J. A., STEELMAN, L. S., CHAPPELL, W. H., ABRAMS, S. L., MONTALTO, G., CERVELLO, M., NICOLETTI, F., FAGONE, P., MALAPONTE, G., MAZZARINO, M. C., CANDIDO, S., LIBRA, M., BASECKE, J., MIJATOVIC, S., MAKSIMOVIC-IVANIC, D., MILELLA, M., TAFURI, A., COCCO, L., EVANGELISTI, C., CHIARINI, F. & MARTELLI, A. M. 2012b. Mutations and deregulation of Ras/Raf/MEK/ERK and PI3K/PTEN/Akt/mTOR cascades which alter therapy response. *Oncotarget,* 3**,** 954-87.

MCMENAMIN, M. E., SOUNG, P., PERERA, S., KAPLAN, I., LODA, M. & SELLERS, W. R. 1999. Loss of PTEN expression in paraffin-embedded primary prostate cancer correlates with high Gleason score and advanced stage. *Cancer Res,* 59**,** 4291-6.

MCNEAL, J. E. 1981. The zonal anatomy of the prostate. *Prostate,* 2**,** 35-49.

MCNEAL, J. E. 1988. Normal anatomy of the prostate and changes in benign prostatic hypertrophy and carcinoma. *Semin Ultrasound CT MR,* 9**,** 329-34.

MEHRIAN-SHAI, R., CHEN, C. D., SHI, T., HORVATH, S., NELSON, S. F., REICHARDT, J. K. V. & SAWYERS, C. L. 2007. Insulin growth factor-binding protein 2 is a candidate biomarker for PTEN status and PI3K-Akt pathway activation in glioblastoma and prostate cancer. *Proceedings of the National Academy of Sciences of the United States of America,* 104**,** 5563-5568.

MENDOZA, M. C., ER, E. E. & BLENIS, J. 2011. The Ras-ERK and PI3K-mTOR pathways: cross-talk and compensation. *Trends Biochem Sci,* 36**,** 320-8.

MERIC-BERNSTAM, F. & GONZALEZ-ANGULO, A. M. 2009. Targeting the mTOR signaling network for cancer therapy. *J Clin Oncol,* 27**,** 2278-87.

MITHAL, P., ALLOTT, E., GERBER, L., REID, J., WELBOURN, W., TIKISHVILI, E., PARK, J., YOUNUS, A., SANGALE, Z., LANCHBURY, J. S., STONE, S. & FREEDLAND, S. J. 2014. PTEN loss in biopsy tissue predicts poor clinical outcomes in prostate cancer. *Int J Urol*.

MORGAN, T. M., KORECKIJ, T. D. & COREY, E. 2009. Targeted therapy for advanced prostate cancer: inhibition of the PI3K/Akt/mTOR pathway. *Curr Cancer Drug Targets,* 9**,** 237-49.

MORRISON, S. J. & KIMBLE, J. 2006. Asymmetric and symmetric stem-cell divisions in development and cancer. *Nature,* 441**,** 1068-74.

MULHOLLAND, D. J., KOBAYASHI, N., RUSCETTI, M., ZHI, A., TRAN, L. M., HUANG, J., GLEAVE, M. & WU, H. 2012. Pten loss and RAS/MAPK activation cooperate to promote EMT and metastasis initiated from prostate cancer stem/progenitor cells. *Cancer Res,* 72**,** 1878-89.

NARDELLA, C., CLOHESSY, J. G., ALIMONTI, A. & PANDOLFI, P. P. 2011. Pro-senescence therapy for cancer treatment. *Nat Rev Cancer,* 11**,** 503-11.

NORMAN, L. L., BRUGUES, J., SENGUPTA, K., SENS, P. & ARANDA-ESPINOZA, H. 2010. Cell blebbing and membrane area homeostasis in spreading and retracting cells. *Biophysical Journal,* 99**,** 1726-33.

O'REILLY, K. E., ROJO, F., SHE, Q. B., SOLIT, D., MILLS, G. B., SMITH, D., LANE, H., HOFMANN, F., HICKLIN, D. J., LUDWIG, D. L., BASELGA, J. & ROSEN, N. 2006. mTOR inhibition induces upstream receptor tyrosine kinase signaling and activates Akt. *Cancer Research,* 66**,** 1500-1508.

OESTERLING, J. E. 1991. Prostate-specific antigen: a valuable clinical tool. *Oncology (Williston Park),* 5**,** 107-22; discussion 122, 125-6, 128.

OHREN, J. F., CHEN, H., PAVLOVSKY, A., WHITEHEAD, C., ZHANG, E., KUFFA, P., YAN, C., MCCONNELL, P., SPESSARD, C., BANOTAI, C., MUELLER, W. T., DELANEY, A., OMER, C., SEBOLT-LEOPOLD, J., DUDLEY, D. T., LEUNG, I. K., FLAMME, C., WARMUS, J., KAUFMAN, M., BARRETT, S., TECLE, H. & HASEMANN, C. A. 2004. Structures of human MAP kinase kinase 1 (MEK1) and MEK2 describe novel noncompetitive kinase inhibition. *Nat Struct Mol Biol,* 11**,** 1192-7.

OKUZUMI, T., FIEDLER, D., ZHANG, C., GRAY, D. C., AIZENSTEIN, B., HOFFMAN, R. & SHOKAT, K. M. 2009. Inhibitor hijacking of Akt activation. *Nat Chem Biol,* 5**,** 484-93.

OLDRIDGE, E. E., PELLACANI, D., COLLINS, A. T. & MAITLAND, N. J. 2012. Prostate cancer stem cells: are they androgen-responsive? *Mol Cell Endocrinol,* 360**,** 14-24.

PLACER, J. & MOROTE, J. 2011. [Usefulness of prostatic specific antigen (PSA) for diagnosis and staging of patients with prostate cancer]. *Arch Esp Urol,* 64**,** 659-80.

PODSYPANINA, K., ELLENSON, L. H., NEMES, A., GU, J., TAMURA, M., YAMADA, K. M., CORDON-CARDO, C., CATORETTI, G., FISHER, P. E. & PARSONS, R. 1999. Mutation of Pten/Mmac1 in mice causes neoplasia in multiple organ systems. *Proc Natl Acad Sci U S A,* 96**,** 1563-8.

POWIS, G., BONJOUKLIAN, R., BERGGREN, M. M., GALLEGOS, A., ABRAHAM, R., ASHENDEL, C., ZALKOW, L., MATTER, W. F., DODGE, J., GRINDEY, G. & ET AL. 1994. Wortmannin, a potent and selective inhibitor of phosphatidylinositol-3-kinase. *Cancer Res,* 54**,** 2419-23.

PULIDO, R., ZUNIGA, A. & ULLRICH, A. 1998. PTP-SL and STEP protein tyrosine phosphatases regulate the activation of the extracellular signal-regulated kinases ERK1 and ERK2 by association through a kinase interaction motif. *EMBO J,* 17**,** 7337-50.

RAMEH, L. E. & CANTLEY, L. C. 1999. The role of phosphoinositide 3-kinase lipid products in cell function. *J Biol Chem,* 274**,** 8347-50.

RATNACARAM, C. K., TELETIN, M., JIANG, M., MENG, X., CHAMBON, P. & METZGER, D. 2008. Temporally controlled ablation of PTEN in adult mouse prostate epithelium generates a model of invasive prostatic adenocarcinoma. *Proc Natl Acad Sci U S A,* 105**,** 2521-6.

REYA, T., MORRISON, S. J., CLARKE, M. F. & WEISSMAN, I. L. 2001. Stem cells, cancer, and cancer stem cells. *Nature,* 414**,** 105-11.

RHODES, N., HEERDING, D. A., DUCKETT, D. R., EBERWEIN, D. J., KNICK, V. B., LANSING, T. J., MCCONNELL, R. T., GILMER, T. M., ZHANG, S. Y., ROBELL, K., KAHANA, J. A., GESKE, R. S., KLEYMENOVA, E. V., CHOUDHRY, A. E., LAI, Z., LEBER, J. D., MINTHORN, E. A., STRUM, S. L., WOOD, E. R., HUANG, P. S., COPELAND, R. A. & KUMAR, R. 2008. Characterization of an Akt kinase inhibitor with potent pharmacodynamic and antitumor activity. *Cancer Res,* 68**,** 2366-74.

RODRIGUEZ-VICIANA, P., WARNE, P. H., DHAND, R., VANHAESEBROECK, B., GOUT, I., FRY, M. J., WATERFIELD, M. D. & DOWNWARD, J. 1994. Phosphatidylinositol-3-OH kinase as a direct target of Ras. *Nature,* 370**,** 527-32.

RONINSON, I. B. 2003. Tumor cell senescence in cancer treatment. *Cancer Res,* 63**,** 2705-15.

SABATINI, D. M. 2006. mTOR and cancer: insights into a complex relationship. *Nature Reviews Cancer,* 6**,** 729-734.

SALMENA, L., CARRACEDO, A. & PANDOLFI, P. P. 2008. Tenets of PTEN tumor suppression. *Cell,* 133**,** 403-14.

SANO, H., KANE, S., SANO, E., MIINEA, C. P., ASARA, J. M., LANE, W. S., GARNER, C. W. & LIENHARD, G. E. 2003. Insulin-stimulated phosphorylation of a Rab GTPase-activating protein regulates GLUT4 translocation. *J Biol Chem,* 278**,** 14599-602.

SANTARPIA, L., LIPPMAN, S. M. & EL-NAGGAR, A. K. 2012. Targeting the MAPK-RAS-RAF signaling pathway in cancer therapy. *Expert Opin Ther Targets,* 16**,** 103-19.

SAR, M., LUBAHN, D. B., FRENCH, F. S. & WILSON, E. M. 1990. Immunohistochemical localization of the androgen receptor in rat and human tissues. *Endocrinology,* 127**,** 3180-6.

SARBASSOV, D. D., ALI, S. M., SENGUPTA, S., SHEEN, J. H., HSU, P. P., BAGLEY, A. F., MARKHARD, A. L. & SABATINI, D. M. 2006a. Prolonged rapamycin treatment inhibits mTORC2 assembly and Akt/PKB. *Molecular Cell,* 22**,** 159-68.

SARBASSOV, D. D., ALI, S. M., SENGUPTA, S., SHEEN, J. H., HSU, P. P., BAGLEY, A. F., MARKHARD, A. L. & SABATINI, D. M. 2006b. Prolonged rapamycin treatment inhibits mTORC2 assembly and Akt/PKB. *Mol Cell,* 22**,** 159-68.

SARBASSOV, D. D., GUERTIN, D. A., ALI, S. M. & SABATINI, D. M. 2005. Phosphorylation and regulation of Akt/PKB by the rictor-mTOR complex. *Science,* 307**,** 1098-1101.

SARKER, D., REID, A. H. M., YAP, T. A. & DE BONO, J. S. 2009. Targeting the PI3K/AKT Pathway for the Treatment of Prostate Cancer. *Clinical Cancer Research,* 15**,** 4799-4805.

SARRIS, E. G., SAIF, M. W. & SYRIGOS, K. N. 2012. The Biological Role of PI3K Pathway in Lung Cancer. *Pharmaceuticals (Basel),* 5**,** 1236-64.

SCHRODER, F. H. & BLOM, J. H. 1989. Natural history of benign prostatic hyperplasia (BPH). *Prostate Suppl,* 2**,** 17-22.

SEBOLT-LEOPOLD, J. S. 2008. Advances in the development of cancer therapeutics directed against the RAS-mitogen-activated protein kinase pathway. *Clin Cancer Res,* 14**,** 3651-6.

SEGER, R., AHN, N. G., POSADA, J., MUNAR, E. S., JENSEN, A. M., COOPER, J. A., COBB, M. H. & KREBS, E. G. 1992. Purification and characterization of mitogen-activated protein kinase activator(s) from epidermal growth factor-stimulated A431 cells. *J Biol Chem,* 267**,** 14373-81.

SEOL, J. W., LEE, Y. J., KANG, H. S., KIM, I. S., KIM, N. S., KWAK, Y. G., KIM, T. H., SEOL, D. W. & PARK, S. Y. 2005. Wortmannin elevates tumor necrosis factor-related apoptosis-inducing ligand sensitivity in LNCaP cells through down-regulation of IAP-2 protein. *Exp Oncol,* 27**,** 120-4.

SERRA, V., MARKMAN, B., SCALTRITI, M., EICHHORN, P. J., VALERO, V., GUZMAN, M., BOTERO, M. L., LLONCH, E., ATZORI, F., DI COSIMO, S., MAIRA, M., GARCIA-ECHEVERRIA, C., PARRA, J. L., ARRIBAS, J. & BASELGA, J. 2008. NVP-BEZ235, a dual PI3K/mTOR inhibitor, prevents PI3K signaling and inhibits the growth of cancer cells with activating PI3K mutations. *Cancer Res,* 68**,** 8022-30.

SHARRARD, R. M. & MAITLAND, N. J. 2000. Phenotypic effects of overexpression of the MMAC1 gene in prostate epithelial cells. *Br J Cancer,* 83**,** 1102-9.

SHARRARD, R. M. & MAITLAND, N. J. 2007. Regulation of protein kinase B activity by PTEN and SHIP2 in human prostate-derived cell lines. *Cell Signal,* 19**,** 129-38.

SHAUL, Y. D. & SEGER, R. 2007. The MEK/ERK cascade: from signaling specificity to diverse functions. *Biochimica Et Biophysica Acta,* 1773**,** 1213-26.

SHAW, R. J. & CANTLEY, L. C. 2006. Ras, PI(3)K and mTOR signalling controls tumour cell growth. *Nature,* 441**,** 424-30.

SHEN, M. M. & ABATE-SHEN, C. 2010. Molecular genetics of prostate cancer: new prospects for old challenges. *Genes Dev,* 24**,** 1967-2000.

SHERWOOD, E. R., THEYER, G., STEINER, G., BERG, L. A., KOZLOWSKI, J. M. & LEE, C. 1991. Differential expression of specific cytokeratin polypeptides in the basal and luminal epithelia of the human prostate. *Prostate,* 18**,** 303-14.

SHIN, S. & BLENIS, J. 2010. ERK2/Fra1/ZEB pathway induces epithelial-to-mesenchymal transition. *Cell Cycle,* 9**,** 2483-4.

SHIN, S., DIMITRI, C. A., YOON, S. O., DOWDLE, W. & BLENIS, J. 2010. ERK2 but not ERK1 induces epithelial-to-mesenchymal transformation via DEF motif-dependent signaling events. *Molecular Cell,* 38**,** 114-27.

SHUKLA, S., MACLENNAN, G. T., HARTMAN, D. J., FU, P., RESNICK, M. I. & GUPTA, S. 2007. Activation of PI3K-Akt signaling pathway promotes prostate cancer cell invasion. *Int J Cancer,* 121**,** 1424-32.

SIGNORETTI, S., WALTREGNY, D., DILKS, J., ISAAC, B., LIN, D., GARRAWAY, L., YANG, A., MONTIRONI, R., MCKEON, F. & LODA, M. 2000. p63 is a prostate basal cell marker and is required for prostate development. *Am J Pathol,* 157**,** 1769-75.

SINGH, S. K., CLARKE, I. D., TERASAKI, M., BONN, V. E., HAWKINS, C., SQUIRE, J. & DIRKS, P. B. 2003. Identification of a cancer stem cell in human brain tumors. *Cancer Res,* 63**,** 5821-8.

SONTAG, E., FEDOROV, S., KAMIBAYASHI, C., ROBBINS, D., COBB, M. & MUMBY, M. 1993. The interaction of SV40 small tumor antigen with protein phosphatase 2A stimulates the map kinase pathway and induces cell proliferation. *Cell,* 75**,** 887-97.

SPARKS, C. A. & GUERTIN, D. A. 2010. Targeting mTOR: prospects for mTOR complex 2 inhibitors in cancer therapy. *Oncogene,* 29**,** 3733-3744.

STAMPFER, M. J., JAHN, J. L. & GANN, P. H. 2014. Further evidence that prostate-specific antigen screening reduces prostate cancer mortality. *J Natl Cancer Inst,* 106**,** dju026.

STEELMAN, L. S., CHAPPELL, W. H., ABRAMS, S. L., KEMPF, R. C., LONG, J., LAIDLER, P., MIJATOVIC, S., MAKSIMOVIC-IVANIC, D., STIVALA, F., MAZZARINO, M. C., DONIA, M., FAGONE, P., MALAPONTE, G., NICOLETTI, F., LIBRA, M., MILELLA, M., TAFURI, A., BONATI, A., BASECKE, J., COCCO, L., EVANGELISTI, C., MARTELLI, A. M., MONTALTO, G., CERVELLO, M. & MCCUBREY, J. A. 2011. Roles of the Raf/MEK/ERK and PI3K/PTEN/Akt/mTOR pathways in controlling growth and sensitivity to therapy-implications for cancer and aging. *Aging (Albany NY),* 3**,** 192-222.

STEINBRUNN, T., STUHMER, T., SAYEHLI, C., CHATTERJEE, M., EINSELE, H. & BARGOU, R. C. 2012. Combined targeting of MEK/MAPK and PI3K/Akt signalling in multiple myeloma. *Br J Haematol,* 159**,** 430-40.

STEVERMER, J. J. & EASLEY, S. K. 2000. Treatment of prostatitis. *Am Fam Physician,* 61**,** 3015-22, 3025-6.

STONE, K. R., MICKEY, D. D., WUNDERLI, H., MICKEY, G. H. & PAULSON, D. F. 1978. Isolation of a human prostate carcinoma cell line (DU 145). *Int J Cancer,* 21**,** 274-81.

SUGGITT, M. & BIBBY, M. C. 2005. 50 years of preclinical anticancer drug screening: empirical to target-driven approaches. *Clin Cancer Res,* 11**,** 971-81.

SULIS, M. L. & PARSONS, R. 2003. PTEN: from pathology to biology. *Trends in Cell Biology,* 13**,** 478-483.

SUN, S., SPRENGER, C. C., VESSELLA, R. L., HAUGK, K., SORIANO, K., MOSTAGHEL, E. A., PAGE, S. T., COLEMAN, I. M., NGUYEN, H. M., SUN, H., NELSON, P. S. & PLYMATE, S. R. 2010. Castration resistance in human prostate cancer is conferred by a frequently occurring androgen receptor splice variant. *J Clin Invest,* 120**,** 2715-30.

SUZUKI, H., FREIJE, D., NUSSKERN, D. R., OKAMI, K., CAIRNS, P., SIDRANSKY, D., ISAACS, W. B. & BOVA, G. S. 1998. Interfocal heterogeneity of PTEN/MMAC1 gene alterations in multiple metastatic prostate cancer tissues. *Cancer Res,* 58**,** 204-9.

TAICHMAN, R. S., LOBERG, R. D., MEHRA, R. & PIENTA, K. J. 2007. The evolving biology and treatment of prostate cancer. *J Clin Invest,* 117**,** 2351-61.

TAKAMURA, A., KOMATSU, M., HARA, T., SAKAMOTO, A., KISHI, C., WAGURI, S., EISHI, Y., HINO, O., TANAKA, K. & MIZUSHIMA, N. 2011. Autophagy-deficient mice develop multiple liver tumors. *Genes Dev,* 25**,** 795-800.

TANNOCK, I. F., DE WIT, R., BERRY, W. R., HORTI, J., PLUZANSKA, A., CHI, K. N., OUDARD, S., THEODORE, C., JAMES, N. D., TURESSON, I., ROSENTHAL, M. A. & EISENBERGER, M. A. 2004. Docetaxel plus prednisone or mitoxantrone plus prednisone for advanced prostate cancer. *N Engl J Med,* 351**,** 1502-12.

TEE, A. R., FINGAR, D. C., MANNING, B. D., KWIATKOWSKI, D. J., CANTLEY, L. C. & BLENIS, J. 2002. Tuberous sclerosis complex-1 and -2 gene products function together to inhibit mammalian target of rapamycin (mTOR)-mediated downstream signaling. *Proc Natl Acad Sci U S A,* 99**,** 13571-6.

TINDALL, D. E. O. C. *Prostate cancer : biochemistry, molecular biology and genetics*.

TORII, S., NAKAYAMA, K., YAMAMOTO, T. & NISHIDA, E. 2004. Regulatory mechanisms and function of ERK MAP kinases. *J Biochem,* 136**,** 557-61.

TURKE, A. B., SONG, Y., COSTA, C., COOK, R., ARTEAGA, C. L., ASARA, J. M. & ENGELMAN, J. A. 2012. MEK inhibition leads to PI3K/AKT activation by relieving a negative feedback on ERBB receptors. *Cancer Res,* 72**,** 3228-37.

VANHAESEBROECK, B., STEPHENS, L. & HAWKINS, P. 2012. PI3K signalling: the path to discovery and understanding. *Nat Rev Mol Cell Biol,* 13**,** 195-203.

VANTAGGIATO, C., FORMENTINI, I., BONDANZA, A., BONINI, C., NALDINI, L. & BRAMBILLA, R. 2006. ERK1 and ERK2 mitogen-activated protein kinases affect Ras-dependent cell signaling differentially. *J Biol,* 5**,** 14.

VASSILOPOULOS, A., XIAO, C., CHISHOLM, C., CHEN, W., XU, X., LAHUSEN, T. J., BEWLEY, C. & DENG, C. X. 2014. Synergistic Therapeutic Effect of Cisplatin and Phosphatidylinositol 3-Kinase (PI3K) Inhibitors in Cancer Growth and Metastasis of Brca1 Mutant Tumors. *J Biol Chem,* 289**,** 24202-14.

VAZQUEZ, F., RAMASWAMY, S., NAKAMURA, N. & SELLERS, W. R. 2000. Phosphorylation of the PTEN tail regulates protein stability and function. *Mol Cell Biol,* 20**,** 5010-8.

VELDSCHOLTE, J., BERREVOETS, C. A., RIS-STALPERS, C., KUIPER, G. G., JENSTER, G., TRAPMAN, J., BRINKMANN, A. O. & MULDER, E. 1992. The androgen receptor in LNCaP cells contains a mutation in the ligand binding domain which affects steroid binding characteristics and response to antiandrogens. *J Steroid Biochem Mol Biol,* 41**,** 665-9.

VILAR, E., PEREZ-GARCIA, J. & TABERNERO, J. 2011. Pushing the envelope in the mTOR pathway: the second generation of inhibitors. *Molecular Cancer Therapeutics,* 10**,** 395-403.

VISAKORPI, T., HYYTINEN, E., KOIVISTO, P., TANNER, M., KEINANEN, R., PALMBERG, C., PALOTIE, A., TAMMELA, T., ISOLA, J. & KALLIONIEMI, O. P. 1995. In vivo amplification of the androgen receptor gene and progression of human prostate cancer. *Nature Genetics,* 9**,** 401-6.

VIVANCO, I. & SAWYERS, C. L. 2002. The phosphatidylinositol 3-kinase-AKT pathway in human cancer. *Nature Reviews Cancer,* 2**,** 489-501.

VOGELSTEIN, B. & KINZLER, K. W. 1993. The multistep nature of cancer. *Trends Genet,* 9**,** 138-41.

WALSH, P. C. 2007. The discovery of the cavernous nerves and development of nerve sparing radical retropubic prostatectomy. *J Urol,* 177**,** 1632-5.

WANG, X. & JIANG, X. 2008. Post-translational regulation of PTEN. *Oncogene,* 27**,** 5454-63.

WELLBROCK, C., KARASARIDES, M. & MARAIS, R. 2004. The RAF proteins take centre stage. *Nat Rev Mol Cell Biol,* 5**,** 875-85.

WENDEL, H. G., DE STANCHINA, E., FRIDMAN, J. S., MALINA, A., RAY, S., KOGAN, S., CORDON-CARDO, C., PELLETIER, J. & LOWE, S. W. 2004. Survival signalling by Akt and eIF4E in oncogenesis and cancer therapy. *Nature,* 428**,** 332-7.

WU, L., BIRLE, D. C. & TANNOCK, I. F. 2005. Effects of the mammalian target of rapamycin inhibitor CCI-779 used alone or with chemotherapy on human prostate cancer cells and xenografts. *Cancer Res,* 65**,** 2825-31.

YANG, J. Y., ZONG, C. S., XIA, W., YAMAGUCHI, H., DING, Q., XIE, X., LANG, J. Y., LAI, C. C., CHANG, C. J., HUANG, W. C., HUANG, H., KUO, H. P., LEE, D. F., LI, L. Y., LIEN, H. C., CHENG, X., CHANG, K. J., HSIAO, C. D., TSAI, F. J., TSAI, C. H., SAHIN, A. A., MULLER, W. J., MILLS, G. B., YU, D., HORTOBAGYI, G. N. & HUNG, M. C. 2008. ERK promotes tumorigenesis by inhibiting FOXO3a via MDM2-mediated degradation. *Nat Cell Biol,* 10**,** 138-48.

YAP, T. A., GARRETT, M. D., WALTON, M. I., RAYNAUD, F., DE BONO, J. S. & WORKMAN, P. 2008. Targeting the PI3K-AKT-mTOR pathway: progress, pitfalls, and promises. *Curr Opin Pharmacol,* 8**,** 393-412.

YILMAZ, O. H. & MORRISON, S. J. 2008. The PI-3kinase pathway in hematopoietic stem cells and leukemia-initiating cells: A mechanistic difference between normal and cancer stem cells. *Blood Cells Molecules and Diseases,* 41**,** 73-76.

YOON, S. & SEGER, R. 2006. The extracellular signal-regulated kinase: multiple substrates regulate diverse cellular functions. *Growth Factors,* 24**,** 21-44.

YOSHIMOTO, M., CUNHA, I. W., COUDRY, R. A., FONSECA, F. P., TORRES, C. H., SOARES, F. A. & SQUIRE, J. A. 2007. FISH analysis of 107 prostate cancers shows that PTEN genomic deletion is associated with poor clinical outcome. *British Journal of Cancer,* 97**,** 678-685.

YUEN, H. F., ABRAMCZYK, O., MONTGOMERY, G., CHAN, K. K., HUANG, Y. H., SASAZUKI, T., SHIRASAWA, S., GOPESH, S., CHAN, K. W., FENNELL, D., JANNE, P., EL-TANANI, M. & MURRAY, J. T. 2012. Impact of oncogenic driver mutations on feedback between the PI3K and MEK pathways in cancer cells. *Biosci Rep,* 32**,** 413-22.

ZHANG, H., BAJRASZEWSKI, N., WU, E., WANG, H., MOSEMAN, A. P., DABORA, S. L., GRIFFIN, J. D. & KWIATKOWSKI, D. J. 2007. PDGFRs are critical for PI3K/Akt activation and negatively regulated by mTOR. *J Clin Invest,* 117**,** 730-8.

ZHANG, S. & YU, D. 2010. PI(3)king apart PTEN's role in cancer. *Clin Cancer Res,* 16**,** 4325-30.

ZHANG, W., HAINES, B. B., EFFERSON, C., ZHU, J., WARE, C., KUNII, K., TAMMAM, J., ANGAGAW, M., HINTON, M. C., KEILHACK, H., PAWELETZ, C. P., ZHANG, T., WINTER, C., SATHYANARAYANAN, S., CHENG, J., ZAWEL, L., FAWELL, S., GILLILAND, G. & MAJUMDER, P. K. 2012. Evidence of mTOR Activation by an AKT-Independent Mechanism Provides Support for the Combined Treatment of PTEN-Deficient Prostate Tumors with mTOR and AKT Inhibitors. *Transl Oncol,* 5**,** 422-9.

ZIMMERMANN, S. & MOELLING, K. 1999. Phosphorylation and regulation of Raf by Akt (protein kinase B). *Science,* 286**,** 1741-4.

ZINDA, M. J., JOHNSON, M. A., PAUL, J. D., HORN, C., KONICEK, B. W., LU, Z. H., SANDUSKY, G., THOMAS, J. E., NEUBAUER, B. L., LAI, M. T. & GRAFF, J. R. 2001. AKT-1,-2, and-3 are expressed in both normal and tumor tissues of the lung, breast, prostate, and colon. *Clinical Cancer Research,* 7**,** 2475-2479.

ZONCU, R., EFEYAN, A. & SABATINI, D. M. 2011. mTOR: from growth signal integration to cancer, diabetes and ageing. *Nat Rev Mol Cell Biol,* 12**,** 21-35.

Websites:

Harvard Prostate Knowledge; http://www.harvardprostateknowledge.org/prostate-basics

National Health Service, UK

http://www.nhs.uk/Conditions/Prostate-enlargement/Pages/Treatment.aspx

Urology Care Foundation

http://www.urologyhealth.org/urology/index.cfm?article=144

National Cancer Institute;

https://visuals.nci.nih.gov/details.cfm?imageid=7137

http://www.cancer.gov/cancertopics/factsheet/detection/PSA

Cancer Research UK

http://www.cancerresearchuk.org/cancer-info/cancerstats/types/prostate/incidence/

http://www.cancerresearchuk.org/cancer-info/cancerstats/types/prostate/mortality/

Cell Signaling Technology;
http://www.cellsignal.com/common/content/content.jsp?id=pathways-mtor-signaling

http://www.clinicaltrials.gov

http://venture-pharmaceuticals.com/what-is-drug-development/olddrugs2/

Book chapters:

Maitland N.J., The future: What's in the toolkit for prostate cancer diagnosis and treatment?, p.313-330, 2014, book title: Prostate cancer, Diagnosis and clinical management, edited by Ashutosh K. Tewari, Peter Whelan and John D. Graham. /Wiley Blackwell

Frame F.M. and Maitland N.J. (2013) Cancer stem cells provide new insights into the therapeutic responses of human prostate cancer (Chapter 4). In 'Stem Cells and Prostate Cancer'. S. Cramer, ed. (Springer Science + Business Media, LLC).